UNIVERSITY *of the*
WESTERN CAPE

University of the Western Cape

ASSESSING HYDROCARBON POTENTIAL IN CRETACEOUS SEDIMENTS IN THE WESTERN BREDASDORP SUB-BASIN IN THE OUTENIQUA BASIN SOUTH AFRICA.

A thesis submitted in fulfilment of the requirements for a Magister degree (MSc) Petroleum Geology, Department of Earth Science University of the Western Cape.

Presented by:

COLLINS BANAJEM ACHO

SUERVISOR	**:**	**Dr. MOMINITU OPUWARI**
CO-SUPERVISOR	**:**	**Prof. JAN VAN BERVER DONKER**

(July 2015).

ABSTRACT

The Bredasdorp Basin is one of the largest hydrocarbon producing blocks within Southern Africa. The E-M field is situated approximate 50 km west from the FA platform and was brought into commission due to the potential hydrocarbons it may hold. If this field is brought up to full producing capability it will extend the lifespan of the refining station in Mosselbay, situated on the south coast of South Africa, by approximately 8-10 years. This study is focused in block 9 off shore western part of the Bredasdorp Basin in the main Outeniqua Basin South Africa. Cretaceous Sandstone reservoirs are commonly heterogeneous consequently they may require special methods and techniques for description and evaluation. Reservoir characterization is the study of the reservoir rocks, their petrophysical properties, the fluids they contain or the manner in which they influence the movement of fluids in the subsurface. The main goal of the research is to assess the potentials of hydrocarbons in Cretaceous sediments in the Bredasdorp Basin through the integration and comparison of results from core analysis, production data and petrography studies for the evaluation and correction of key petrophysical parameters from wireline logs which could be used to generate an effective reservoir model for wells (E-BB1, E-BD2, E-A01) in the Bredasdorp Basin.

Porosity and permeability relationships, wire-line log data have been examined and analysed to determine how the porosity and permeability influence reservoir quality which further influences the potential of hydrocarbon accumulation in the reservoirs. The reservoir sandstone is composed mainly of fine to medium grained Sandstones with intercalation of finger stringers of Siltstone and Shale. In carrying out this research the samples are used to characterize reservoir zones through core observation, description and analyses and compare the findings with electronic data obtained from Petroleum Agency of South Africa (PASA). Secondary data obtained from (PASA) was analysed using softwares such as Interactive Petrophysics (IP), Ms Word, Ms excel and Surfer. Wireline logs of selected wells (E-BB1, E-BD2, E-A01) were generated, analysed and correlated. Surfer software also used to digitize maps of project area, porosity and permeability plotted using IP. Formation of the Bredasdorp Basin and it surrounding basins during the Gondwana breakup. The Bredasdorp Basin consists mainly of tilting half graben structures that formed through rifting with the break-up of Gondwanaland. The model also revealed that these

faults segregate the reservoir which explains the pressure loss within the block. The production well was drilled, confining pressure relieved and pressure dropped hence production decreases. The age, transportation, deposition and thermal history of sediment in the basin, all plays a vital role in the type of hydrocarbon formation. Structural features such as faults, pore spaces determines the presence of a hydrocarbon in the reservoir. Traps could be stratigraphic or structural which helps prevent the migration of hydrocarbons from the source rock to reservoir rock or from reservoir rock to the surface over a period of time. The textural aspects included the identification of grain sizes, sorting and grain shapes. The diagenetic history, constructed from the results of the reservoir quality study revealed that there were several stages involved in the diagenetic process.

It illustrated several phases of cementation with quartz, carbonate and dolomite with dissolution of feldspar. A potentially good reservoir interval was identified from the data and was characterized by several heterogeneous zones. Identifying reservoir zones was highly beneficial during devising recovery techniques for production of hydrocarbons. Secondary recovery methods have thus been devised to enhance well performance. As recommendation, additional wells are required to appraise the E-M structure and determine to what extent the cement present in the basin has affected fluid flow as well as the degree of sedimentation that could impede fluid flow. There are areas still containing untapped resources thus the recommendation for extra wells. This research may well be reviewed with more data input from PetroSA (wells, seismic and production data) for additional studies, predominantly with respect to reservoir modelling and flow simulation. Based on the findings of this research, summary of calculated Net Pay shows that in well E-BB1, reservoir (1) is at depth 2841.5m – 2874.9m has a Gross Thickness of 33.40m, Net Pay of 29.72 and Pay Summary of 29.57 and reservoir (2) has depth of 2888.1m – 2910.5m, Gross Thickness of 22.40m, Net Pay of 19.92m and Pay summary of 1.48m. Well E-AO1 has depth from 2669.5m – 2684.5m and Gross Thickness of 15.00m and has Net Pay of 10.37m and Pay Summary of 10.37m. Based on the values obtained from the data analysed the above two wells displays high potential of hydrocarbon present in the reservoirs. Meanwhile well E-BD2 has depth from 2576.2m – 2602.5m and has Gross Thickness of 350.00m, Net Pay of 28.96m and Pay Summary of 4.57 hence from data analysis this reservoir displays poor values which is an indication of poor hydrocarbon potentials.

DECLARATION

I the undersigned hereby declare that the work contained in this thesis is my own original work and has not previously in its entirety or in part been submitted at any university for a degree. I hereby declare that any material or knowledge (from previous studies) used in this thesis has been acknowledged and referenced appropriately.

Signature:……Date……..

DEDICATION

I would like to dedicate this project to God Almighty for keeping me alive, protecting and providing me with knowledge, wisdom and good health to be able to attain this achievement. I would also like to dedicate this work to my parents, Mr. Alex Musi Acho and Mrs Sabina Chi Acho for the prayers and support they gave me during my studies and in my undertakings. Also to my entire family members and friends for their support and prayers.

ACKNOWLEDGEMENT

I would like to thank God Almighty for given me the knowledge and good health throughout my study, my parents Mr. Alex Musi Acho and Mrs Sabina Chi Acho, the family of Dr. Abongdia Jane-francis, the family of Mr. Eugene Alfred and friends for their prayers and support. Big thanks go to Petroleum Agency of South Africa (PASA) for providing me with data (hard and soft copy) used for this thesis. Thanks also go to Dr. Mimonitu Opuwari my supervisor and Prof. Jan Van Bever Donker my co-supervisor for their continuous input and support from the beginning of my project till the end. I would like to thank the department and faculty staffs especially Mrs. Wasielah Davids administrative officer and Mrs. Mandy Naidoo postgraduate coordinator for their support and encouragement. Many thanks to Inkaba Ye-Africa for the financial assistance throughout my project and finally to my classmates and friends Moses Magoba, Nehemiarh Dominick, Stephane Tsakou, Dr. Nokulunga S. Majozi and Dr. Mpho P. Dikgale for their massive contributions and support. Thank you all very much without your contributions, support and prayers this wouldn't have happened thank you and God bless us all.

TABLE OF CONTENT

LIST OF FIGURES

LIST OF TABLES

LIST OF PLATES

1 CHAPTER

1.1 Introduction

The Bredasdorp Basin and its environs, is located on the South Africa continental shelf between Cape Agulhas and Mossel Bay (fig:1.1). The basin, one of four delineated by the results from seismic surveys and the ~200 wells drilled during the course of exploration for hydrocarbons, extends for approximately 150 km E-W and 100 km N-S, having a total area of ~15 000km^2. Prior to the start of hydrocarbon exploration in the South African offshore in the late 1960's, there had been no geological studies of the continental shelf of the Bredasdorp Basin in particular therefore stems from this hydrocarbon exploration effort, which is still continuing. Indeed, it is only during the past 10 years, after many regional and local studies, that the geologic history has become well understood enough for exploration success rates to improve dramatically. However, few of these studies have been published apart from some general reviews e.g. Burden, (1992) and presentations at Geocongress, Cape Town (1990). In step with this advancement, comes an explosive growth in the understanding of the petroleum geochemistry of the basin.

Many regional studies of this nature have also been undertaken in offshore areas, almost entirely by SOEKOR. Very little of this information has been published. Within the Bredasdorp Basin, many hydrocarbon reservoirs have been found in Creataceous sandstones. It is thought that the gas and oil they contain have been generated in one or more of the carbon-rich source rocks found within the limits of the basin or in the western part of the southern Outerniqua Basin. These hydrocarbons comprise liquid oils and traces of high molecular weight hydrocarbons, considered to be residues after earlier oil charges, and wet gas with condensate. Concentrations of these hydrocarbons are commercially significant and are actively explored. Two reservoirs are currently producing gas-condensate and oil. The commercial viability of these occurrences is primarily related to the high monetary value of the liquid fraction compared to that of gas. Therefore it is of paramount importance for exploration efforts to concentrate their search in those parts of the basin where such hydrocarbons are preferentially reserved. This is achieved if:

(a) The route(s) these hydrocarbons took when migrating from their source rock to the present reservoir rock are known,
(b) Where the timing of the migration episodes is understood and
(c) The volume available for migration through each route can be reliably estimated. These can only be evaluated once:

- The source rock for the hydrocarbon is identified,
- The fetch area is delineated,
- The maturation history is known and
- The relative quantities expellable from each source are calculated.

Each of these is very difficult to determine and represents major challenges to the exploration geologist. Prior to the present study, the distribution, thickness and richness of source rocks in the Bredasdorp Basin wells were established from inter-well comparisons using pyrolysis analyses (>24000) and optical studies (>3500) carried out on core and sidewall core samples from 150 wells and 75 wells respectively. From these data it was determined that there were several different source rocks and that some were within the oil window, whereas some had passed through the oil window. No intersections of immature wet gas or oil-prone source rocks have been found. The search for inherited characteristics of source rocks has been actively pursued by petroleum geochemistry elsewhere for some time Philippi, (1956).

These earliest efforts concentrated on the composition of the oil amenable to gas chromatographic analysis. Those early methods were quickly adopted by other companies and refined so that correlations between source rocks and oils were frequently attempted using more detailed comparisons of the chemical and physical properties of hydrocarbons, with similar properties of bituments in the supposed source rocks Dow, (1974) and Williams, (1974). Those comparisons were based on the fact that hydrocarbons derived from each source rock should be distinguishable because they inherit characteristic of the original biological source material. Since it is known that some hydrocarbons are left behind in the source rock as bitumens after migration Tissot and Welte, (1984), it is likely that chemical 'fossils' in the bitumens should match those found in reservoired hydrocarbons Eglinton and Calvin, (1967). These early correlation studies largely addressed characteristic aspects of low maturity whole oil and bulk source rock extracts using medium resolution gas

chromatography. As the techniques became more widely used, the complexity of the hydrocarbons became apparent. The high molecular weight fractions of the oils were evidently comprised of mixtures of hundreds of components which could only be separated by high resolution gas chromatography and later by mass spectrometry analysis. However, these methods proved less successful when dealing with higher maturity condensate and their sources, because the proportions of bulk and chromatographically resolvable groups of hydrocarbons decreased with increasing maturity. As a result, various fractionation and concentration steps were employed. The added advantage of using high resolution analyses of specific fractions was that they were able to establish identities of characteristic groups of compounds which could differentiate oils and source rocks without recourse to the short to medium-chain alkanes previously employed. This was a step forward as those alkanes were often subject to severe in-reservoir alteration by biodegration (Rogers et al., 1974). The discovery (1986) of reservoir oil in the previously unexplored centre of the Bredasdorp Basin led to a concerted effort to discover further reserves of oil, which in turn led to a need to understand the sourcing and migration timing of oil in the basin. This could only be done using the techniques of biological marker (or biomarker) analysis and provide a new impetus for the use of these analyses.

A few such analyses were carried out at the University of Stellenbosch but equipment problem, and the inability to correlate the peaks found with those of published biomarkers because of the lack of suitable standards, and led to a cessation of the attempt. However, after the easing of sanctions in the early 1990's it became possible to have samples from South Africa analysed for their biomarker contents and to use those results as standards to calibrate the local equipment. The arrival of the first available biomarker results in 1992 sparked a fresh start to oil, source correlation studies. The ability to carry out these analyses in-house led to a rapid growth in their utilisation and helped in the understanding of the hydrocarbon history of the basin. In addition, most of the work has been targeted at local studies which have immediate commercial benefits and not at the long-term aims of regional appraisal. This study, however, aims at redressing the imbalance and shows that studies outside the main hydrocarbon trend can also yield information which is of direct importance to more local oil and gas exploration projects. A second major advancement came with the adoption of a commercial burial history programme (Basin-mod) in the late

1980's for use in basin modelling studies aimed at understanding the generation history of the basin. This capability was further enhanced by the acquisition of the OPTKIN programme for the Rock-Eval pyrolysis instrument which allowed for the determination of kinetic generation parameters from source rock samples. These two techniques together allowed a more rigorous assessment of the generation and expulsion of hydrocarbons from source rocks, which in turn led to the appreciation that the previously accepted gradualistic thermal history model of the basin, i.e. continuous cool-down after Late Jurassic rifting, did not take account of all the facts. Hence a new thermal model of the basin had to be formulated.

It is anticipated that deep marine plays are likely to hold hydrocarbon resources which are presently in high demand. To ensure characterization of the sand-rich intervals in the Bredasdorp Basin deep marine play with respect to controls on their porosity and permeability distribution is required. Knowledge of porosity and permeability heterogeneity is essential to exploration geologist, production geologist and reservoir engineers for accurate evaluation of economic resources. A higher porosity and permeability coupled with other favourable conditions such as trap and seal for hydrocarbon accumulation within a reservoir zone implies greater probability of producing a commercially viable resource. Sandstone reservoirs are commonly heterogeneous consequently they may require special methods and techniques for description and evaluation.

Reservoir characterization is the study of the reservoir rocks, their petrophysical properties, the fluids they contain or the manner in which they influence the movement of fluids in the subsurface. This study focuses on the description of core samples and the pore network of reservoir intervals of wells in the western part of the Bredasdorp Basin. Porosity and permeability relationships, wire-line log data (signals) have been examined and analysed to determine how the porosity and permeability influence reservoir quality which further influences the potential of hydrocarbon accumulation in the reservoirs. The reservoir sandstone is composed mainly of fine to coarse grained Sandstones with thin intercalation of Siltstone and Shale. In carrying out this research the samples are used to characterize reservoir zones through core observation, description and analyses and compare the findings with electronic data obtained from Petroleum Agency of South Africa (PASA).

1.1.1 Aim

The aim of this study is to critically assess the characteristics of the reservoir zones and the different lithology associated with petrophysical characteristics such as porosity, permeability, grain size and shape by integrating basic core observation and descriptive analyses, wireline log analyses to understand the potential of hydrocarbon in the reservoirs.

1.1.2 Objectives

i. Characterisation of different sand units with the reservoir zones.

ii. Assess the impact of clay and cement on porosity and permeability

iii. Complete well log correlation of wells with the study area to identify clean sand zone with favourable porosity and permeability.

v. Critically determine the impact of petroleum systems that may be present within the reservoirs.

vi. Determine the age of material transported, deposition and timing.

1.1.3 Location of study area

Bredasdorp Basin is a sub-basin in the greater Outeniqua Basin which lies between the Columbine-Agalhas and Infanta arches (fig1.1) is situated off the south coast of South Africa, South East of Cape Town and South West of Port Elizabeth. It is a ~200km long and 80km wide and occupying about 18,00km^2. The sub-basin was formed as a result of extensional episodes during the initial stages of rifting during the Jurassic period. There are intersections in offshore well basement consists of slates of the Bokkeveld group (Devonian) or quartzite of the Table Mountain Supergroup (Ordovician-Silurian). The Bredasdorp sub-basin is to the South and NW, SE shallow water fault trend. This research is focused on reservoir zones encountered by three selected wells in the Western Bredasdorp Basin; E-BD2, E-BB1, E-AO1, in block 9.

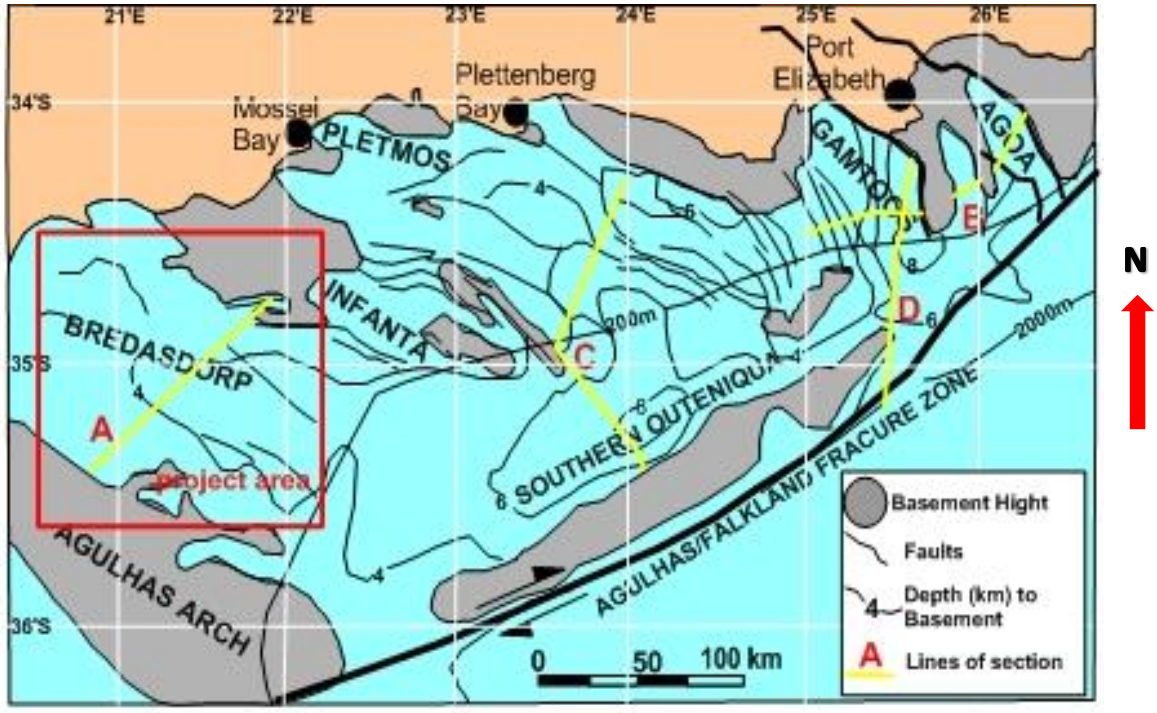

Figure 1.1 Location map of Bredasdorp Basin source; modified after Petroleum Agency SA, (2003). Transtention generation along the Agulhas-Falkland Zone initiated Right Lateral movement which separated the South American and African plates and effected tectonic development of the Bredasdorp Basin.

1.1.4 Literature review

According to Shanmugan and Moiola (1985), submarine fans constitute major hydrocarbon reservoirs on a world wide scale. There are three major controls on the nature of submarine fans; sediment type and their supply, tectonic settings and sea level changes Stow et al.,(1985) and Stow (1985). These controls aid in determining the potential of a reservoir. The most common sediment is terrigenous materials Stow et al., 1985. Grain sizes of sediments and distance of transport affects the geometry of the deposit, these along with the volume and the rate at which sediments reach the area for deposition also plays key roles Stow et al., (1985). The number of entry points of sediment supply determines whether single, multiple or overlapping fans will develop. Source rock types determine the composition, particle sizes, ability to be eroded and end products of submarine fans. The climate and vegetation in the source area determines the weathering processes and mode of transportation Stow et al., (1985). Relief and tectonic activity would influence the rate of sediments transport, for instance shown in (fig 1.02) sediments travelling down a submarine canyon would be faster than sediments travelling over a plain.

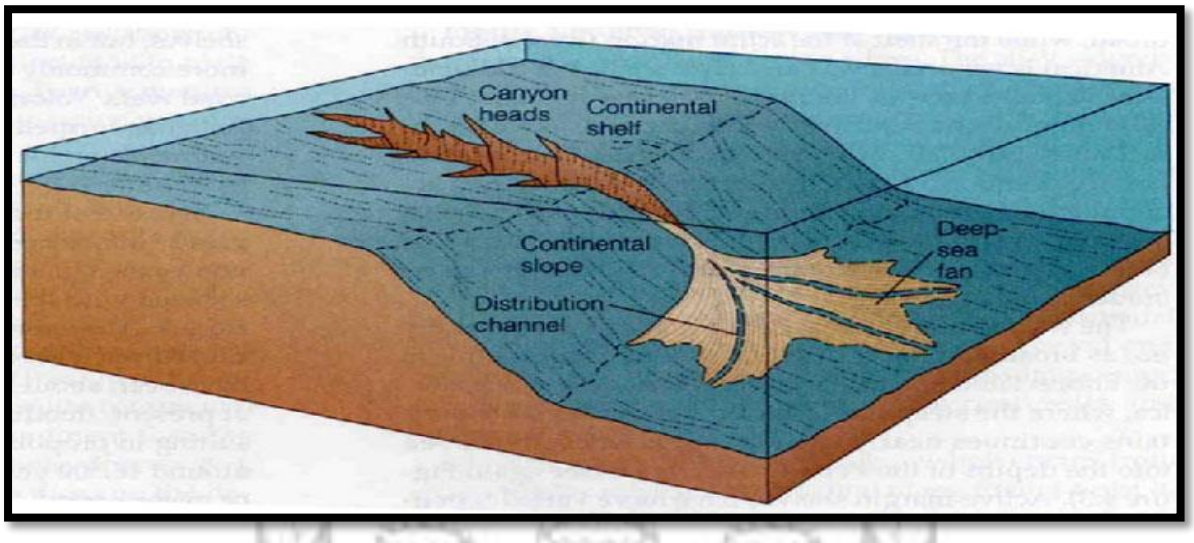

Figure 1.2 Diagram showing transportation of sediments faster down a submarine canyon. Source: http://blogs.denison.edu/geosciences/2012/04/27/the-erosive-and-depositional-poperties-of-turbidty-currents/

Marine conditions would affect the biogenic and organic carbon supply depending on currents such as coriolis force, water temperature and upwelling Stow et al., (1985). Coriolis force is the deflection of a water body towards the left (in the Southern hemisphere) affected by the Earth's rotation Kearey (1996). Deep water fans can develop as a result of major tectonic activity such as the rifting of margins Stow et al., (1985). These activities affect uplift and denudation rates, drainage patterns, and sediment supply and relative sea-level changes. The rate of tectonic uplift and subsidence are secondary factors controlling submarine fan development.

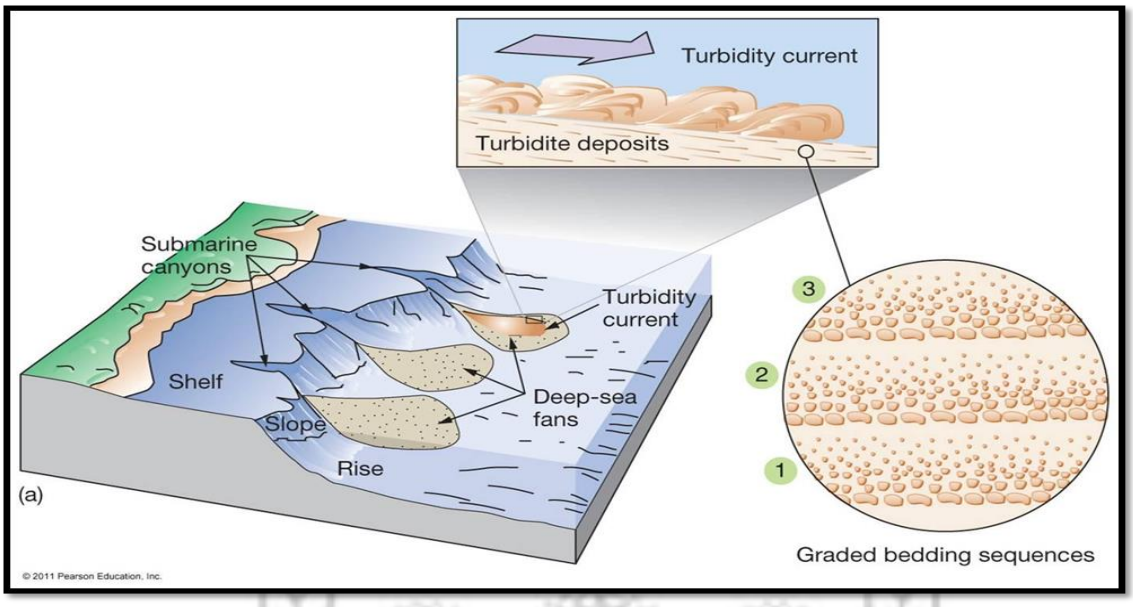

Figure 1.3 Diagram showing deep-sea fans formed as a result of submarine canyon, (http://www.studyblue.com/notes/note/n/planet-earth-16-deep-ocean/deck/4681998).

The nature and frequency of tectonic activity in the source and transitional areas determines the rate and volume of transport by gravity flows deeper into the basin. Sediment gravity flows will thus be greater in volume (in an area marked by less frequent but high magnitude tectonic events) than an area which experiences more frequent activity at a lesser magnitude Stow et al., (1985). As in the case of the Bredasdorp sub-basin, having greater magnitude of earthquakes during rifting (due to stress release), larger slumps during failure developed large debris flow and turbidity currents. According to Amy et al., (2005) physical experiment has shown that turbidite bed geometries are spatially extensive deposits with tapered margins. These high density (built up over a long period of time) turbidity currents carrying along with it different grained size particles were gradually particle begins settling out of the turbulent suspension Amy et al., (2005). Some turbidites may even contain debris flow deposits in large proportions which often occur in conjunction with forced removal from the transition zone during tectonic activity Amy et al., (2005). Changes in sea level have effects on near shore areas as well as deep sea regions with regard to sedimentation. Submarine fans are mostly active during periods of low sea level Stow et al., (1985). This is a result of the direct access of rivers (as a result of low sea level exposure) which feed deeper areas. These controlling factors merely contribute to the

development of reservoirs in deep marine conditions. Basic requisites for the accumulation of hydrocarbons in near shore and deep marine conditions are relatively similar Wilde et al., (1985). Source rocks should have an abundance of suitable thermal maturation levels for generation and be connected to reservoir beds Wilde et al., (1985). The reservoir rocks require adequate porosity and permeability in the form of a network for petroleum migration Karmaker et al., (2003). Matthews and Ridgway (1996) eloquently state that the void space within a porous solid can be regarded as a network of void volumes (pores) connected by a network of smaller void channels (throats). A study of the main controls on reservoir quality for sandstones Hamel and Thom (2001) would be porosity and permeability. Adequate trapping mechanisms are required for petroleum accumulation. Two types of traps are recognised; structural and stratigraphic traps. The Bredasdorp sub-basin has a structural trap characteristic mirroring fault planes which trap hydrocarbons and seal them in. The sealing of accumulated hydrocarbons is vital in determining the extent of the reserves which also determines its commercial viability Wilde et al., (1985).

1.1.5 Diagenesis

The process of hydrocarbon generation to maturation occurs in conjunction with a vital process of sediment evolution known as diagenesis. Diagenesis involves all low temperature and low pressure changes to sediments including lithification and delithification Press et al., (2004), Kearey, (1996). These processes aid in transforming sediments into sedimentary rocks Karmaker et al., (2003). Temperature and pressure realms of diagenesis are between near surface weathering conditions and metamorphism Boggs, (2001). Taylor et al., (2004) stated that diagenetic processes are controlled by and dependant on spatial and temporal patterns of sedimentary successions. Thus stages of diagenesis exists which occur at different levels of depth and time. These stages are shallow burial (Eodiagenesis), deep burial (Mesodiagenesis) and late stages diagenesis (Telodiagenesis) Boggs, (2001). Shallow burial is characterised by bioturbation, compaction with grain repacking and mineralogical evolution Boggs, (2001). Compaction of sediments is minor at this stage due to the shallow burial depth. Compaction is a mechanical process causing volume reduction and promoting pore fluid expulsion thus decreasing the pore volume of the rock Kearey, (1996). Mineralogical changes are, minerals precipitated out of solution (pore fluids at this stage)

Boggs, (2001). In reducing conditions particularly in marine environments, the precipitation of pyrite occurs at this stage as a cement or replacement mineral through pyritization Keary, (1996). Many other minerals and cements are formed such as clays, carbonate cements, quartz and feldspar overgrowths and glauconite. Glauconite forms at the sediment water interface Rasmussen, (2005)., Pasqini et al., (2004), ideally under conditions of slow sedimentation, Weaver and Pollard, (1975), agitated saline water with reducing conditions thus forms quite early during burial. Glauconite occurs in two forms as minerals pellets containing iron-rich clays and as the authigenic recrystallized form Weaver and Pollard, (1975), Pasquini et al., (2004). Most cements are allogenic (precipitated during or shortly after deposition) at this stage. Quartz carbonates and calcites are precipitated during burial. The presence of clays would inhibit quartz cementation Storvoll et al., (2002) and enhance the dissolution of quartz Renard et al., (1997), when in contact with each other.

Clay is precipitated from solutions containing potassium and silicates sourced from K-feldspar. Chlorite, kaolinite and Smectite precipitate at relatively low temperatures of about 25^{o}C and thus form early in the diagenetic process. Illite requires a higher temperature of about 100^{o}C threshold for precipitation McHardy et al., (1982). Deep burial involves mechanical and chemical compaction. Mechanical compaction is the physical aspect whereby the weight of the overlying deposited sediments causes load pressure forcing grains to become more tightly packed together. This would reduce the primary porosity of that layer. As grain boundaries move closer together, their contacts become soluble Boggs, (2001). Grains then become partially dissolved at the contacts by a process known as pressure solution Kearey, (1996), Boggs, (2001) or chemical compaction. This process further reduces porosity Boggs, (2001) and forms sutured contacts between grains with the principle stress being perpendicular to the length of the sutured grain Kuntcheva et al., (2006). Dissolution of minerals such as feldspar during pressure solution is as a result of contact with under saturated pore fluids Wilkinson et al., (2001).

The sites of feldspar and carbonate dissolution are economically important as they generate secondary porosity. Gier and Johns, (2005). On the other hand, as more elements are dissolved from framework grains inevitable precipitation would form authigenic minerals by cementation. The cementation intern reduces the porosity available for hydrocarbon migration and accumulation. Haszeldine et al., (2003). This cycle of dissolution and

precipitation is aided by heat from brine solutions which flow into the basin Lee et al., (2005) and fill up the pores. Thus diagenesis forms the restructuring of pore networks by these processes Karmakar et al., (2003). These secondary pore networks can either remain intact to become a net contribution to total rock porosity Wilkinson et al., (2001) or they could be filled by authigenic clays and other cementing materials. As the sandstone becomes more deeply buried, the Illitization of shallow authigenic and detrital clays becomes prominent. These clays fill pores and aid in reducing porosity. Late stage diagenesis begins once deeply buried rocks experiences uplift Boggs, (2001). The rocks thus experience lower temperatures and pressures along with oxygen-rich meteoric water having low salinities. Thus the mineralogical framework is altered by continued dissolution of cements and framework minerals. Grain replacement reactions of feldspar by clays prevail. In certain cases kaolinite could replace feldspar after dissolution Gier and Johns, (2005). Precipitation of new cements occurs. These processes continue along with chemical weathering due to uplift Boggs, (2001).

1.1.6 Methodology

In this section, the lists of available data within the study area and outlines the various methods employed to characterize the reservoir zones. The flow chart (Fig 2.0) below illustrates the steps taken in carrying out this research. The method starts with the review of previous studies and literature search in analogous oil and gas fields. The data collection section has the list of data collected from the Petroleum Agency SA, which is used in this study. They are carefully arranged, and prepared for easy access (Data Development). Well log correlation and delineation of reservoir sand units together with reservoir studies using Interactive petrophysics (IP) software characterize the reservoir quality and possible pays and other softwares like Excel, Ms Word and Surfer for digitizing.

1.1.7 Previous work

Given the nature of this research, this section begins with an overview of several significant geological, stratigraphic and structural characteristics as well as the hydrocarbon potential of reservoir rocks studies conducted on the Bredasdorp Basin and associated formations

from surface exposures and through subsurface studies. The Bredasdorp Basin is characterized by deep marine sedimentation. Sedimentary processes such as bulk emplacement, debris flow, turbidity current and slumping have put together its sequence and reservoir geometry. Accumulation of terriginous materials (land derived) on the continental slope and continental rise are deposited into the deep sea by slumping (movement of sediment piles as a mass) or by turbidity currents which is the rapid movement of large slurries (mixture of sediment and water) down slope. Turbidity currents are driven by gravity and can move far into the sea. Sediment deposition is accelerated by sea-level falls during which the coast is at the shelf break causing rivers to empty sediment directly on the slope. According to Turner (2000), the sea-level fall during early Aptian and mid-Albian, resulted in material eroded from pre-existing highstand shelf sandstones and transported into the central basin by turbidity currents from the west-southwest flank. He also pointed out that sandstone reservoirs in the Bredasdorp Basin consist of stacked and amalgamated channels and lobes. Fan lobes have a coarsening-upward pattern, whereas channelised reservoirs are fining upward. By using core, well log and dip data, it is concluded that the massive, amalgamated deep-marine sandstones, which make up the larger part of the E-BD reservoir, represent extensive mass-flow deposits. Additionally, the distribution of these deposits has been controlled by a significant erosional feature on a regional unconformity, which basically represented a major easterly-trending valley on basin floor. It is analogous to a submarine canyon extending through the E-BD area and acting as a conduit for sand sourced from the shelf to the west. The Oribi and Oryx oil fields; both being reservoir accumulations within the same turbidite system in the Cretaceous drift succession of the Bredasdorp Basin. Based on the seismic recognition of multiple unconformities within the drift successions, stratigraphic naming reflects a sequence stratigraphic approach. According to Brown et al, (1996); sequences defined by significant unconformities recognized on seismic sections, were assigned numbers (1 to 22). Third and higher order sequences; composite sequences and sequence sets recognized subsequently were designated by letters (A, B, C etc). Unconformities are designated by the sequence overlying them (1A, 4B etc) and by their nature chart, (Petroleum Agency SA, brochure, 2004/05). Turner *et al*., (2000) focusing on sequences 13A and 14A addressed the fact that reservoirs in the Bredasdorp Basin principally within Block 9 generally consist of stacked, deep-marine channel/lobe sandstones of Aptian age. The work had the objective of predicting and

delineating additional hydrocarbon reservoirs, based on geological modelling of the Aptian and Albian sequences within Block 9. Generally, for an overview of natural gas resources and petroleum exploration offshore South Africa, the reader is directed to the Petroleum Agency SA brochure (2003/4/5), McLachlan, *et al.* (2000) and Wood (1995). These studies have helped to provide information for improved understanding of the stratigraphic architecture and geological development utilized for the present research.

1.1.8 Equipment/material used

The following tools/material were used to obtain and load data in to a computer; Canon digital camera, Measuring tape, Hand lens, Water, Note book, pen and pencil, Software (Ms word, Excel, Surfer, Interactive Petrophysics (IP). Below is the flow chat illustrating the rout taken for this research;

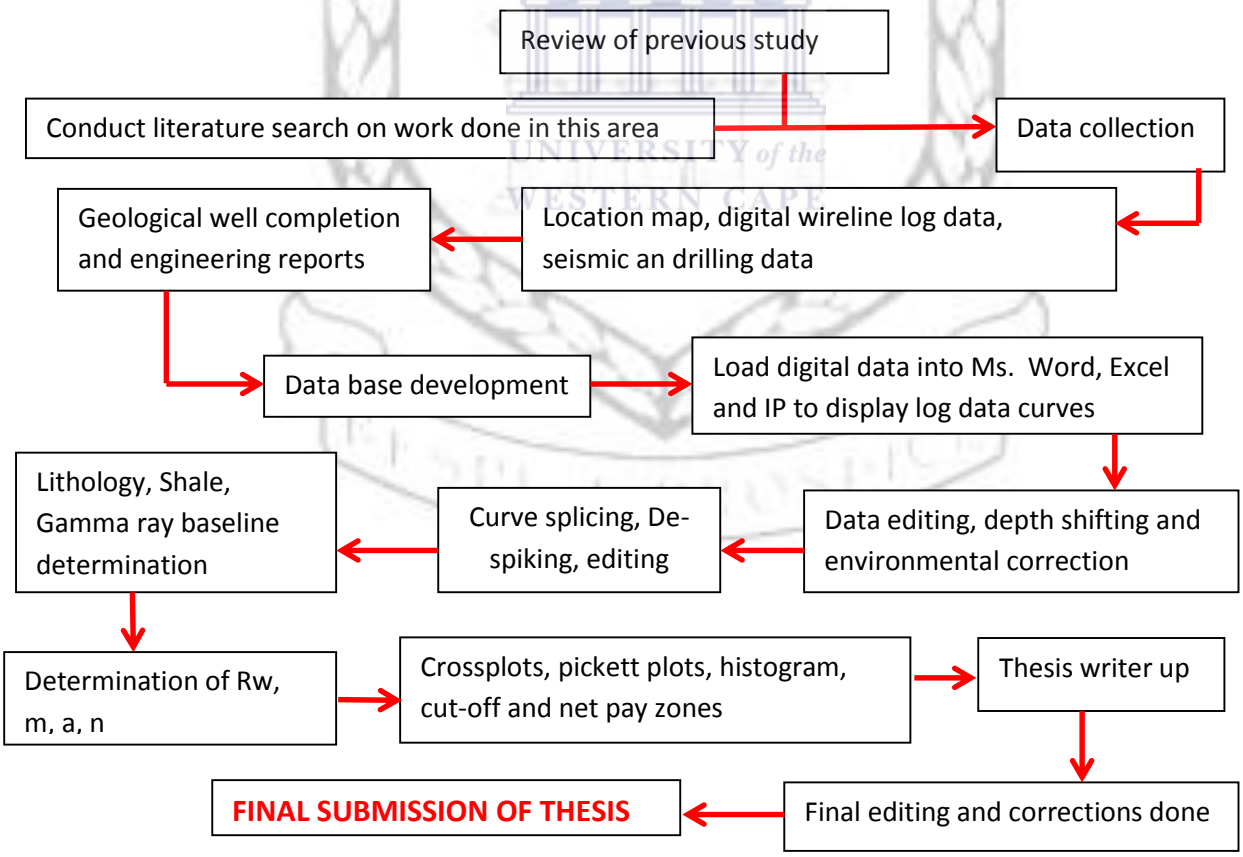

Figure 1.4 Flow chat diagram of methodology.

2 CHAPTER

2.1 REGIONAL GEOLOGY

2.2 Pre-rift geology

Cape Supergroup sandstone and shales were deposited on the southern perimeter of the Kaapvaal Craton during the late Palaeozoic and were overlaid in the present day onshore regions by sedimentary rocks of the Karoo Supergroup (table: 2.1). These rocks were deposited in a retro-arc foreland basin (McLachlan and McMillan, 1979; Johnson, 1990). Deposits of the Cape Supergroup are Table Mountain series Metasandstones. There is no evidence that Witteberg series rock were present across the area. Their absence, and that of Karoo rocks, may reflect non-deposition (Biddle et al., 1986) or erosion (Rowsell and De Swardt, (1976); Cole, (1992). There is evidence that these rocks indeed extend further south at the Southern African continental shelf. Deposits of Devonian age, possibly equivalent to Bokkeveld Group rocks, comprises of the basement of the Falkland Island (Lawrence and Johnson, 1995). Banks et al. (1976) show that sediments equivalent to Lower Ecca beds of the Karoo Supergroup are present in the Falklands showing that at least some earliest Karoo rocks were present south of the Cape Fold Belt mountains. Indeed, Lawrence and Johnson (1995) show that some of these possess source potential.

Rowsell and De Swardt (1976) shows that burial of pre-Karoo rocks to a depth of several thousand meters is necessary to account for the high maturity of the Bokkeveld series rocks both onshore and offshore. Indeed, Bokkeveld series slates, intersected in two offshore wells, have vitrinite reflectances commensurate of burial to 4000-6000 metres at moderate heat flow rate, whilst reflectance in the overlying Mesozoic deposits in those wells have maturity levels typical of <2000 metres of burial at similar heating rates. The maturation levels of the Bokkeveld rocks have been confirmed by fission tract analyses in the southern Cape (Brown et al., (1990); it may be that these Bokkeveld rocks represent the basal formations and that burial caused by the originally great thickness of Bokkeveld rocks about four kilometres (Theron, 1970) plus a small thickness of early Karoo rocks could have caused the evidence of deep burial. It is therefore considered that Karoo rocks, of at least early Karoo age, were originally present in southernmost South Africa and possibly even reached

as far as southern South Africa. During the Cape Orogeny (215-278Ma; Hälbich et al., 1983) which was largely coeval with Karoo sedimentation, Cape Supergroup (and possibly early Karoo Supergroup rocks) were folded and faulted to form the present-day WNW-ESE structural grain which now underlies all the offshore basins of Southern Africa (Hälbich et al., op cit., 1983). The orogeny is considered to have commenced when the Gondwana landmass started to override the Pacific plate producing oblique subduction (Dingle et al., 1983). A recent plate reconstruction of Western Gondwana records this disposition just after this event (Lawver et al., 1992).

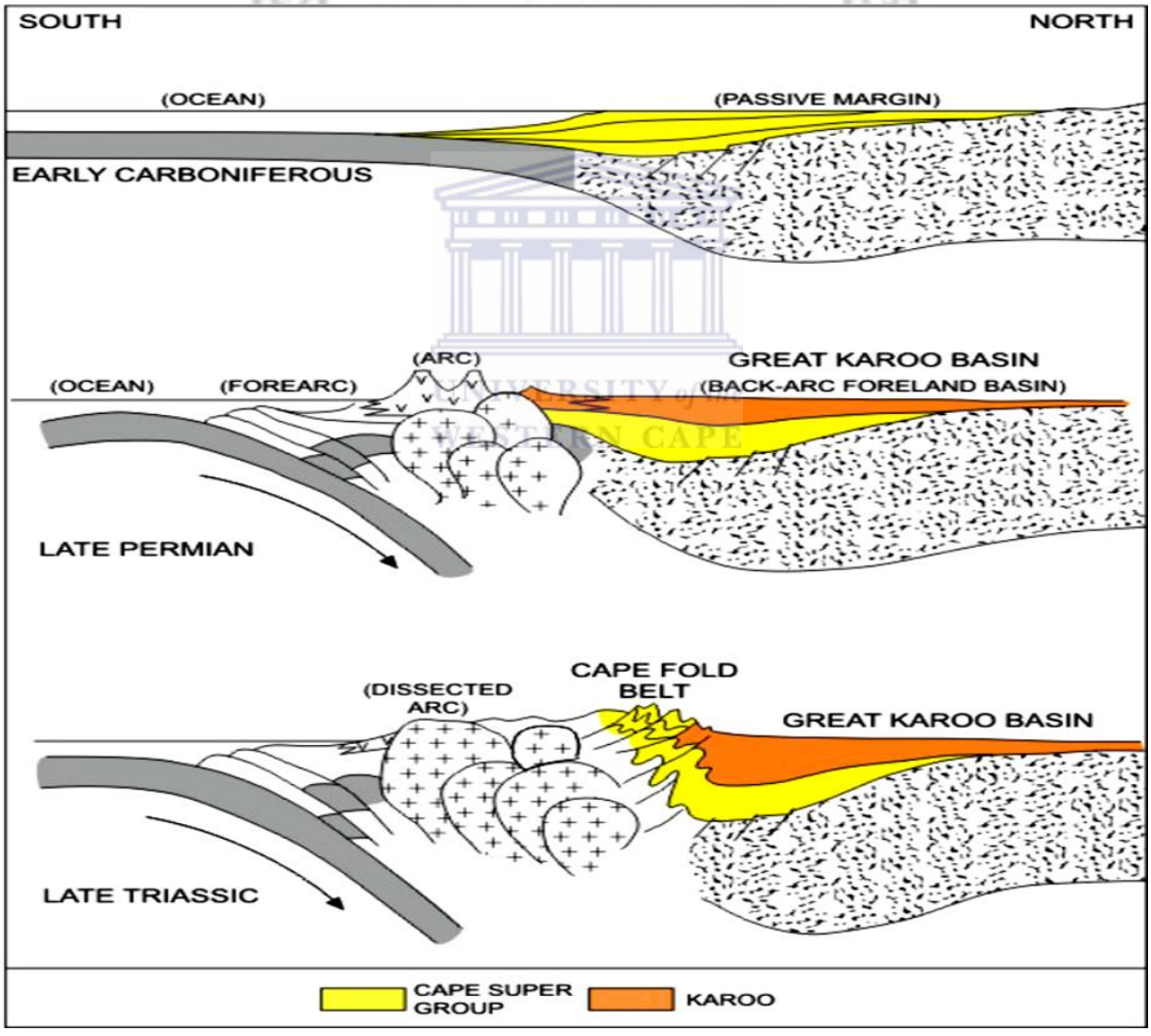

Figure 2.1 Evolution of Cape Fold Belt source; (Petroleum Agency SA, 2003).

MEGA-SEQUENCES	FORMATION NAME	ENVIRONMENT	LITHOLOGY	PERIOD	AGE
KAROO SUPER GROUP	Stormberg Series	Continental - shallow marine	extrussive with some sandstone	Late Triassic and Early Jurassic	~180-230Ma
	Beaufort Series	Fluvial-transitional marine	Siltstone and occ. shales	Late Permian and Triassi	~230-255Ma
	Ecca Series	Two upward-coarsening deep-marine megacycles	Claystone with occ. coals	Permian	255-270Ma
	Dwyka Tilite	Glacio-marine	Tillites and claystones	Carboniferous	278~290Ma
CAPESUPERGROUP	Witteberg Series	Shallow marine and transitional	Shoreface sandstone and siltstones	Late Devonian-Early Carboniferous	~320-390Ma
	Bokkeveld Series	Deep marine	Turbidity claystones and sandstones	Devonian and late Silurian	~390-410Ma
	Table mountain Series	Continental and nearshore	Sandstones and acc. Claystones	Ordovician	410-500Ma
BASEMENT	Cape Granite & Metasediment	continental	Sandstones and arkoses	Cambrian and Pre-Cambrian	>500Ma

Table 2.1 Generalised chronostratigraphic, environmental and lithologic description of basement, Cape and Karoo Supergroup rocks in the Western Cape (after Wickens, 1987).

Subsequent to this early deformation, Gondwana started to fragment resulting in the development of the subsequent syn-rift and post-rift basins (Fig. 2.02). Dingle et al. (1983) and Biddle et al. (1986) show that the Magellanes Basin of South Argentina, based on its present day position West of the Falklands Islands and Falklands Island, was located South of the Agulhas bank prior to continental separation. The Falklands Islands and Falklands Plateau Basin were probably South-east of Port Elizabeth. The present day South Africa offshore is considered to comprise the Outeniqua Basin (Du Toit, 1976; Dingle et al., 1983), which is subdivided into five basins, separated by ridges of Palaeozoic metasediments (Dingle et al., 1983). The four inboard basins (Bredasdorp, Pletmos, Gamtoos and Algoa) arbitrarily extend to the 200 metre isobaths. The outboard deep water basin is the Southern Outeniqua Basin (Fig.1.1).

2.2.1 Syn-rift geology

It has been suggested that regional igneous events is a major cause of the break-up of the continents as a result of the increasingly focussed heat flow along mantle trends (Condie, 1989). There is support for this suggestion from the igneous events around Southern Africa/South America. An extensive igneous episode affected the eastern part of South Africa and adjacent plates and resulted in the extrusion of basaltic material forming the Drakensberg basalts and Lebombo igneous centres in Southern Africa and basaltic intrusions in the Trans Antarctic Mountains (Dingle et al., 1983; Dalziel et al., 1987) (Fig. 2.2). The age of this episode is reportedly between 162 Ma and 200 Ma (Dingle et as., 1983, although there is evidence that intermittent volcanism probably extended as late as 130 Ma. Indeed, Brown et al. (1990) record a period of uplift and unroofing episode formed the Etendeka formation volcanic of central Namibia and the Parana volcanic province of South America dated around 134±5 Ma (Milner, 1992). Igneous and extrusive basaltic material has also been found in Cretaceous sediments in several wells drilled in the Orange Basin (Gerrard and Smith, 1983; Erlank et al., 1990).

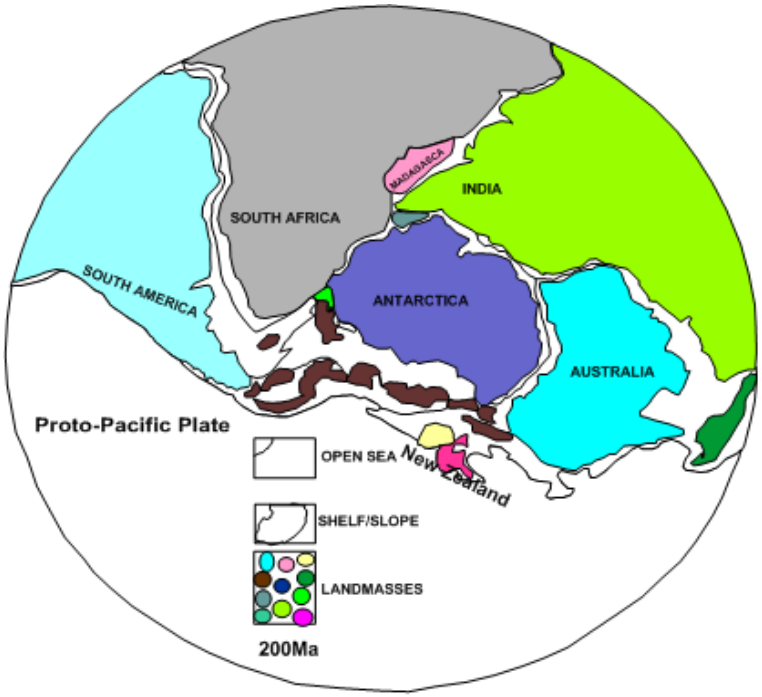

Figure 2.2 View of Gondwana plate reconstruction at 200Ma prior to the commencement of proto-pacific subduction (after Lawver et al., 1992).

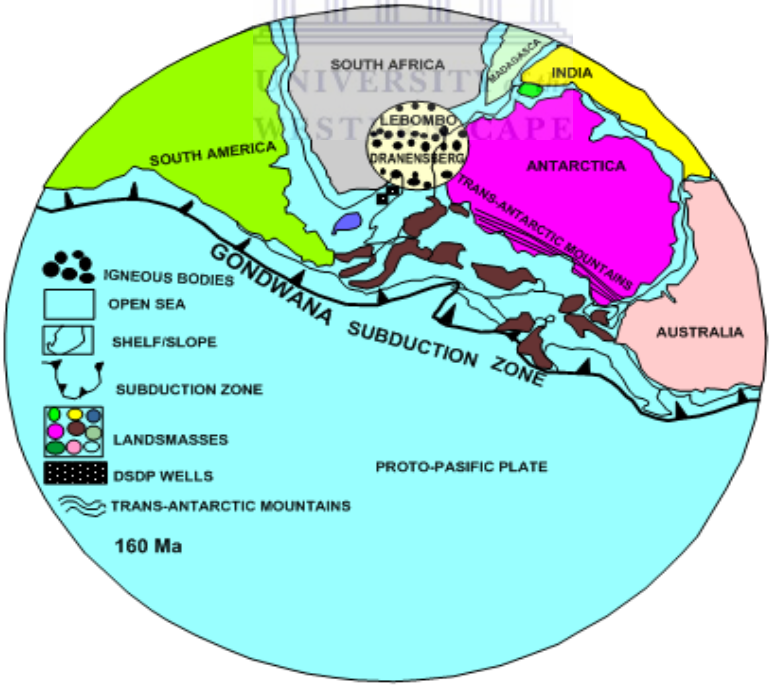

Figure 2.3 View of Gondwana plate reconstruction at 160Ma (after Lawver et al., 1992). Proto-Pacific plate subduction started at 180-190Ma.

The date of the earliest break-up of Gondwana, based on the volcanic evidence from eastern South Africa is therefore taken to be approximately 160±30 Ma, whilst in the Western part of South Africa it is approximately 150±15 Ma. Rifting appears to have started earlier in the east than in the West. This conclusion agrees well with the proposed time of the first rifting events in the southern part of Africa based on the presence of mid-late Jurassic (possibly Oxfordian) rock in DSDP 327 AND 511 IN THE South Atlantic (Gilbert, 1977). It is considered that the Agulhas-Falkands fracture zone is characterised by ultramafic rocks which upwelled into the fracture zone (Talwani and Eldholm, 1973) and which cause the strong magnetic signature evident in the regional aeromagnetic survey (GETECH, 1992).

2.2.2 Sedimentary deposits

The earliest of the post-basement and pre-rift sediments were deposited in continental fluviatile, lacustrine and estuarine environments and comprise mainly red and green sandstones and shales. Rigassi and Dixon (1970) subdivided these rocks into three main units which they interpreted as Lower Cretaceous based on field evidence only:

1. Sundays River beds (marine to estuarine grey shales and clastics)
2. Marls and Wood beds (estuarine to lacustrine clastics and shales)
3. Enon conglomerates (fluviatile coarse red beds).

Du Toit (1976) also stated that both the Kirkwood Bridge Formation (previously called Marls and Wood Beds) and the Enon Formation were of Early Cretaceous age and both were overlain by the Sundays River Formation. The latter was subdivided into two units separated by a major unconformity, seismic horizon C. From microfaunal data, McLachlan and McMillan (1979) showed the Kirkwood Bridge and Enon Formations to be Late Jurassic in age and that Du Toit's seismic horizon B was in fact the Jurassic-Cretaceous boundary (dated to 131Ma by Haq et al., 1987). Later work (McMillan et al., in press) has shown that Du Toit's seismic horizon C (now named 1At1, Burden, 1992) is of Baleanginian age. During the earliest stages of the rifting, when the crust had just started to sag and prior to the development of the marine environment, lacustrine sediments might be expected to have developed due to ponding of rivers in the lowest areas. Where such sediments were

deposited in large lakes, source rocks could have formed. Such sediments have not only been encountered in a number of wells in the Algoa Basin (McLachlan and McMillan, 1979)

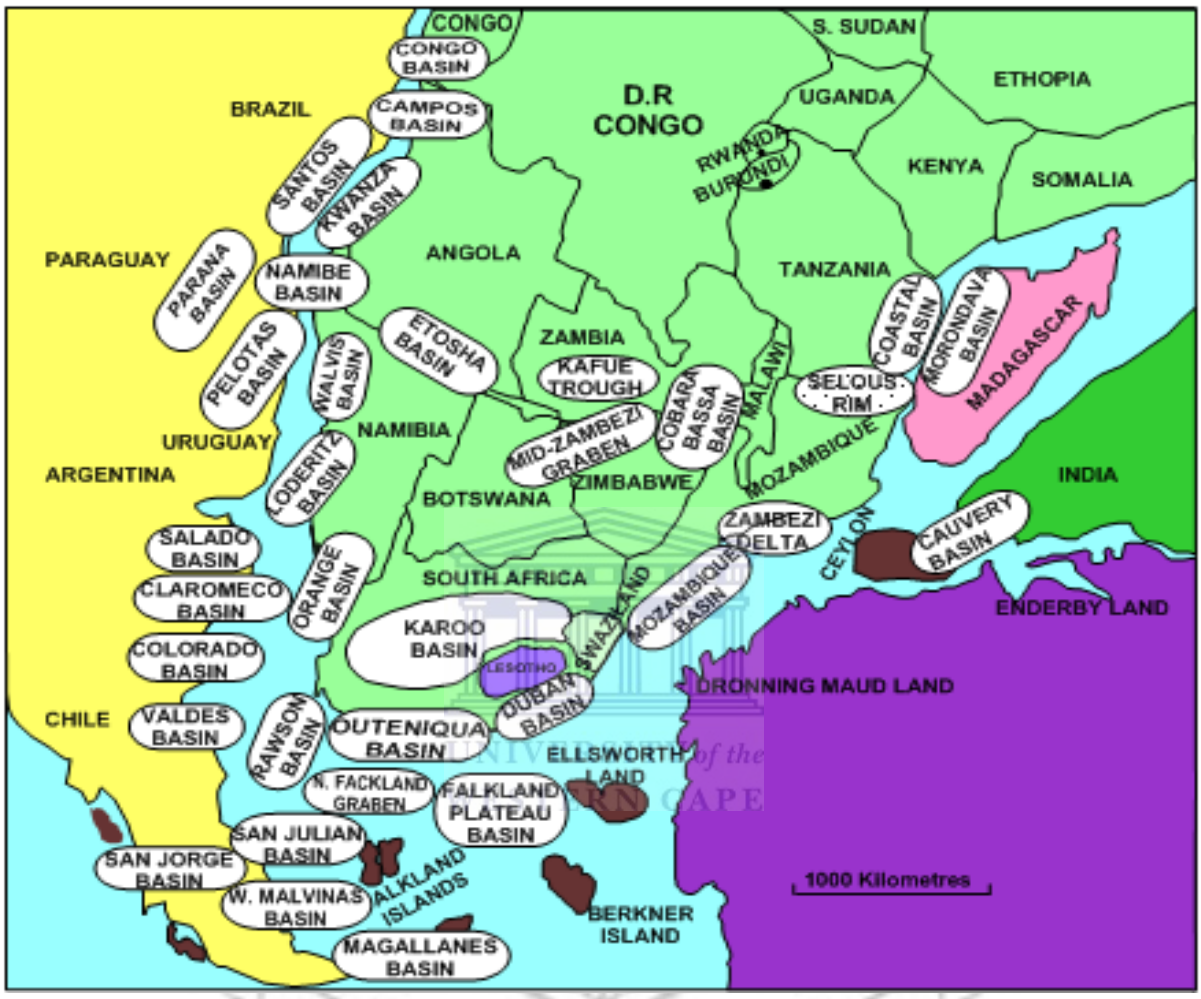

Figure 2.4 Regional map of plate reconstruction at ~ 121 Ma (after De Wit et al., 1988) showing the location of Mesozoic basins along the proto-coastlines.

also in the Bredasdorp Basin and in the onshore Haasvlakte Graben. In addition, since the Southern Outeniqua Basin contains great thicknesses of syn-rift sediments (Wenham et al., 1991), it is possible that a similar lithology could be present there. The best known example of such lacustrine source rock is the Colchester member of the Infanta Formation. This is locally well developed in the onshore Algoa Basin in the form of pyritic black shales intercalated with fluviatile and deltaic sands and silts (McLachlan and McMillan, (1979).

Ostracode datings show it to be Kimmeridgian-Portlandian in age (Valicenti and Stephens, 1984). As the separation of Gondwana continued, the marine transgression continued southwards along the eastern seaboard of Africa and into the more westerly basins, progressively overstepping the earlier continental sediments and heralded the drift onset unconformity. Late Jurassic marine source rocks deposited in a deep marine and match those in DSDP 511 and 330 on the Falkland Plateau (Barker et al., 1977a; Herbin et al., 1986; Davies et al., 1991).

2.2.3 Post-rift geology

More recent studies have addressed the post-rift geology because of the importance of that time interval to commercial exploration. As a result of these studies, the classification table of Du Toit (1976) has been found to be inadequate and a more correct chronostratigraphic table was constructed. This table is used exclusively hereafter. The drift onset unconformity has been determined from astracode, foram and palynologic data to be at ~126Ma in the Bredasdorp Basin (Valicenti and Broad, 1994). The oldest rocks overlying horizon 1At1 are deep marine shales of the Upper Sundays River Formation. These shales have occasional interbeds of basin floor turbiditic and fan sandstone, deposited following the major sea level rise during the Valanginian which was due in part to post-rift thermal subsidence.

They overlap a basin-wide veneer of transgressive coastal sandstone considered equivalent to the lower part of sequence LZB 2.1 Haq et al., (1987). The base of the shales is marked by a characteristic angular unconformity mapped as seismic horizon 1At1. Seismically this is characterised by a surface of downlap onto impedance contrast. The regional extent of this seismic evidence suggests the shales have a basin-wide distribution. The location of this shale immediately above extensive shallow marine sandstones, where there is no evidence either lithologically or seismically of intervening transgressive sediments shows that the basin subsided rapidly (McMillan et al., 1997).

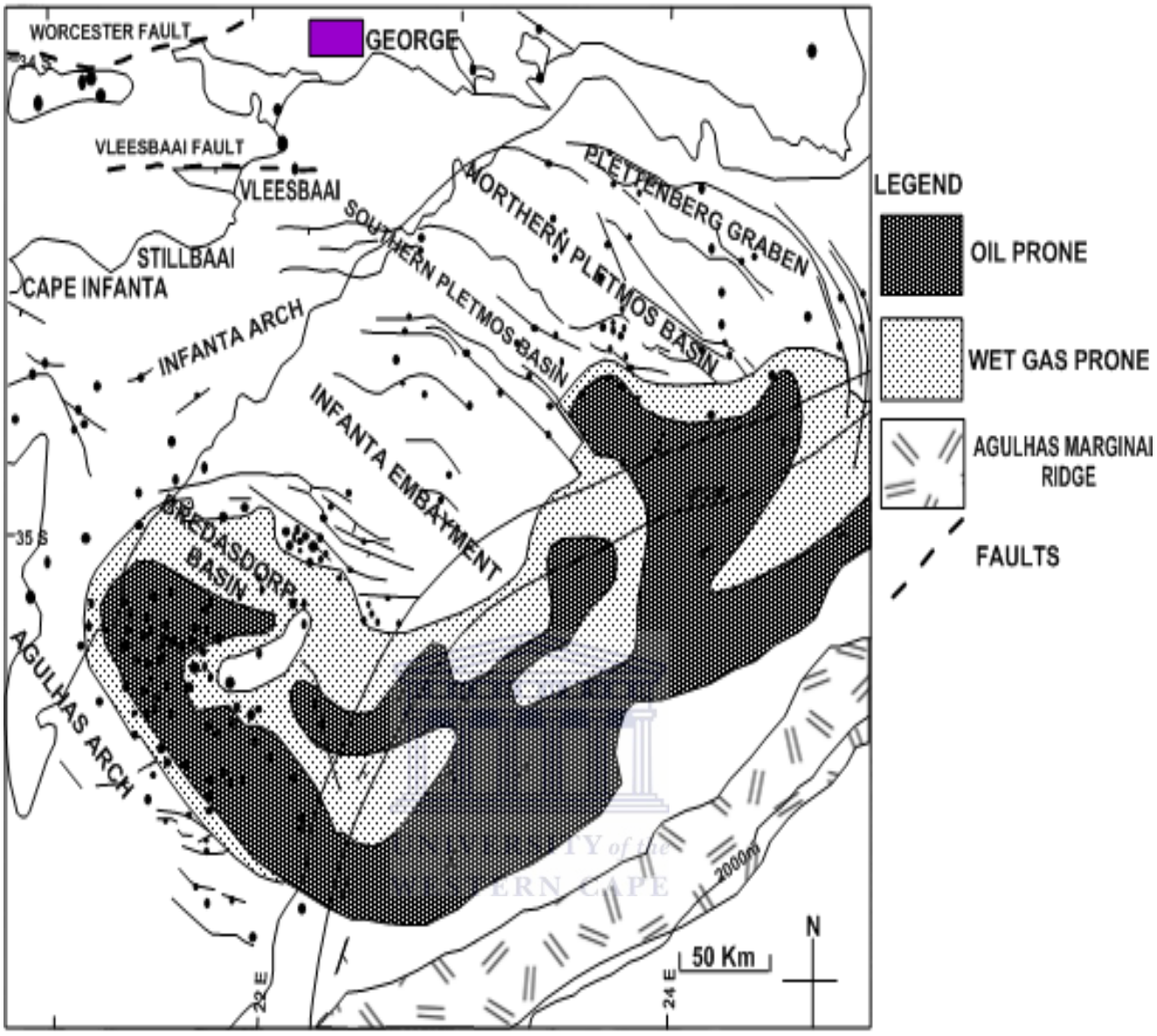

Figure 2.5 Map of wells drilled to date in the Western part of the Outeniqua Basin. This locates the Bradesdorp Basin, Southern Outeniqua Basin, Western Pletmos and Infanta embayment, the onshore Haasvlakte Graben and major onshore and offshore faults Broad and Turner (1982), and unpublished SOEKOR data.

Du Toit (1976)						Van Wyk et al. (1994)	
Chrono Stratigraphy	Formation	Member	Seismic Horizon	Sequence	Rift Drift Phase	Sequence Boundaries	Age
Tertiary	Alexandria				DRIFT	22At1	Tertiary
Upper Cretaceous	Agulhas			Agulhas			Cretaceous
Lower Cretaceous	Sundays River	SR-4.5	A	Upper Sundays River		13At1	
		SR-3					
		SR-2	C	Lower Sundays River	RIFT	1At1	
		SR-1					
	Kirlowood		B	Pre-Sundays River		B	Jurasic
	Infanta	Colchester					
		Swartkops					
	Enon		D			D	
Palaeozoic and Older					SYN & PRE-RIFT		Palaeozoic and Older

Table 2.2 Classification of Mesozoic and Tertiary sediments (and their bounding horizons) after Du Toit (1976) compared to the recent biostratigraphically and seismically characterised sequence stratigraphic boundaries. Modern sequence stratigraphic and tectonic subdivisions are now used in preference to this less practical classification.

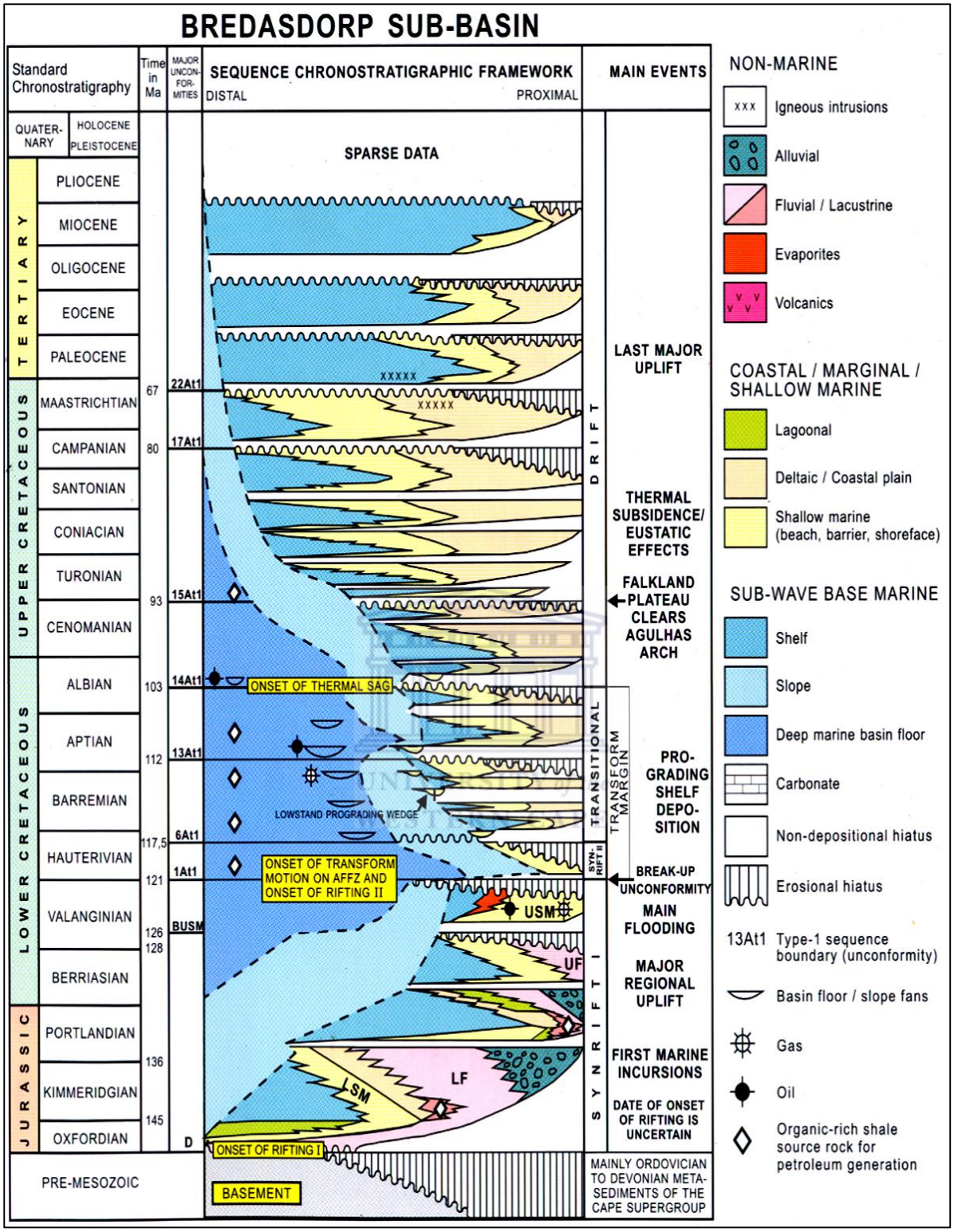

Table 2.3 Chronostratigraphic column of the Mesozoic and Tertiary strata in the Bredasdorp Basin (after Dingle et al., 1983; Burden, 1992 and McMillan et al., in press). The sequence of events and the stratigraphy are generally applicable for the greater southern African region and the Mesozoic part of the succession in the DSDP wells in the Falklands Plateau Basin.

During the Hauterivian, a second major tectonic episode resulted in rejuvenation of many of the earlier horst and graben features (Jungslager, 1996). This episode probably resulted from transgression during early movement alone the Agulhas-Falklands fracture zone (AFFZ). Coevally, a tectonically-enhanced sea level fall resulted in a major regression in the Bredasdorp Basin, mapped as seismic horizon 5At1. Deep marine rocks of the ensuing 5A sequence have not been intersected to data owing to their great depth of burial. They are only likely to be found in the centre of the basin and are largely infill. No evidence of progradation or aggradation is recorded from seismic or drilling data to date (Jungslager, 1996). However remnant shelf rocks have been intersected in boreholes around the basin edge. Further regional sag occurred after Hauterivian times and the transgression brought the coastline close its present day location. Marine sedimentation dominated up to the present, but owing to the closeness of the Falkland Islands Plateau which was a positive feature, circulation was restricted during Early to Mid-Cretaceous. During this period, the seafloor (and probably much of the water column) was intermittently depleted of oxygen, perhaps because of short periods of restriction, resulting in the development of dysoxic conditions which promoted the better preservation of organic material.

These organic-rich intervals have source potential for gas and oil. Oceanic circulation improved after the rift had opened further and open marine conditions extended around the southern tip of Africa joining the incipient North Atlantic rift during the Mid-Cretaceous (Zimmerman et al., 1987). Evidence for this is that Early Aptian marine conditions extend up the west coast of Africa, at least as far as the Kudu wells (Wickens and McLachlan, 1990; Benson 1990). The presences of thick Aptian salt deposits in Angola Basin formed by the occasional overtopping of the Walvis Ridge during the high stands, demonstrate that the transgression was regionally extensive. Four of these spill-over events are demonstrated to have occurred in the Angola Basin (Schlumberger, 1991a). Several sea level adjustments during the Cretaceous resulted in widespread erosive events mapped regionally (partly because of their down lapping relationship with underlying reflectors) as type 1 unconformities (Vail et al., 1977). These occurred notably during the Aptian (13At1), Albian (14At1), Turonian (15At1) and at the Cretaceous-Tertiary boundary (22At1). Post-Hauterivian, active progradation can be seen on seismic records to continue up to the Cretaceous-Tertiary boundary. Above this, the sedimentation appears largely aggradational

although seismic data near the sea-floor are badly affected by noise multiples. The biostratigraphic definition of several of these hiatuses has been discussed by McMillan, (1990). He addressed the susceptibility of the benthic and pelagic fauna to changes in water depth and commented on the environmental implications of the faunal changes across the boundary, pointing out that most of these unconformities are relatively short duration. Deep marine sediments deposited immediately after many of the hiatuses during periods of transgression and early high stand sedimentation, are associated with sediments with elevated contents of organic carbon. Many of these intervals have source potential. The most widespread of these is found in Upper Barremian to Lower Aptian transgressive to high stand sediments in the 13A sequence. Cretaceous rocks can be separated into four units based on the oxygen level in the water:

(a) 1A-4A rocks tend to be dominated by relatively low levels of oxygen
(b) 5A-12A rocks tend to be generally oxidising although in some areas oxygen levels are lower
(c) 13A rocks which were deposited under low oxygen (dysoxic-anoxic) conditions and
(d) Post-13A rocks which, with one exception in the Turanian, were deposited in oxygen-rich water.

The exception is found in the Turanian 15A sequence which is dominated by a sediment-starved environment in which organic-rich claystones are found (McMillan, 1990). The clasystones are considered to be equivalent to the Turonian source rocks accumulated in the Tethyan region and thought to represent a regional oceanic anoxic event, possibly related to the final opening of the Atlantic (Schlanger et al., 1987). Arthur et al (1987) show that this was a short-lived period of intense organic carbon burial coinciding with a maximum sea level high stand when strong upwelling enhanced the surface productivity. This high stand is believed to be due to higher global temperatures which reduced ice caps to a minimum and which led to greater precipitation and higher surface runoff. This would in turn lead to larger quantities of fresh water entering the marine environment resulting in density stratification in deep basins and an increase in deep marine salinity and anoxicity. These conditions have been noted in Angola and Nigeria as probably being responsible for the presence of source rocks and oils with dominant biomarkers which are characteristic of hypersaline conditions (Burwood et al., 1990; Ekweozor and Telnaes, 1990). More locally,

there is micro-faunal evidence of uplift of the western South African offshore and downwrap of the eastern area (McMillan, 1990; McMillan et al., 1997). Above these Turonian source rock, a thick package of Mid-Late Cretaceous claystones and siltstones prograded across the basin from the west. These argillites are devoid of source potential, mainly because the dominantly oxygenated environment precluded preservation of aliphatic organic matter (Comford et al., 1983). The persistent influx of cold, oxygen-rich Antarctic bottom water is given as the main reason for the largely oxygenated sedimentary environment (Zimmerman et al., 1987).

2.2.4 Tertiary

The Tertiary sediments were deposited in a strongly oxidising environment in higher water temperatures and have low organic carbon contents. The sediments are calcite-rich, largely biogenic and occasionally form calcite layers. These are thought to be associated with winnowing current action resulting from the occasional warm water eddies which separate from the Agulhas current and sweep the shelf. The core of the Agulhas current (Fig 2.6) is at a temperature of 25-29^{0}C, i.e. 10-15^{0}C warmer than the water on the Atlantic side of South Africa, and >20^{0}C warmer than the bottom water in the Outeniqua Basin (Derbyshire, 1964). The current is considered to have been active at least since the Early to Mid-Tertiary (Winter and Martin, 1990; McMillan, 1986; McMillan, 1989) and to have influenced the near shore land temperatures (Frakes and Kemp, 1972). The core of the current generally flows near the surface along the shelf break although it occasionally deflects southwards or northwards impinging on the bottom water of the shelf.

Examples of this happening recently have been demonstrated from anchored current meter data (Gründlingh, 1984). During periods of northern hemisphere glaciation, though, it has been shown that the current swings southwards (Winter and Martin, 1990) so that the present day shelf and continental rise were no longer swept by the current. The Tertiary sedimentary history of the continental shelf of the south coast has been studied using shallow seismic profiles in conjunction with bottom dredged and gravity cored sample (Dingle, 1971) and occasional samples from offshore wells (McMillan, 1989). These data allowed for the subdivision of the Tertiary into three packages separated by major

unconformities during the Late Palaeocene, Eocene-Early Oligocene and Late Miocene-Pliocene. Tertiary sediments commonly have a large biogenic component and include phosphatic muds, chalks and chalk marls.

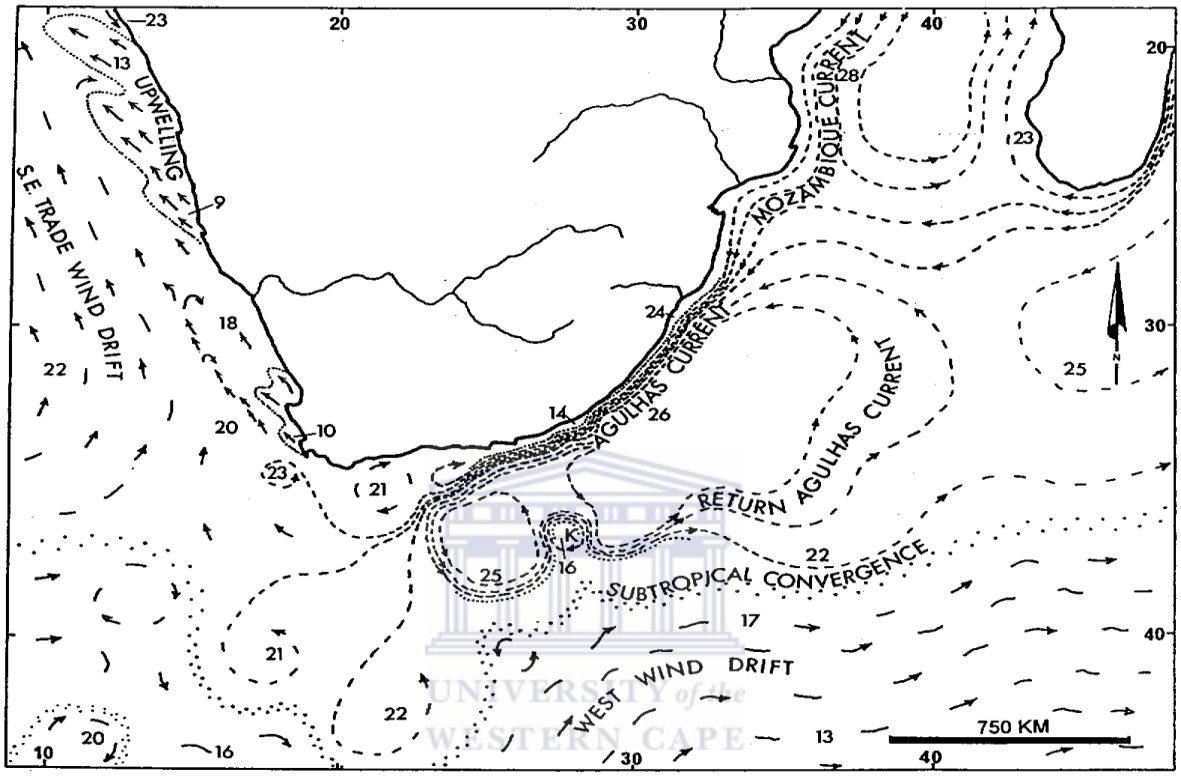

Figure 2.6 Oceanography of the Southern African region showing direction and temperature of Cape Agulhas currents modified from (Nasou, 1973).

McMillan (1989) confirmed the latter two of these unconformities and pointed out that no boreholes on the South African offshore had ever intersected deposits of Late Oligocene. This supports the conclusions of Vail et al., (1977) who showed that the Mid to Late Oligocene was a period of major world-wide sea level fall during which sedimentation probably continued, but only in the deepest parts of the basin. Unfortunately, the Late Tertiary is consistently thin an all the basins, and seismic sea bottom noise multiple mask evidence of possible erosion at this horizon. Micro-faunal studies (McMillan, 1996, pers comm.) have shown evidence of reworked Mid-Oligocene fauna indicating that there had been at least some erosion.

No sediments of Late Oligocene age were reported from the DSDP 361 well, although they were expected because the well is in a more distal location than oil exploration well drilled in the South African offshore to date. The incompleteness of the core record in the well (less than 10% of the upper 1000 metres was sampled) may be responsible for this absence. Lower Oligocene sediments have also been eroded from the Bredasdorp Basin, most severely in the proximal portions. Locally this planation extends down to the latest Eocene (McMillan, 1993; pers comm.). McMillan (1989) demonstrated that Upper Miocene, line-rich sediments have also been eroded leaving only the Lower Miocene. This surface forms a calcrete on which Late Pliocene, Early Pleistocene and Holocene fauna are preserved.

2.3 IGNEOUS BODIES, MANTLE SWELLS AND HOTSPOTS

2.3.1 Post-rift igneous bodies

Alkaline, locally under saturated, igneous bodies (Fig 2.7) have been found in two regions of the Bredasdorp Basin and in one region of the Orange Basin Gerrard and Smith, 1983 and unpublished SOEKOR data). In the Bredasdorp Basin, these areally extensive intrusives are readily detected from seismic data and a map of their distribution has been compiled. Similar igneous bodies are also found in a number of onshore locations (Duncan et al., 1978; Duncan, 1981). A number of samples of these igneous bodies, both onshore and offshore, have been subjected to isotopic age dating (K-Ar and Rb-Sr) as indicated.

Nepheline-syenite and aegirine-trachyte dykes and sills intruded the western Bredasdorp Basin in the area around well three during the Early Tertiary, drawn after Broad and Turner, (1982) and unpublished SOEKOR data; fig 2.7). Isotopic dating of sea floor and borehole samples of these intrusives provides dates ranging from 52-59 Ma (Dingle and Gentle, 1972; Rowsell et al., 1979). Coevally, calc-alkaline lamprophyric and possible carbonatitic dykes and sills intruded the eastern end of the basin (Rowsell et al., 1979) especially in the vicinity of well 8. Isotopic dating of these revealed ages ranging from 53-57 Ma (Eglington et al., 1990). Although from the descriptions they appear to differ chemically and petrologically, Rowsell et al., (1979) and Eglington et al., (1990) considered these intrusives to represent early and late fractions of the same magma which may be related

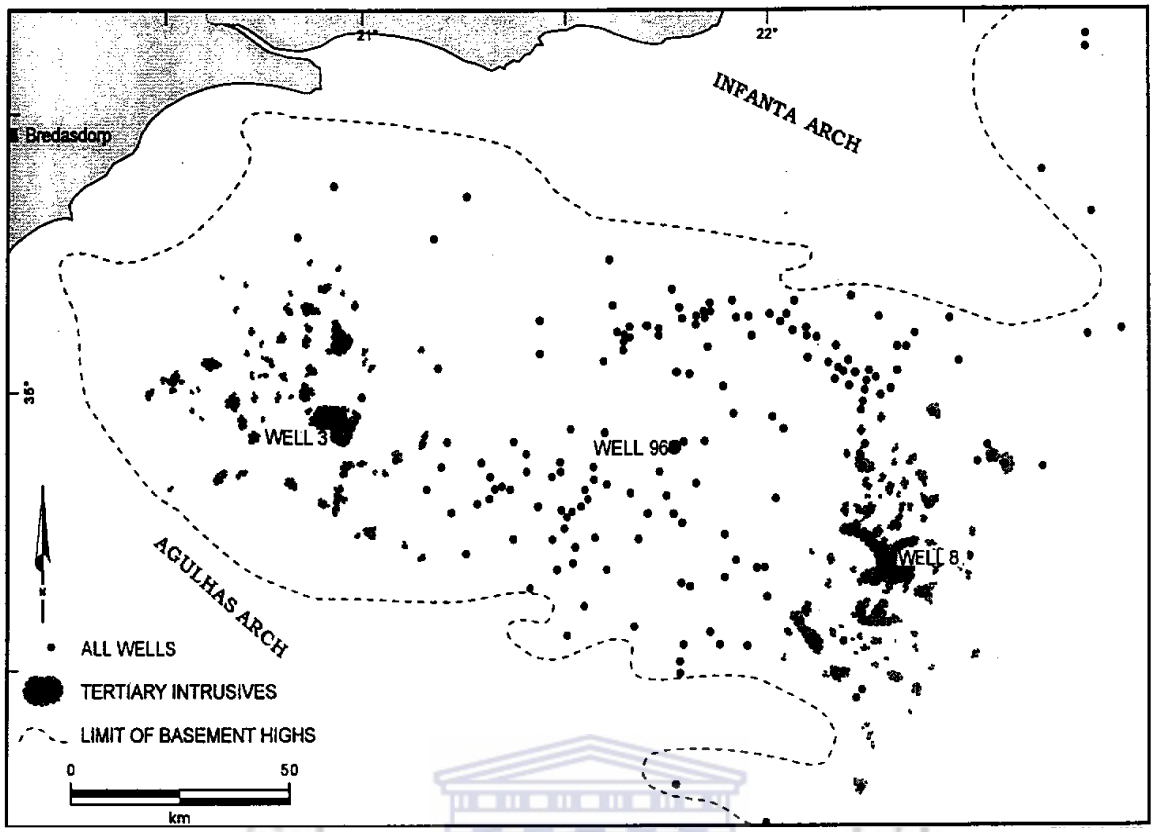

Figure 2.7 Map showing the distribution of igneous rocks in the Bredasdorp Basin (after Broad and Turner, (1982) modified using unpublished SOEKOR seismic and borehole data.

(Hatch et al., 1961, p. 373-379). Alternatively, the differences may result from biased sampling because the more basic intrusions are often severely altered, apparently by hydrothermal fluids. Examples of this were noted in well 8, (Marot, 1990, pers comm.). Some of the lamprophyre samples effervesce strongly in dilute acid and may represent carbonate intrusives, hydrothermally altered sediments or lamprophre (Rowsell et al., 1979). Trace element analysis of some sidewall core samples from these rocks record locally high contents of Rb, Y and Zr suggesting non-sedimentary origin (McCarthy, 1978) but do not could not help confirm whether they are original carbonatites or altered lampropyres.

Onshore, alkaline melitite-rich basalts plugs are reported from several locations in the south-western Cape and some of these have been dated as Latest Cretaceous and Early Tertiary (table 2.04 and references therein). The mililite basalts at Saltpeter Kop, in the southern Cape, which Duncan (1981) considers to be part of this igneous trend, are indeed

chemically similar to the intrusions in the western Bredasdorp Basin (Mclver and Ferguson, 1978; Duncan et al., 1978).

2.3.2 Mantle swells and Cretaceous –Tertiary hotspot

It has been suggested that these intrusions are associated with proposed mantle swells and the ensuing hotspot activity (Duncan, 1981; Hartnady and Le Roex, 1985). Mantle swells are considered to originate at the lower mantle boundary where periodic outbursts of excess heat initiate rising plumes from the mantle (white and McKenzie, 1989; Condie, 1989). These rising plumes of mantle material usually develop large heads up to 1000 km in diameter (Underhill and Partington, 1993) and can result in the transfer of large quantities of heat to the lithosphere where they form hotspots. Where these hotspots result in decompressive melting of localised buoyant up-wellings (De Paolo et al., 1996) they often take the form of regional lava extrusion.

With time the head dissipates leaving persistent plumes, which may be only a few hundred kilometres across but which continue to give rise to repeated outbursts of igneous activity in a series of loosely associated intrusive events. Since hotspots tend to be fixed relative to crustal motion, they leave distinct linear tracks of volcanic emanations which are especially noticeable in oceanic crust as bathymetric highs (Wright, 1973; Duncan, 1981; Morgan, 1983). Some hotspots leave a very narrow surface track because they have essentially no plume head. The hotspot considered to have formed the Hawaiian chain is of this type (Wright, 1973). It is also possible that the Bouvet/Shona hotspot is of this type. The African plate is unusual in being characterised by a large number of hotspots. Each has a surface expression of a volcanic centre.

The separation of the African and South American continents after initiation of the Agulhas-Falkland Fracture zone (AFFZ) transform motion resulted in the northward rotational movement of the African plate (Duncan, 1981; Lawver et al., 1992) about a pole located off north-west Africa, hence these hotspots racks are arcuate. Duncan (1981) suggested that one of these hotspots migrated pass the Bredasdorp Basin during the Late Cretaceous-Early Tertiary. There are also abrupt changes in the direction of the bathymetric tracks which may be a result of the impingement of the hotspot plume alternately on opposite sides of transform faults (Hartnady and Le Roex, 1985). In addition to this explanation, a change in

the pole of rotation also resulted in the tracks showing a matching change in direction at about 40 Ma, Duncan, (1981). The increments of motion of these hotspots indicate that the Bredasdorp Basin would have overlain the hotspot at ~70 Ma, i.e. there is a discrepancy between the date of transit of the hotspot and the dates of the intrusions. De Paolo et al., (1996) show that hotspot volcanoes tend to have an active lifetime of only about 1 Ma. It is considered likely that magma generated in the upper mantle could have taken 10-20 Ma to travel to the lithosphere (Condie, 1989; Underhill and Partington, 1993), hence ages of the near-surface bodies would be expected to have a range of 50 Ma. Many of the dated intrusives lie on a track from the Bouvet/Shona hotspot, which continues into the Bredasdorp Basin. This may extend to the kimberlite intrusions of the Norther Cape (Duncan, 1981; Hartnady and Le Roex, 1985).

The footprint of this track is relatively narrow, apparently about 200 km wide, typical of an ascending plume without plumehead (Wright, 1973). The present day position of the hotspot is shown by Duncan (1981) to be near Bouvet Island, althouth Hartnady and Le Roex (1985) suggest it may be closer to the probable Shona hotspot several hundred kilometres noth-west of Bouvet Island. Fission track analyses of two Late Cretaceous samples from well 96, located at least 50 km distant from the nearest intrusive either intersected or visualised seismically, are available for temperature study. These data record a heating event to 100^0C or more during the period 60± 5 Ma (Eurotrack, 1996). This high Palaeocene temperature may be due to a more regional heat input such as might arise during the hotspot transit. This needs to be tested by study of fission track data from other wells in the basin.

3 CHAPTER

3.1 Geology of Bredasdorp Basin

Among the 5 basins (Bredasdorp, Infanta, Pletmoos, Gamtos, Algoa) in the southern part of South Africa, Bredasdorp Basin is situated in the western part of the rift basins on the southern border of the African continent (fig 1.1). These basins together make up the greater Outeniqua basin. This basin is arbitrarily divided in two at the 200m isobaths. the inboard component is subdivided into four basins (Bredasdorp, Infanta, Pletmos, Gamtoos and Algoa) whilst the outboard component is the Southern Outeniqua Basin. The Bredasdorp Basin is underlain by metasedimentary rocks of the Palaeozoic Table Mountain and Bokkeveld Groups which also form the dividing highs e.g. the Agulhas and Infanta Arches. The geometry of the basin follows the grain of the underlying Cape Fold Belt (Fouché et al., 1992) raising the possibility that structural control is related to reactivation of earlier lines of weakness. To the east, the basin is separated from the western part of the Southern Outeniqua Basin by a moth-south lineation of early structural horsts (Roux, 1996). Much of the tectonism affecting the basin after formation is attributable to differential plate motion during the separation of Africa and South America, the transit of the Bouvet/Shona hotspot and the initiation of the African Super-swell.

3.1.1 Periods of tectonic adjustment

A phase of compression in the Mid-Jurassic, probably coincident with early separation of the Falklands Plate, affected all offshore basins (Van der Merwe and Fouché, 1992). It resulted in uplift and erosion of Palaeozoic metasediments, and extant Lower Mesozoic Karoo sedimentary rocks, (Rowsell and De Swardt, 1976). Later downwarp, associated with the initial southward propagation of the rift between East and West Gondwana along the East African seaboard, was initiated as early as Oxfordian based on palaeontological results (Barker et al., 1977a and 1977b). The second phase of compression, during the Hauterivian, possibly related to impact of the Falklands Plate on the south coast of Africa, coincided with a major uplift and erosive event resulting in an angular unconformity at horizon 5At1. The third phase of compression occurred shortly after deposition of the Albian 14A sequence (Van der Merwe and Fouché, 1992) and formed the central basin structural highs. This

phase of compression is probably related to the passage of the eastern end of the Falklands Plate past the Agulhas Arch. Subsequently the basin subsided again, probably when the Falkland Islands finally cleared the south tip of the Agulhas Arch (Honiball, 1995), and no further compressional events occurred.

The last major uplift of the Agulhas Arch started in Late Maastrichtian (McMillan, 1986) reaching a maximum of ~300 metres during the period 66-64 Ma, although the arch only became exposed during the Early Palaeocene (McMillan, 1986). This uplift, and associated erosion, was probably due to heat flux during passage of the Bouvet/Shona hotspot. A more detailed appraisal of the tectonic development of the basin is provided in McMillan et al., (1997). A major uplift of the western end of the basin, evident from seismic data, reaches a maximum in the D-block wells where Cenomanian deposits are at the sea floor (fig. 8 of Brink et all., 1991) indicating probable erosion of >1000 metres. This uplift is thought to have been the result of Mid-Oligocene tilting (McMillan, 1996, pers. comm.) but did not affect the central and eastern areas. Alternatively, the tilting may reflect initiation of the African Superswell (Hartnady and Partridge, 1995).

3.1.2 Faulting

Early rift-faulting during the period of formation of the Bredasdorp Basin resulted in a WNW-ESE parallel-sided graben with a number of marginal half-graben. This fault trend is most evident in the north and south flanks. At the same time, in the eastern part of the basin, on both north and south flanks, as well as in the eastern central basin, a series of structural highs developed (Fridinger, 1988; Roux, 1995; Pferdekämper, 1996, pers. comm.). These highs include all the eastern highs (wells 10,12,13,24 and 47) and the high immediately to the south-west (well 9,11, 14 and 17). The regional WNW-ESE fault trend is modified in the Bredasdorp Basin (and indeed in other south coast basins) by trending NW-SE at the western and eastern ends. All these similar fault trends are considered to be due to drag along the Agulhas-Falklands Fracture Zone (Du Toit, 1976; Fouché et al., 1992) or to inherited Cape Fold Belt fault (Cartwright, 1989) or possibly to tension gash style faulting (Cartwright, 1989; Malan et al., 1990).

Some of these faults are thought to have rejuvenated at 5At1 times (Late Hauterivian, ~118 Ma) as many extend to this surface. Details of these movements are given in (Jungslager, 1996). Some of the faults have been rejuvenated much later and extend to 9At1 (Hodges, 1996), probably representing a combination of compactional drape over the central high and Albian compression, and locally even into the Tertiary (Strauss and Noble, 1996). These faults have been suggested to be conduits for gas migration into those wells from deeper in the succession (Davies, 1996c). Indeed, in the western part of the basin, in the area of well 16 and particularly near well 3, seafloor steps and ridges are evident on seismic lines which may be surface manifestations of very shallow faults. However, few faults smaller that ~10metres are seismically mapped because they cannot be effectively imaged. Hence most of the faults which intersect the sea floor cannot be mapped at depth. On the north flank, a few faults extend shallower than 6At1 (Latest Hauterivian) but none appear to reach the Tertiary.

The most readily mappable of these faults is in the area of well 78 due north of the E-M structure. The presence of apparently bacterially degraded oil in syn-rift sandstones down-dip of the fault intersection may be evidence that the fault allowed the ingress of fresh, oxygenated water. There is, however, no evidence of a step in the sea floor although the movement may have been too small (<2 metres). In general, although the basin has been extensively faulted during at least three episodes in the Late Jurassic, Early Hauterivian and Barremian, (syn-rift, 5At1 and post 9At1 times) and there are also faults which appear to be related to an inherited Cape Fold Belt trend, there are essentially only four main fault regions. These four regions all have similar trends i.e. W-E to NW-SE:

1. south flank essentially between wells 19 and 9, down throwing north and north-east
2. north flank essentially between wells 46 and 1, down throwing to the south
3. central basin near wells 96 and 163, forming a deep-seated horst block
4. north of the central basin between wells 46 and 8, down throwing to the south (this fault acts as the main pressure boundary between high pressure 9A sandstones to the south and low pressure 1A-10 A sandstones to the north).

3.1.3 Sedimentation

The pattern of sediment distribution in the Bredasdorp Basin has been broadly controlled by global sea level changes (Haq et al., 1987) superimposed on regional tectonism. Since some of these sediments are potential source rocks for hydrocarbons and others are possible reservoir rocks, the tectonic control on the sediment distribution is of importance. The developing Mid-Late Jurassic rift created accommodation space for fluvial sedimentation. Intersections of up to 900 metres of largely fluvial sandstones and claystones have been made in wells around the margins of the Bredasdorp Basin. There is only one intersection of these sediments in the basin centre as only that well (# 160) was targeted at the break-up unconformity (horizon 1At1)- elsewhere it is far below the temperature limit for oil preservation. Basement rocks too, have only been intersected by a few wells around the edges of the basin and in each case; seismic data suggest great thicknesses of pre-rift sedimentary rocks were eroded during this period (Du Toit, 1976).

3.1.4 Syn-rift period, Jurassic-to-Earliest Cretaceous

Early sedimentological studies subdivided Post-Palaeozoic metasediments into four main intervals of non-marine deposits separated by major erosive unconformities (Du Toit, 1976) (Table 2.1). The non-marine Kirkwood, Infanta and Enon Formations (collectively known as the Pre-Sundays River sequence) were stratigraphicallly defined in the onshore Algoa Basin and interpreted as Lower Cretaceous (Du Toit, 1979) or Upper Jurassic-Uppermost Cretaceous (McLachlan and McMillan, 1979). These intervals were deposited during the pre-rift period. The Lower Sundays River Formation extended from the pre-rift sedimentary rocks up to the onset of drift, horizon C≡1At1 (Du Toit, 1976 and Burden, 1992). This formation comprises transitional-to-shallow marine sedimentary rocks.

The distribution of the pre-Sundays River rocks has been tentatively extended into the offshore basins and time-equivalent intervals have been intersected in the Bredasdorp Basin. These formations separate the Devonian and old basement rocks from the Cretaceous marine sedimentary rocks. Continuation of the rift caused increased sag which resulted in the lowering of base level in the Bredasdorp Basin causing fluvial systems to locally pound, resulting in the formation of lakes. Shaly and silty intervals containing

freshwater fauna (e.g. carophytes) were found in a few wells and are considered to indicate a nearby lacustrine environment (Valicenti, 1995, pers. comm.). Thin (<30m) Early Tithonian (Kimmeridgian) lacustrine shales with local oil source potential, are found in one well in a marginal half-graben in the Bredasdorp Basin and another well (DWK-1) in the coeval onshore Haasvlakte Graben (Davies et al., 1991). The source potential is variable but locally very high, as seen in the type intersection for Late Jurassic lacustrine source rocks, the Colchester shales of the onshore Algoa Basin (McLachlan and McMillan, 1979). However, well 89did not continue deep enough to establish the overall thickness of these sedimentary rocks. In addition, their presence elsewhere in the area has not been confirmed largely because most wells did not penetrate deep enough. It is likely that lacustrine shale development in the Bredasdorp Basin is not as sparing as these few intersections show and could be similar to the distribution of coeval sedimentary rocks in the Springhill Formation, Magellanes Basin, South America (Biddle et al., 1986; Maslanyi it al.,1992) i.e. in the basal parts of most marginal half-graben.

3.1.5 Evaporites

Well 16 drilled into a small sub-basin in the western part of the basin and intersected a 409 metre thick interval of red siltstones and claystones thinly interbedded with halite-rich sediments. A total of 53 individual salt layers up to several metres thick in places were found, totalling ~209 metres, although more may be present as seismic data show that the interval continues below TD. Salt swells are evident on seismic line throughout this region. Evarporites are Earliest Cretaceous (Dingle et al., 1983; Lawver et al., 1992) and from the present day climatic regime (cool and moist) formations of evaporates is unlikely. However, warm water Ostracode species found in sediments of similar age in the onshore Algoa Basin, indicate that the water temperature was higher than today implying significantly warmer weather (Valicenti and Stephens, 1984).

These warmer conditions may have been a consequence of the higher proportions of CO_2 interpreted to characterise the Mesozoic atmosphere and which resulted in the development of “greenhouse” conditions (Barron and Moore, 1993; Larsen, 1991). It is thought that this evaporate-bearing sub-basin was located close to the palaeo-coast-ling

and filled with sea-water each time the barrier between it and the sea was breached- most likely during periodic highstands. Log data show the thickness of the salt layers to vary between 1-8 metres with a mean of 3.5 metres. Evaporation of a 220 metres column of present-day sea-water is required to deposit this average thickness of salt, although the actual thicknesses of salt layers most probably reflect frequent fill and evaporation episodes-enhanced by intermittent tectonism. After each major tectonic deepening event, the basin gradually filled with both salt and sediments reducing the accommodation space. Hence salt layer thicknesses progressively decrease. These sediments are time-equivalents of 3rd order transgressive and highstand portions of the earliest Valanginian LZB 2.1 sequence (Haq et al., 1987 and Valicenti, 1995, pers comm.) and represent some 60% of the sequence duration, i.e. ~1.9-2.1 Ma. Hence each average salt layer could equate to a period of ~40000 years. This time interval could differ if the salt layers resulted from partial or multiple fill and evaporation episodes as shown for Messinian salt layers in the Mediterranean (Butler et al., 1995). This figure is closed enough to the accepted average period of global orbital obliquity (Hays et al., 1976; Heckel, 1986; Smith, 1990) of 41000 years to temperature comparison. Elsewhere in the basin, high gamma claystones are thought to characterise equivalents of these highstands, e.g. in wells 65/75 (Valicenti, 1995, pers comm.).

3.1.6 Syn-rift period, Early Cretaceous

Regional relative sea level rise in the Early Valanginian brought an extensive marine incursion into the Outeniqua Basin and with it a diachronous coastal environment which transgressed the region. Littoral, shallow marine and marine glauconitic sandstones up to 100-200 metres thick, the latter originally interpreted to be lag sands, were deposited (Du Toit, 1976). Recent studies show that they represent the earliest phase of marine incursion during the final stages of rifting and sag (Valicenti and Broad, 1994 and McMillan et al., in press). Indeed, the most recent biostratigraphic interpretations place the 1A type 1 unconformity (1At1) at the base of these transgressive coastal sandstones rather that the top (Valicenti, 1995). However, the top of these sandstones is still called 1At1 for purely descriptive reasons. As the transgression continued into the western Bredasdorp Basin, the coastal sands were in turn overlain by basin-wide deep marine infill sediments of the Upper

Sundays River Formation which encroached from the east. The contact is diachronous (Valicenti and Broad, 1994).

3.1.7 Post-rift period, Mid-Cretaceous

Subsequent sea level rise resulted in the establishment of open marine conditions in the basin which prevailed to the Albian. Sediments deposited during this episode were shelf and slope shales and silts but several persistent channelized sandstones have been identified. These sandstones are important petroleum migration conduits. The upper boundary of the Upper Sundays River Formation, Seismic horizon A≡E≡13At1 (Du Toit, 1976; McLachlan and McMillan, 1979; Burden, 1992) also marks the base of the Agulhas Formation. Dominantly argillaceous marine sedimentation continued in the Lower Agulhas Formation deposits until global lowering of sea level in Early Albian (14At1) resulted in a major erosive period when the shelf edge was dissected by submarine canyons. These canyons subsequently filled with further channelized sandstones which are important oil reservoirs. Sediments in the 1At1-to-13At1 interval belong to the Upper Sundays River Formation.

3.1.8 Cretaceous sequence stratigraphy

Recent seismic studies of marine Cretaceous sediments (Van Wyk, 1990; Brown et al., 1995) saw the application of sequence stratigraphic concepts to the Bredasdorp Basin. A sequence is defined as ‘’a relatively conformable succession of genetically related strata bounded by unconformities and their correlative conformities’’ (Vail et al., 1977). Benefits of this interpretation method are the ability to predict lithology, particularly that of reservoir quality sandstone, and the basin-wide correlation of sedimentary units. After the sequences in the Cretaceous had been fully delineated, the success rate of the technique for lithological prediction was evaluated by (Brown and Doherty, 1992).

They showed that the ability to predict the continuation of individual units across the basin was high by comparison with the results obtained from previous facies correlation methods. Results from drilling confirmed the predicted depositional system in 75% of all cases although only approximately 50% of predicted lithologies were found. The application of the method resulted in the basin-wide correlation of 22 Cretaceous third-order sequences; each

bounded by type 1 unconformity surfaces (Van Wyk, 1990). Such surfaces (labelled 't1') are considered to reflect sea level fall below the shelf break (Vail, 1987) and so indicate episodes of shelf edge erosion. Individual sequences have been established from seismic and borehole data. Precise ages of sequences and their boundaries, based on biostratigraphic information (using palynological. Ostracode and foraminiferal dating), match the major sequence boundaries of (Haq et al., 1987). Their basin-wide definition has allowed the construction of detailed distribution and isopach maps for the 14A sequence (Benson et al., 1993 and Wickens, 1993), the 13A sequence (Brink et al., 1991), the 9A-12A sequences (Smith, 1992) and 1A-8A sequences (Burden and Gasson, 1992). The studies also confirmed that the stratigraphic subdivision of the Sundays River Formation of (Du Toit, 1976) (Table 2.03) was essentially valid but too imprecise for current detailed exploration work. Therefore horizon correlations used in his report all reflect the sequence stratigraphic concept. Each sequence commenced with deposition of isolated or amalgamated lowstand fan deposits on the unconformity surface (Van Wyk, 1990).

These deposits are inferred to be connected by channels to submarine canyons incised into the previous shelf. Seismic evidence of shelf-edge canyons and the channels themselves is largely lacking perhaps because of their small size and lack of lithologic contrast although recent developments in seismic continuity mapping show some features which could be channels (Barton and Grobbler, 1997). Many of the clastic sediments derived from onshore are polycyclic and where reworked, especially into lowstand deposits. They generally comprise fine sandstones and silts. Occasionally, however, coarse material was transported into the basin. Examples of these deposits are found in the basin floor sandstones of the 14A sequence which form the reservoir facies for some of the oil reservoirs sampled for this study (Wickens, 1993).

In general, sandstones nearest the shelf are poorly sorted and characteristic of mass-flow deposits (Gilbert, 1990) but more distally they are well-sorted and channels and lobes dominate (Beamish, 1990). One important consequence of the continued and extensive transgression is that the central part of the basin became progressively sediment starved, typified by thinly bedded pelagic, organic-rich shales draped over the basin floor fans. At the time of greatest landward transgression (13A mfs), these shales are characterised by maximum sediment starvation i.e. greatest concentration of fauna (especially radiolarian),

maximum preservation of organic matter and lowest oxygen contents (McMillan et al., 1997). Development of oil-prone source rocks in the 13A sequence is considered to be an example of this process (Demaison et al., 1988). Shelf progradation or aggradation, following the period of highstand sedimentation, accompanied a return to oxygenated conditions, and resulted in dilution of faunal concentrations and decreased preservation of organic matter in shales. Associated deltaic systems, rich in clastic debris, advanced into the basin and deposited extensive, mainly fine-grained, sandstones across the shelf edge. Eventually these systems advanced across the pre-existing shelf edge and onto the slop following discreet channels as in the present day Mississippi delta. Depending on distance from the sediment source, these resulting deposits can be fine-grained (as in the 9A-10A sandstones) or relatively coarse (as in the 14A channel sandstones).

3.1.9 Post-rift period, Late Mid-to-Late Cretaceous

Environments of deposition prevailing through the later part of the Cretaceous were dominated by gradual cooling from 'greenhouse' conditions (Veevers, 1990; Barron and Moore, 1993; Larsen, 1991) and a long period when temperate conditions dominated. Deposits during this period are dominated by relatively high energy sedimentary rocks (sandstones and siltstones) and only occasional shales indicative of erosion of pre-existing sediments. The greater rate of sediment input reflects the wetter climate and elevated hinterland topography. The remainder of the Cretaceous comprises the clastic-rich later parts of the Agulhas Formation and is separated from the overlying carbonate-rich Tertiary Alexandria Formation by the basal Palaeocene unconformity horizon L≡22At1 (Du Toit, 1976; Burden, 1992).

Completion of separation between Africa and South America in the Early Turonian allowed the establishment of open marine circulation between northern and southern hermisphere throughout the Atlantic. This resulted in changed global oceanic circulation (Arthur et al., 1987; Schlanger et al., 1987; Zimmerman et al., 1987) which is inferred to have initiated the formation of locally anoxic bottom waters and caused the deposition of thin, but persistent, organic-rich shales in the 15A sequence. These constitute a regional source rock overlying the 15At1 unconformity. Matching sediments are found in wells in the offshore Gamtoos

and Pletmos Basins and in many wells on the west coast of South Africa, although without the rich source potential of the Bredasdorp Basin. Climatic changes culminated in cooler conditions in the Campanian and Maastrichtian (Huber and Watkins, 1992). These sedimentary rocks contain significant amounts of calcite, mostly in the form of abundant Inoceramus spines, reflection the change to cooler water.

3.2 FORMATION FLUIDS

3.2.1 Hydrocarbons

Reservoirs containing gas with condensate or oil have been found below horizon 13At1 throughout the basin. Those gases reservoired below 9At1 tend to be condensate-rich whilst those below 1At1 generally have very little condensate. Oil reservoirs have been found mostly in Albian (14A) sandstones in the basin centre and occasionally in north flank area wells below horizon 1At1. The distribution of these oil and gas prone zone is shown in (fig 2.5). The results of drilling offshore have shown the Palaeozoic metasediments contain neither significant hydrocarbon source potential nor potential reservoir rocks (except where locally fractured) and they are currently considered to be the economic limit for hydrocarbon exploration. It is possible that locally the Bokkeveld Group slates could source non-hydrocarbon gases (e.g. CO_2, H_2S) as well as some methane gas.

3.2.2 Water

Where the Agulhas (and possible Infanta) Arch were subaerially exposed, they could have been sources of water influx to the basin, especially where highly faulted. Resent mapping has shown faults which extend to the basal Palaeocene on the Agulhas Arch (Strauss and Noble, 1996). Rain falling on such exposed highs percolated through these faults, entering juxtaposed sandstone bodies where through-flow of fluids was possible. Also, porosity resurrection prevails in syn-rift reservoir sandstones in the north flank of the basin, caused by dissolution of intergranular poikilotopic calcite cement (Hill, 1995a and b) probably by meteoric fluids. Even today, formation water salinities in these reservoirs are low (locally <20000 ppm NaCl, Davies, 1995a) this dissolution must have occurred late, after the period

of Cretaceous rapid burial, otherwise the secondary pores would have been compacted. This could be at, or shortly after, the Cretaceous-Tertiary boundary because sedimentation rate decreased greatly during Late Cretaceous (McMillan et al., 1997) leading to a reduced likelihood of further compaction.

In addition, recent studies have shown evidence of a possible bolide impact at the Cretaceous/Tertiary boundary (Alvarez et al., 1980; Hildebrand et al., 1991). One global consequence was markedly elevated rain-water acidity during the succeeding 0.01-0.1 Ma (Retallack, 1996). This rain-water would have been able to percolate from the exposed basin margins into the sandstones resulting in dissolution of calcite-rich pore-filling material. In support of this scenario, an apparently partly biodegraded oil, with depleted normal alkanes, was found in well 78 close to a major fault which extends close to the Early Tertiary palaeo-surface. Burial and thermal history modelling of the well data show the sandstone is presently at ~80^{0}C (at which temperature any bacteria are essentially inactive), but during the Early Tertiary, formation temperature was closer to 60^{0}C, when bacteria were active (Connan, 1984). In other areas, compaction resulted in expulsion of saline water from deeper sediments, and this connate water flowed up-dip, locally mingling with the incoming meteoric water and possibly resulting in the brackish water found in many sandstones in marginal highs (Davies, 1995a).

Erosion during the Early Eocene mainly occurred on the north flank and reached a maximum at the eastern end of the basin but was still <50-100m. It was probably caused by thermal uplift due to the near-surface intrusion of the alkaline igneous bodies. Erosion during the latter part of the Mid-Oligocene is considered to be a result of the global sea-level lowstand (Haq et al., 1987; McMillan, 1989) rather than local tectonic uplift. Erosion of Early to Mid-Oligocene (and presumably Late Eocene) sedimentary rocks may have reached 100m during this lowstand (McMillan, 1995, pers. comm.). The event has only been recognised very locally from biostratigraphic data, mainly because few samples of the interval were collected from the wells. Flushing by meteoric water of north flank pre 1A and central basin 13B-14A (Albian) channel sandstones may also have happened during Plio-Pleistocene sea-level falls caused by northern hemisphere glaciation. The resulting eustatic sea level falls could have reached 200m and probably averaged 150m for each glacial advance (Dingle et al., 1983; Malan, 1990; Ben-Avraham, 1994, pers comm.).

At that time, various topographic sub-sea highs around the margins of the basin and to some extent the centre of the basin would have been exposed to rainfall. In addition, annual rainfall rates are shown to have been at least twice as high as presently for periods of several tens of thousands of years within the Plio-Pleistocene (Butzer et al., 1973). Fresh-water flushing might have occurred during this period but until samples of formation water have been dated (possibly using ^{14}C isotope techniques) this will remain uncertain.

3.2.3 Formation pressures

Regional pressure studies, based almost wholly on data from Cretaceous reservoirs, show three pressure regimes to exist in the basin (Winter, 1981; Brink and Winters, 1989; McAloon et al., 1990; Larsen, 1995). These are:

(i) a normally pressured zone, largely down to ~3000m. in parts of this zone, fluids readily interchange with surface water causing low salinity trends and locally gas seeps (Davies, 1988b),

(ii) a second zone, largely associated with thick source rocks (mainly 13A Aptian), in which the equivalent mud weight (MW_{eqquiv}) reaches values up to 1.15 ppg,

(iii) a third zone in which very high overpressures are developed (up to >3000 psi above hydrostatic or MW_{equiv}**. >**1.60). These pressures are estimated in many sandstones from the drilling and log parameters but are locally recorded from RFT and DST pressures (Verfaille, 1993).

Very high formation pressures are also found in Valanginian sandstones in well 128 some 80km east, in the highest pressured reservoirs, Hauterivian (5A) sandstones in wells 83 and 88, pressures approach ~0.73 psi/ft, similar to that found in North Sea reservoirs (Miles, 1990) and possibly represent the local fracture gradient. Indeed, their matching pressure and close proximity suggest they are part of the same pressure cell although it is possible that the matching overpressures reflect matching seal efficiencies rather than connectivity. It is possible that thermally-induced hydrocarbon cracking during hotspot events or pulses of migration may have caused pressures to locally exceed this amount only to be almost instantly reduced by seal rupturing. In a few reservoirs, the regional pressure distribution shown above differs. For example, in well 123, overpressure is recorded in Lower Albian

(13B) sandstones just above ~2600m bKb. Associated oil-bearing fractures in apparently diagenetically calcitised sandstones attest to possible intermittent pressure build-up/release episodes (Brown, 1991; Davies, 1995c). In well 142, Barremian (9A-12A) sandstones are also overpressured and fractured (although not to the same extent as above) and contain gas shows and fluorescence traces (possibly residual condensate) below~2700m bKb.

3.2.4 Late Tertiary slump

Large volumes of Tertiary (and locally Upper Cretaceous) sediments were removed from the present day shelf edge by Late Tertiary slumping (or creep) along a composite glide plane resulting in the present day rugose sea floor topography (Dingle, 1977). Indeed De Swardt and McLachlan (1982) commented that up to 1000m of sediment was removed at this time (although they considered that erosion was the cause). Several prominent, regionally sub-parallel slump scars are interpreted on the available seismic records from the area. These sediments were re-deposited further down dip in a partially consolidated state (Dingle, 1977; Dingle et al., 1983, p. 307). The exact timing of the slump event is not known but is discussed in section 3.9.5. Dingle (1977) comments on a core sample from the slump which contains Upper Miocene sedimentary rocks suggesting a Pliocene age for the slump although this may only reflect the age of the last slump. Certainly the disposition of the apparent slump scars lends support to the suggestion of multiple slumps over period of time.

3.2.5 Age

Biostratigraphic data horizons in nearby SOEKOR wells can be extrapolated into the Southern Outeniqua Basin using seismic data and it is evident that the slumps do affect the latest correlatable sediments, which are Early Miocene in age. Available seismic data were recently re-interpreted to take into account recent stratigraphic data from distal wells drilled around the northern and western rum of the Southern Outerniqua Basin. Palaeocene rocks are shown to be consistently thick as far offshore as the main slump scar whilst the Eocene rocks appear to gradually thin. This supports the contention of Partidge and Maud (1987) that the Early Palaeogene sedimentation rate was high but gradually decreased into

the Neogene. All Tertiary and Latest Cretaceous sediment packages terminate at the glide place which suggests that the strata were originally continuous into the basin. If so, this indicates that large volumes of these sediments (up to ~20000km^3, Dingle, 1977) must have existed further offshore prior to the slump.

The timing of the slump event has been modelled using Basinmod 1D (Platte River Associates, 1995). The timing of the slumping has been assumed as between 10-9 Ma, midway between the latest microfaunal age dating in the nearest well (McMillan and Valicenti, 1986), the suggestion of an Early Pliocene date by Dingle, (1977). The model shows the subsequent build-up and dissipation of excess pressure to occur during the succeeding 9 Ma. The slumping may however have occurred later that this and it is possible that the event was Pliocene in age rather than Late Miocene. It is unlikely that the slumping took as long as 1 Ma, rather each of the several slump episodes would have been considerably more rapid. In geological terms, slumping is essentially instantaneous although some develop over periods of weeks or years (probably more likely creep) whilst other slumps occur within a day. In the marine environment, slumps could be much more rapid (Holmes, 1965, p. 482-486; Piper et al., 1985). However, where slumps are caused by slope-steepening as a result of a regional tilting event, it is likely that each slump was separated from the next by a lengthy hiatus during which the expelled water migrated up-dip dissipating the excess pressure. Thus the period of slumping and hot-water flow could have spanned several millions years.

3.2.6 Volumetric

These large volumes of sediments removed from the shelf and re-deposited in the basin must have profoundly affected the compaction and fluid flow from the pre-existing sediments. Not only would the flow direction of water from the sediment pile due to normal compaction have been directed toward the Bredasdorp Basin by the relative uplift of the continental plate and down-warp of the oceanic plate, but water expressed from the sediment pile as a result of the slumping would also migrate into the Bredasdorp Basin, Dingle (1977) comments on a maximum estimated thickness of the slump debris of 324 m form the interpretation of a few seismic lines, whilst De Swardt and McLachlan (1982)

commented on thicknesses up to 700m. This study shows up to 750 milli-seconds (two-way line) thickness of slump sediments in the central part of the Southern Outeniqua Basin (Roux, 1997, pers. comm.). Since these sediments could have been re-deposited in a partly consolidated state (Dingle, 1977) and almost certainly were if they were affected by creep (Paull et al., 1996), they would be equivalent to at least 800m (possibly in excess of 900m) based on equivalent non-slumped sediments in surrounding wells. The area of the Southern Outeniqua Basin cover by the slump where expressed water could migrate into the Bredasdorp Basin, the area is essentially that of south of the southern Infanta Arch and its south-eastward projection.

3.3 Cause of slumping

The reasons for the slope instability, and by extension the age of slumping, are not known for certain because of the lack of suitable rock samples, although several possibilities exist:

(i) seismic shocks from fault movements (Dingle, 1977) although few faults extend shallower than the base of the Oligocene (Strauss et al., 1996),

(ii) increased sediment load from rapid deposition (Dingle, 1977) although Partridge and Maud (1987) show this to be unlikely,

(iii) slope undercutting by shelf edge erosion,

(iv) dip steepening as the Southern Outeniqua Basin (and probably the Agulhas Fracture Ridge) foundered (Dingle et al., 1983),

(v) Released of gas from hydrates during pressure reduction by low sea level action as a plane of decollement (Paull et al., 1996).

3.3.1 Slope undercutting by shelf erosion.

Sea-level oscillation was more intermittent during the Plio-Pleistocene than at present, but shelf edge erosion could not have happened then because the Agulhas Current was much further south as far as latitude 38^0S and only weekly developed (Winter and Martin, 1990). In addition, there is little likelihood of the wave-base erosion of sediments downdip because the maximum Late Tertiary sea-level lowstand was only ~150m (Partridge and Maud, 1987) yet the slumped area is now in >700m of water. Erosion due to the Agulhas Current has

been postulated (Winter and Martin, 1990). If erosion were the cause of the sediment planation, the current velocity would have to be higher than the minimum needed to remove claystone (i.e. ~0.2-0.4 m/s) in order to overcome the cohesion of the sediments and to remove partially compacted Upper Cretaceous sediments (Potter et al., 1980, pp. 10-12). However, the Agulhas Current velocity decreases markedly with depth (Derbyshire, 1964). For example, the high velocity part of the Agulhas Current, where velocities attain 2m/s, is the warmest part where temperatures generally exceed 20^0C. This is called the high temperature Agulhas Current (HTAC) and it flows near surface. By contrast, the cool Agulhas Current barely reaches temperature of 17-20^0C and generally flows at much less than half the speed of the HTAC. In fact, at depths below ~140m, the temperature rapidly decreases to <<15^0C (SOEKOR unpublished Sniffer survey data, Davies, 1988a) and the velocity drops substantially. Below 170m the mean velocity falls to <~0.2m/s (Derbyshire, 1964; Lutjeharms et al., 1981; Van Heerden, 1984) and it is this water which locally impinges on the sea floor. Indeed, silt and clay deposition dominates where the velocity drops below ~0.2m/s (Birch et al., 1986).

3.3.2 Dip steepening

A strong possibility for the cause of slumping is dip oversteepening. The driving force behind this could be tilting of the continental plate and localised downwraping of the oceanic plate as a result of the physical and thermal doming during development of the a new mantle plume below south-eastern Africa, the 'African Superswell' (Hartnady and Partridge, 1995). The earliest evidence of formation of this swell is given as Late Miocene (Hartnady and Partridge, op cit.), i.e. coincident with the estimated age of slumping. Uplift during this event is thought to be ~900m on the east coast but only ~100m on the south-western coast. Accompanying the tilting, there would likely have been considerable seismic activity which could have added to the sediment instability as seen in other examples (Piper et al., 1985).

3.3.3 Fluid flow

The sudden addition for several hundred metres of partly compacted overburden would rapidly increase pore pressures in those sediments and since the pressure could not

dissipate rapidly because of the overburden, it would bleed off slowly (Deming, 1994). Basinmod 1D modelling of the pressure build-up in these sediments has been carried out. This type of modelling is, however, less than perfect as it takes no cognisance of the lack of well data in the area. Nevertheless, it indicates pore pressure increases of several hundred psi and a 'bleed-off' period of some Ma, both dependent on assumptions of the lithologic type based on data from the surrounding wells. Immediately after each slump, pressure would build up in the sediments deeper than ~2000m (bmsl), i.e. below the Turonian source rock claystones (but not above as those sediments are too porous and permeable to sustain overpressures). This claystone layer forms a regionally extensive seal to fluid flow and would channel fluids laterally up-dip rather than vertically. Modelled excess pressure does not build up in sediments in the top 200m, probably because their high permeability allows near-instantaneous expulsion of water. Below that depth the model shows a rapid rise in the excess pressure and a slow fall-off over the succeeding few million years. The top 1500-2000meters of original (pre-Miocene) sediments presently retain high permeability and porosity. Partial compaction of these sediments by deposition of 800m (or more) of sediments, would result in the expulsion of large volumes of water which should be able to flow essentially unimpeded up-dip and out of the basin through the shallow overburden.

The remainder of the Cretaceous and Jurassic rocks in the basin, locally in excess of 8km thick (Ben Avraham et al., 1993), were already partially compacted and slump-related compaction effects would be less but nevertheless likely. The volumes of water expelled during this slump event could be very large. Estimates can be made from modelled porosity changes. Based on compilations of porosity versus depth data (North, 1985), and the calculated depths to the seismic horizons (Van Wyk et al., 1992; Wenham et al., 1991), model of the porosity changes match those shown by North (1985). Evaluation of log porosities in sandstones in wells at the margins of the Southern Outeniqua Basin supports these estimates. The hydrothermal change due to this slumping significantly altered the thermal regime of the Bredasdorp Basin, influencing hydrocarbon generation in this region.

4 CHAPTER

4.1 Geophysical tools used for the study

The following list of data was used to carry out this research and will be discoursed below: Core Samples, Productivity Test Data, Drill stem test (DST), Wireline formation testing, Well Logs, Porosity, Permeability, Resistivity, Gamma Ray (GR), Spontaneous potential (SP), Induction, Neutron, Electrode resistivity, Density, Combination neutron-Density, Sonic.

Data for this project was collected over the period of April 2013 to March 2014 obtaining well completion reports and other hard copied data as well as digital data from the Petroleum Agency of South Africa (PASA). In block 9 of the Bredasdorp Basin, three wells which situated in close proximity to each other were selected for this study. The selected cores were laid out within a core shed supplied by (PASA) and approximately 4-5 hours spent daily physically investigating the cores of each well. The extensive time where spent to describe, correlate and depth match different horizons. Logging was carried out to identify different geological features such as imbrications, minor faults, presence of fossils and folds to the corresponding depths. The cores used in this study are located at the Petroleum Agency of South Africa (PASA) core library. Petroleum Agency of South Africa provided all the data used for this study.

4.1.1 Core Samples

These are cylindrical samples of rock taken from a formation in situ for analysis purposes. This is done by substituting a conventional drill pipe core barrel and core bit for the drilling bit to obtain samples as it penetrates the formation. Usually cores are cut using a special coring bit and are retrieved in a long core barrel. The core barrel is a hollow cylindrical device 7.6m to 18m in length with a hollow drill bit which can be attached to the bottom of the drill pipe for the purpose of recovering continuous samples of the formation while the hole is being drilled. The samples recovered are cylindrical cores and can be as long as the core barrel, (Reifenstuhl 2002). Core samples provide a full sample of rocks penetrated.

It is used both for qualitative (visual lithology) and quantitative analysis which is a laboratory analysis of recovered reservoir formation samples of the purpose of measuring porosity,

directional permeability, residual fluid saturation, grain size, density and other properties of the rock formation contained fluids. It is also used to calibrate wireline logs. Additional coring methods such as sidewall coring could be carried out when extra rock samples are necessary after the well has been drilled and before it has been cased. Sidewall cores are obtained with a wireline tool from which a hollow cylindrical bullet is fired into the formation and retrieved after each bullet has been fired into the formation was by a free pull by wires connection the barrel to the gun. Core barrels are accessible for piercing formation s of different hardness. The type of barrel and size of charge varies to optimize recovery in different formations. The problem with coring lies in the tendency of the formation samples to undergo physical changes on its way from the bottom of the well to the surface. More sophisticated coring mechanisms that can preserve the orientation, pressure and original fluid saturations of the core samples have been developed. The cores are held within core boxes delineating the location and the depth to which recovered core belong to. Parts of core where still encased within waxed cylinders to preserve the original environmental fluids as well as the original sediment from the subsurface.

These waxed units are randomly selected on basis of how important certain units of core were to the study. Certain parts of the waxed units visually obscured the investigation of the core and obstructed conformation to contacts between sedimentological units and grain size distribution between different sections of the core and were left to proficient decision making as well as assumption on the continuum of the stratigraphic sequence. Random core plugs where selected within each well to further evaluation to grain size distribution and the porosity and permeability traits each core attained.

4.1.2 Productivity Test Data

A well test is the execution of a set of planned data acquisition activities to broaden the knowledge and understanding of hydrocarbons properties and characteristics of the underground reservoir where hydrocarbons are trapped. The test will also provide information about the state of the particular well used to collect data. The overall objective is identifying the reservoir's capacity to produce hydrocarbons, such as oil, natural gas and condensate. Data gathered during the test period includes volumetric flow rate and

pressure observed in the selected well. Outcomes of a well test, for instance flow rate data and gas oil ratio data, may support the well allocation process for an ongoing production phase, while other data about the reservoir capabilities will support reservoir management. Productivity Test Data include: Formation Tester and Drill Stem Test (DST). Obviously, not all of these measurements are made in any single well. A careful selection of a specific measurement is made in order to completely identify and evaluate the commercially productive hydrocarbon bearing zones. Formation testing presents collection of data on a formation to determine its potential productivity before installing casing in a well. If a well flow's hydrocarbon during a drill stem test, no amount of log or core samples analyses can deny that a productive zone has been found.

4.1.3 Drill stem test (DST) and wireline formation testing

Drill Stem Test which is defined as a temporary completion of a well is a procedure for testing a formation through a drill pipe. Incorporated in the drill stem testing tool are packers, valves or ports that can be opened and closed from the surface and a pressure recording device. The formation fluid is recovered in the drill pipe through temporary relief of back pressure imposed on the formation. Hydrostatic flowing and shut in pressures are recorded against time. A (DST) do not only provides the proof that hydrocarbons exist in the formation and that it will flow but it also supplies very important data concerning both size of the reservoir and its capability to produce. Interpretation of pressure records from drill test adds greatly to the overall formation evaluation. Wireline Formation Testing complements drill stem test by their ability to sample several different zones encountered by the well. They provide fluid samples and detailed formation pressure data that is almost impossible to obtain from DST alone, (Reifenstuhl, 2002).

4.1.4 Well Logs

Well logs are a class of the most useful and important tools available to petroleum geologists. They are products of survey operations consisting of one or more set of digitized data or curves which display an array of permanent record of one or more physical measurement as a function of depth in a well bore. They are used to identify and correlate

underground rocks, determine their mineralogy, generate their physical properties and the nature of the fluids they contain. During drilling a well, relatively little can be learned about the potential of the penetrated formation. The analyses of the returned cuttings, sometimes referred to as Measurement While Drilling (MWD), reveal the general lithology.

Geological sampling during drilling leaves a precise record of the formation encountered. Mechanical coring is slow and expensive. Even though geophysical logs need interpretation to bring it to the level of geological or petrophysical experience, the strong points are in the precision and ability to bridge the gap between well cutting and core samples, (Levorsen, 1967). The geophysical wireline logs are the continuous records of geophysical parameters along a borehole. They are products of wireline logging which involves inserting a logging sensor or a combination of (Sonde) in the drill collar is lowered into the well bore by a survey cable and a continuous physical measurements (electrical, acoustical, nuclear, thermal and dimensional) are made. A sensor and its associated electronics are housed in a sonde, which is suspended in the hole by an armored electric cable. The sensor is separated from the virgin formation by the drilling mud, mud cake, and often by an invaded zone in the formation. Signals from the sensor are conditioned by down-hole electronics for transmission up the cable to the surface electronics, which in turn conditions the signals for output and recording. As the cable is raised or lowered, it activates a depth measuring device which provides depth information to the surface electronics and recording devices. The data is recorded on digital tape, film or paper, (Levorsen, 1967). Necessary geophysical measurements are obtained to allow a quantitative evaluation of hydrocarbon in place. It is very important to get accurate well calibrated and complete data. The cost of wireline logging generally amount to less than 6% of the total well budget. Some well logs are made of data collected at the surface; example are core logs, drilling time logs, mud sample logs, hydrocarbon well logs etc. Other types such as movable oil plots, computed logs, etc. Show quantities calculated from other measurements**.**

4.1.5 Porosity

This is defined as the ratio of void space to the bulk volume of rock containing the void space. It can be expressed as a fraction on percentage of pore volume in a volume of rock and has a symbol (Φ). It is represented with the formula stated below:

$$\text{Porosity } (\Phi) = \frac{\text{Volume of Pores}}{\text{Total Volume of Rock}}$$

The amount of internal space in a given rock volume is a measure of the amount of fluids the rock will hold. The amount of interconnected void spaces excluding isolated pores and pore volume occupied by adsorbed water available to free fluids is referred to as effective porosity. The effective porosity can also be defined as the fraction or percentage of interconnected pore or void space volume in a volume of rock. It excludes isolated pores and pore volumes occupied by the water adsorbed on clay minerals or other grains. The total porosity is all void space in a rock and matrix whether effective or non-effective. It includes porosity in isolated pores adsorbed water on grains or particle surface and associated with clay, (Levorsen, 1967).

Porosity in sedimentary rocks can be primary or secondary; Primary porosity refers to the porosity remaining after the sediments have been compacted but without considering changes resulting from subsequent chemical action or flow of water through the sediments. Secondary porosity on the other hand is the additional porosity resulting from fractures, vugs, solution channels, diagenesis, and dolomitization. The three common types of secondary porosity are: fracture porosity, shrinkage porosity and dissolution porosity.

4.1.6 Permeability

This is the property a rock has to transmit fluids. It is related to the effective porosity but not always dependent on it. Permeability is controlled by the size of the connecting passages (pore throats or capillaries) between pores. It is measured in Darcies, more commonly in millidarcies and represented by the symbol K_{a-}. A measure of the ability of a rock to conduct a single fluid through its interconnected pores when it is 100% saturated

with that fluid is called absolute permeability while effective permeability refers to the ability of a rock to transmit a fluid in the presence of another fluid when the two fluids are immiscible. The ratio of the effective permeability of a fluid at partial saturation to its permeability at 100% saturation (absolute permeability) is the relative permeability. It is also defined as the ratio of the amount of a specific fluid that will flow at a given saturation in the presence of other fluids to the amount of the same fluid that will flow at a saturation of 100%, other factors remaining the same. It ranges in value from zero at low saturation to 1.0 at 100% saturation of the specific fluid. Since different fluid phases inhibit the flow of each other, the sum of the relative permeability of all phases is always less than unity.

4.1.7 Resistivity

This is the rock property on which the entire science of logging was initially developed. The resistance of a material which is its ability to resist the flow of the electric current at a particular temperature is directly proportional to its length **(ℓ)** and decreases with increasing cross-sectional area **(A)**. The proportionality constant is resistivity **(ρ)** of the material. The resistivity of a material is its resistance **(R)** over a specified length and cross sectional area. It is defined by:

$$\text{Resistivity } (\rho) = \frac{RA}{\ell}$$

In log interpretation, the rock and fresh water all act as insulators and are therefore non-conductive and highly resistive to electric flow. The resistivity recorded on a resistivity well log may differ from true resistivity because of the influence on the measured response caused by the presence of the mud column invaded zone adjacent beds and borehole cavities. This is referred to as apparent resistivity and may need correction prior to use in any computation. The measure units are ohm-meters (ohm-m). The figure below shows the flow of current in the resistivity tool during its measurement.

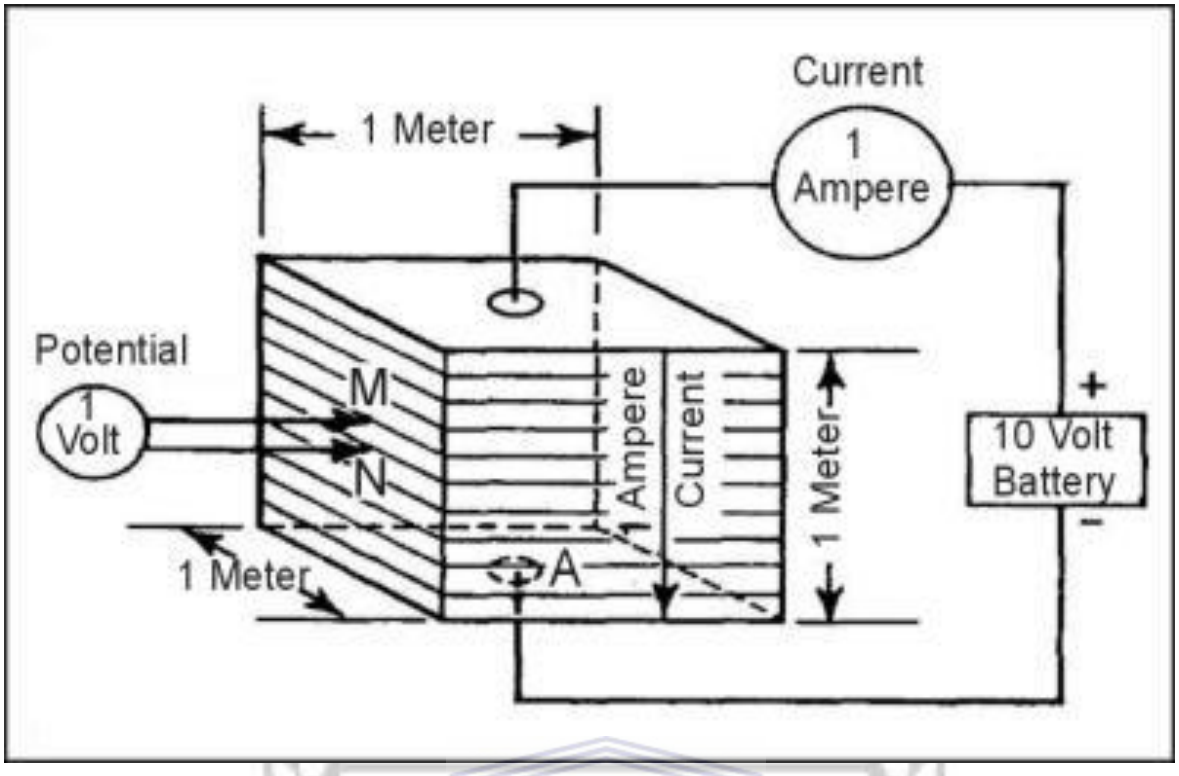

Figure 4.1 Principles of measuring resistivity in Ohm-meter. Example is 10 Ohm-meter modified from Wightman, W. E., Fluid Saturation.

This is the fraction or percentage of the pore volume occupied by a specific fluid (oil, gas, water). It is generally defined by:

Fluid Saturation (S_f) = <u>Formation fluid occupying ores</u>

Total pore space in the rock

The fluid in the pore spaces of a rock may be wetting or non-wetting. In most reservoirs, water is in the wetting phase while few reservoirs are known to be wet oil. The wetting phase exists as an adhesive film on the solid surfaces. Water saturation is an important log interpretation concept because hydrocarbon saturation of a reservoir can be determined by subtracting water saturation value from a unit value (1), where a unit value (1) equals 100% water saturation. Water saturation $\mathbf{S_w}$ is measured in percentage. Irreducible water saturation $\mathbf{Sw_{irr}}$ is the term used to describe the water saturation at which the water is adsorbed on the grains in the rock or held in capillaries by capillary pressures. At irreducible water saturation, water (wetting phase) will not move implying a zero relative permeability

and the non-wetting phase is usually continuous and is producible under a pressure gradient of the well bore. The occupation of fluids in a pore may take different forms:

i. Funicular saturation. A form of saturation in which the non-wetting phase exists as a continuous web throughout the interstices which make it to be mobile under the influence of the hydrodynamic pressure gradient. The wetting phase may or may not be at irreducible saturation. Figure (4.2 A) illustrates the oil (non-wetting phase). As funicular.

ii. Pendular saturation. Here the wetting phase exists in a pendular form of saturation in which an adhesive fluid film of the wetting phase coasts solid surfaces, grain to grain contacts and bridges pore throats. The wetting phase may or may not be at irreducible saturation. In (Fig: 4.2 B), water (wetting phase) in A and B is pendular.

iii. Insular saturation. A type of saturation in which the non-wetting phase exists as isolated insular globules within the continuous wetting phase. Here it is uncertain that a decrease in pressure may cause the insular globules to collect into a continuous phase. Illustration in B and C (figure 4.2) shows that the oil (non-wetting phase) is insular, (Levorsen, 1967).

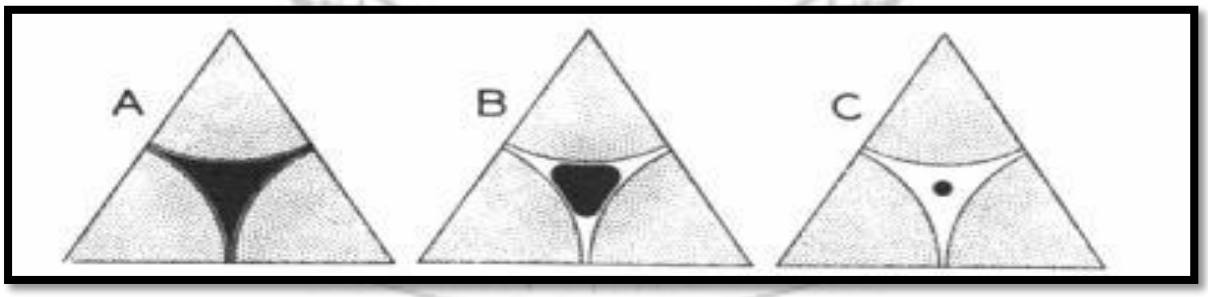

Figure 4.2 None wetting oil (black) and water (clear) in a single water-wet pore modified from Levorsen, (1967).

4.2 Characteristics of Selected Wireline Logging Tools

Wireline logging tools are numerous and new models designed to handle specific logging restrictions. Therefore for the purpose of this study, a few logging tools have been selected for short description of their distinctiveness:

4.2.1 Gamma Ray (GR)

Gamma ray log are designed to measure the natural radioactivity in formations (fig: 4.3). The number of energy of the naturally occurring gamma ray in the formation is measured and distinguished between elements of parent and daughter products of the three main radioactive families Uranium, Thorium and Potassium. In sediments the log mainly reflects clay content because clay contains the radioisotopes of potassium, uranium and thorium. Potassium feldspars, volcanic ash, granite wash and some salt rich deposits containing potassium (e.g. potash) may also give significant gamma ray readings.

Shale free sandstones and carbonates have low concentrations of radioactive materials and give low gamma ray readings. The standard unit of measurement is American Petroleum Institute (API). High gamma ray may often not imply shaliness but a reflection of radioactive sands such as potassium rich feldspathic, glauconitic or micaceous sandstones. Gamma ray log is usually preferred to spontaneous potential logs for correlation purposes in open holes nonconductive borehole fluids for thick carbonate intervals and to correlate cased-hole logs with open-hole logs.

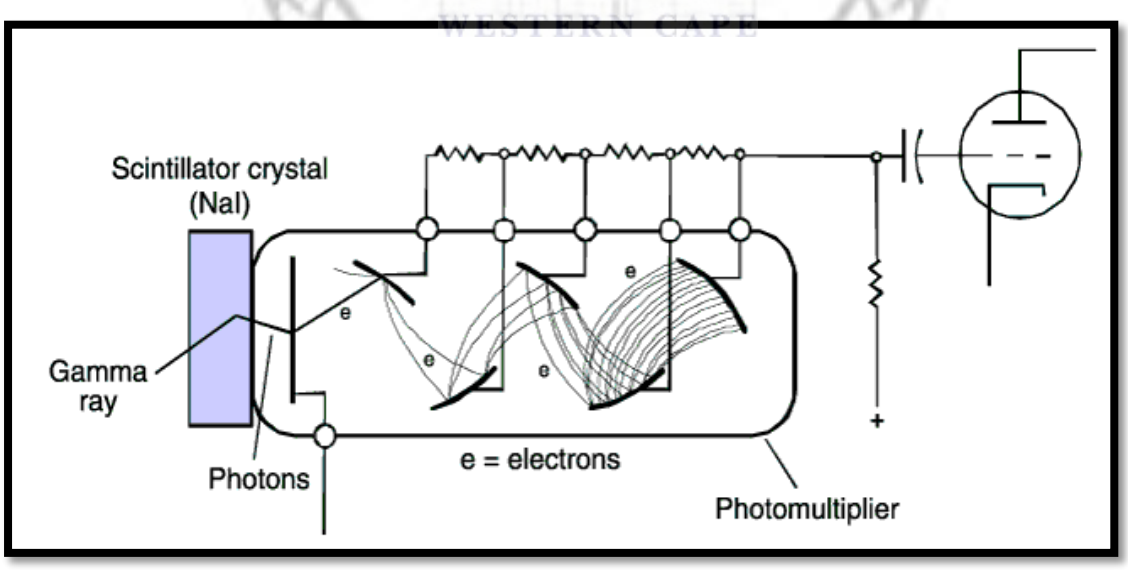

Figure 4.3 Schematic drawing of a gamma ray tool (redrawn from Serra, 1979).

4.2.2 Spontaneous Potential (SP)

Also known as self-potential logs, it measures potential (DC voltage) difference between a movable electrode in the borehole and a distant reference usually at the surface (fig: 4.4, 4.05). The SP results from the measurable voltage drop in the borehole produced by the flow of SP currents generated by electrochemical and electrokinetic potentials in the hole. The SP tends to follow a fairly constant shale base line in impermeable shales while in permeable formations; the deflection depends on the contrast between the ion content of the formation water and that of the following:

i. Drilling mud filtrate
ii. Clay content
iii. Bed thickness and resistivity
iv. Hole size
v. Invasion
vi. Bed boundary effect.

In thick permeable, thick non-shale formations, the SP value approach the fairly constant value (static SP), which will change if the formation water salinity changes. It varies in dirty reservoir rocks and a set of pseudo-static SP value is recorded.

SP is most useful when:

i. Drilling mud is fresher than the formation water
ii. A good contrast exists between mud filtrate and formation water resistivity
iii. Formation resistivity is moderately low.

The SP curve becomes featureless when the mud column becomes so conductive that it fails to display a demonstrable voltage drop which the tool can support SP response of large negative deflection in permeable beds enhances easy sand-shale discrimination, correction and under favourable conditions estimation of formation water resistivity, (Rider, 1996). The SP measuring equipment consists of a lead or stainless steel electrode in the well connected through a millivolt meter or comparably sensitive recorder channel to a second electrode that is grounded at the surface. The SP electrode usually is incorporated in a

probe that makes other types of electric logs simultaneously so it is usually recorded at no additional cost.

Spontaneous potential is a function of the chemical activities of fluids in the borehole and adjacent rocks, the temperature, and the type and amount of clay present; it is not directly related to porosity and permeability. The chief sources of spontaneous potential in a drill hole are electrochemical, electrokinetic, or streaming potentials and redox effects. When the fluid column is fresher than the formation water, current flow and the SP log are as illustrated in Figure 1; if the fluid column is more saline than water in the aquifer, current flow and the log will be reversed. Streaming potentials are caused by the movement of an electrolyte through permeable media. In water wells, streaming potential may be significant at depth intervals where water is moving in or out of the hole. These permeable intervals frequently are indicated by rapid oscillations on an otherwise smooth curve. Spontaneous potential logs are recorded in millivolts per unit of t paper or full scale on the recorder. Any type of accurate millivolt source may be connected across the SP electrodes to provide calibration or standardization at the well. The volume of investigation of an SP sonde is highly variable, because it depends on the resistivity and cross sectional area of beds intersected by the borehole. Spontaneous potential logs are more affected by stray electrical currents and equipment problems than most other logs. These extraneous effects produce both noise and anomalous deflections on the logs. An increase in borehole diameter or depth of invasion decreases the magnitude of the SP recorded. Obviously, changes in depth of invasion with time will cause changes in periodic SP logs. Because the SP is largely a function of the relation between the salinity of the borehole fluid and the formation water, any changes in either will cause the log to change.

Spontaneous potential logs have been used widely in the petroleum industry for determining lithology, bed thickness, and the salinity of formation water. SP is one of the oldest types of logs, and is still a standard curve included in the left track of most electric logs. The chief limitation that has reduced the application of SP logs to groundwater studies has been the wide range of response characteristics in freshwater environments. If the borehole fluid is fresher than the native interstitial water, a negative SP occurs opposite sand beds; this is the so‑called standard response typically found in oil wells. If the salinities

are reversed, then the SP response also will be reversed, which will produce a positive SP opposite sand beds.

Thus, the range of response possibilities is very large and includes zero SP (straight line), when the salinity of the borehole and interstitial fluids are the same. Lithologic contacts are located on SP logs at the point of curve inflection, where current density is maximum. When the response is typical, a line can be drawn through the positive SP curve values recorded in shale beds, and a parallel line may be drawn through negative values that represent intervals of clean sand.

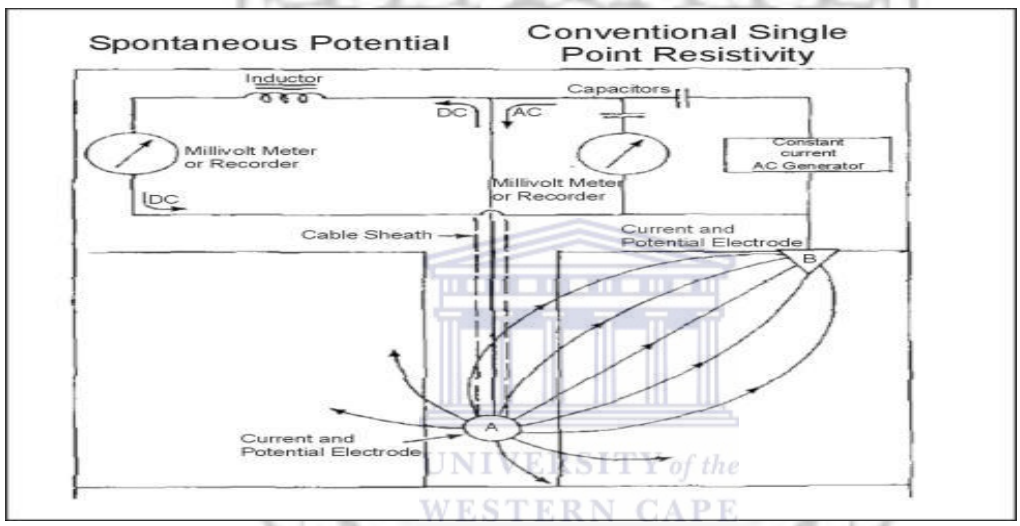

Figure 4.4 Spontaneous potential logging tool modified from Wightman, W. E., Jalinoos, F., Sirles, P., and Hanna, K. (2003).

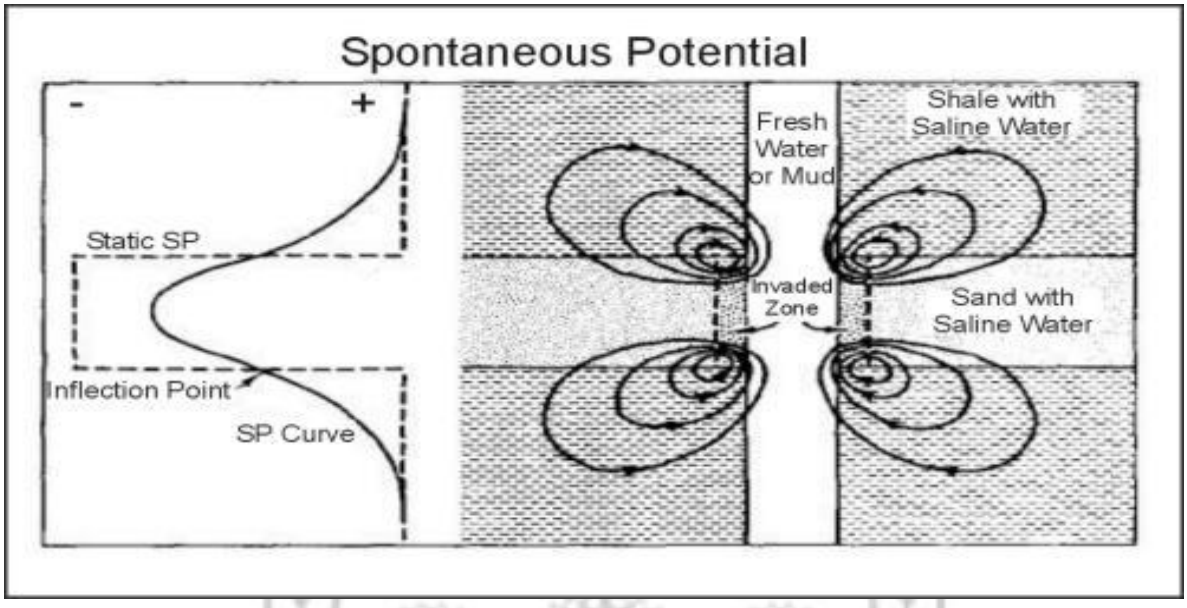

Figure 4.5 Flow of current at typical bed contacts and the resulting spontaneous potential curve and static values. Modified from Wightman, W. E., Jalinoos, F., Sirles, P., and Hanna, K. (2003). http://www.cflhd.gov/resources/agm/

4.2.3 Induction tool

Induction logs are a class of resistivity logs which are recorded in uncased boreholes and involve the application of electromagnetic induction principles for the measurement of formation resistivity or conductivity. It has an advantage of being used in nonconductive borehole fluids such as air, oil and gas in which other electrical resistivity logging tools cannot be easily used. It works well with electrically conductive drilling mud provided the mud is not too saline and the borehole diameter not too large (SPWLA Glossary, 1984-97). Practical induction tools include an array of several transmitter and receiver coils designed to provide focusing and deep investigation to minimize borehole and adjacent formation effect

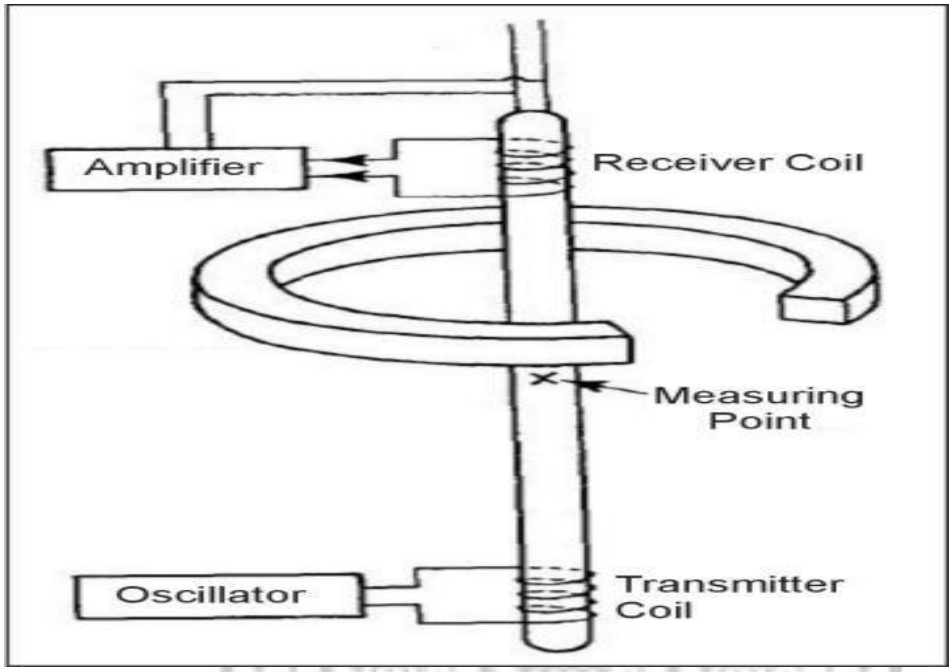

Figure 4.6 Induction equipment modified from Wightman, W. E., Jalinoos, F., Sirles, P., and Hanna, K., (2003). http://www.cflhd.gov/resources/agm/

The transmitting coils emit a high frequency alternating current of constant intensity resulting in an alternating magnetic field which in turn induces secondary current in the formation. The multiple coils are used focusing so that the resistivity measurement is done to minimize the effect of materials in the borehole invaded zone and other nearby formations. The induced current flows in circular ground-loop paths coaxial with the sonde. These ground loop current also generate their one magnetic fields inducing signals in the receiver coils which at low conductivities are essentially proportional to formation conductivity. However at high conductivities, the magnetic fields of the ground-loop currents induce additional eddy currents in adjacent ground loops which are superimposed on those induced by the transmitter coil field. This is referred to as skin effects and affects the reading. Induction tools can be run separately or combined with other devices. Integrated tools such as the induction with a deep depth of investigation (ILD) with another induction device having shallower depth of investigation (ILM) and invaded zone investigative devices (short normal device, short laterolog or spherically focused logging device) are common examples.

4.2.4 Electrode Resistivity tool

The second class of resistivity measuring device is the electrode log. Electrodes in the borehole are connected to a power source (generator) and the current flows from the electrodes through the borehole fluid into the formation and then to remote reference electrode. Examples of electrode resistivity tools include: Normal devices, Lateral logs, Laterolog, Macrolaterolog, Micro log, Proximity log, and Spherically Focused logs.

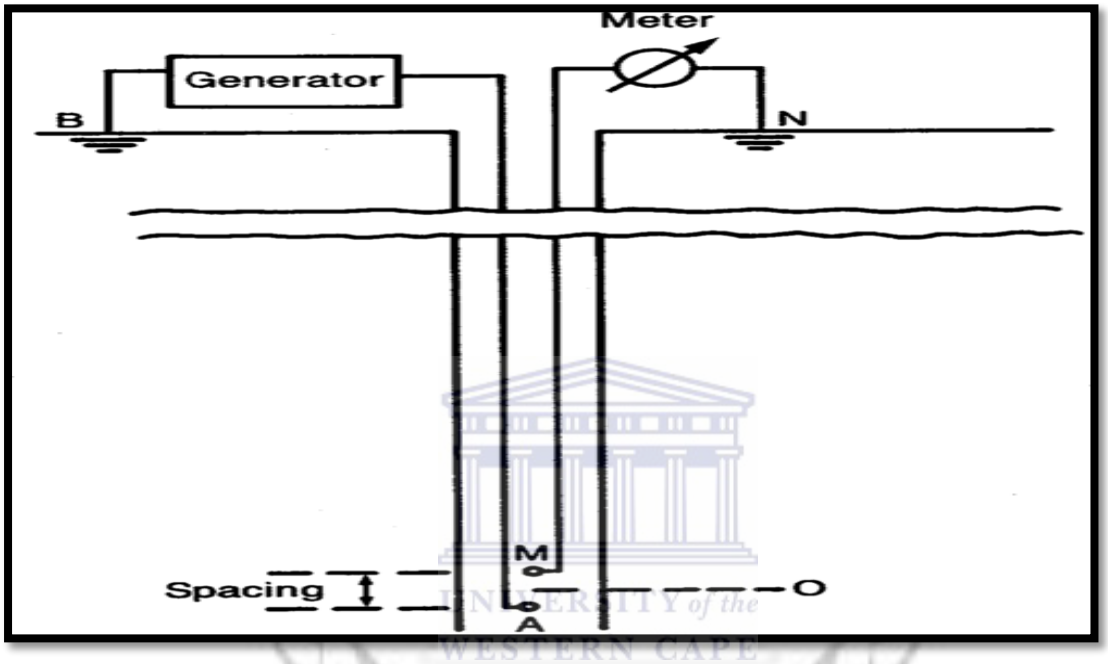

Figure 4.7 Normal device with electrodes Boreholes filled with salt-saturated drilling muds require electrode logs such as Laterolog or Dual Laterolog to determine accurate true resistivity values of the uninvaded zones. (Society of Petroleum Engineer, 2013).

4.2.5 Neutron tool

Neutron logs are porosity logs that measure primarily the hydrogen ion concentration in a formation but also affected by mineralogy and borehole effects. In clean formations where the porosity is filled with water or oil, the neutron log measures liquid-filled porosity. Whenever pores are filled with gas rather than oil and water, neutron reads low values. This occurs as a result of less concentration of hydrogen in gas compared to oil or water. The lowering of neutron porosity by gas is called Gas Effect. The tool contains a continuously emitting source and either be a neutron (neutron-neutron tool) or a gamma ray detector (neutron- gamma tool). High energy neutrons from the source are slowed down by collisions

with atomic nuclei (fig: 4.8). The hydrogen atoms are by far the most effective in the neutron. Hence the distribution of the neutrons at the time of detection is primarily determined by the hydrogen concentration.

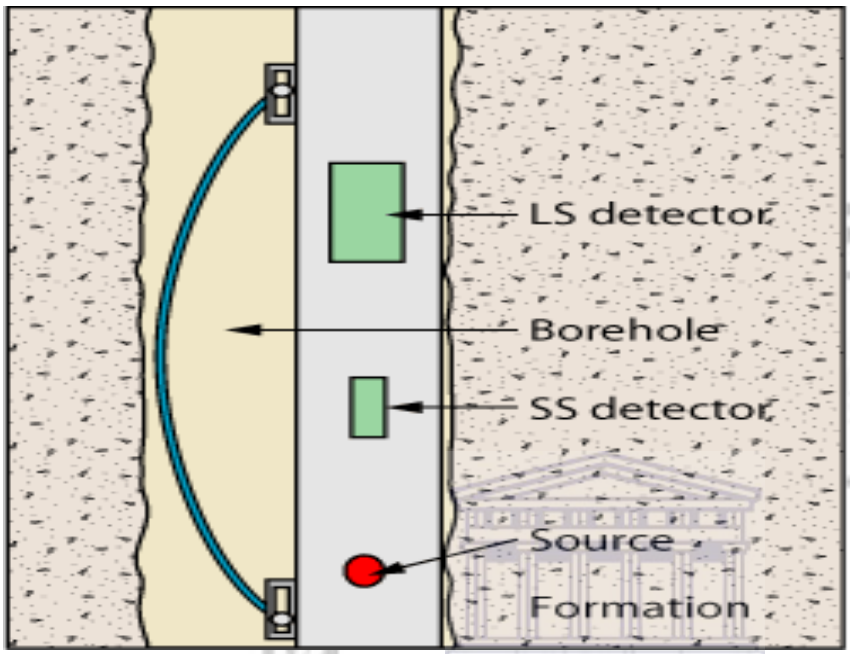

Figure 4.8 Compensated neutron tool drawing. (Society of Petroleum Engineer, 2013).

Neutron log responses vary depending on:

i. Difference in detector types
ii. Spacing between source and detectors
iii. Lithology (i.e. sandstone, limestone and dolomite).

4.2.6 Density tool

This is a well log that records formation density. The logging tool consists of a gamma ray source (e.g. Cs^{137}) and a detector shielded from the source so that it records backscattered gamma rays from the formation depending on the electron density of the formation (fig: 4.9). The formation electron density is proportional to its bulk density. Like in neutron tool

the source and the detector are usually mounted on a skid which is pressed against the borehole wall.

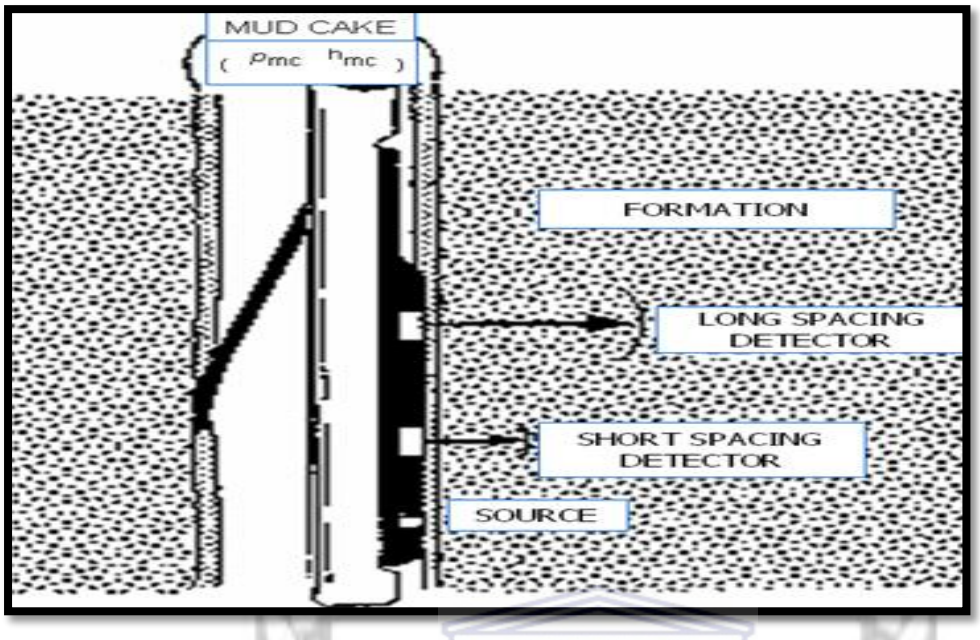

Figure 4.9 Density Log showing the configuration of the source and detectors of a compensated density logging tool. Courtesy of Schlumberger

The compensated density logging tool includes a secondary detector which responds more to the mud cake and small borehole irregularities. The response of the second detector is used to correct the measurements of the primary detector. Density log is applied primarily to uncased holes.

4.2.7 Combination Neutron-Density tool

This is a combination porosity log, besides its use as a porosity device; it is also used to determine lithology and to detect gas bearing zones. Both the neutron and density curves are normally recorded in limestone porosity units with each division equal to either 2% or 3% porosity. Limestone and dolomite porosity units can also be recorded. An increase in density porosity occurring with a decrease in neutron porosity indicates a gas bearing zone usually referred to as Gas Effect. Gas Effect is created by gas in the pore as it caused the density log to record too high a porosity (i.e. gas is lighter that oil or water) while the

neutron log record too low a porosity reflecting lower concentration of hydrogen atom than oil or water.

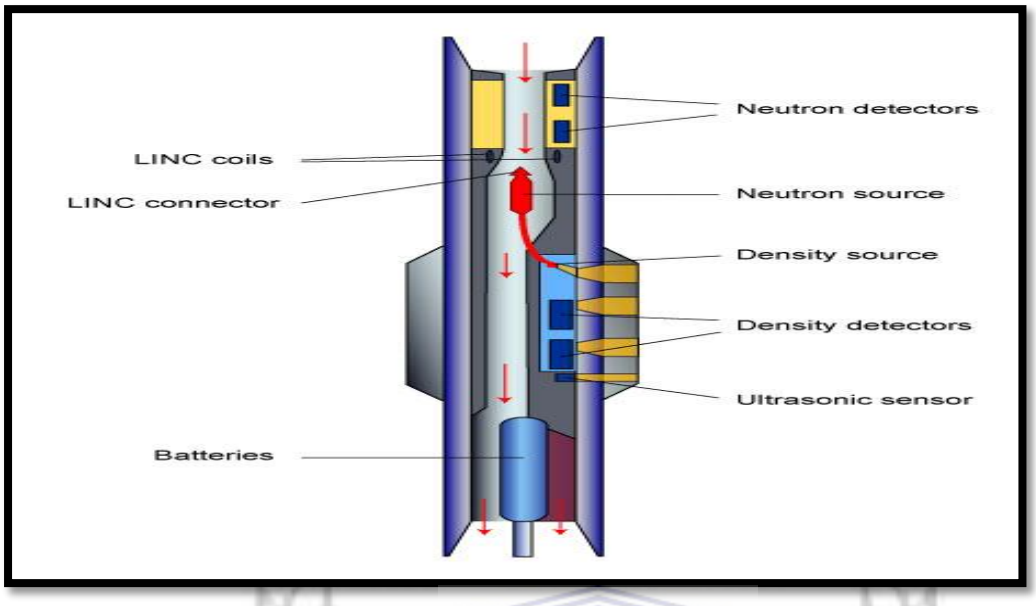

Figure 4.10 A combination neutron/density tool.
(http://iodp.ldeo.columbia.edu/TOOLS_LABS/LWD/lwd_adn.html)

4.2.8 Sonic tool

A sonic log measures interval transit time (Δt) of a compressional sound wave in feet per second and hence a reciprocal of the compressional wave velocity. The sonic log device consists of one or more transmitters and two or more receivers (fig: 4.11). The time for the acoustic energy to travel a distance through the formation equals to the distance spanned by the two receivers is the desired measurement and the unit expressed as microseconds per foot. The interval travel time can be integrated to give the total travel time over the logged interval. Borehole compensated sonic log consists of two transmitters located above and below the receiver which are pulsed alternately to produce an improved log. Errors due to sonde tilt or changes in the hole six are minimized by averaging the measurements.

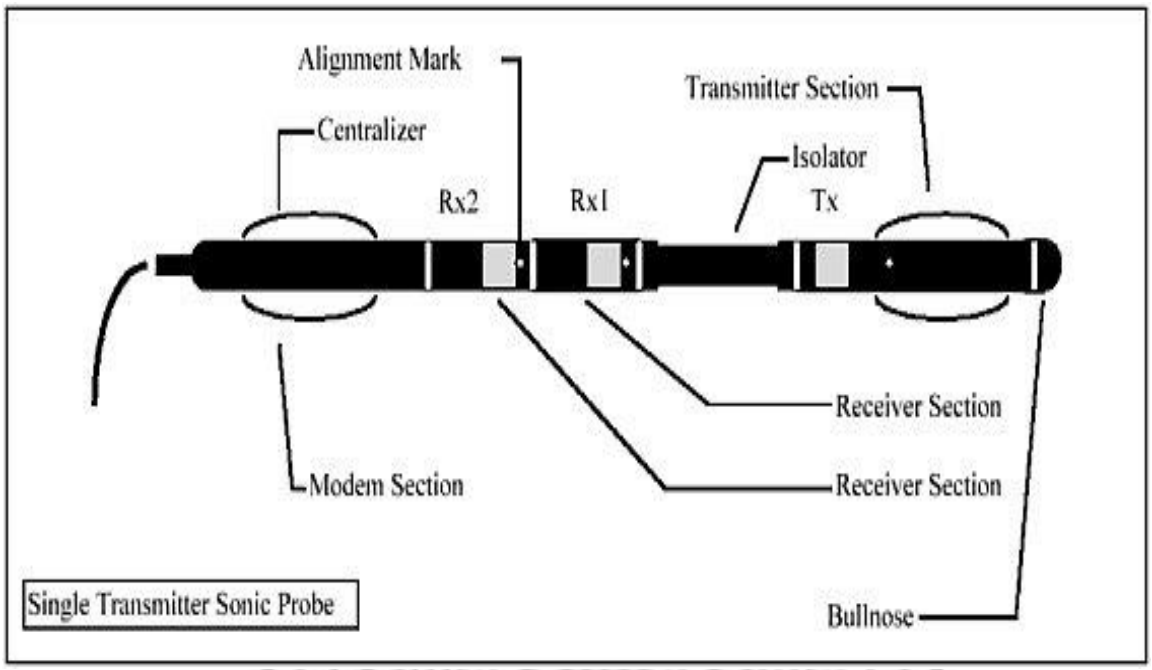

Figure 4.11 Sonic logging tool modified from (http://terraplus.ca/products/borehole/sonic-probe.aspx)

The sonic log is used in combination with other logs (e.g. density and neutron logs) for porosity, shalyness, and lithology interpretation. Integrated transit time is also helpful in interpreting seismic records. A simpler but efficient approach is taken to evaluate the core using a measuring tape, a hand lens and a digital camera was used to be able to compile imperative information from the cores such as:

i. Mineral inhibition
ii. Grain size distribution
iii. Changes in facies
iv. Fining sequences
v. Contacts between facies successions
vi. Environments of deposition
vii. Sequence alternation
viii. Fluid alteration.

Most importantly the structure implications of the granulation distribution as well as the facets of compartmentalization within the different core sections. The granulation had no

specific orientation within the cores and in some areas they were chaotic and occurred as areas which were highly fractured. During the investigation it was discovered that the granulated beds actually accompanied a distinct sequence, which in this case was shale unit ranging sizes which stretched straight through all the cores. This shale layer stepped up or down within a few meters within the cores.

5 CHAPTER

5.1 Petroleum geochemistry of the Bredasdorp Basin and adjacent Basins

The Bredasdorp Basin and adjacent Southern Outeniqua Basin contain all the factors usually considered necessary for hydrocarbon prospective namely:

(i) Source rocks that have demonstrated expelled hydrocarbons

(ii) Conduits for hydrocarbons migration and reservoiring (i.e. continuous sandstones and fault-connected sandstones) exist several levels in the basin

(iii) Sandstones retain enough original porosity (or have diagenetically-enhanced porosity) to reservoir large volume of hydrocarbons

(iv) Many of these sandstones are over and underlain by claystones which are locally over-pressured capillary seals preventing escape of hydrocarbons

(v) Several families of hydrocarbons have been reservoired and can be correlated to nearby source rocks.

Relevant aspects of each of these factors will be addressed in this section whilst the samples and analyses are discussed subsequently.

5.1.1 Source rock

Source rocks have been define as “a volume of rock that has generated, or is generating, and expelling hydrocarbons in sufficient quantities to form commercial oil and gas accumulation” (Brooks et al., 1987). A potential source rock is one which “could generate hydrocarbons given the right conditions” (Brooks et al., 1987). Other authors omit the commercial reference but comment on maturation, e.g., “rocks containing sufficient organic matter of a suitable chemical composition to generate and expel hydrocarbons at appropriate maturity levels” (Miles, 1989). In order to be a viable source rock, the quantities of hydrocarbons which can be (or have been) generated must exceed the amount necessary to fill a portion of the pore spaces in the source rock and satisfy the adsorbency of the maceral grains before expulsion can commenced. Indeed many source rock definitions include comment on the both the quantity of sedimentary organic matter and the amount

of hydrocarbons generated. Source rocks can form in both non-marine (fluvial and lacustrine) and marine detrital environments and can be clastic-dominated or carbonate-rich and biogenic-dominated.

5.1.2 Source potential of clastic lithologies

Clastic rocks are fine-grained, clay-rich sediments combining larger than average quantities of organic matter. Clay-rich rocks are generally only considered to be potential source rocks if the total organic carbon (TOC) content exceeds 1% by weight (Tissot and Welte, 1984). Since the average organic carbon content of several of these fine-grained sediments is <1% by weight, they are considered potential source rocks (Ronov, 1958; Dow, 1977). This cut-off is an empirical one, based on data from various studies which show that sedimentary rock with TOC contents less than this, even though they may generate hydrocarbons, do not expel them in any significant quantity. This is largely because smaller amounts or organic matter are generally widely dispersed through the rock and not concentrated in one region. In practice, effective source rocks often contain >2% TOC and may even exceed 10%, e.g. Bakken Shale (Welliston Basin, Canada) and Kimmeridge Sahle (North Sea). It is also shown (Ronov, 1958; Dow, 1977; Demaison and Moore, 1980) that many non-source argillaceous sediments contain <<1.0% TOC and that the difference between TOC contents in prolific source rocks and no-source rocks can be greater than an order of magnitude. Large amounts of organic matter, suitable to form source rocks, can be concentrated in clastic sedimentary rocks as a result of three processes:

(i) Enhanced preservation
(ii) High organic productivity
(iii) Sediment starvation

Considerable study has taken place during the past two decades in attempting to understand the relative importance of each TOC enhancement process.

5.1.3 Enhanced preservation of organic matter.

Enhanced preservation is due mainly to the development of anoxia. In low oxygen environments, there are few organisms at the sea-floor or in the topmost sediments which can scavenge organic material (Demaison et al., 1988) hence; the organic matter content of sediments preserved under such conditions is higher than in oxidising environments. Anoxia can develop regionally for a number of reasons but dominates in one of two main depositional settings:

(i) Restricted circulation due to the presence of a barrier (such as a landmass) to open ocean circulation. (Fig.5.1)

(ii) Water stratification due either to the development of a halocline or separate water masses having different temperature (Fig. 5.2).

5.1.4 Enhanced productivity of organic matter

Pederson and Calvert (1990) showed that biogenic decomposition of organic matter occurred at the same rate whether the seafloor conditions were oxic or anoxic.

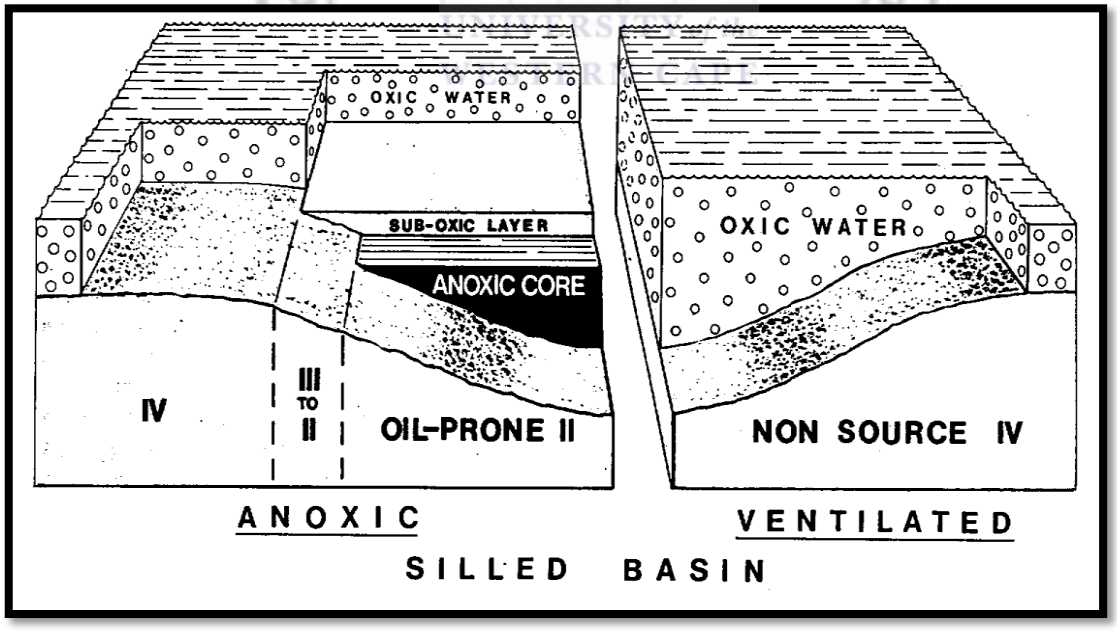

Figure 5.1 Schematic sections through anoxic and ventilated silled basin (from Demaison et al., 1988).

The anoxic basin has a core in which oxygen levels are low. In such situations, organic matter generation is high in the surface waters and its presentation through the passage from sea level to sea floor is enhanced because of the limited scavenging of organisms. Hence high proportions of organic matter, in particular high hydrogen material are preserved.

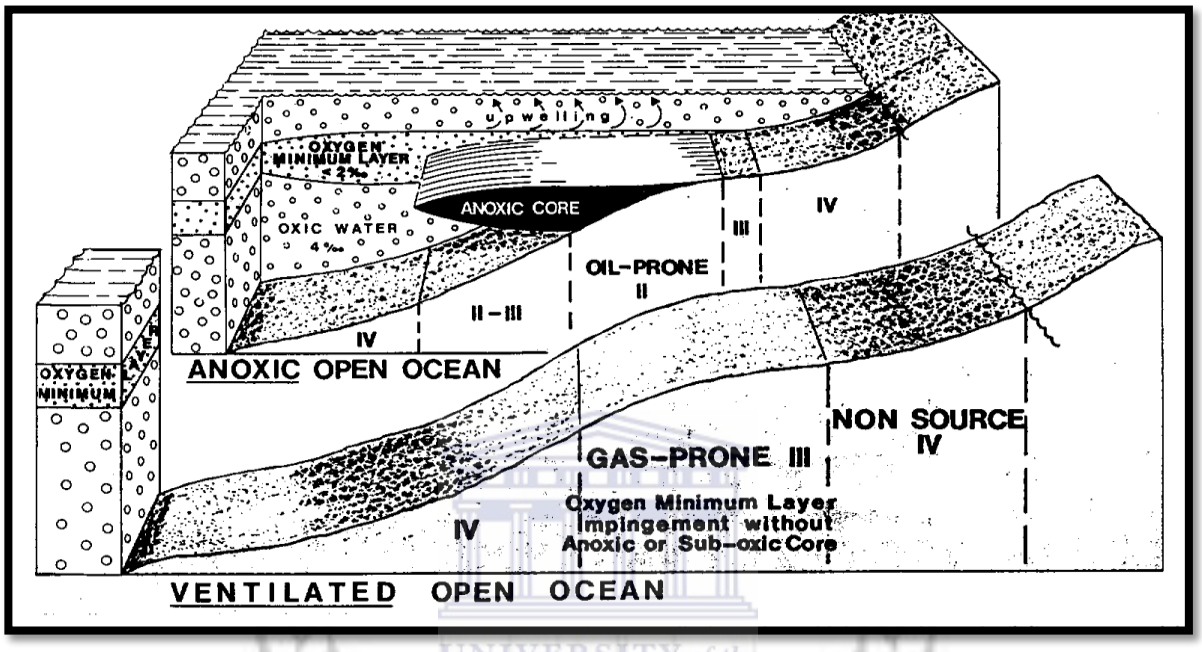

Figure 5.2 Schematic section through a basin in which open ocean circulation prevails but where high organic productivity occurs and bacterial decay is enhanced which results in development of an oxygen minimum layer (after Demainson et al., 1988).

Where this impinges on the basin floor and margins, or even where it closely approaches these regions, scavenging destruction of the most lipid material is largely prevented. Large amounts of high hydrogen organic matter becomes deposited and incorporated in the sediments. In this situation, and mixed oil and gas prone zone is commonly found seaward of the main oil prone (oxygen minimum), zone. They favour a model which relies on an increased organic productivity to result in the formation of source rocks. In this model, the oxygen minimum is located in the mid-water column (rather than at the sea floor) and organic-rich sediments are deposited directly beneath it. One such location where this commonly occurs is in mid-latitudes (i.e. 30-40^{0}S and N) where a large temperature

difference exists between deep oxygen-poor bottom water and oxygen-rich surface water. This results in a relatively stable water column with essentially no mixing (Denainson et al., 1988). At the contact between these two layers, a prolific food-chain develops and oxidation of the resulting large amounts of organic material uses up the free oxygen in the water resulting in a low oxygen layer (Fig. 5.2). This is occasionally enhanced where trade winds blow continuously on the south-western side of southern hemisphere continents. Warmer surface waters are forced westwards, cold water wells up from below and the waters mix, so that in the nutrient-rich water, an explosive organic growth results. Decay processes, operating with consumption of the organisms by bacteria and plankton, uses up oxygen in the water column and 'blooms' of phytoplankton occur. This effect is likely to result in high concentrations of organic matter entering the sediment cycle partly because the scavenging organisms are overwhelmed by the large amounts of organic matter and cannot reduce it. Demaison and Moore (1980), however suggested that periodic wholesale mixing of water column, thought to be responsible for much of the source rock deposition, is likely to occur where there is a stable warm upper-water surface column.

Under those conditions, the high rate of input of organic matter to the bottom water is exacerbated during overturning events when high-oxygen, nutrient-rich, cold bottom-water upwells and biotic blooms occur. Assuming present climatic conditions prevailed, the early Cretaceous Palaeo-lacation of South Africa at `55^0S (McMillan, 1986) places the continent in a cool surface water environment where continuous mixing is likely, which would result in the development of a large scavenging community in the water column and at the sea floor so that periodic development of anoxia would not occur. Pederson and Calvert (1990) consider that these conditions may not have been operative in South African waters during the Late Jurassic and Early Cretaceous because open marine conditions had not developed.

However, once the continents had separated enough to allow establishment of open marine condition, during the Mid-Late Cretaceous and even into the Tertiary (Frakes and Kemp, 1972), such stability would occur. Under the greenhouse conditions prevailing in Mid-Late Cretaceous, stable warm water column extended further south (Barron, 1983; Pederson and Calvert, 1990) and water-column mixing was less regular, resulting in periodic development of biotic blooms which, where preserved resulted in source rock formation. Cornford et al., (1986) suggest that the Kimmeridge Shale may be an example of this type of source rock

and it is thought that the Hauterivian-Aptian sources in the Bredasdorp Basin also represent such an example.

5.1.5 Sediment starvation

Lautit et al., (1989) shows that organic carbon enrichment and source rock development usually occur during periods of highstands associated with sediment starvation episodes. Burden (1992) therefore suggested that the 13A source rock interval was deposited during a period of sediment starvation. However, the average sedimentation rate of this source sequence (SOEKOR unpublished biostratigraphic data) is ~47m/Ma (using the time scale of Haq et al., 1987) which does not indicate any significant sediment starvation. By way of contrast, in the northern part of the North Sea, the richest source shales are approximately 200m thick (Bailey et al., 1990). They were deposited during the Brent and Early Heather periods, which Thomas et al, (1985) show to extend from Bajocian through Callovian (i.e.~18 Ma). This indicates a sedimentation rate of about 11m/Ma, typical of that in periods of sediments starvation (Loutit et al., op cit.). In the Bredasdorp Basin, the Turonian source rock interval was deposited at an even lower sedimentation rate (~7m/Ma) suggesting sediment starvation as the prime cause. However, the existence of intervals of sediments starvation (typified by condensed sequences) without source rock development (Benson et al., 1993) demonstrates that starvation does not always ensure source rock development.

5.1.6 Source potential of carbonate lithologies

Carbonate sediments deposited in shallow, warm-water, low-oxygen environments are common world-wide and often prolific source rocks. Their kerogen is often comprised of finely disseminated amorphous material with a high oil potential. The Bredasdorp Basin has been a deep, cool-water mud-rich basin (McMillan et al., 1997) and contains little carbonate sediment except in the Tertiary. In those carbonates, source potential is uniformly low.

5.1.7 Other factors

Whichever model of source rock development is more likely, if indeed is possible to select one or the other- the conditions responsible for their formation were enhanced by the following additional factors:

(i) The period of major development of Mid-Cretaceous source rocks has been correlated with sea level fluctuations, Palaeo-surface temperature maxima and the 'Long Cretaceous Normal' magnetic non-reversal period. All of these can be related to periods of increased mantle activity and initiation of plume generation (Veevers, 1990; Larsen, 1991) and related increases in carbon recycling from the mantle. These result in a propensity of Mid-Upper Mesozoic sedimentary rocks to be organic-rich.

(ii) Pederson and Calvert (1990) and Larson (1991) also demonstrate that with the high CO_2 contents though to have dominated during the Mesozoic (Barron and Moore, 1993) a global 'greenhouse' could have prevailed. This would have resulted in higher water temperatures. Warmer water tends to have reduced oxygen levels resulting in sediments being deposited in a dominantly low oxygen environment with fewer bottom-living organic matter scavengers.

(iii) Pederson and Calvert (1990) also suggest that globally, wind speeds would have been higher because of enhanced Hadley cells. This could result in increased influx of moist air from high latitudes to the tropics and hence globally, rainfall would have been higher. This generally moister climate would be enhanced in Southern Africa by the presence of the Cape Fold Belt Mountains which acted as an obstacle to the northward movement of these air masses. These conditions would result in greater plant growth and increased runoff resulting in larger inputs of terrigenous organic material to the marine environment, which would become more organic-rich. In offshore basins, all sediments contain some terrigenous material. Sediments deposited during the syn-rift period are generally coarse and oxidised so that remnant organic matter tends to be only the most refractory material.

Indeed, many of the sediment intersections contain wood in the form of tree trunks or fragments of wood (Du Toit, 1954, p. 374-387; McLachlan and McMillan, 1979). Where recognised in the onshore Algoa and offshore Bredasdorp Basins, lacustrine rocks contain remnants such as reeds and limnological fauna. Sedimentary rocks preserved from post-rift

periods, especially Mid-Cretaceous, locally contain woody material (Du Toit, 1954, p. 393-395) and thick coals are developed (wells 3 and Ga-D1, Davies, 1979). A significant proportion of organic material in the marine sediments is also shown optically or chemically to be terrigenous. Much of this material probably comes from a coastal vegetated belt, similar to the present, as Du Toit (1954, p. 408) shows that most the interior of the continent was relatively dry throughout the Late Mesozoic.

5.2 Types of organic matter and their products

There are four main types of detrital organic matters found in source rocks:

(i) Refractory (e.g. inrtinite or vitrinite) with low hydrogen

(ii) Structured (lipid-rich, e.g. algal, exinite) fluorescent, high hydrogen

(iii) Amorphous/sapropelic (e.g. lipid-rich), fluorescent, high hydrogen

(iv) Amorphous (low hydrogen, non-fluorescent), low hydrogen.

The relative proportions of these four types of organic matter determine the source potential.

(i) Refractory organic matter is comprised largely of condensed, polycyclic aromatic rings with few alkyl groups and little hydrogen so they cannot be readily converted to hydrocarbons. They also require high activation energy to crack their condensed structures and tend to mature later than aliphatic material. Such material is generally terrigenous, being mainly comprised of cellulose-rich woody material rich in oxygen. Most woody material is deposited in near-shore estuarine and deltaic-continental environments where plant input is high and sediments reworking common both contributing to continual attack by scavengers. Woody material has a high preservation potential because it has few chemically reactive moieties hence the lipid fraction is generally removed from the material leaving the highly condensed core of the lignin. If this kerogen has any source potential, it is largely for gas although some forms of terrigenous material can generate waxy oil (Fleet and Scott, 1994).

(ii) Structured high-hydrogen material generally comprises exinite (e.g. spores, pollen) and has the potential to generate wet gas and oil. Algal material, which is also structured but often only in the form of flowed structures, has a very high oil potential.

(iii) Amorphous organic material is usually assumed to be high-hydrogen forms such as bacterially altered marine organic matter. This is formed under low oxygen conditions where anaerobic bacteria reduce sulphates and oxygenated organic matter for oxygen and deposit the sulphur as H_2S, pyrite or other metal sulphides. Thus these amorphous sapropelic claystones are often black partly from the finely disseminated organic matter and partly from the presence of sulphides. In the oil window, this material fluoresce which distinguishes it from low-hydrogen material.

(iv) Low-hydrogen amorphous material is commonly found only where humid acids are incorporated into the sediment in large volumes. Even where matured into the oil window, this material does not fluoresce, by contrast with high-hydrogen material. Fluorescence is therefore only used to differentiate the two types in the oil window. In the absence of first cycle vitrinite, this maturity level can only be determined from chemical parameters, such as Tmax, production index and extracted hydrocarbon GC's and other optical parameters such as TAI, spore fluorescence.

5.3 Distribution of organic-rich sediments in Bredasdorp Basin

In the oxygen minimum model, the basin would be expected to have a band of source rock around the edge of the basin coinciding partly with the intersection of the oxygen minimum layer and its shadow with the sea floor. Hence, where source rocks are present mainly in the basin centre this provides support for the restricted anoxic basin model; it lends support to the oxygen minimum model. Where source rocks are only locally developed (and not restricted for tectonic reasons) it could indicate the local sediment starvation model. Each of these three types of source rocks are found developed in the marine drift sediments in the Bredasdorp Basin. Isolated half-graben infilled with clastic non-marine sediments characterised the pre-rift sedimentation. In some of them, lacustrine argillites are found, and in two wells, DWK-1 onshore (Davies et al., 1991) and well 89 offshore, these locally possess oil source potential.

Marine source rocks are associated with rapid sea-level rise and continental shelf flooding during which explosive colonisation of hitherto exposed (nutrient-rich) shelf occurred. Yet the rate of subsidence needed to generate each sequence boundary I far greater and far more rapid than could be accounted for by regional thermal decay and probably indicates a tectonic influence. In general, each post-rich transgression extended further landward culminating in the Turonian when sea-level advance reached a maximum. Under these conditions, increasing distance from the sediment input results in sediment starvation which in turn leads to increased proportions of organic matter incorporated into the sediment.

The general trend of rising sea-level through the Early and Mid-Cretaceous may be related to post-rich thermal decay which gradually lowered level (Haq et al., 1987). Hence most source rocks are formed partly as a result of sediment starvation. After deposition, diagenetic alteration of the organic material in the first few hundred metres of burial reduces most of the oxygenated functional groups and converts most hydrolysable material to polycondensed macro-molecules, while micro-organisms recycle amino acids and sugars. Below these depths, the resulting organic material has a much higher preservation potential than detrital organic matter and is referred to as kerogen (Tissot and Welte, 1984).

The type of hydrocarbons generated and expelled classify the source rocks as “oil-prone”, “wet gas-prone” and “dry gas-prone”. In general, all source rocks generate both oil and gas but in different proportions, e.g. oil represents 60-70% of the hydrocarbons generated by oil-prone (i.e. sapropelic) source rocks but only ~ 5% of the products of dry gas-prone (i.e. refractory) source rocks.

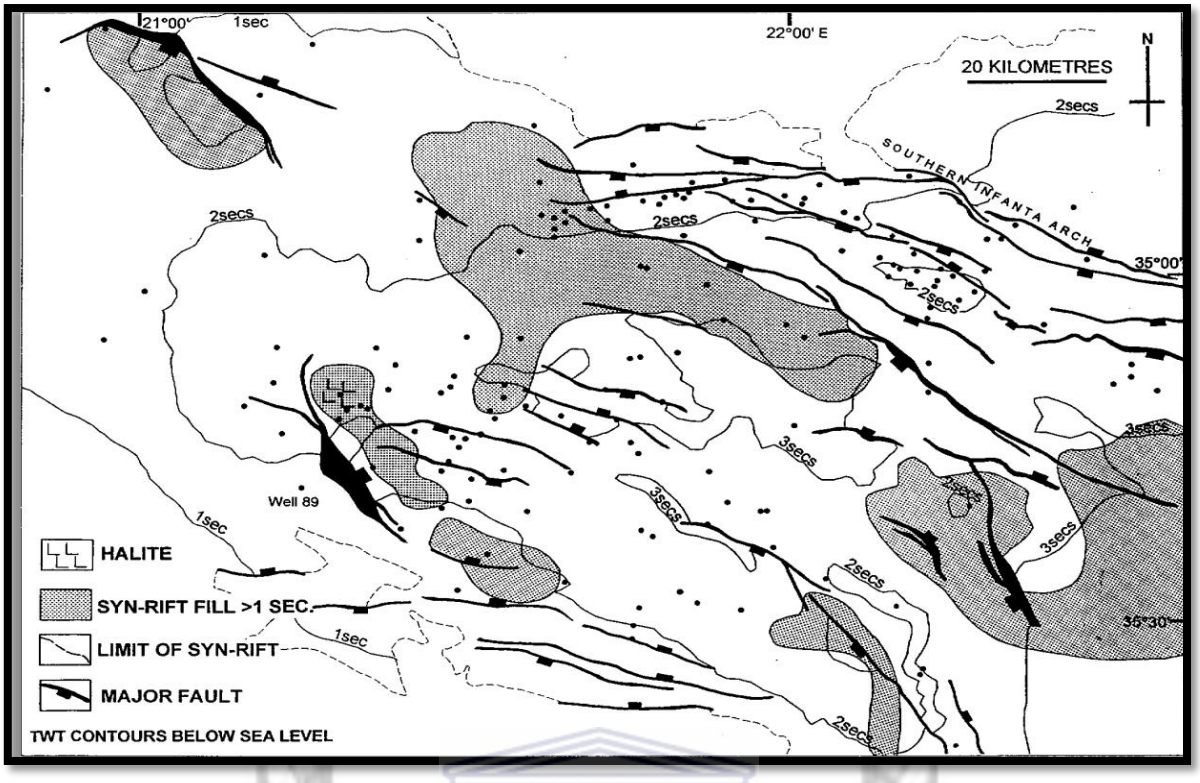

Figure 5.3 Two-way time control map to horizon 1At1 in the Bredasdorp Basin showing the graben in which syn-rift sediments exceed 1500ms in TWT thickness (from Burden, 1993).

5.4 Distribution of organic-rich sediments in Southern Outeniqua Basin

As the western part of this basin lie immediately down-dip of the Bredasdorp Basin, mature organic-rich rocks could act as sources for hydrocarbons in the Bredasdorp Basin. Predictions of source rock development can be made based on the known distribution of source rocks in the surrounding basins, their regional synchronicity and their matching seismic signatures, namely a high impedance contrast with the super-and subjacent rocks. In addition, DSDP wells on the Maurice Ewing Bank, east of the Falkland Islands, which was conjugate with Outeniqua Basin, also contain matching Aptian and Upper Jurassic source rocks. There is no reason to suppose they were not deposited in the Southern Outeniqua Basin when the landmasses were in contact. However, as no wells have yet been drilled in this basin, discussion of source rocks there is speculative.

5.5 Chemical and optical analyses

The minimum amount generally regarded as necessary to constitute a source rock is TOC 1% (mass). For convenience, this is usually measured by combustion (e.g. using a LECO instrument) although a wet chemical process (Loring and Rantala, 1992) was used for some of the earliest analyses. An estimation of the quantity of kerogen can be made from the amount of material recovered during the kerogen separation process, but this depends largely on which processed fraction is used. Of equal importance to the study of quantity and quality are: (i) there type of organic material, as this must be able to generate hydrocarbons within the oil or gas windows and (ii) its thermal maturation, which determines the depth at which hydrocarbons are generated. Fine-grained sediments generally contain larger proportions of hydrogen-rich organic matter (e.g. sapropels) and constitute source rock for oil, in contrast with coarse-grained rocks (e.g. silts) in which the organic carbon is generally refractory, hydrogen-poor, (e.g. vitrinite) and largely gas-prone (Tissot and Walte, 1984).

The character of the organic matter is often best determined from optical studies in which the kerogen is separated from the mineral matrix (by acid dissolution of the minerals) and studied under transmitted light. Structurally distinct hydrogen-rich material (e.g. spores, algal masses) or amorphous matter, usually fluoresces except where over-mature. As the material is matured, hydrogen-rich chemical compounds are generated and the organic matter becomes less hydrogen-rich hence any evaluation of the potential of source rocks should be carried out in conjunction with maturity analyses. The hydrogen proportion can also be estimated from chemical analyses using the Rock-Eval method. This is a method which requires minimal sample work-up and is carried out routinely on all samples. Chemically, hydrogen-rich macerals have high S2 (remaining hydrocarbon potential) and low S3 oxycarbon (≡ carbon dioxide and monoxide) potential at low maturity, whereas structured low-hydrogen high-oxygen macerals (e.g. vitrinite, inertinite) have low S2 and high S3 values. The ratio S2/TOC is the hydrogen index (OI) a measure of the oxygen content of the kerogen. Rich source rocks, including some coal kerongens (Espitalié et al., 1985; Fleet and Scott, 1994) have original HI values in excess of 400. This figure reduces with increasing maturation as hydrocarbons are generated and expelled but some are retained as increased S1.

A further analytical approach used with immature samples is that of kerogen kinetic analysis. The results of these analyses provide not only a detailed understanding of the chemical kinetic break-down rate of the organic material but also the maturation levels at which that occurs. A detailed description of the hydrocarbon characteristics of source rocks is summarised in Tissot and Welte (1984) and Brooks et al., (1987). During maturation, the kerogen breaks down at characteristic rates initiated above specific energy thresholds. These break-down characteristics have been measured on a number of samples using a Rock-Eval 2 instrument. The results of these analyses are used in the hydrocarbon generation modelling carried out for this study (table 5.1).

5.6 Log character

Source rocks are often recognisable by their geophysical log characteristics. For example higher-than background log responses, i.e. gamma log (+10 API), slow sonic travel time (commonly accentuated by compaction disequilibrium and overpressure) (+15µsec/ft), high resistivity (+2-5Ω/m) and lower density are common in source rocks (Cornford, 1986; Davies, 1990; Van der Spuy, 1991; Creaney and Passey, 1993). The common paucity of accurately located samples in wells (e.g. sidewall cores and cores frequently leads to a reliance on log character to extrapolate between samples.

5.7 Seismic character

Marine source rocks are usually found in sediments deposited in specific deep marine environments (e.g. overlying transgressive system tracts tracts and in basal highstand tracts) and these often have a characteristic and recognisable seismic signature (Loutit et al, 1989). As a result of their slower time and lower densities (because of the organic matter contents and the commonly high proportions of under compacted clays) they often show strong impedance contrasts with normally compacted and organic-poor beds above and below. This results in the characteristic “tramline” response i.e. high contrast parallel reflectors enclosing a low contrast interval (Brink et al., 1991). Indeed source rocks distributions in the distal Bredasdorp and Southern Outeniqua Basins are largely extrapolated from adjacent wells using this aspect. However, the distinction of source rocks near the edge of the basin is

made more difficult because sequences thin below seismic resolution, by onlap, offlap and erosion (Beamish, 1990).

5.8 Measurement of source potential

Estimates of the proportions of different macerals, essentially proposed by Correia and Peniguel (1975) are used to evaluate the quality of the organic matter. The fourfold subdivision used, with certain diagnostic chemical parameters, is given in (Table 5.2) below.

5.9 Bredasdorp Basin source rocks

Source rocks have been intersected in wells in the Bredasdorp Basin in each of the major sequences as shown in (Table 5.2).

5.9.1 Syn-rift source rock (Late Jurassic)

Syn-rift source rocks have been intersected in only one offshore well (# 89) in the Bredasdorp Basin and in one onshore well (DWK/1) in the Haasvlakte graben an onshore extension from the western end of the Bredasdorp Basin. In these wells, thin intervals of interbedded lacustrine source rocks and coaly silts were intersected in each case totalling <20m. TOC contents vary from 1-3% and in many samples; a large proportion of the organic matter is amorphous although bottryococcus masses do occur (Davies it al., 1991). In well 89, the WG-OIL prone lacustrine shales have a total thickness of 13m spread over a 70m section, i.e. ~20% of the whole interval has source potential (Table 5.4). Potential ranges up to ~20 kg/tonne rock (HI=764) but averages 7 kg/tonne (HI=523). The few data points plot in the type 1 region of the HI vs Tmax plot. (This plot style, commonly called the Espitalié plot, was pioneered by Espitalié et al., 1977). The maturation level is recorded at R_0~0.8%.

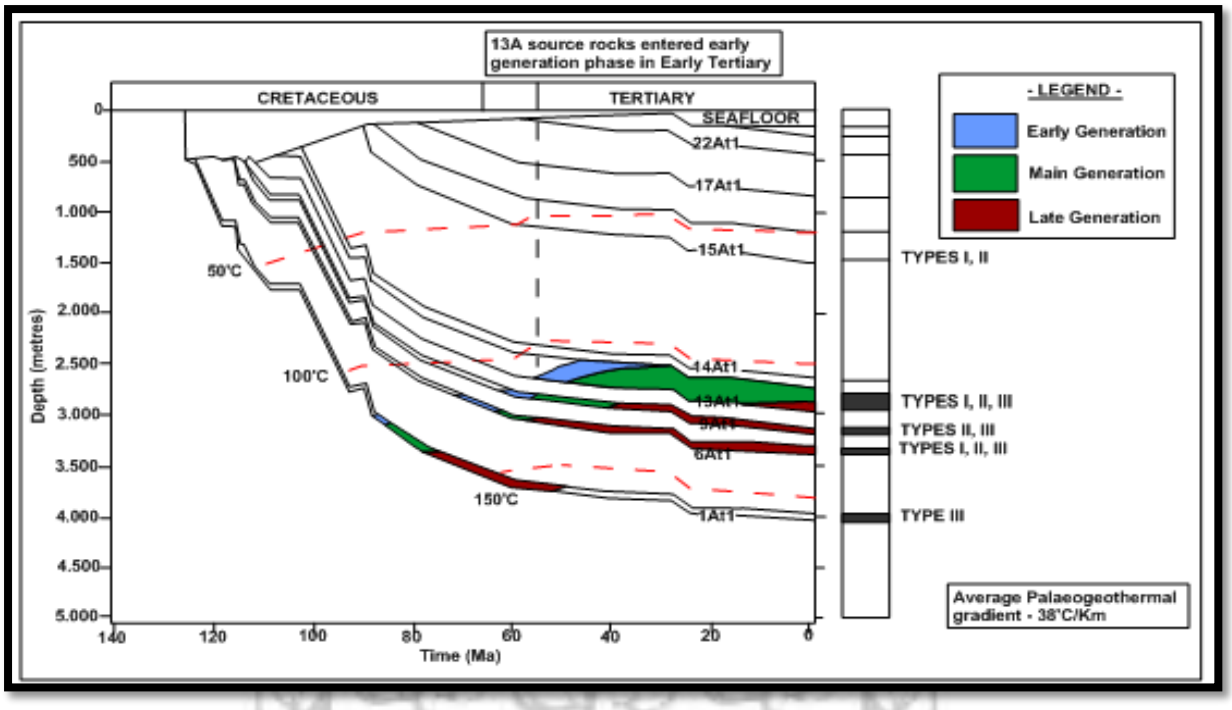

Figure 5.4 Schematic diagram showing Burial history graph for Bredasdorp Basin. Modified after Soekor (1994).

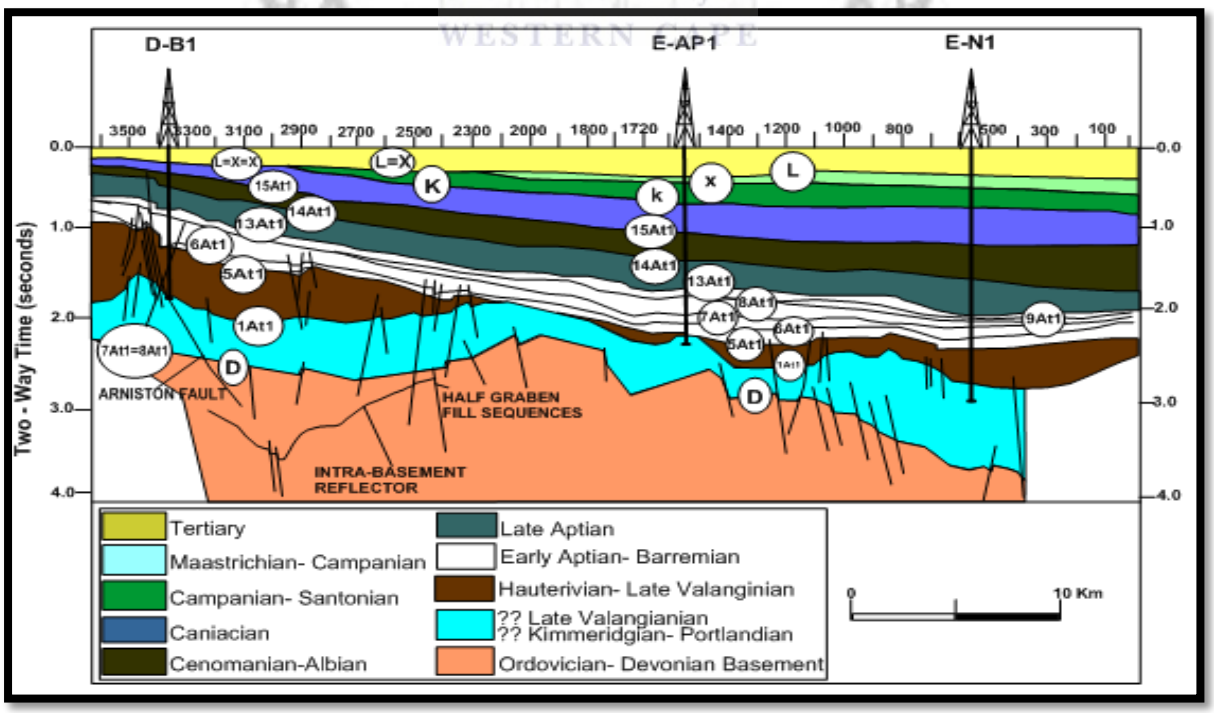

Figure 5.5 Schematic diagram showing seismic section A-A and geological interpretation across the Bredasdorp Basin. Modified after McMillan et al. (1997).

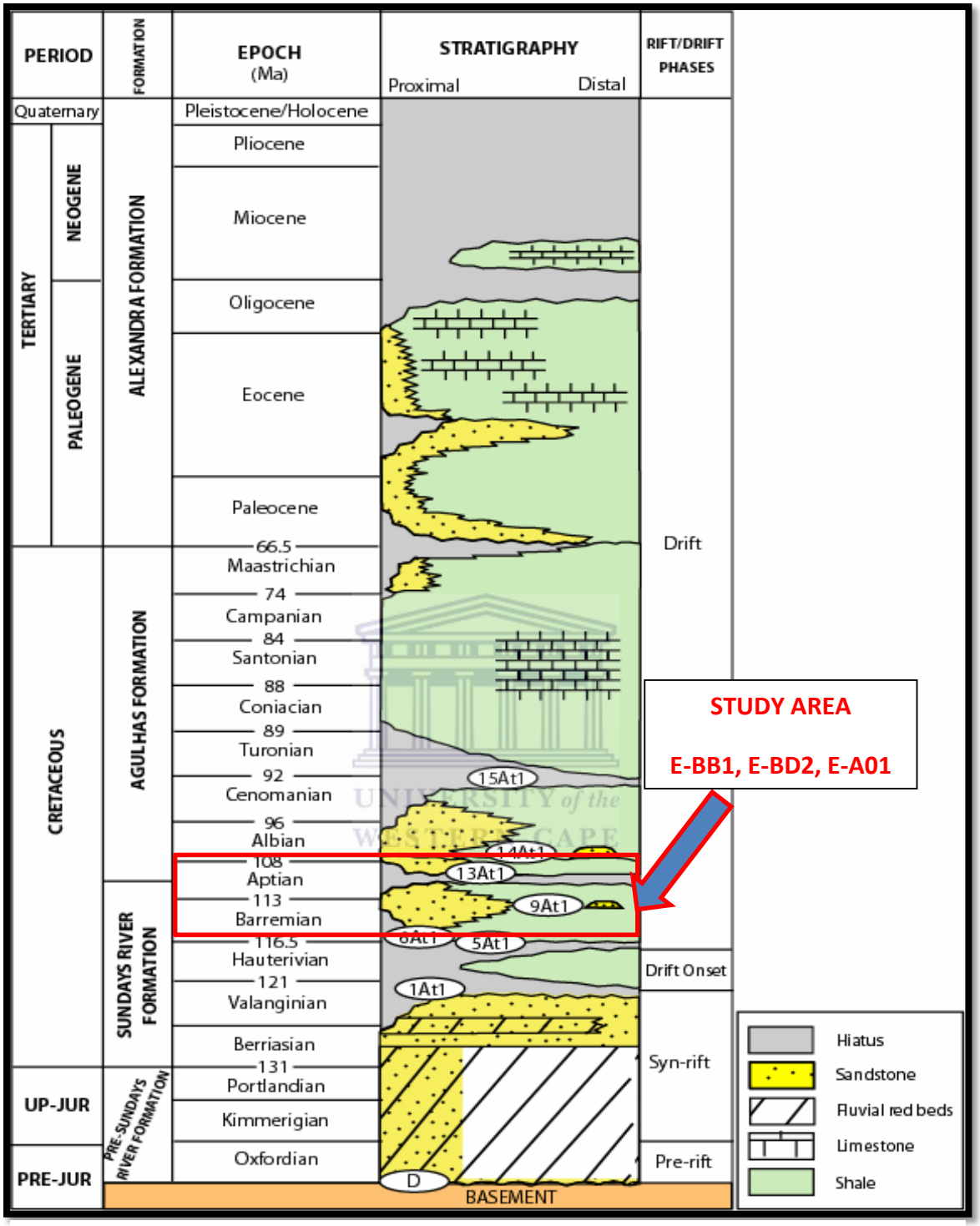

Figure 5.6 Schematic diagram showing the stratigraphic chart of the Bredasdorp Basin. (Modified from Burden, 1992).

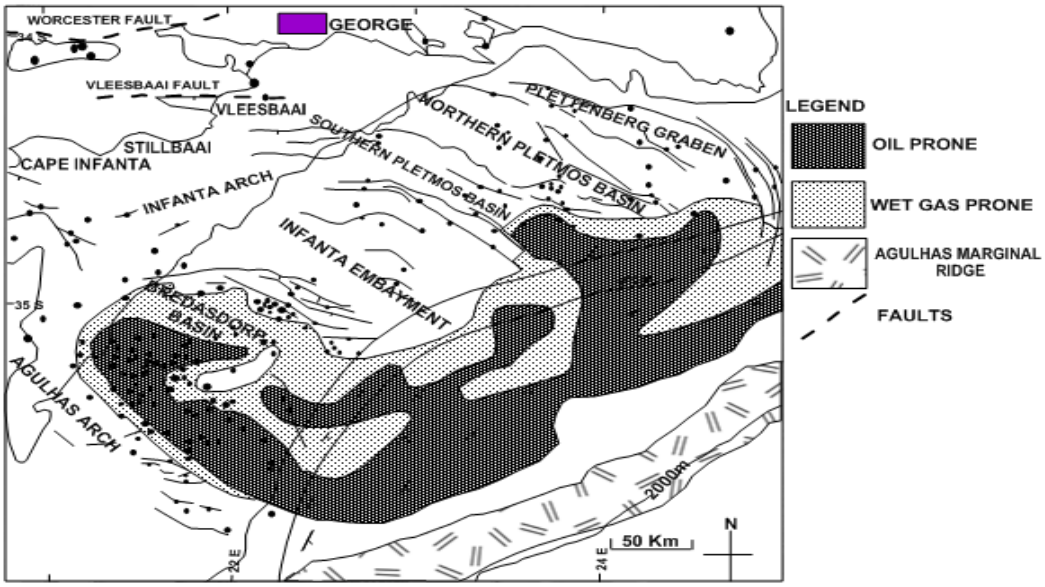

Figure 5.7 Distribution of wet gas and oil prone source rocks in Outeniqua Basin, early Aptian 13A sequence. (Modified from Davies it al., 1991).

Kerogen Type	**Optical description**	**Hydrocarbon/ Oxycarbon ratio S2/S3**	**Hydrogen indexS2 mg/gm TOC**	**Oxygen index mg/gm TOC**
MOC	Amorphous/ sapropelic	>10	>400	<30
MOV	Structured terrigenous algal	~5 >20	250-450 >600	20-50 10-30
MOT	Tracheid	1-3	150-300	40-100
MOL	lignitic	≤1	<150	>80

Table 5.1 Chemical source potential of the four main types of organic matter distinguished by optical means (after Correia and Peniguel, 1975).

5.9.2 Measurement of source potential

Estimates of the proportions of different macerals, essentially proposed by Correia and Peniguel (1975) are used to evaluate the quality of the organic matter. The fourfold subdivision used, with certain diagnostic chemical parameters, is given in (Table 5.2).

AGE	SEQUECNCE NAME	OVERALL HYDROCARBON POTENTIAL	OVERALL MATURIT (R_0%)
TURONIAN	15A	Oil	0.5-0.7%
EARLY APTIAN	13A	Oil	0.7-1.2%
BARREMIAN	9A-12A	Wet gas-oil	0.8-1.3%
EARLY BARREMIAN	6A-12A	Wet gas-oil	0.8-1.3%
LATE HARTERIVIAN	5A	Gas	0.9-1.5%
LATER VALANGINIAN-EARLY HAUTERIVIAN	1A-4A	Gas	1.0-1.5%
LATE JURASSIC-EARLY VALANIGIAN	Syn-rift	Dry gas or Oil	1.0-1.5%
DEVONIAN	Bokkeveld	Dry gas and non-hyrocarbons	>3%

Table 5.2 Overall maturity and gas/oil potential of source rocks in the Bredasdorp Basin, (from Davies et al., 1994).

RICHNESS	TOC %	HYDROCARBON POTENTIAL (S2kg/tone rock)
EXCELLENT	10-20%	>50
VERY GOOD	5-10%	10-50
GOOD	2-5%	5-10
FAIR	1-2%	2-5
POOR	<1%	<2

Table 5.3 Generation potential of hydrocabon.(after Davies et al., 1994)

TYPE (Organic matter types)	HYDROGEN INDEX (original estimate) (100*S2/TOC)	S2/S3	OPTICAL	HALF HEIGHT (width in T^0C of S2 peak at half maximum height)
OIL (I/II)	>>400	>5(>10 where TOC >5%)	>60% amorphous exinite or liptinite	$<45^0C$
WG-OIL (II)	300->400			
WG (II/III)	250-350	2.5-5(>5 where resinous or woody OM)	40-60% amorphous, exinitic or liptinite	$50-60^0C$
DG-WG (III/II)	200-300			
DG (III)	100-200	1-2.5 (>5 where resinous or woody OM)	>60% structured exinite, vitrinite and inertinite	$>70^0C$

Table 5.4 Hydrocarbon potential and organic matter types showing values of each parameter used to describe source rocks of various types and potential (from Davies et al., 1994).

Source potential in this interval is largely developed immediately above 6At1. In some cases, source rock have been assigned to the 7A or 8A sequences but there is some doubt regarding the correctness of those assignments. Indeed those horizons are no longer routinely picked because at the basin edge they become indistinguishable from other horizons. Biostratigraphic data is not able to differentiate these individual sequences. Horizon 6At1 is relatevely easy to pick on seismic records as it is often an angular break and marks the base of basin-wide progradation. The present distribution of source rock in the interval, i.e. largely away from the south flank, may be a function of tectonism in post-6A times when the south flank was uplifted relative to the north flank and eroded. It may also be that as with the 5A sequence, source rock are better developed in the depositional lows which are undrilled. The distribution of these source rocks cluster in two distinct zones, one in the south-east and the other in the north-western part of the basin. These two marginal zones shows that the location of better quality source rocks is not a funtion of water depth, which was greatest near the basin centre, or of sediment starvation.

The 6A-8A source rocks may be an example of the high productivity model in which the prevalence in the western end of the basin indicates an input point for organic carbon. There is however no evidence for sediment input from that direction (Burden and Gasson, 1993). These source rocks have thickness of a few tens of metres with variable but generally modest TOC contents (1.8-2.5%). Overall the source potential is shown in the HI vs Tmax plot as wet gas-oil prone. All the data locate within the Type 2 limits but are widely scattered. This wide variation is mirrored by the chemical data which locally show the potential to range from oil-prone to dry gas-prone within just a few metres (e.g. well no. 93, core 1, 2850.85-2852.30m), where maturity is high (R_0=1.03%). HI varies between 275 and 119). Notwithstanding the location of many points to the left of the Espitalié et al., (1985) 0.5% line, the samples are not of such low maturity. Other chamicals and optical maturity data place all of these samples in the main oil window at R_{equiv} = >0.7%. As with the 5A sequence source rocks, the reduced Tmax is probably due to a large proportion of bitumen (Peters, 1986). Some of this bitumen is detrital as many of the lowest maturity samples have significant free hydrocarbon contents (S1 > 0.2 and generaly >0.6kg/toone rock). Three representative samples from this interval are used the the detailed study.

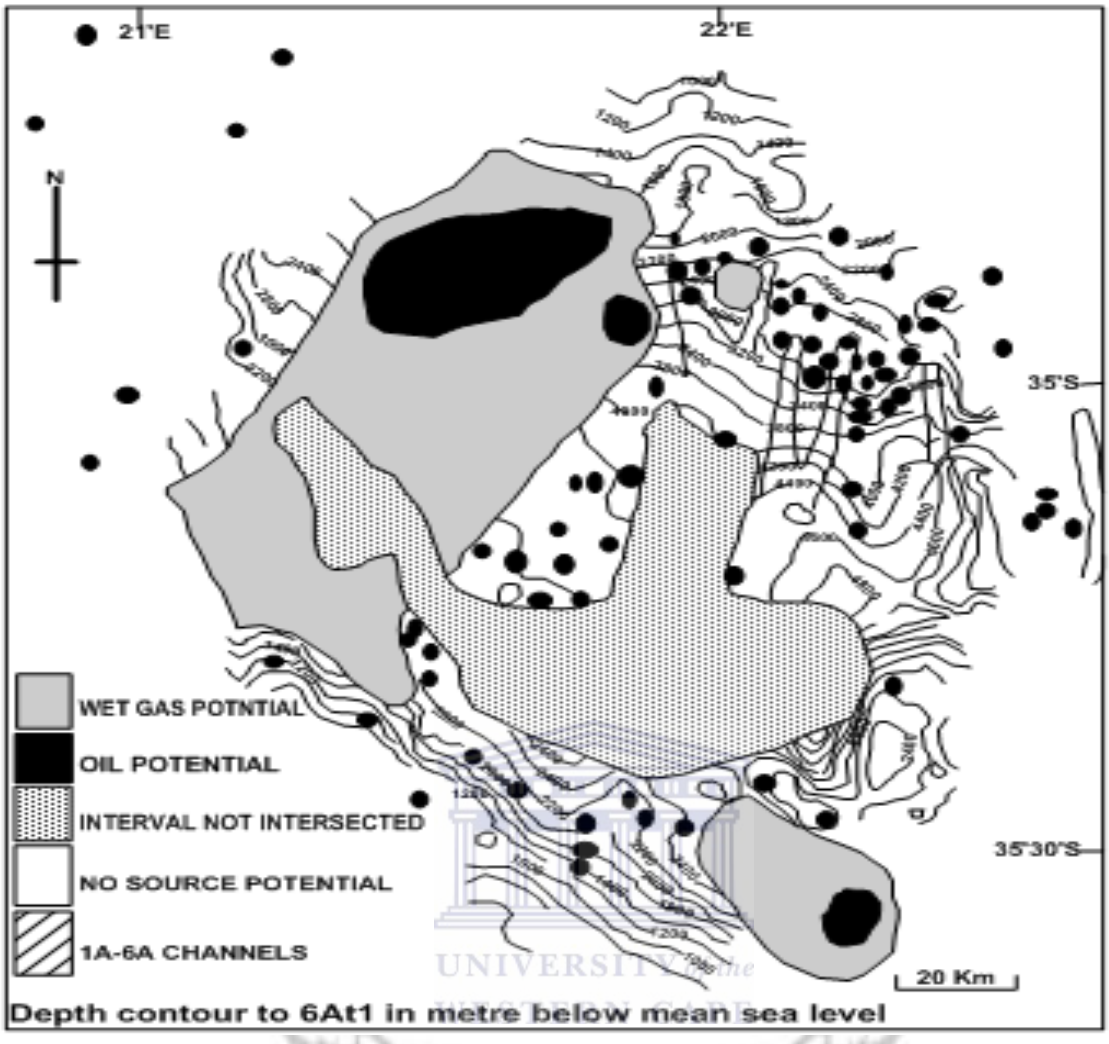

Figure 5.8 Map of the distribution of source rock quality in the 6A sequence in the Bredasdorp Basin, (after Jungslager, 1996).

5.9.3 Source rocks in sequences 9A-12A (Late Barremian)

In most cases, the source rocks are located at the base of the 9A sequence. This makes the interval relatively easy to pick on seismic lines as it marks the start of widespread aggradation. In the central part of the basin, early lowstand channelisation of pre-existing sediments and later infill of the channel with relatively coarse clastic late lowstand sediment fill (Hodges, 1996). Result in the source rocks are found largely in the basal section fo the 9A-12A sequences, but only along the south flank and in the western central parts of the basin. The maturation data show that these source rocks are buried through the base of the oil window and into the top of the gas window (R_0~1.1%) in different locations. The HI vs

Tmax plot shows a wide maturity variation but the source quality data all locate within the Type 2 region. Unusually , the best quality source potential is found associated with the southern flank highs (near wells 9, 35 and 42) and not with the onlap position on the Agulhas Arch. One possible explanation is that these highs are inverted lows although the distribution of onlaps of the preceding sequences do not support this interpretation (Burden, 1992). Alternatively the distribution may indicate the development of a shallow oxygen minimum which impinged on the highs, yet where the oxygen minimum layer deepens, sediment starvation resulted in widespread oxidation. Source rocks are unlikely to have been present in this interval closer to the arch (and consequently eroded during later lowstands) because there is no evisence of an angular break between these rocks and the later 13A sediments. These source rocks have TOC's ranging from 1.8-2.5% with quite high original HI values (table 5.03).

Areally, the distribution of oil-prone source rocks is very limited (~300lm^2) but some of the intersections of we gas-prone shales may, based on the log character, actually be interlaminated oil and wet gas-prone shales. However, overlaying the source map with the maturity map shows that only the central area of wet gas-prone source rocks is buried deeper than R_0=1.1% and therefore the source rocks are largely immature for gas yet the oil potential in 9A-12A source rocks although it is restricted to the areas as hown.

5.9.4 Source rocks in sequence 13A (Early Aptian)

Source rocks in the 13A sequence are developed across most of the basin (Davies, 1988b and Brink et al., 1991). The considerable thickness and extent of this source and its significantly higher richness than any of the other source rocks make it highly prospective. The Early Aptian source is considered to have been formed in an anoxic basin in which organic matter deposited in the core of the basin was dominated by oil-prone material and was rimmed by gas-prone sourec rocks. There is a small area near the basin centre where no source rocks have been found (between wells 124 and 160). This dows not negate the anoxic basin model as it is though that this was a high during deposition of Lower Aptian rocks, possibly a relict of an earlier inversion (perhaps during Hauterivian), when the sea floor may have been above the oxygen minimum.

Support for this comes from the thinly bedded nature of the sands in over and underlying sequences, evidence of a topographic high lasting a considerable time. Indeed, this region is still a relative high in post-13A, based on the bifurcation of the 14A sandstone-rich trend around it (Hill, 1991). In well123 at the western end of this high there are thin intervals of source rock indication that potential existed at least intermittently for source rock deposition. This suggests that the 13A source rock was deposited in the "silled basin" model probably silled by the early eastern highs. The 13A sequence is seen to blanket all the highs in the eastern part of the basin and it is therefore likely that the source rock was deposited by hemi-pelagic sedimentation (Benson, J.M,. 1993, pers.comm.).

In the northern flank of the basin, in spite of the considrable areal extent of wet gas-prone source rocks, the maturation level is generally too low to result in significant gas generation, except in the eastern region were sediments have been matured into the gas window by the instrusions. The buld of the oil-prone material is found to the south of the present day basin axis. As with other source rock intervals, HI vs Tmax shows all samples located in the Type 2 region, but towards the upper side in contrast with all other intervals. This indicates a greater oil potential in this interval than in any other. Average TOC's are significantly higher than in other intervals, ranging up to 4.0% with HI's ranging up to >500. Generation potential exceed 12 kg/tonne at the present day. Extrapolation along the trend shown in Davies (1990) suggests that original potentials could have been in excess of 14 kg/tonne rock.

6 CHAPTER

6.1 CORE ANALYSIS AND INTERPRETATION OF BOREHOLE LOGS

The core analysis is done to establish ground truth for other formation evaluation measurements and is essential for calibration of well logs. Core analysis is a tool in reservoir assessment that directly measures many important formation properties. The objective of performing this analysis is to bring a sample of the formation and its pore fluids to the surface in an unaltered state to preserve the sample and then transport it to the laboratory for analysis. The analysis may aim to determine porosity, permeability, fluid saturation, grain size distribution, mineral composition, grain density; etc. samples for this analysis may come from conventional core, sidewall cores or plugs, and cuttings (Bateman, 1985). The core analysis is usually carried out on core plugs, samples that are taken from the bulk core. In the core laboratory, core plugs are drilled from whole core that typically have a length of about 5cm in diameter of 2.5cm. The petrophysical properties are then measured on these core plugs. Laboratory core analysis can provide very accurate measurements and are regarded as the ground truth.

Porosity determinations in the laboratory are accurate within ±0.5% of the porosity value and ±5% of permeability when the limits and procedures are properly observed. Samples of core taken with either water or oil base mud and are preserved and subsequently tested without cleaning and drying are referred to as fresh cores. Sample of cores cleaned and dried prior to testing are referred to as restored core. An advantage is that air permeability and porosity are available to assist in sample selection (Core laboratories, 1973). The special core analysis (SCAL) are measurements that are made on core plugs that complement the routine core analysis measurements which provides information on the electrical properties, relative permeability, capillary pressure, cation exchange capacity (CEC) and wettability. The results of electrical properties of rock measured from SCAL analysis include the resistivity formation factor, cementation exponent, resistivity index, and also the determination of saturation exponent. The results of the relative permeability measurements helps to make quantitative estimates of formation damage, quantifies effective permeabilities of water, oil and gas, and calculate cumulative permeabilities to each different fluid.

The common goal in the oil industry is to maximize the net revenue from the hydrocarbon-bearing resources that we discover and develop. This can be summarized in the following equation:

Profit=f(A*H*N/G*Ø*S_h*R)

Where: A*H = Gross rock volume,

N/G = Net to gross ratio,

Ø = Porosity,

S_h = Hydrocarbon Saturation,

R = Recovery factor.

This equation illustrates that the economic result is a function of the volume of hydrocarbons in place in the reservoir at any time. Log analysis concentrates on quantifying the petrophysical parameters such as G/G, Ø, S_h and input to R.

6.1.1 Lithology

This is a geological description of a formation in terms of sedimentology, petrology, diagenesis and mineralogy. The source of such information are; cuttings, sidewall cores and whole cores. Whole cores are considered the best source for quantitative data. Logs can be calibrated to core data and be used for prediction of mineralogy using for example Natural Gamma Spectrometry (NGS) log or the Gamma Spectrometry tool (GST). In normal cases the combination of the porosity logs can be used to predict lithology from crossplots or from clustering techniques (electrofacies). When properly calibrated to core data, electrofacies can give a useful prediction of lithology and provide the foundation for an improved application of petrophysical models. Mineralogical information can affect the log analysis (Hurst 1986) as all the logs are functions of the physical and chemical composition of the formation. The capabilities to increase the understanding of log responses need accurate mineral data from core. The Element Mineral Catalogue (Schlumberger, 1990) constitutes a

reference to measured and theoretical properties of 125 minerals. Shaly or dirty formations have been and still are one of the major challenges to log analysis. Shale/clay can affect both porosity and resistivity logs because their properties are different from the clean lithologies, especially in terms of conductivity. The terms clay and shale have both mineral and grain size definitions and can mean different things to different analysis. One is calculating the shale volume (V_{sh}) from logs as described by Fert (1987). The other is the measurements of Cation Exchange Capacity (CEC) developed by Waxman and Smith (1986) which is measured on cores. The measurements of CEC can be quite uncertain (Drønen, 1990) and systematic differences may exist between laboratories and measuring techniques. (Fig 6.1) shows typical occurrences and modes of shale/clay in sandstone. The petrophysical properties of the rock will be affected according to the type of shale and the way it is distributed.

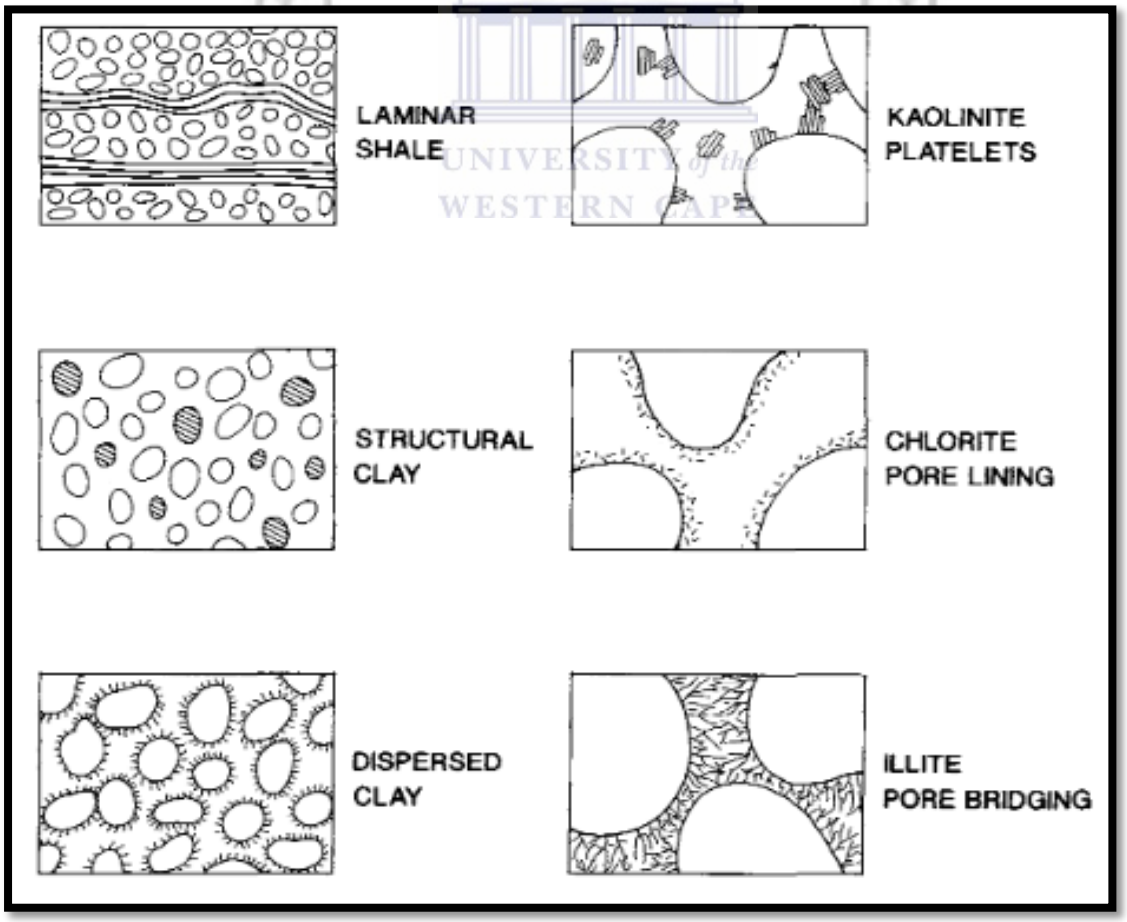

Figure 6.1 Occurrence of shale/clay in reservoired sandstone (from Hurst, 1987).

Clay mineral	Density g/cm^3	Hydrogen index	CEC (mEq/100g)	Natural gamma radioactivity		
				K(%)	Th(ppm)	U(ppm)
Kaolinite	2.60-2.68	0.36	3-5	0.42	6-19	1.5-3.0
Chlorite	2.60-2.96	0.34	10-40	0.1	3-8	
Smectite	2.20-2.70	0.13	80-150	0.16	14-24	2.0-5.0
Illite	2.64-2.69	0.12	10-40	4.5	<2.0	1.5

Table 6.1 (from Hurst, 1987); Schlumberger, 1990) describes the variation in properties of four clay minerals:

6.1.2 Porosity

Porosity (Ø) is defined as the ration of void volume filled with fluids to the bulk volume. (Fig 6.2) after Juhasz, (1986) shows the unit volume of sandstone as a function of shaliness. This illustrates the difference between the total and effective porosity. Log porosity can be calculated from a tool response equation such as the one below by applying density, neutron, sonic or a combination of those logs.

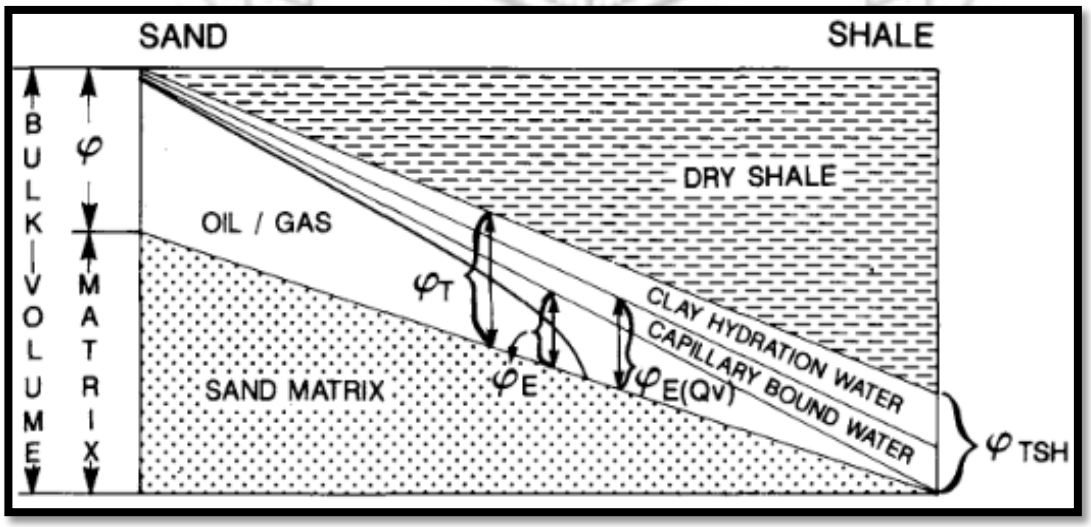

Figure 6.2 Shaly sand Ø, Sw definitions (after Juhasz, 1986).

Core measurements can be used to determine the matrix and shale parameters entering the response equations and total porosity can one measured on cores. The following equation is one response equation for porosity logs (Crain, 1986):

$$X = (1 - Ø - V_{sh})*X_{ma} + V_{sh}*X_{sh} + Ø*S_w*X_w + Ø(1 - S_w)X_{hc}$$

Where:

$Ø$	=	Porosity
X	=	Log value
X_{ma}	=	Matrix log reading
V_{sh}	=	Shale log reading
X_w	=	Formation water log reading
X_{hc}	=	Hydrocarbon log reading
V_{sh}	=	Shale volume
S_w	=	Water Saturation

Sometimes porosity logs are calibrated to core data using a linear fit:

$$Ø = A + B*X$$

Where A and B are constants. This may be necessary in some formations where the log responses are not fully understood and core data can bot be used to verify log analysis. Verification is done by comparing average values of porosity over representative zones.

6.1.3 Saturation

Water saturation (S_w) is defined as that fraction of the pore volume which is filled with water such that the sum of water and hydrocarbon saturations are one ($S_w + S_h = 1$). Achie suggested the following relationship between the resistivity of the rock, formation factor, water saturation and the resistivity of the brine in the formation: $R_t = a*Ø^{-m}*S_w^{-n}*R_w$ (Archie, 1942);

Where: **Ø** = Porosity (fraction)

R_t = Resistivity of virgin zone (ohm m)

a = Lithology factor

m = Cementation exponent

S_w = Water saturation (decimal)

n = Saturation exponent

R_w = Formation water resistivity (ohm m)

6.1.4 Well logs

This is a continuous recording of a geophysical parameter along a borehole produces a geophysical well log. The value of the measurement is plotted continuously against depth in the well (fig 6.3). For example, the resistivity log is a continuous plot of a formation's resistivity from the bottom of the well to the top and may represent over 4 kilometres (2.5 miles) of readings. The most appropriate name for this continuous depth-related record is a wireline geophysical well log, conveniently shortened to well log or log. It has often been called an 'electrical log' because historically the first logs were electrical measurements of electrical properties. However the measurements are no longer simply electrical and modern methods of the data transmission do not necessarily need a wire line so name above is recommended.

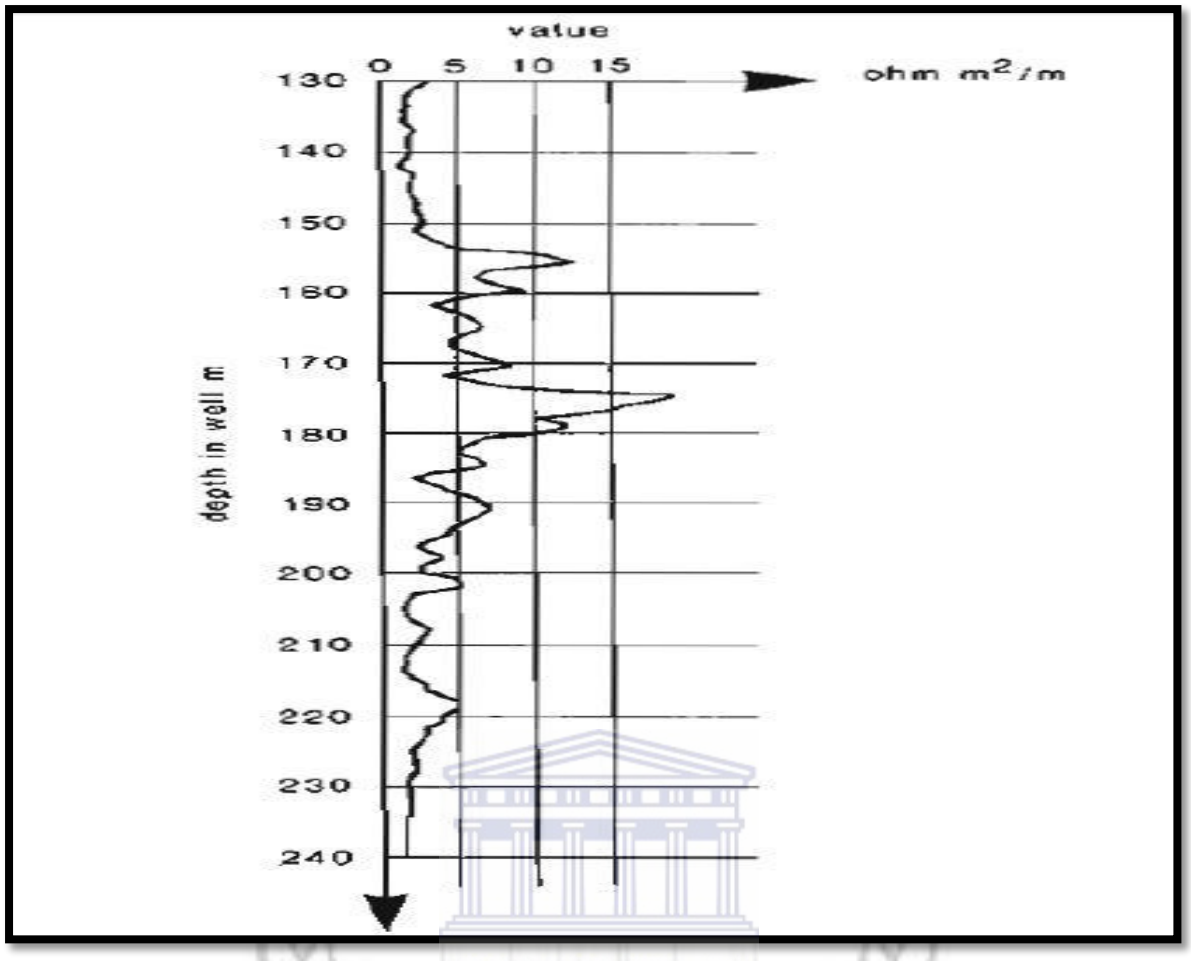

Figure 6.3 Showing a geophysical well log in a borehole (from M. H. Rider, 2002).

6.1.5 Caliper log

Caliper tools measure hole size and shape. The simple mechanical Caliper measures a vertical profile of hole diameter. The more sophisticated borehole geometry tools record two simultaneous calipers and give an accurate borehole shape and orientation. The mechanical Caliper measures variations in borehole diameter with depth. The measurements are made by two articulated arms pushed against the borehole wall. The arms are linked to the cursor of a variable resistance. Lateral movement of the arms is translated into movements of the cursor along the resistance, and hence variations in electrical output. The variations in out are translated into diameter variations after a simple calibration. Frequently logging tools are automatically equipped with a caliper, such as the micrologs and the density-neutron tools where the caliper arm is used to apply the measuring head of the tool to the borehole wall.

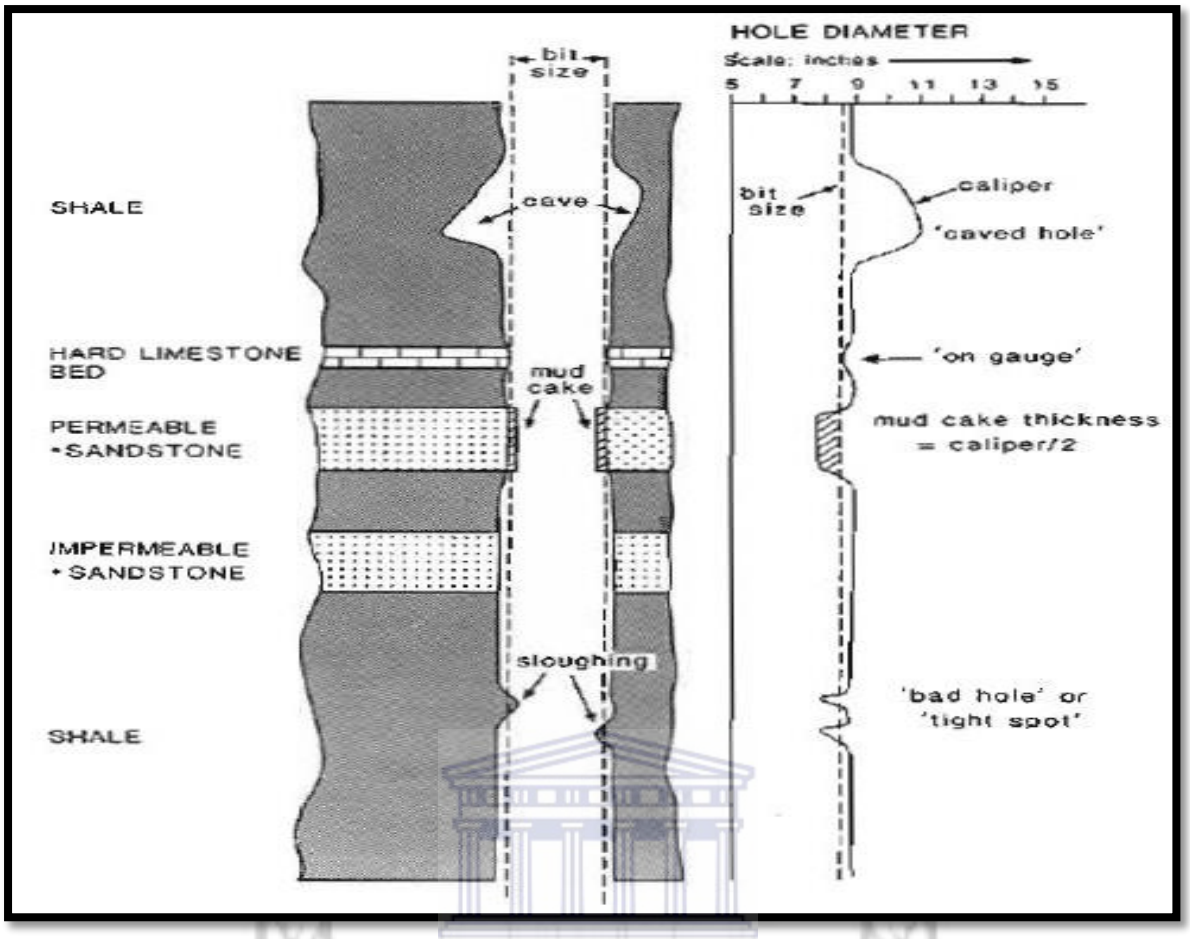

Figure 6.4 Caliper log showing hole diameter: some typical responses, limestone, dolomite, sandstone, shale etc (from M. H. Rider, 2002).

6.1.6 Resistivity log

Of all the logging tools, those that measure resistivity are archetypical. The resistivity log is a measurement of a formation's resistivity that is its resistance to the passage of an electric current. It is measured by resistivity tools. Conductivity tools measure a formation's conductivity or its ability to conduct an electric current. It is measured by the induction tools. Conductivity is generally converted directly and plotted as resistivity on log plots. Most rock materials are essentially insulators, while their enclosed fluids are conductors. Hydrocarbons are exception to fluid conductivity, and on the contrary, they are infinitely resistive. A current is induced in the formation around the borehole and the capacity to carry the current is observed. This carrying capacity is the conductivity. The resistivity is simply the reciprocal of the conductivity. Thus the equation:

Resistivity (ohms m^2/m) $= \frac{1x1000}{\text{conductivity}}$ (millimhos/m)

When a formation is porous and contains salty water the overall resistivity will be low, when this same formation contains hydrocarbons, its resistivity will be very high (Rider, 20020). It is the character that is exploited by the resistivity logs: high resistivity values may indicate a porous, hydrocarbon-bearing formation.

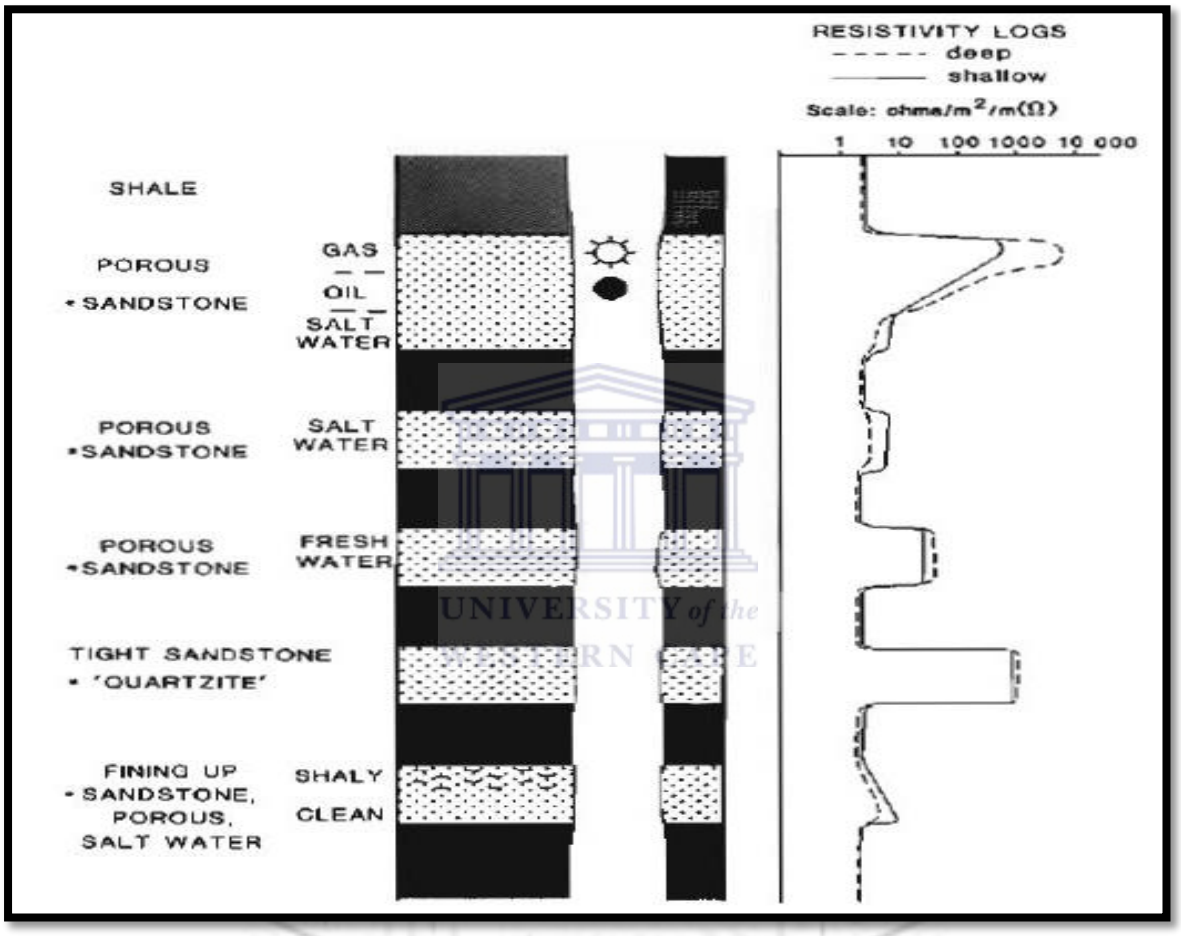

Figure 6.5 Resistivity log: some typical responses, the resistivity log show the effects of the formation and its contained fluids on the passage of an electric current (from M. H. Rider, 2002).

6.1.7 Gamma ray log

The gamma ray log is a record of a formation's radioactivity. The radiation emanates from naturally-occurring uranium, thorium, and potassium. The simple gamma ray log gives the radioactivity of the three elements combined, while the spectral gamma ray log shows the amount of each individual element contributing to this radioactivity. The geological

significance of radioactivity lies in the distribution of these three elements. Most rocks are radioactive to some degree, igneous, and metamorphic rocks more so than sediments. However, amongst the sediments, shales have by far the strongest radiation. It is for this reason that the simple gamma ray log has been called the 'shale log'. Although modern thinking shows that it is quite insufficient to equate gamma ray emission with shale occurrence. Not all shales are radioactive, and all that is radioactive is not necessarily shale (Adams and Weaver, 1958), (Rider, 2002).

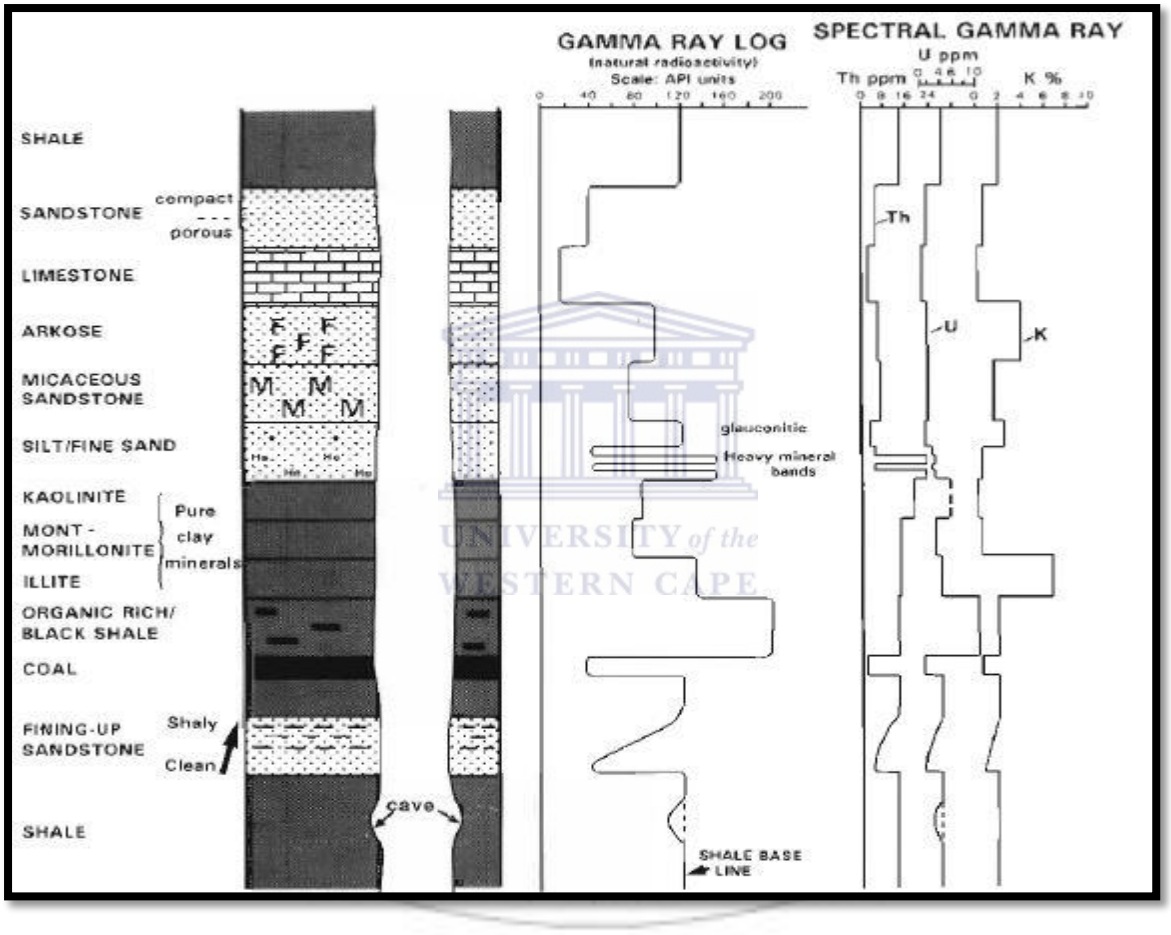

Figure 6.6 Gamma ray log and spectral gamma ray log showing typical responses of radioactivity of some elements modified from (Adams and Weaver, 1958), (Rider, 2002).

6.1.8 Sonic log

The sonic log provides a formation's interval transit time, designated Δt (delta-t, the reciprocal of the velocity). It is a measure of the formation's capacity varies with lithology and rock texture, notably porosity. Quantitatively, the sonic log is used to evaluate porosity

in liquid-filled holes. As an aid to seismic interpretation it can be used to give interval velocity profiles, and can be calibrated with the seismic section. Cross-multiplied with the density, the sonic is used to produce the acoustic impendence log, the first step in making a synthetic seismic trace. Qualitatively, for the geologist, the sonic log is sensitive to subtle textural variations (of which porosity is only one) in both sands and shales. It can help to identified lithology and may help to indicate source rock, normal compaction and overpressure and to some extent fractures. It is frequently used in correlation to the typical seismic signal (sonic and seismic velocities are routinely compared).

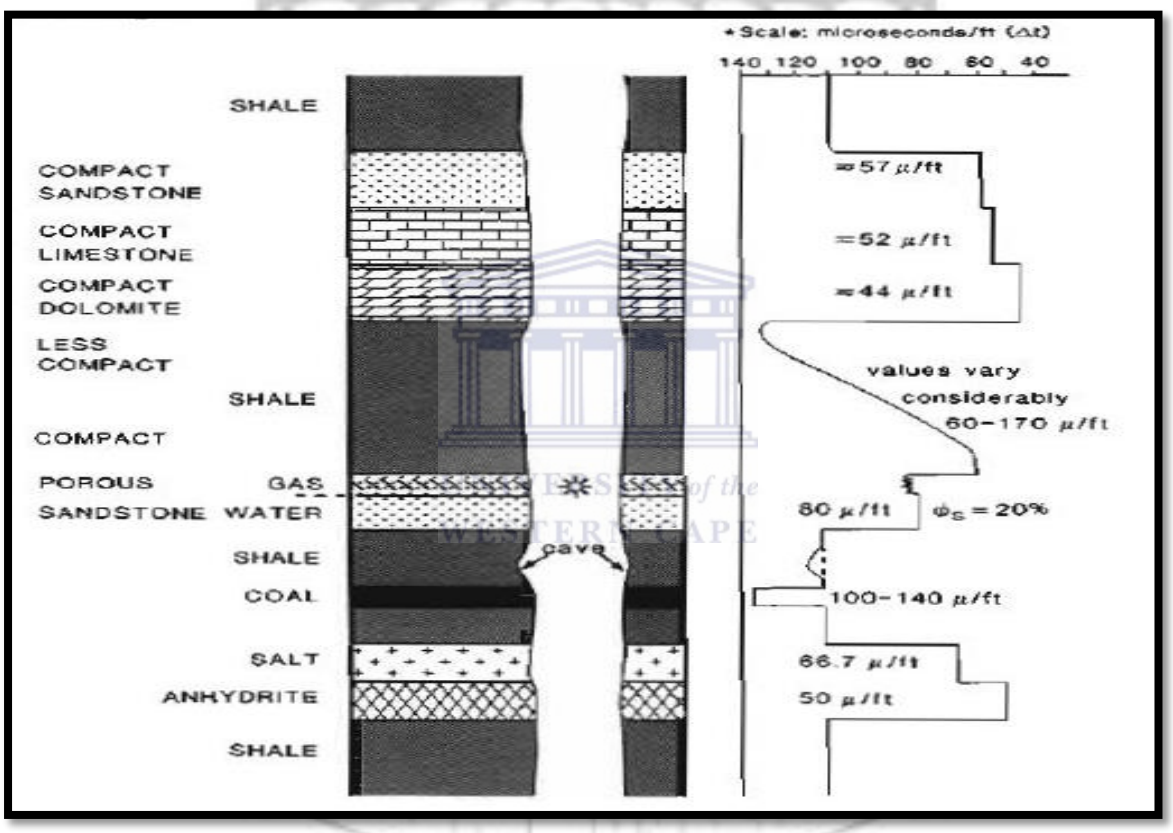

Figure 6.7 Sonic log showing some typical responses in a formation's ability to transmit waves. It is expressed as Interval Transit Time, Δt.*(1x106)/Δt = sonic velocity, ft/sec from (Adams and Weaver, 1958), (Rider, 2002).

6.1.9 Density log

Density log is a continuous record of a formation's bulk density. This is the overall density of a rock including solid matrix and the fluid enclosed in the pores. Geologically bulk density is

a function of the density of the minerals forming a rock (i.e. matrix) and the volume of free fluids which it encloses (i.e. porosity). For example, sandstone with no porosity will have a bulk density of 2.65g/cm^3, the density of pure quartz. At 10% porosity the bulk density is only 2.49g/cm^3, being the sum of 90% quartz grains (density 2.65g/cm^3) and 10% water (density 1.0g/cm^3). Quantitatively, the density log is used to calculate porosity and indirectly, hydrocarbon density. It is also used to calculate acoustic impendence. Qualitatively, it is a useful lithology indicator, can be used to identify certain minerals and also help to assess source rock organic matter content (even quantitatively) and may help to identify overpressure and fracture porosity from (Rider, 2002).

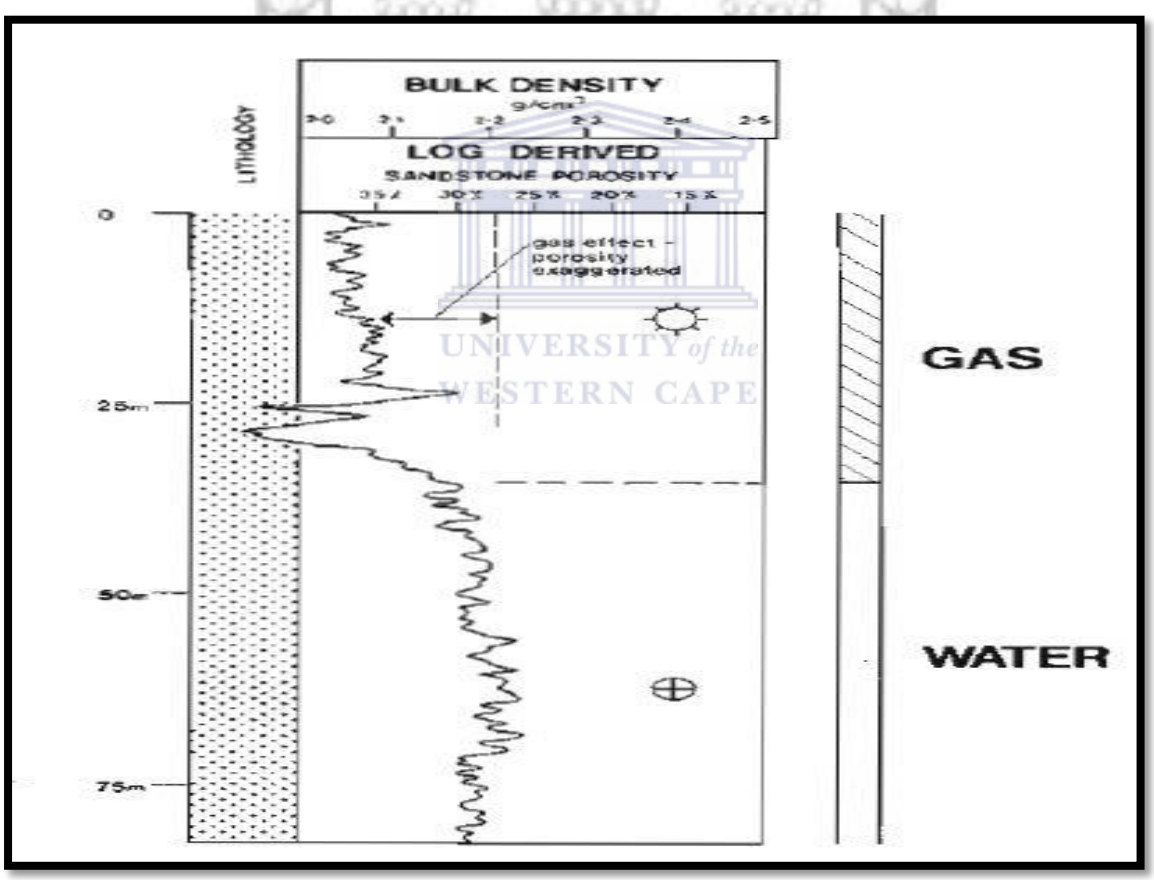

Figure 6.8 Showing density log with some typical responses of bulk density, density and porosity with fresh water formation 1.0g/cm3 (Adams and Weaver, 1958), (Rider, 2002).

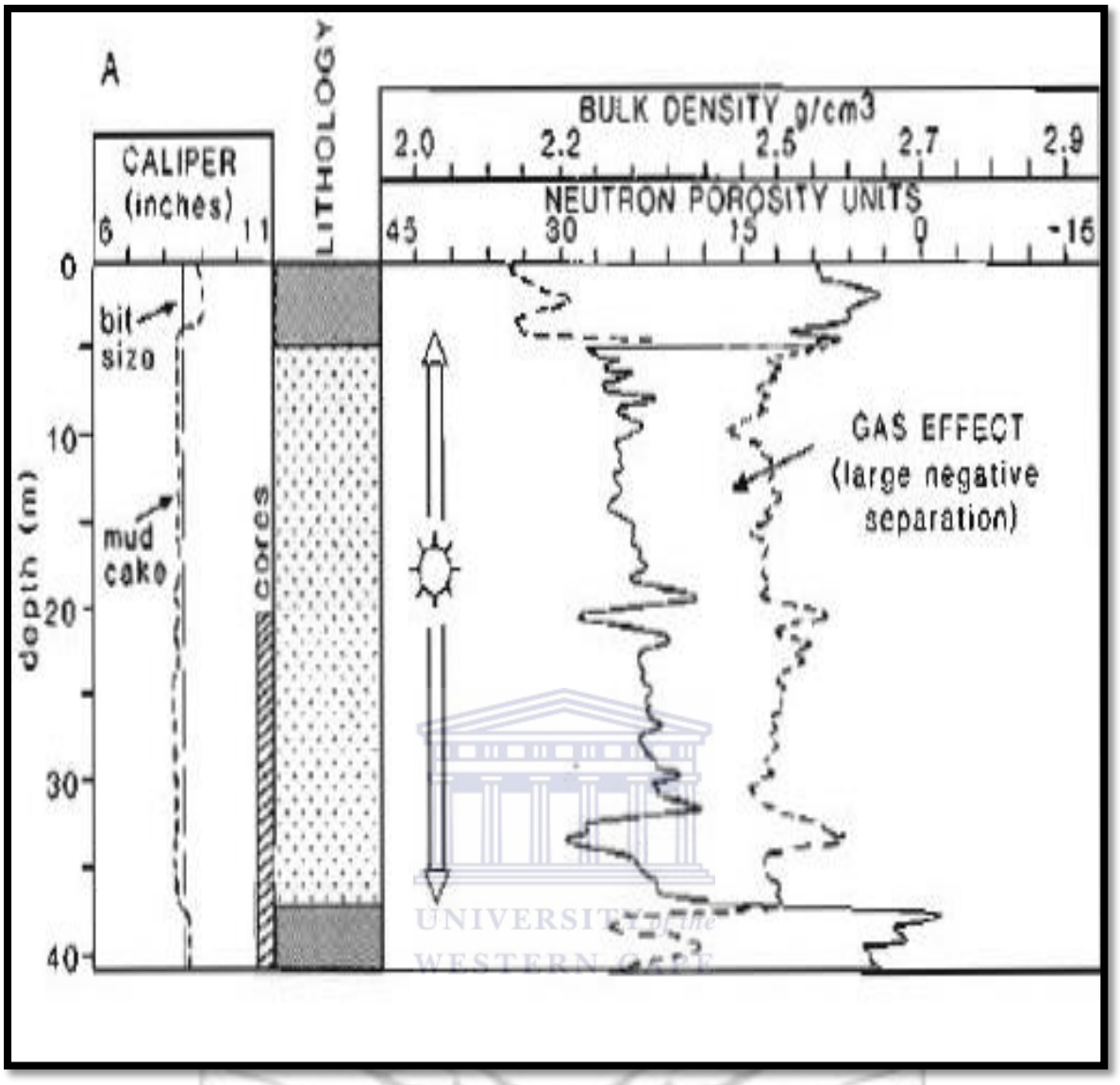

Figure 6.9 Showing combination bulk density and neutron porosity responses by the gas effect. (Rider, 2002).

6.1.10 Neutron log

Neutron log provides a continuous record of a formation's reaction to fast neutron bombardment. It is quoted in terms of neutron porosity units. Which are related to a formation's hydrogen index, an indication of its richness in hydrogen. Formation modifies neutrons rapidly when they contain abundant hydrogen nuclei, which in the geological context are supplied by water (H_20). The log is therefore principally a measure of a formation's water content, be in bound water, water of crystallization or free pore-water.

The hydrogen richness is called hydrogen index (HI) which is defined as the weight % hydrogen in the formation/wt % hydrogen in water, where HI water= 1.

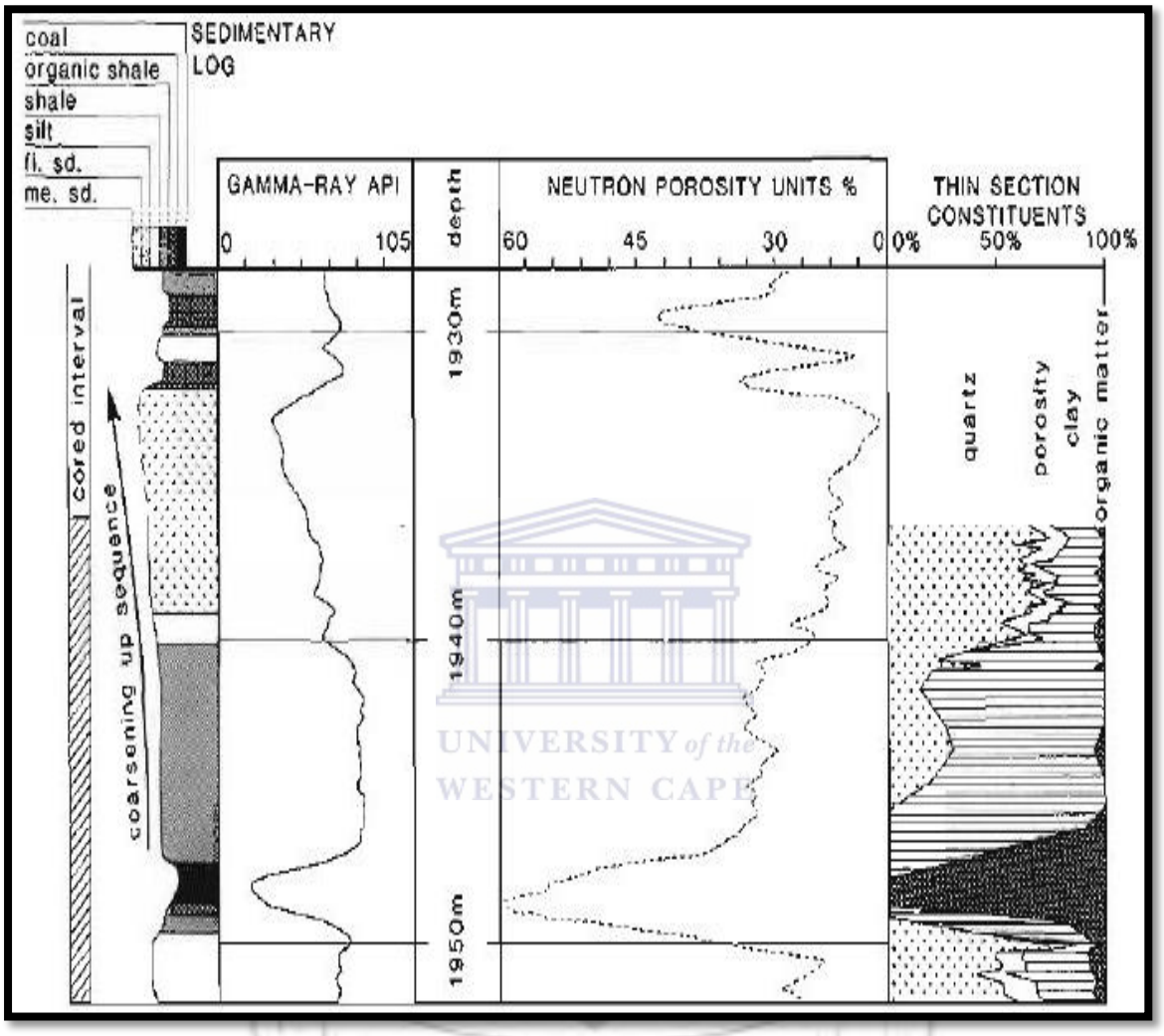

Figure 6.10 Neutron log response in a clean formation, neutron shows a very low value in the gas zone.(Heslop, 1974).

However the oilfield interest in water is as a pore fluid filler and porosity indicator so that the neutron log response is given directly in neutron porosity units. Neutron porosity is real porosity in clean limestones, but other lithologies require conversion factors. Since it is calibrated to limestones, the log is sometimes called the limestone Curve.

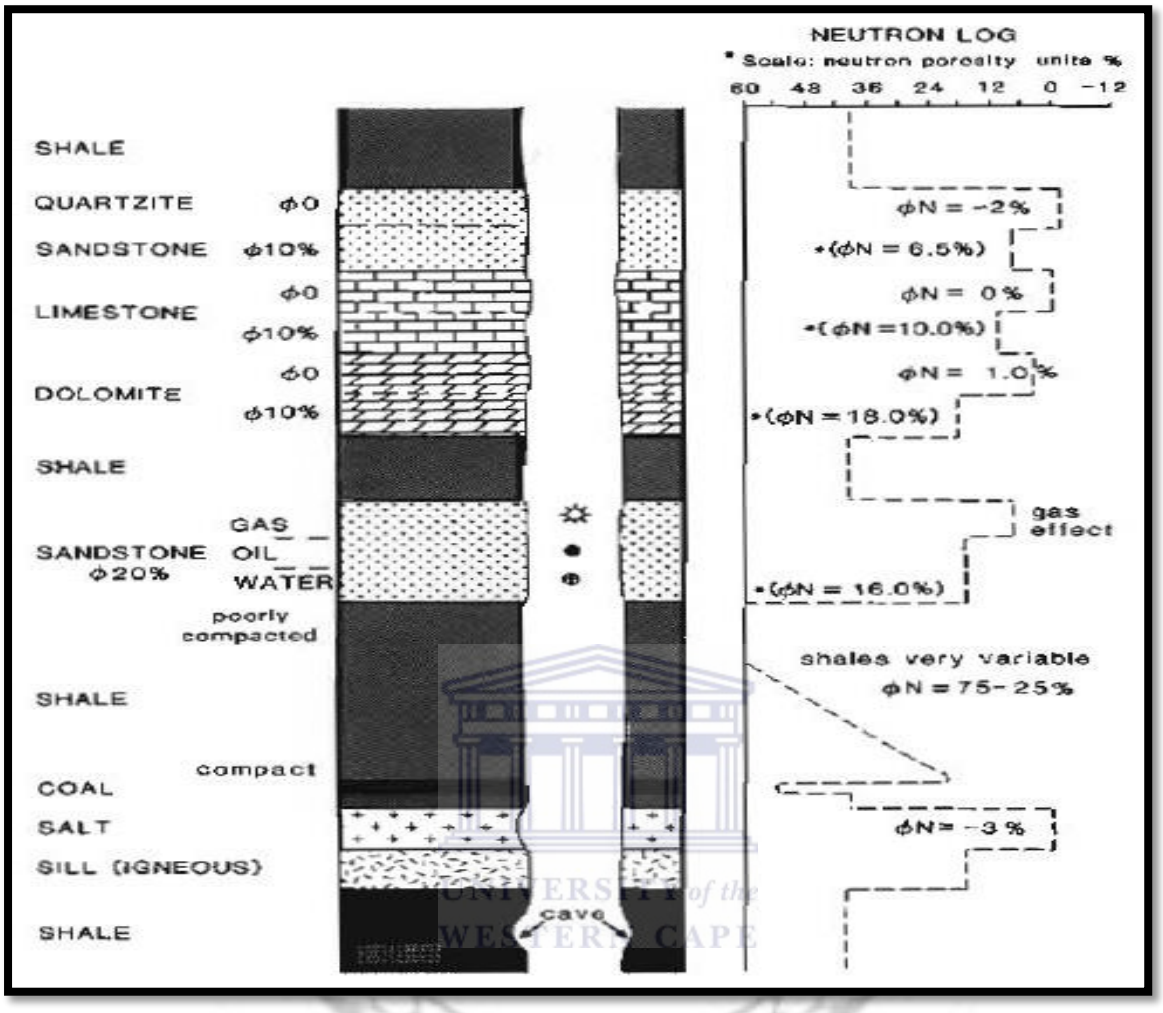

Figure 6.11 Showing the effect of gas on the neutron (and density) logs, neutron shows a very low value in the gas zone.(Heslop, 1974).

6.2 CONVENTIONAL CORE ANALYSIS

The conventional or plug type core analysis is the logging, sampling, and analysis of cores where by a portion of each interval to be analysed is selected to represent the interval of interest. This analysis is performed on homogeneous formations such as sandstones, clay and shaly-sandstone formations at three to four inches of each foot of core. This analysis was performed in three randomly selected wells E-BB1, E-BD2 and E-AO1 of the study area by SOEKOR in order to determine the petrophysical properties of the reservoir formations. Below is the result obtained from the conventional core measurements of well E-BB1. The

tabulated result compiled by (Hill, 1991) courtesy of PASA is found in the appendix page below

6.2.1 Summary of borehole (E-BB1)

Borehole E-BB1 located 5,9km southwest of E-AD1 and 5,4km southwest of E-AY1. All together eight cores were cut (table 6.03 below). Correlation with geophysical logs indicates that logger's depth is 2m deeper than driller's depth over the cored interval and cores were cut and analysed but in the case of this research, much focus is placed in core 5 where the target zone is found at depth (2846-2864m).

6.2.2 Core 5: 2846.0-2864.0m (Sequence 13A)

Core 5 was cut within the massive sandstone unit immediately above 13At1. The sandstone is clean, moderately sorted and medium grained. It contains common to abundant metaquartzite and claystone clasts, is carbonaceous, slightly feldspathic and locally contains minor amounts of mica. Poroperm characteristics are generally good, with 8.4-14.4% porosity and 0.10-39mD permeability (average 11%, 13mD respectively), recorded. Porosity is secondary after dissolution of an early intergranular cement, probably calcite. Quartz overgrowths, vug filling kaolinite, and, below 2853.5m, fibrous Illite reduce porosity and permeability. Minor amounts of ferroan dolomite, pyrite, and, in places, siderite are also developed. Samples with poorer poroperms (2859.98m) have undergone pressure solution along carbonaceous streaks, resulting in more extension quartz and kaolinite cementation.

6.2.3 Summary of borehole interval (Sequence 13A 2688-2877m)

A predominantly claystone interval, with occasional thin (up to 3m) sandstones. Cores 4, 5 and 6 were cut in this sequence. The sandstones above 2840m are clean, well sorted and very fine to fine grained. They are glauconitic, lithic (with claystone and metaquartzite clasts), and slightly micaceous, carbonaceous and feldspathic. Poroperm characteristics range from very poor to good. Secondary porosity is developed in places by leaching of calcite cement and detrital grains. Quartz overgrowths, ferroan dolomite and Illite are the main authigenic phases affecting porosity and permeability, though calcite cements are preserved in places. Pseudomatrix, from compaction of clay and glauconite clasts, has also reduced porosity in places. Core 5 and 6 were cut in the massive sandstone from 2845-

2875m. The sandstone is clean, moderately sorted and medium grained. It is lithic, with metaquartzite and claystone clasts, carbonaceous, and slightly feldspathic and micaceous. Poroperms are good, with secondary porosity developed by leaching of early calcite cement. Quartz overgrowths, kaolinite and Illite are the main permeability restriction phases. Minor amounts of ferroan dolomite, pyrite and, locally, siderite are also developed.

Core No.	DEPTH OF CORED INTERVAL (m)		RECOVARY %	STRATIGRAPHIC LEVEL (Sequence)
	Driller	Schlumberger (logger)		
1	2537.0 - 2537.8	2539.0 - 2539.8	60.0	14A
2	2537.8 - 2556.42	2539.8 - 2558.42	100	14A
3	2556.0 - 2669.0	2663.0 - 2673.0	92.0	13B
4	2717.5 - 2724.5	2721.5 - 2726.0	97.4	13A
5	2846.0 - 2864.0	2848.0 - 2861.5	58.0	9A
6	2872.0 - 2877.0	2874.5 - 2879.0	92.6	9A
7	2894.0 - 2895.0	2896.0 - 2897.0	65.0	9A
8	3280.0 - 3297.0	3284.0 - 3301.0	95.0	Pre-6A

Table 6.2 showing core depths, recovery rate and stratigraphic sequences, compiled by Grobbler, (1991) well site geologist for SOEKOR. SOE-RPT-003.

6.2.4 Description and interpretation of facies (Core #5 E-BB1)

Facies are physical, chemical, and biological aspects of a sedimentary bed and the lateral change within sequences of beds of the same geologic age.

Core #5 was cut to evaluate the reservoir properties of the primary target sandstones in the 9A sequence and was prompted by an increase in ROP, sandstone content, fluorescence and ditch gas below 2843m. (as highlighted in table 6.2 above);

6.2.5 Facies description

Facies A: Only one facie type occurs in the core, namely homogenous massive sandstone. The sandstone is fine to medium grained, well sorted and clean. Possibly amalgamated contacts are hardly visible. No grading of grains size can be detected. Calcareous material, TMS and claystone lithic fragments and feldspar grains are present in the sandstone. Stylolite development is common in the form of millimeter thick black layers in the sandstone. At the top of the core the stylolites are inclined and could be developed along cross-bedding surfaces. At the bottom of the core the stylolite development is influenced by concave-up dish structures.

DEPTH	OBSERVATION AND DESCRIPTION OF CORE
2846.0 – 2847.0	Clean sandstone, fine to medium , well sorted, loose packing, round, lithic, carbonaceous mineral, feldspar, mica, vug filling kaoline, silica cement, grain dissolution, porosity, Illite from grain alteration, kaolinite, oil stained.
2847.98 – 2850.0	Same as above, and carbonaceous material, very lithic, no mica observed
2851.0	As seen above but here mica is present
2851.98	Clean sandstone, tight packing, rounded, very lithic, (TMS, claystone, very carbonaceous, mica, Illite poor porosity, quartz, silica, kaoline, stylolite oil stained.
2853.06 - 2856.0	Clean sandstone, loose packing, rounded, lithic, (TMS, claystone, carbonaceous, mica, good cement and grain dissolution, kaoline, Illite and siderite from grain alteration, oil stained.
2856 - 2876	Same as above.

Table 6.3 Detailed description of core #5 E-BB1. (1991) well site geologist for SOEKOR. SOE-RPT-003.

Plate 6.1 Core #5 showing some sedimentary features in well E-BB1 (courtesy of PASA).

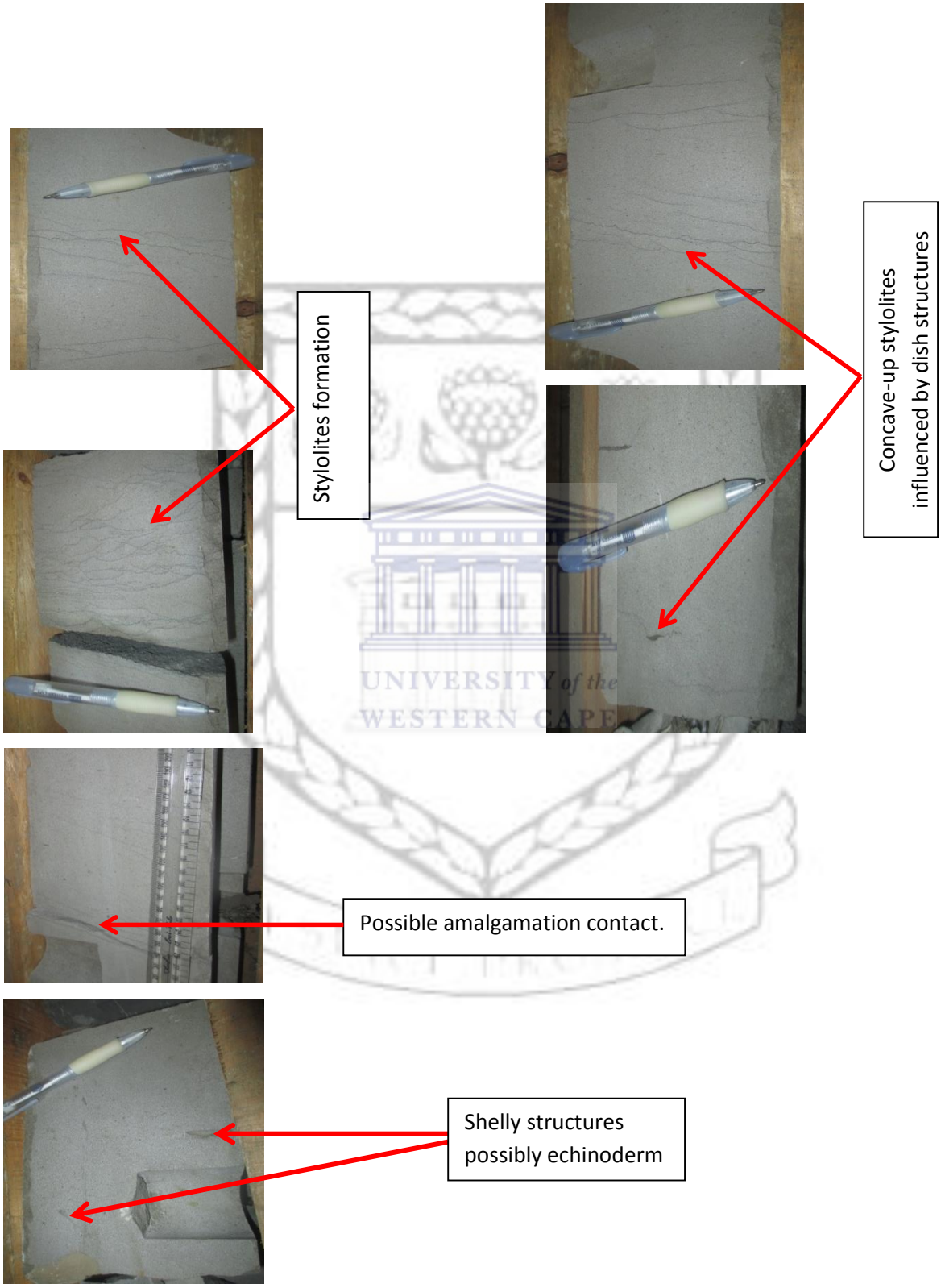

6.3 Summary of borehole interval E-BD2 Sequence 13A (1980-2622m).

A 25m thick massive sandstone unit developed just above the 13At1 unconformity, from 2576.9-2604m.The sandstone was intersected by core# 1. The sandstone is clean, moderately sorted and medium grained, with common metaquartzite clasts, and minor feldspar and carbonaceous material. Poroperm characteristics are very good (average 17.5%, 287mD from core analysis) with cement dissolution porosity well developed after leaching of early calcite cement. Porosities are slightly reduced by quartz overgrowths and, to a lesser extent, kaolinite, dolomite and siderite.

6.2.6 Summary of core 1 E-BD2 (2579.0-2597m)

The core comprises mostly of clean, moderate sorted, medium grained sandstones. A slightly fine grained unit, with occasional claystone stringers, occur from 2593-2589. The sandstones are lithic, with common metaquartzite clasts, probably derived from Cape Supergroup basement. They are slightly feldspathic and carbonaceous, with traces of mica locally. The poroperm characteristics are very good; average porosity being 17.5% and average permeability 287mD. Secondary porosity is very well developed, as a result of dissolution of intergranular cement, probably calcite. Only minor amounts of pore filling cements are developed, quartz overgrowths being the most abundant, with lesser amounts of ferroan dolomite, siderite and, locally, pyrite. Vug filling kaolinite is the most abundant authigenic clay phase, with minor amounts of Illite (from grain alteration) present locally. After the reservoir bottom depth at 2602.1m, claystone core was observed hence no petrographic observation and analysis was performed on this section. Below is the result obtained from the conventional core measurements of well E-BD2.

6.2.7 Conventional Core Analysis

In this core analysis, there was an incomplete data capture such that missing data such as Sg, So, Sw, Calcite, Dolomite was not captured hence research was done by extrapolating data from the key well E-BB1 hence the research was done with data available from Petroleum Agency of South Africa (PASA). The tabulated result of the conventional core

measurements for well E-BD2 obtained from SOEKOR (Hill, 1991) PASA is found in the appendix page below.

DEPTH	OBSERVATION AND DESCRIPTION OF CORE
2579.30	Clean massive sandstone, loose packing, rounded grains, lithic (TMS), (feldspars), good secondary pores due to cement dissolution, well sorted
2580.35	Clean massive sandstone as above and some siderite present
2581.10-2582.35	Clean massive sandstone as above less siderite and some carbonate present, well sorted
2583.05	Clean massive sandstone, tight packing,(angular), carbonate, lithic (TMS), mica and some feldspar, well sorted
2584.55-2590.89	Clean massive sandstone, as above but some carbonate present
2591.94	Clean massive sandstone, mica, stylolitised carbonate streaks
2592.94-2595.03	Clean massive sandstone, No stylolites present
2595.53	Clean massive sandstone, tight packing, stylolites carbonate streaks, poor lining Illite.

Table 6.4 Detailed description of core #1 E-BD2. (1991) well site geologist for SOEKOR. SOE-RPT-003.

Plate 6.2 Core#1 showing some sedimentary features in well E-BD2 (courtesy of PASA).

Stylolite formation

Carbonaceous shale bed about 10cm

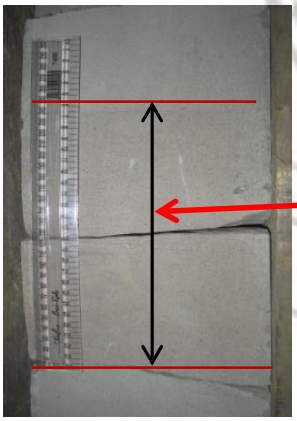

Heavily discoloration from very light to brownish possible due to oxidation

Possible amalgamation contact

Contours formed from fluid escape in the formation fluid and discoloration due to oxidation of iron bearing minerals

Plate 6.3 Core#1 showing some sedimentary features in well E-BD2 (courtesy of PASA).

Brown coloured clast present possibly from a terrestrial origin with high oxidized iron mineralization

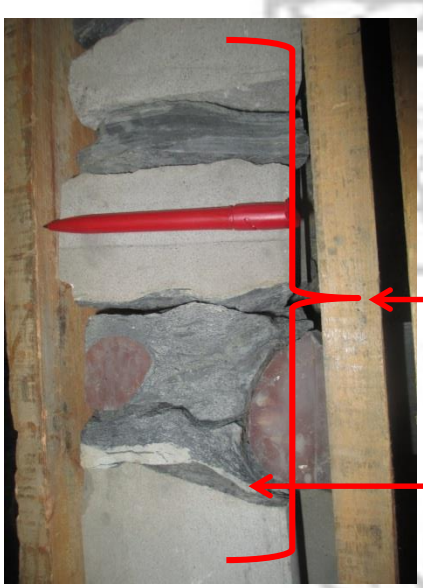

Intercalation of sandstone and shale possibly indication of episodes of high and low sea current flow where during rise in sea water (high current), sand is deposited and during low sea level there little of no current, hence shale is deposited with finer darker grains.

Sandstone lense

6.3 Core description and interpretation (E-AO1)

6.3.1 Summary of core #1 well E-A01

Mostly very fine to medium grained, shelly glauconitic sandstones. Sorting improves with depth through the core. Porosity and permeability are very good at the top of the core, but tend to deteriorate with depth as quartz and calcite/dolomite cements become more abundant, and pore-lining illite and chlorite appear. Preserved porosity is secondary after cement and grain dissolution. Authigenic chlorite, pyrite and fe-rich calcite and dolomite may present reactivity problems if the formation was acidized with Hcl.

6.3.2 Sequence 13Bt1 (2634-2804m)

The reservoir was deposited in this sequence hence it is predominantly clay stone sequence, with thin sandstones throughout. Thick sandstone occurs at 2671m-2682m and this core was cut in the upper thick sandstone unit. The upper sandstones unit is clean, glauconitic and shelly. Secondary porosity and permeability are very good at the top of the unit, but deteriorate with depth as grain size decreases and sorting improves, cementation by quartz, calcite and dolomite becomes more extensive with depth in the unit, as does development of authigenic illite and chlorite. Hence porosity and permeability are poor at the base of the sandstone.

DEPTH	OBSERVATION AND DESCRIPTION OF CORE
2674.00-26775	Clean sandstone with loose packing, rounded grains, glauconitic and some shell present. Cement dissolution, poor glauconitic, dolomite and pyrite. Bivalve and echinoderm present.
2675.00-2675.85	Cleans massive sandstone, as above but echinoderms, bivalves, carbonaceous cement present.
2676.91-2679.84	Clean massive sandstone, loose packing, rounded grains, very glauconitic, shelly-bivalves, echinoderms, brachiopods. Patchy cement grains dissolution and finer grains and good sorting.

Table 6.5 Detailed description of core #1 E-A01. (1991) well site geologist for SOEKOR. SOE-RPT-003.

Plate 6.4 Core#1 showing some sedimentary features in well E-A01 displayed in boxes for observation and description (courtesy of PASA).

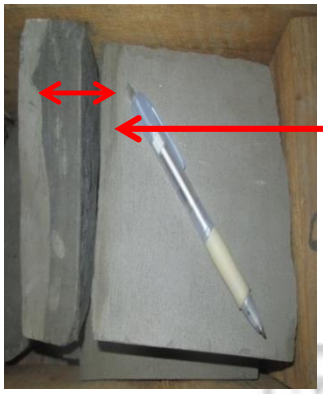

Thin shale bed about 3-4cm with clast present

Stylolites formation present

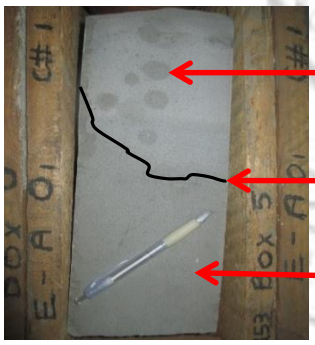

Light coloured massive sandstone with oil stains

Contour of top light coloured sand and lower darker sandstone with signs of oil presence

Darker base sandstone with signs of oil presence

Well cores displayed in boxes for observation. Petroleum Agency of South Africa (PASA)

7 CHAPTER

7.1 Wireline log interpretation

It is generally assumed that 100% water saturation in porous and permeable beds, the resistivity variations being due to mud filtrate and formation water mixing, a two phase system of miscible fluids occur. In well E-BB1 which is used in this research as a key well because it has all the required data needed for this research whereas E-BD2 and E-A01 are not complete hence some data was extrapolated from E-BB1 to E-BD2 and E-A01. E-BB1 has two reservoirs and the (top) upper reservoir is where the zone of interest was identify as the resistivity logs are significantly displaced than in (bottom) lower reservoir with little displacement of these curves. When hydrocarbons are present as in the case in well E-BB1 (fig 7.1) at depth (2844.1 to 2865.6m), the system becomes a three phase and much more complex.

The mud filtrate will replace the hydrocarbon immediately around the borehole essentially replacing them through the flushed zone, while the original saturation in hydrocarbons is only found in the virgin formation. As in well E-BB1, a resistivity profile across a hydrocarbon zone will show a flushed zone with a moderate to low resistivity filled with mud filtrate although resistivity will depend on mud type and the virgin formation with an extremely high resistivity because of the high saturation in hydrocarbons. Both oil and gas are infinitely resistive and show the same effect on resistivity logs as shown in the (Figure 7.1 track #9). The resistivity profile then shows a big increase away from the borehole, the exact reverse of a water zone were the resistivity curve profile shift towards the borehole as in (Figure 7.1) below at depth (2865.6 to 2874.0m).

This increase in resistivity deeper into the formation away from the borehole is expressed very distinctly on the logs. Shallow looking tools which read in the flushed zone show relatively low resistivity values while deep reading tools show very high resistivity as in (fig 6.5) above and in (fig 7.1) below. The separation between the curves from the shallow and deep tools is a diagnostic of the presence of hydrocarbons and it is some time called the (hydrocarbon separation) and used in a quick look technique for locating oil and gas in a reservoir. This quick look can be however, verified by calculation since curve separation can

be caused by fresh water and many hydrocarbon zones do not give any obvious separation. Theoretically there is a differential rate of flushing of formation water and of oil or gas by the mud filtrate. This is supposed to create a zone where there is a high volume of formation water with only residual hydrocarbons, the so called low resistivity annulus on the outer fringe of the flushed zone, (Threadgold, 1971). It is clear that there is a considerable fluid movement not only during drilling when invasion occurs, but also when drilling ceases. The fluid equilibrium which existed before drilling attempts to re-establish itself, especially in gas filled reservoirs or those with very high permeability.

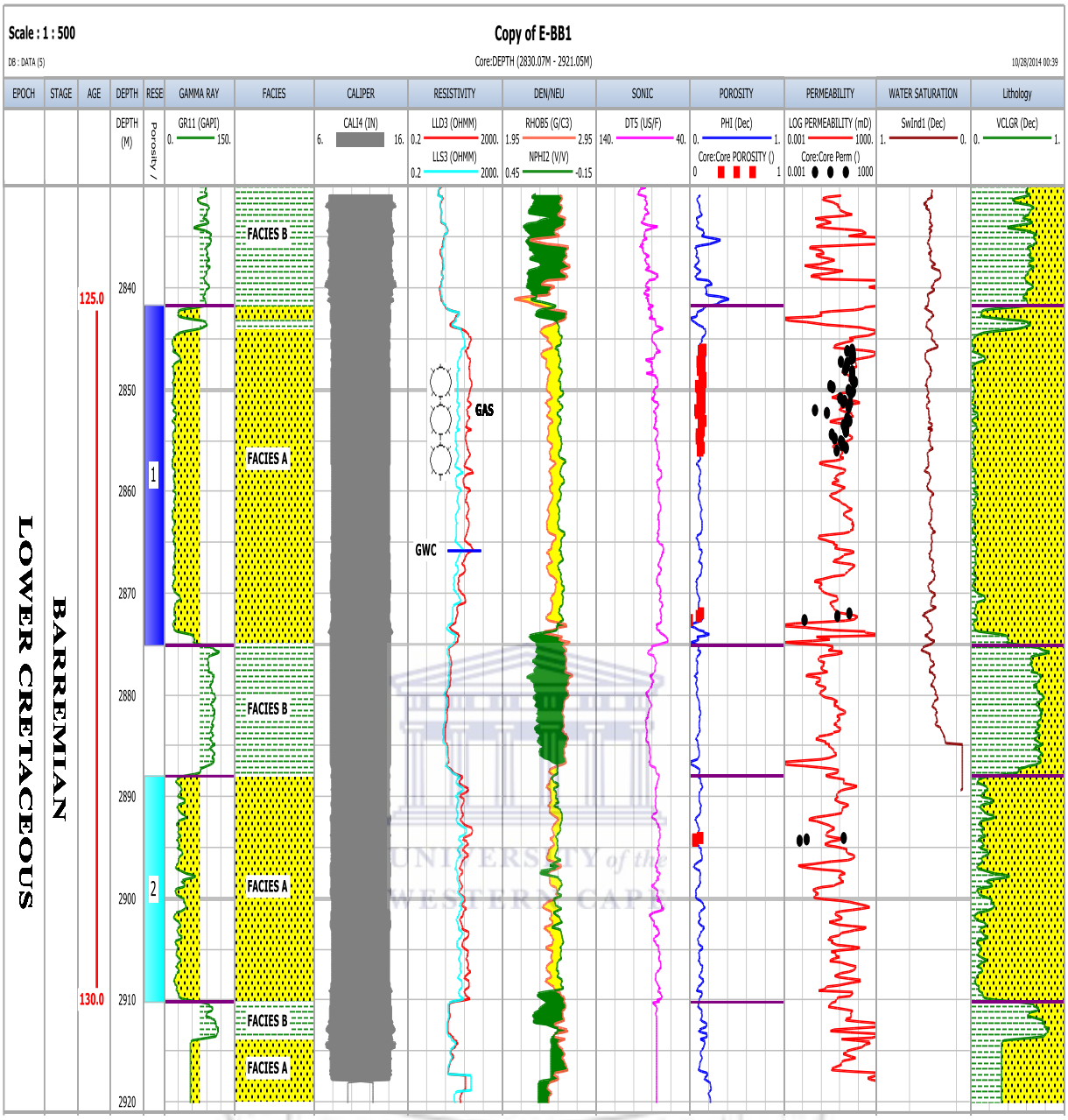

Figure 7.1 Showing various curves behaviour in a hydrocarbon bearing formation of well E-BB1. (courtesy of PASA).

7.1.1 Well E-BB1 Curve interpretation

In the above well E-BB1, core #5 was studied and found some hydrocarbon potential. Only one dominant facies was identified, massive clean fine to medium-grained sandstone, well sorted, TMS and some lithic siltstone clasts and calcareous concretions are contained within the sandstone. No sedimentary structure present and the best facies for this well is facies "A". In this well two reservoirs were identified; #1 ranges from depth 2841.5m to 2875.0m and reservoir #2 ranges from depth 2887.7m to 2909.9m. Although two reservoirs were

identified only reservoir #1 is of high interest for this study due to the factors that are discussed below.

In track #14 (brown colour curve water saturation) is the water saturation curve which has higher values 0.441(Dec) at the top of the reservoir at depth 2841.0m and lower value at the bottom of the reservoir 2874.6m. In a pickett standalone cross plot (in the index page), plotted points that are less than 100% show a potential of hydrocarbon show.

In track #13 (red permeability curve), the permeability curve which show a good matching relationship with permeability plots (black plots) although some of the points are off curve could be errors caused during data capturing or could be the presence of clay mineral (Illite, chlorite), presence of thin clay beds or tight zone within the reservoir.

In track #12 (blue porosity curve), is a porosity curve which show a good matching relationship with the porosity (indicated in red points) in the reservoir, hence this match does not indicate that the reservoir is good based on the matches but simply means that the data obtained and processed shows a good correlation with the respective curves. Where a high porosity and permeability is a good characteristics of a sandstone reservoir.

In track #11, is the sonic log DT (purple colour sonic curve) which shows a tight wrinkled reading of 80us/f to 87us/f at depth of 2841.5 and reads 67us/f at depth 2854.3m. This tightly wrinkled displacement of curve at this depth is caused by the resistance of the hydrocarbon show in the reservoir zone. This curve became smoother after depth 2854.3m probably due to the presence of water at that reservoir zone.

In track #10, in (fig 7.1) above, there is a negative crossover at top depth 2543.5m to bottom depth 2872.9m of the density log RHOB (light brown density curve) register a significant low value due to the resistivity of hydrocarbon presence and neutron log NPHI (green curve) registering a low value as a result of the resistance of hydrocarbon presence which show a strong indication of hydrocarbon presence probably a gas show (Rider 2002).

In track #9 (the aqua coloured curve being Shallow Resistivity curve and the red being the Deep Resistivity curve). The two curves shows a significant increase in values and separation at top depth 2843.5m to bottom depth 2872.9m where the deep resistivity curve shows a higher value reading away from the borehole deeper towards the formation comparatively

to the shallow resistivity curve which is closer to the borehole. This separation shows an indication of the presence of hydrocarbon preferably gas shows and further deep down into the borehole the two curves show a sharp decrease (represented by the blue line at depth 2865.7m) in value readings towards the borehole an indication of a gas water contact at depth 2865.7m.

In track #8 (caliper log), this may show a diameter smaller than the bit size (diameter). If the log has a smooth profile, a mud-cake build-up is indicated. This is an extremely useful indicator of permeability because only permeable beds allow mud cake to form. The limits of mud-cake indicate clearly the limits of the potential reservoir, (Rider, 2002). Mud-cake thickness can be estimated from the caliper by dividing the decrease in hole size by two, i.e.

$$\frac{\text{Bit size } (diameter) - Caliper\ reading}{2} = \text{mud cake thinkness}$$

DEPTH (m)	PERMEABILITY (mD)	POROSITY (%)
2846.2	29.05	3.8
2847.0	25.94	13.0
2847.2	25.94	13.0
2848.3	10.34	11.2
2849.24	30.47	12.6
2850.21	16.10	12.0
2851.2	9.04	11.9
2852.21	0.21	8.4
2853.29	18.48	13.8
2854.2	11.36	12.5
2855.2	5.64	11.3
2856.28	3.38	11.1

Table 7.1 Summarized value for the above curves depths for well E-BB1, (source SOEKOR).

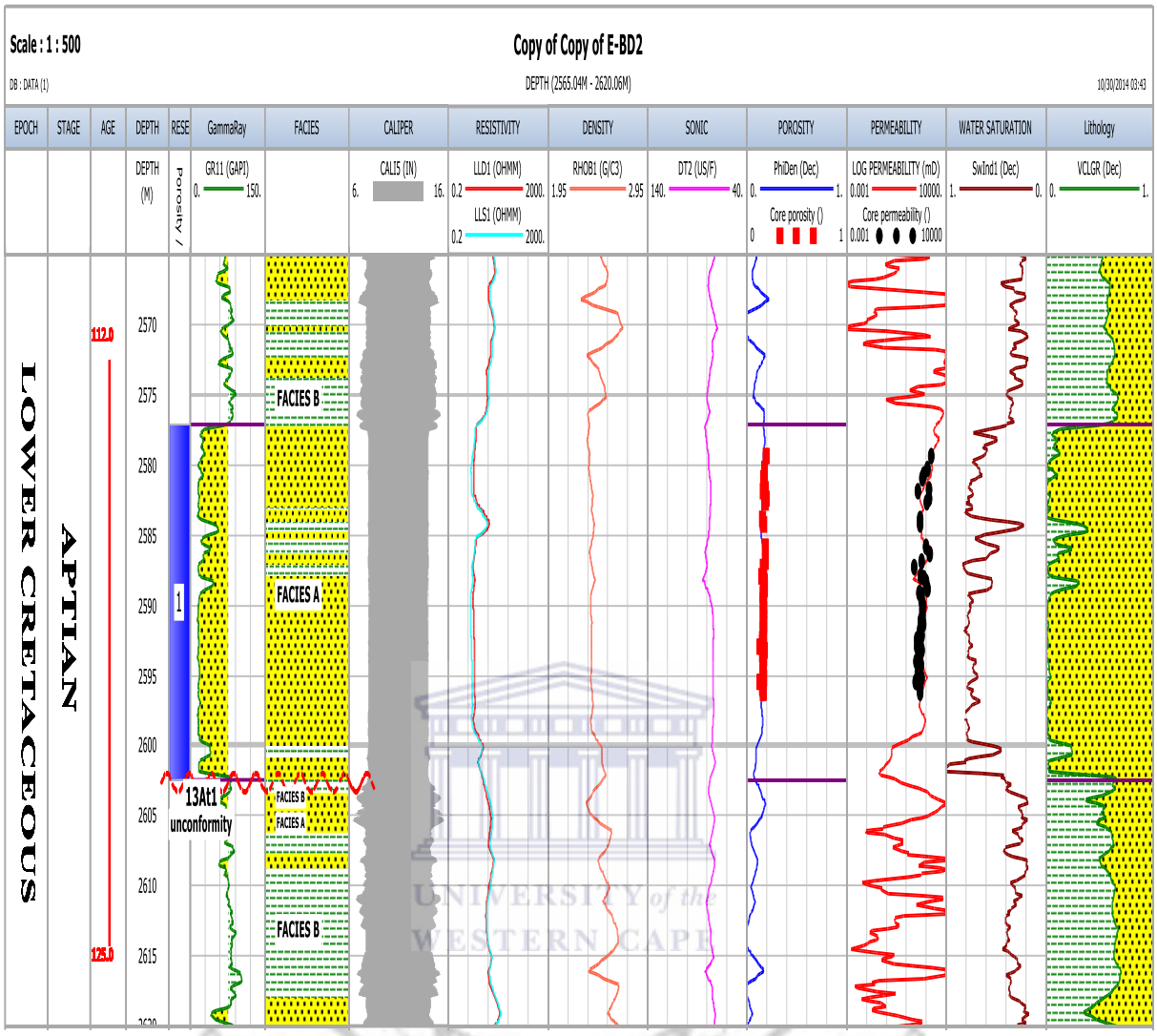

Figure 7.2 Showing various curves behaviour in a hydrocarbon bearing formation of E-BD2. (courtesy of PASA).

7.1.2 Curve interpretation for well E-BD2

Here one reservoir was identified at depth 2576.9m to 2602.4m. The core comprises mostly of clean moderately sorted, fine to medium grained sandstone. A slightly finer grained unit, with occasional claystone stringers, occurs from depth 2584m to 2588.5m and at depth 2600.2m. The sandstone is lithic, with common metaquartzite clasts, probably derived from Cape Supergroup basement. They are slightly feldspathic and carbonaceous, with traces of mica locally.

In track #14 (brown colour water saturation curve), is the water saturation curve which has values 0.565(Dec) at the top of the reservoir at depth 2577.5m, higher value further down of the reservoir at depth 2583.5m. At depth 2584.4m there is a sharp decrease of water saturation and gradually increases to 0.696(Dec) at depth 2589.1m. This decrease here is caused by the presence of the thin claystone stringers that reduces the permeability and porosity at this point of the reservoir. At depth 2600.2m there is another sharp decrease of the water saturation at 0.44(Dec) and again a very high reading of water saturation of 1.3 (Dec) at depth 2601.9m. At this point in the reservoir there is an unconformity at the maximum flooded surface mfs, (Hill, 1991).

In track #13 (red permeability curve) the permeability curve show a good matching relationship with permeability plots (black plots) at depth 2578.8m further down the borehole to depth 2596.9m

In track #12 (blue porosity curve), is a porosity curve which show a good matching relationship with the porosity (indicated in red points) in the reservoir, hence this match does not indicate that the reservoir is a good zone based on the matches but simply it is an indication that the data obtained and processed shows a good correlation with the respective curves. High porosity and permeability are characteristics of a good sandstone reservoir.

In track #11 (the purple coloured sonic curve), is a sonic DT log. The general purpose of sonic log measure the time it takes for a sound pulse to travel between a transmitter and a receiver, mounted on a set distance away along the logging tool. The pulse measured is that of compressional or 'P' wave which is the fastest to arrive at the receiver. A lower to medium velocity reading is recorded due to gas effect in sandstone reservoir hence as shown in well E-BD2 above, (Ellis, 1987).

In track #10 (light brown coloured density curve), is a density (RHOB) curve and shows a lower value of 2.352G/C3 at depth 2576.5m and the reading remains slightly stable further down the curve until at depth 2598.1 were the reading decreases to 2.384G/C3. At depth 2602.1m, there is an increase of 2.531G/C3. There is no neutron (NPHI) curve plotted in this well due to missing data. This increase is as result of an unconformity and a change in lithology from sandstone to claystone stringers at the mfs.

In track #9 (the red coloured resistivity curve is LLD and the aqua coloured curve is the LLS resistivity), here both curves shows low resistivity values at depth 2577.2m, LLD value is 2.59G/C3 and LLS value is 2.61G/C3. At depth 2582.1m, LLD value further decreases to 2.22G/C3 and LLS value decreases to 1.81. At depth 2584.2 there is a sharp spike increase of LLD value to 9.4G/C3 and LLS value to 8.0 then there is a decrease to 2.66G/C3 for LLD and for LLS value to 2.57G/C3. The alternation of values is probably caused by claystone stringers found at this depths, cement, clay minerals present. At depth 2589.6m, LLD value decreases to 2.04G/C3, LLS value decreases to 1.63G/C3 and there is a gradual separation of LLD curve and LLS curve from depth 2589.6m to 2597.7m. This slight separation is a characteristic of fresh water in a porous sandstone formation, (Rider, 2002). At depth 2589.6m to depth 2600.1m there is an increase value, LLD value 5.11D\C3 and LLS value to 4.56D/C3. This increase is caused by the claystone stringers and clay mineralisation present at this zone. Then finally at the base of the sandstone reservoir and on the unconformity (mfs), at depth 2600.1m to 2601.5m there is a decrease of LLD value to 3.46D/C3 to LLS value to 3.56D/C3.

In track #8 (the caliper log), this may show a diameter smaller than the bit size (diameter). If the log has a smooth profile, a mud-cake build-up is indicated. This is an extremely useful indicator of permeability because only permeable beds allow mud cake to form. The limits of mud-cake indicate clearly the limits of the potential reservoir, (Rider, 2002). Mud-cake thickness can be estimated from the caliper by dividing the decrease in hole size by two (the caliper giving the hole diameter), i.e.

$$\frac{\text{Bit size } (diameter) - Caliper\ reading}{2} = \text{mud cake thinkness}$$

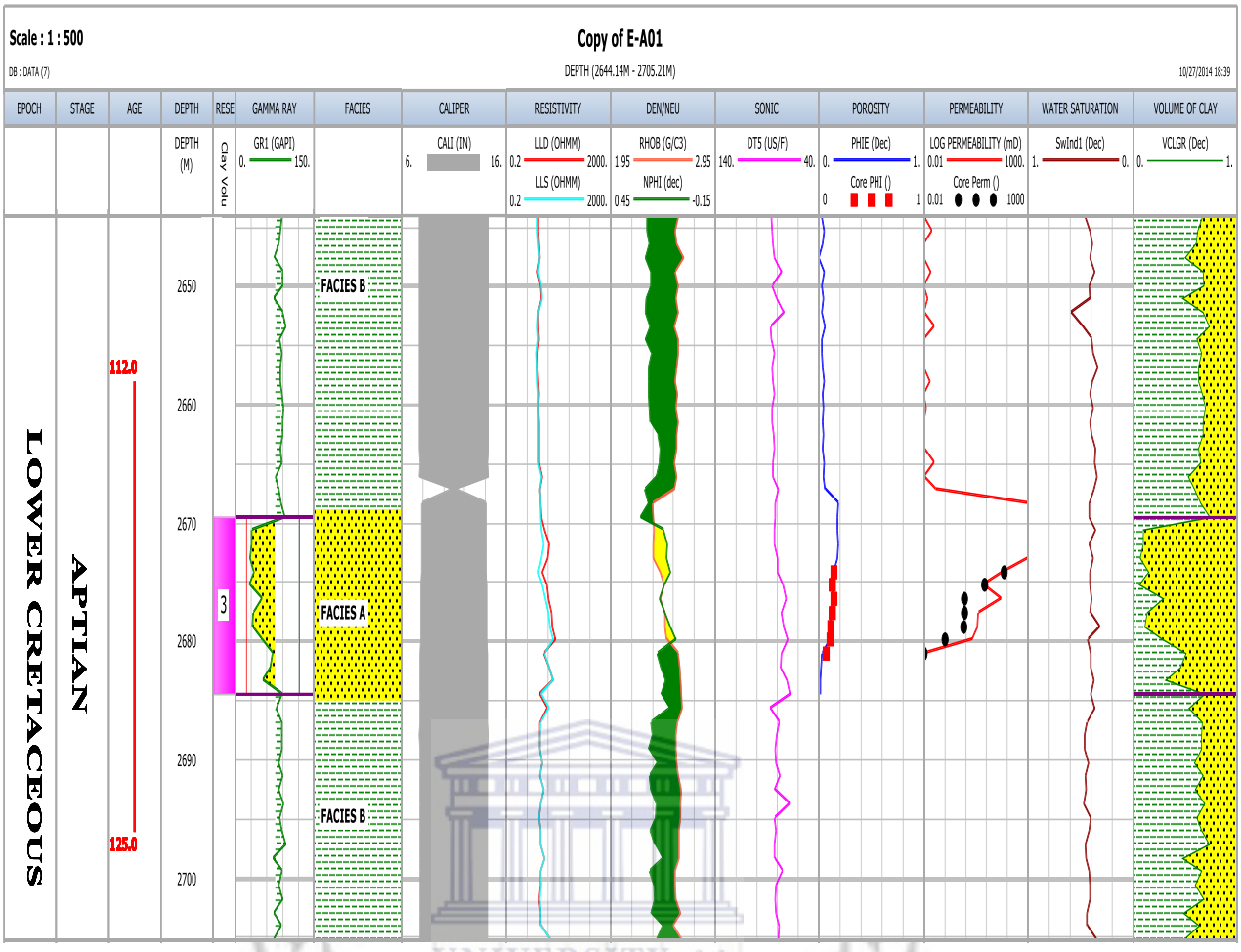

Figure 7.3 Showing various curves behaviour in a hydrocarbon bearing formation of well E-A01 (courtesy of PASA).

7.1.3 Curve interpretation for well E-BD2

Here in well E-A01 three reservoirs were identified but only one is an interest zone. The sandstone here is a clean, very fine to medium grained, shelly, glauconitic section, moderately sorted, comprising of rounded to sub-rounded grains, with loose packing of grains. Porosity and permeability are very good, with 16% porosity and permeability of 106.44mD. Quartz and calcite/dolomite cements appear in minor amounts at depth of 2669.5m to 2684.5m. Preserved porosity is secondary, after cement and grain dissolution. There is alteration of glauconite, and there is also minimal amount of pore filling cements and clays.

In track #14 (brown coloured water saturation curve), at depth 2669.5m the water saturation value reads 0.414mD and suddenly there is a decrease to 0.355mD at depth

2670.6m. There is an increase in water saturation value to 0.413mD at depth 2671.8m and from 2671.8m there is a decrease in water saturation value to 0.38 at depth 2672.9m. At depth 2674.1m water saturation value increases to 0.405mD and then there is a steady trend further downhole till depth 2677.6m to water saturation value 0.405mD. Then there is a sharp decrease at depth 2678.7m and water saturation value is 0.316mD and suddenly there is an increase in water saturation at 0.427mD at depth 2679.9m. Finally at the base of the reservoir at depth 2683.3m there is a decrease in water saturation value reading 0.37mD.

In track #13 (red coloured permeability curve), this is a core permeability curve were permeability is plotted. At depth 2667.2m the core permeability value show a high increase values and then decreases to depth 2675.3m, then increase slightly to depth 2676.4m, increase to depth 2677.6m then to 2679.9m and finally to reservoir base to 2681.0m. This does not show a good match with the facies reason being that the curve could not be generated due to missing data from the data received from PASA, in other to generate this curve, data was gotten from well E-BB1 which is the key well used in this project considering that the wells were drilled at the same site (block 9) hence some E-BB1 data was extrapolated into E-A01 and E-BD2. Such data include water saturation curve, permeability curve. Majority of plotted points are not aligned with the curve only 3 points seem to be aligning with the curve which is not good hence this can be affect by cementation, clay mineral and or claystone stringers cold be present.

In track # 12 (blue coloured porosity curve), this is core density log curve. The plotted point matches well with curve indication that the data show a good correlation with the curve and reservoir. At depth 2667.2m there is an increase of value at Phi value reads 0.0573(Dec). At depth 2668.3m, Phi value reads 0.184(Dec) then Phi curve gradually decreases to 0.0157(Dec) at depth 2683.3m.

In track #11 (the purple coloured sonic curve), is the sonic (DT) log. The general purpose of sonic log measure the time it takes for a sound pulse to travel between a transmitter and a receiver, mounted on a set distance away along the logging tool. The pulse measured is that of compressional or 'P' wave which is the fastest to arrive at the receiver. A lower to medium velocity reading is recorded due to gas effect in sandstone reservoir hence as

shown in well E-A01 (Ellis, 1987). At depth 2667.1m at the top of the reservoir the DT value reads 79us/f meanwhile towards the bottom of the reservoir DT value decreases to about 70us/f at depth of 2679.9m hence decrease in sonic is affected by the presence of hydrocarbon shows in the reservoir.

Track #10 (density curve, light red coloured being RHOB and green coloured curve being NPHI), at depth 2670.6m there is a negative crossover were RHOB value reads 2.369G/C3 and NPHI value reads 0.147 (Dec) to the depth of 2675.3m and RHOB value reads 2.464G/C3 and NPHI value reads 0.142 (Dec). At depth 2677.6m, RHOB value reads 2.473G/C3 and HPHI value reads 0.137(Dec) and at depth 2679.9m, RHOB value reads 2.489G/C3 and HPHI value reads 0.075(Dec) presence of another negative cross over indicating presence of hydrocarbone.

Track #9 (resistivity, red coloured curve being LLD and aqua coloured curve LLS). The LLD measures deeper laterally vertically in to the borehole while the LLS measures shallowly or medium into the lithologies in the borehole. At depth 2669.5m, LLD value reads 4.7 (ohmm) and LLS values reads 4.19ohmm to depth 2678.7m, LLD value reads 12.1ohmm and LLS value reads 9.66 (ohmm). As discussed previously in (chapter 6.1.6) fresh water can also present such displacement in the resistivity logs. This crossover also show the same characteristics as the once in the other reservoir in well E-BB1.

In track #8 (the caliper log), this may show a diameter smaller than the bit size (diameter). If the log has a smooth profile, a mud-cake build-up is indicated. This is an extremely useful indicator of permeability because only permeable beds allow mud cake to form. The limits of mud-cake indicate clearly the limits of the potential reservoir, (Rider, 2002). Mud-cake thickness can be estimated from the caliper by dividing the decrease in hole size by two (the caliper giving the hole diameter), i.e.

$$\frac{\text{Bit size } (diameter) - Caliper\ reading}{2} = \text{mud cake thinkness.}$$

7.1.4 Interpretation of Permeability

The permeability of a rock which is the ability of the rock to allow fluids to flow through its connected pores is controlled by rock grain size, grain shape, degree of cementation or consolidation, grain packing, and clay. Permeability of reservoir rocks may vary from less than 1 mD to over 1000 mD. To determine the permeability of the core plugs, the plugs were placed in a compliant sleeve within a cylinder. A pressure on the sleeve ensures that the injected gas or liquid flows parallel to the core plug axis. Fluid, usually gas is injected with an inflow pressure and flows almost linearly through the plug to atmospheric pressure. The permeability is then determined from Darcy's law. Due to difference in flow physics between gas and liquid especially in low permeability media, a correction is done on the gas or air permeability which is known as Klinkenberg Correction. The permeability values are reported as permeabilities to air and liquid (corrected for the Klinkenberg effect). Gas permeability corrected for the Klinkenberg effect is considered equivalent to the permeability if a liquid medium is present in the pores. The quality of a reservoir as determined by permeability in mD may be scaled as shown in the table below.

PERMEABILITY VALUE (mD)	CLASSIFICATION
Less than 1	Poor
Between 1 and 10	Fair
Between 10 and 50	Moderate
Between 50 and 250	Good
Above 250	Very Good

Table 7.2 Showing Permeability Classification Scale (Modified after Djebbar, 1999).

7.1.5 Well E-BB1 Permeability vs Depth

Core #5 in well E-BB1 borehole permeability plots are concentrated (demarcated in red aquare) at top depth 2845.39m to bottom depth at 2856.60m (fig 7.4). The permeability plots in the zone demarcated in red rectangle is more that 1mD that is between 10mD to 50mD which is classified as fair to moderately and the poor values (less than 1mD) recorded

at reservoir interval as shown in green circles at depth of 2841.5m to 2874.9m. A total of 43 points plotted out of 220 and (177).

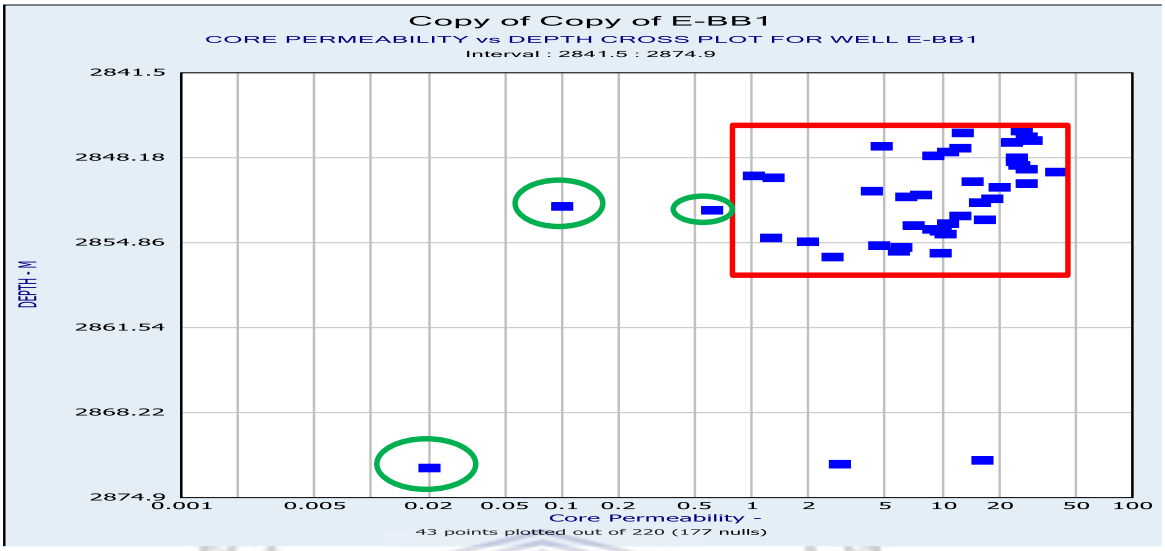

Figure 7.4 Classification of Permeability vs Depth of well E-BB1. (courtesy of PASA).

7.1.6 Well E-BD2 Permeability vs Depth

Core #1 well E-BD2 borehole permeability plots are concentrated (red circle) in the reservoir at top depth 2596.6m to bottom depth at 2587.5m (fig 7.5). The permeability plots in this zone demarcated in red circle are more than 1mD that is between 1mD to more than 250mD which is classified as very good. 84 points plotted out of 168 and (120 nulls).

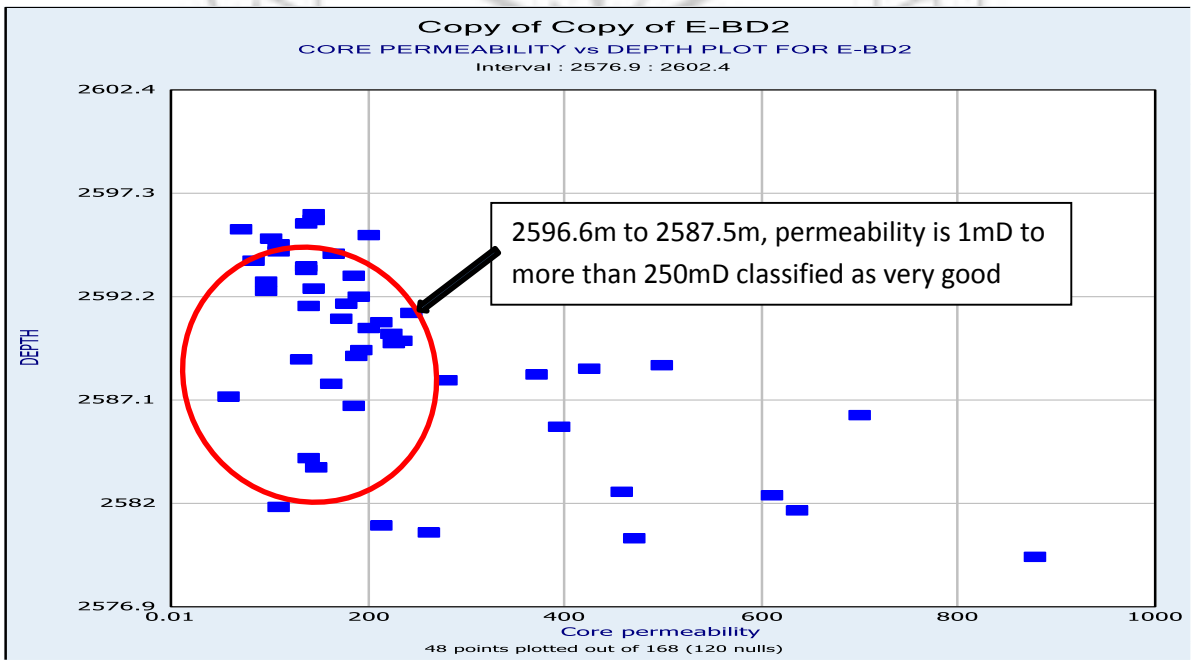

Figure 7.5 Classification of Permeability vs Depth of well E-BD2. (courtesy of PASA).

7.1.7 Well E-A01 Permeability vs Depth

Core #1in well E-A01 borehole permeability plots are concentrated at top depth 2678.89m to bottom depth at 2676.10m (fig 7.6). The permeability plots in the zone demarcated in red circle are less than 1mD hence it is classified as poor permeability for the reservoir. Total of 7 points plotted out of 14 (7 nulls).

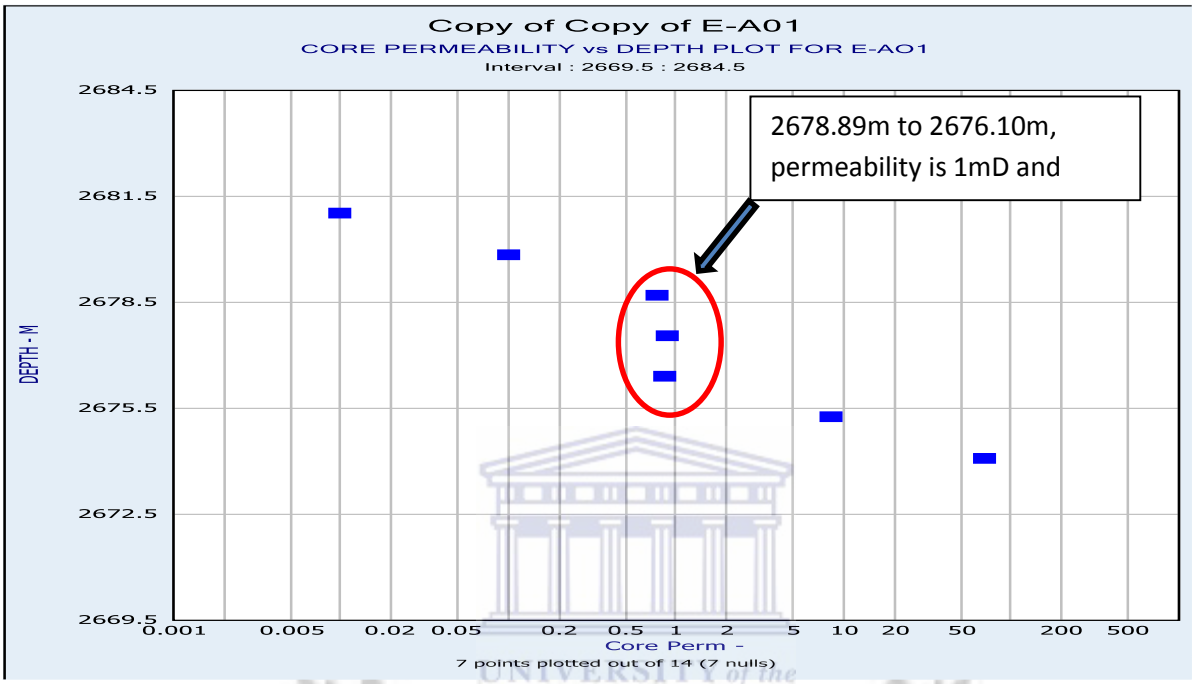

Figure 7.6 Classification of Permeability vs Depth of well E-A01(courtesy of PASA).

7.1.8 Comparison of Core Porosity and Core Permeability

The porosity-permeability cross plots are used to distinguish between rock types and also show the trend between porosity and permeability. Porosity-permeability and facies relationships vary from one exploration well to another well. The Klinkenberg Permeability measured in mD is plotted on a logarithmic scale (y-axis) versus the porosity measured as fraction is plotted on a linear scale (x-axis). Composition and abundance of principal frame work grains have a great impact on diagenetic processes controlling porosity reduction, preservation and enhancement with burial. Heterogeneity and facies variations such as the vertical and lateral changes from cross-bedded to ripple-laminated sandstones, affect reservoir performance.

7.1.9 Well E-BB1

Total of 42 points plotted out of 221 (1 outlier, 175) at top depth 2841.5m to 2874.9m. As shown in the cross plot (fig 7.7) porosity value at 0.1328v/v, permeability value is 22.77mD

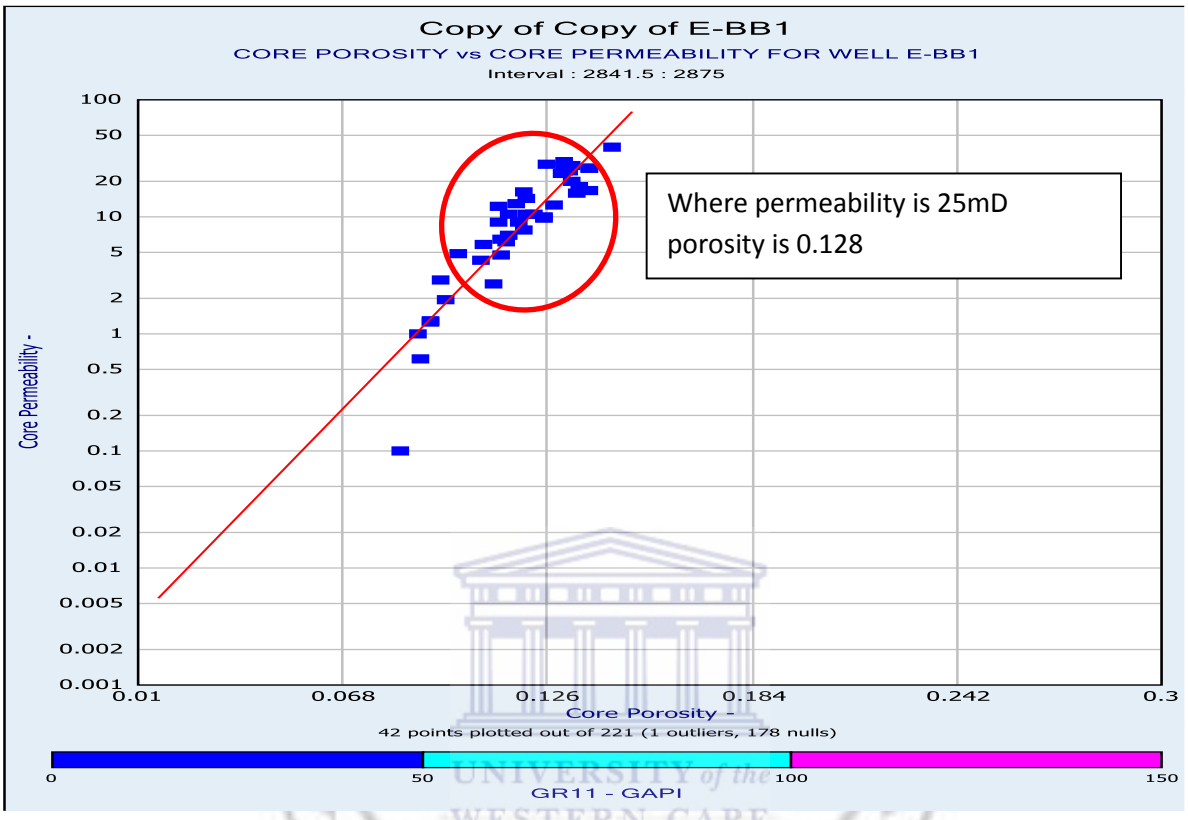

Figure 7.7 Showing comparison of core porosity and core permeability of well E-BB1 (courtesy of PASA).

There is't much clay in this reservoir hence value is more that 1 mD representing a massive sandstone ranging between 1mD to 50mD. The plot show a minimum value of 16 mD, a maximum value of 92 mD and a mean value of 26 mD which is classified as fair to moderate permeability (fig 7.7). Two types of fluid saturation values (saturation of gas, Saturation of water) were reported in well E-BB1. The plot of fluid saturation versus depth present an interval of increasing hydrocarbon saturation (fig 7.8) at depth 2845.5m to 2856.4m which corresponds to the massive sandstone reservoir at depth 2841.5m to 2874.9m. The presence of decreasing water in this interval may represent irreducible water saturation. Below this interval the water saturation increases dramatically with the decrease in gas satureation to the depth of 2874.9m.

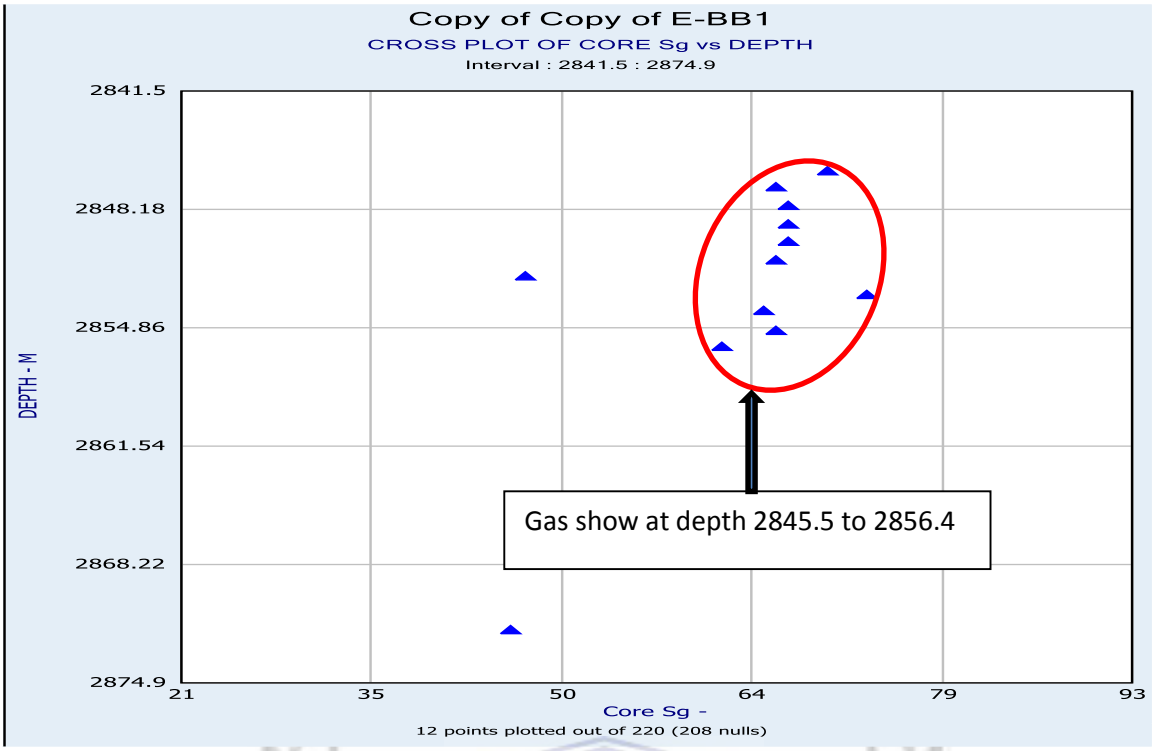

Figure 7.8 Cross plot showing gas concentration in reservoir in well E-BB1(courtesy of PASA).

7.1.10 Comparison of pickett plot for well E-BB1, EBD2 and E-A01

Pickett plot is a visual representation of the Archie equation and therefore is a powerful graphic technique for estimating S_w ranges within a reservoir. All that is needed to make a Pickett plot is a set of porosities and corresponding resistivities taken from well logs. Crossplotted points that lie above the water line have water saturations of less than 100% and complementary hydrocarbon saturations as indicated in (apedix page below). The pickett plots are calculated by plotting deep resistivity log data (LLD) against density log data (Phi) of the same well to be able to have the result. The pickett plots for water resistivity determination for well E-BB1, E-BD2 and E-A01 taken at water bearing zones represented in (figures in apendix). However, their location on the plot does not immediately answer the question concerning the fluids and if the zones will produce when either tested or perforated. Water free hydrocarbons, water-cut hydrocarbons or water alone are all possibilities. The product of porosity and water saturation is the bulk volume of water (BVW) which can give important clues to producibility when related to pore character and reservoir type. As an additional feature, each pair of contiguous zones on Pickett plots

generated are linked by a straight line segment. Taken collectively, the lines sketch out a trace that is the reservoir "trajectory" in the depth dimension of the covariation of resistivity and porosity. Trends, deviations, cut-backs and other features of the trajectory give important clues regarding hydrocarbon column structure, reservoir heterogeneity, cyclic repetition, and changes in pore size. Although the Pickett plot has many useful properties for pattern recognition, there is still room for improvement. When fitting either the water line or a line of irreducible saturation, the resulting values of cementation and saturation exponents are not immediately obvious, but must be calculated from the slopes. The normal range of porosities also means that there is often a fair degree of uncertainty in the estimate of water resistivity when extrapolating to the intercept at 100% porosity.

7.2 Application of result, determination of cut-off and net pay using ϕ, S_w ,V_{sh}.

Net pay (NP) may be defined as “any interval that contains producible hydrocarbon at economic rates given a specific production method”. It thus represents the portion of the reservoir that contains high storability (driven by porosity), high transmissivity (driven by the fluid mobility, which refers to as the ratio of permeability to fluid viscosity), and a significant hydrocarbon saturation (driven by water saturation, Sw). Net pay can be interpreted as an effective thickness that is pertinent to identification of flow units and target intervals for well completions and stimulation programs (Worthington and Cosentino, 2005). The associated net-to-gross ratio (NGR) corresponds to the ratio of the net pay thickness to the total (or gross) thickness of the reservoir under consideration. Net pay (NP) and net-to-gross (NGR) are needed for several reservoir characterization activities. A major use of net pay is to compute volumetric hydrocarbons in-place. Another use of net pay is to determine the total energy of the reservoir i.e. both moveable and non-moveable hydrocarbons are taken into consideration. Net pay for this purpose may be therefore much greater than that for volumetric calculation (George and stiles, 1978). A third use of net pay is to evaluate the potential amount of hydrocarbon available for secondary recovery, meaning net pay with favourable relative permeability to the injected fluid, i.e. “floodable net pay” (Cobb and Marek, 1998). NP and NGR are crucial to quantify the hydrocarbon reserves and have a significant impact on the economic viability of hydrocarbon reservoir production

(Worthington and Casentino, 2005). Net pay determination usually involves defining the threshold values (or cut-offs) of the characteristics of interest. These limiting values are designed to define those rock volumes that are not likely to contribute significantly to the hydrocarbon production although this cut-off values may vary according to the intended application and should be therefore fit for purpose, meaning that " the intended use of the net pay often determines how net pay is picked" (Snyder, 1971). Since the method to pick net pay (and to a larger extent NGR) depends on its usage, these uses determine also the method chosen for establishing cut-off- values.

7.2.1 Summary of the problem

The permeability cut-off is very often considered to be the controlling parameter in net pay and NGR evaluation especially in cases involving the flow regime or the reservoir recovery mechanism. The permeability cut-off, K_c, is dependent on a limited number of parameters including the fluid mobility, the permeability distribution, the reservoir pressure differential, and the reservoir drive mechanism (primary or water-flood). In this research the value considered (for wells E-BB1 which is the key well and E-BD2, E-A01), range typically varies between 0.1 and 100mD depending mainly on the fluid mobility. Because of its low viscosity, gas mobility might remain significant in a tight reservoir (fig 7.01) so the reservoir is still producible: the mobility is therefore an "appropriate starting point" to determine net pay from permeability cut-off (Cobb and Marek, 1998). Nonetheless there is no subsurface continuous permeability measurement (K), ("permeability log") and core permeability measurements are not available throughout all wells.

As a consequence, surrogate variables usually derived from well log measurements, such as porosity (ϕ), amount of shale (V_{sh}) or Clay (V_{cl}) and water saturation (S_w), are generally used to infer the locations and amount of net pay. The selection of cut-off values for these surrogate variable needs to be carefully done in order to avoid introducing further errors into the net pay identification process. It is then necessary for this purpose to test the accuracy and robustness of the availably method providing cut-offs and determine the optimal ones when evaluation either net pay or NGR. In the case where it is already determine based on the mentioned engineering and geological considerations, the

permeability cut-off Kc should be therefore related to those surrogate variables. In this research a common method to identify net pay using porosity (ϕ), (to a larger extent any surrogate variable such as water saturation (S_w), shaliness (V_{sh})) is to use semi logarithmic porosity vs. permeability crossplots (fig 7.9) and a least-squares regression line to obtain the porosity cut-off (Worthington and Cosentino, 2005). A porosity cut-off (ϕ_c) may be obtained from the regression line (fig 7.9). The use of the Y-on-X regression line is an example of methods which may provide porosity cut-off values. These methods were used in this research to obtain the estimates of the "best" cut-off value with associated statistical characteristics.

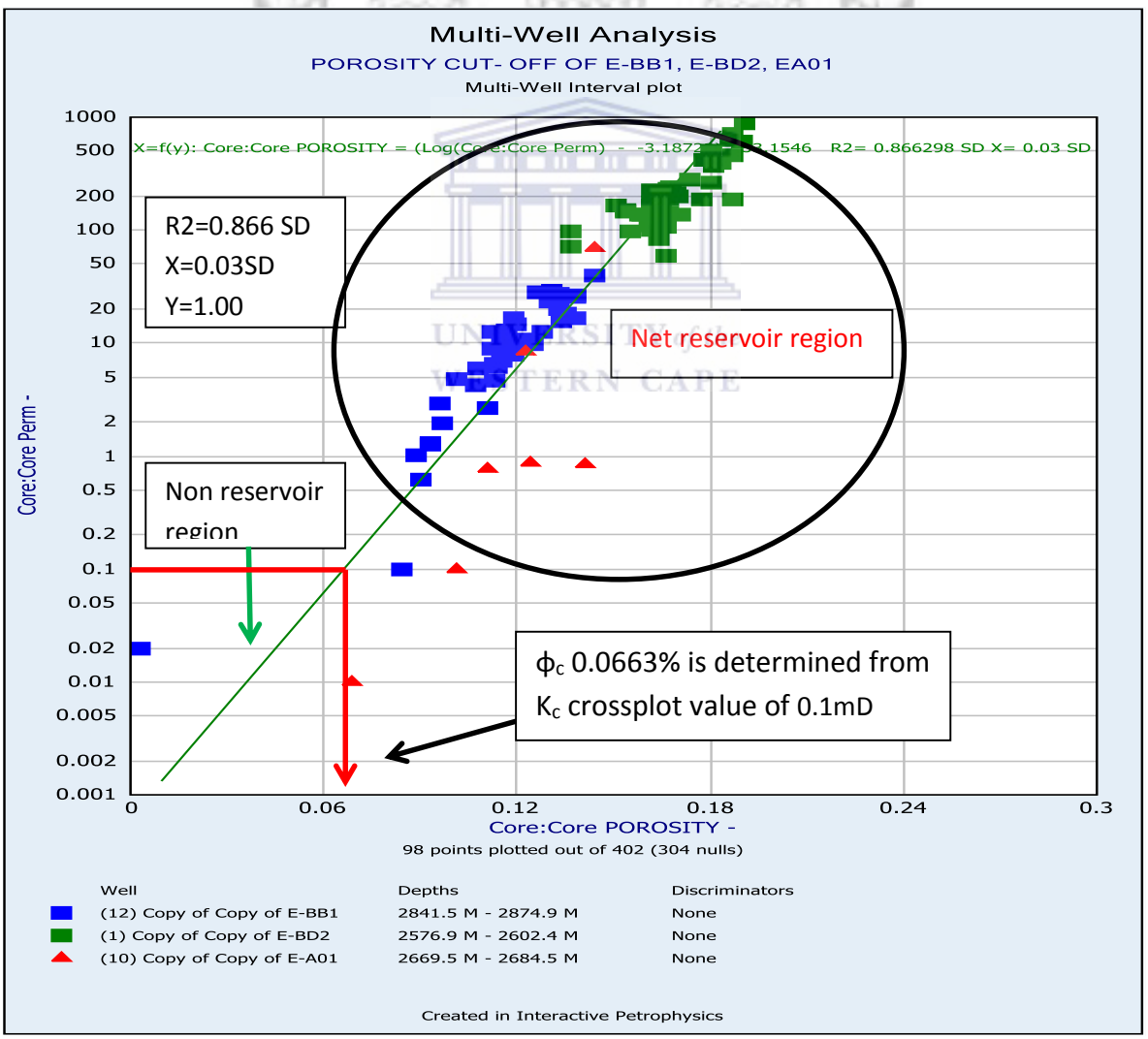

Figure 7.9 Determination of porosity cut-off of multi well E-BB1, E-BD2, E-A01 crossplots (courtesy of PASA).

The best value is the value which when used gives the smallest likelihood error of prediction. This study will investigate which of these several porosity cut-off methods give cut-off values which are optional in terms of bias, efficiency, and robustness when applied to evaluate net pay and NGR for wells E-BB1, E-BD2 and E-A01. A common approach is to define, fixe permeability cut-off values according to the "Rule of Thumb", gas-bearing rocks for which K ≥ 0.1mD are admitted as net pay whereas oil-bearing rocks for which K ≥ 1mD are pay. This approach is arbitrary since the rule of thumb is not taking into consideration the reservoir fluid characteristics. For instance a 1.0mD permeability cut-off is adequate for light, low-viscosity oils (George and Stiles, 1978). Since there is no continuous measurement of permeability, the practice has been therefore to relate core permeability to porosity and/or other log-derivable measurements such as V_{sh}, S_w, and R_t. The cut-off values should be "dynamically conditioned", i.e. they should be tied back to a hydraulic parameter, such as absolute permeability, pore throat radius of fluid mobility (Worthington and Cosentino, 2005). Pirson (1958) developed a "coregraph" method using three independent cut-off for K, ϕ and S_w. Another method from core and log analysis takes account of a different set of three net-pay cut-offs, shale factor V_{sh}, ϕ and S_w (Keener et al., 1967). McKenzie (1975) also defined "producible and non-producible rock types" by establishing an effective pore throat size correlated with the ratio $\frac{K}{\phi}$. A porosity cut-off (ϕ_c) below which there is no commercial permeability can also be considered. Porosity (ϕ), water saturation (S_w) and a bulk-volume ($\phi.S_w$) cut-off value are used for evaluation NP and NGR of oil-bearing carbonates (Teti and Krug, 1987).

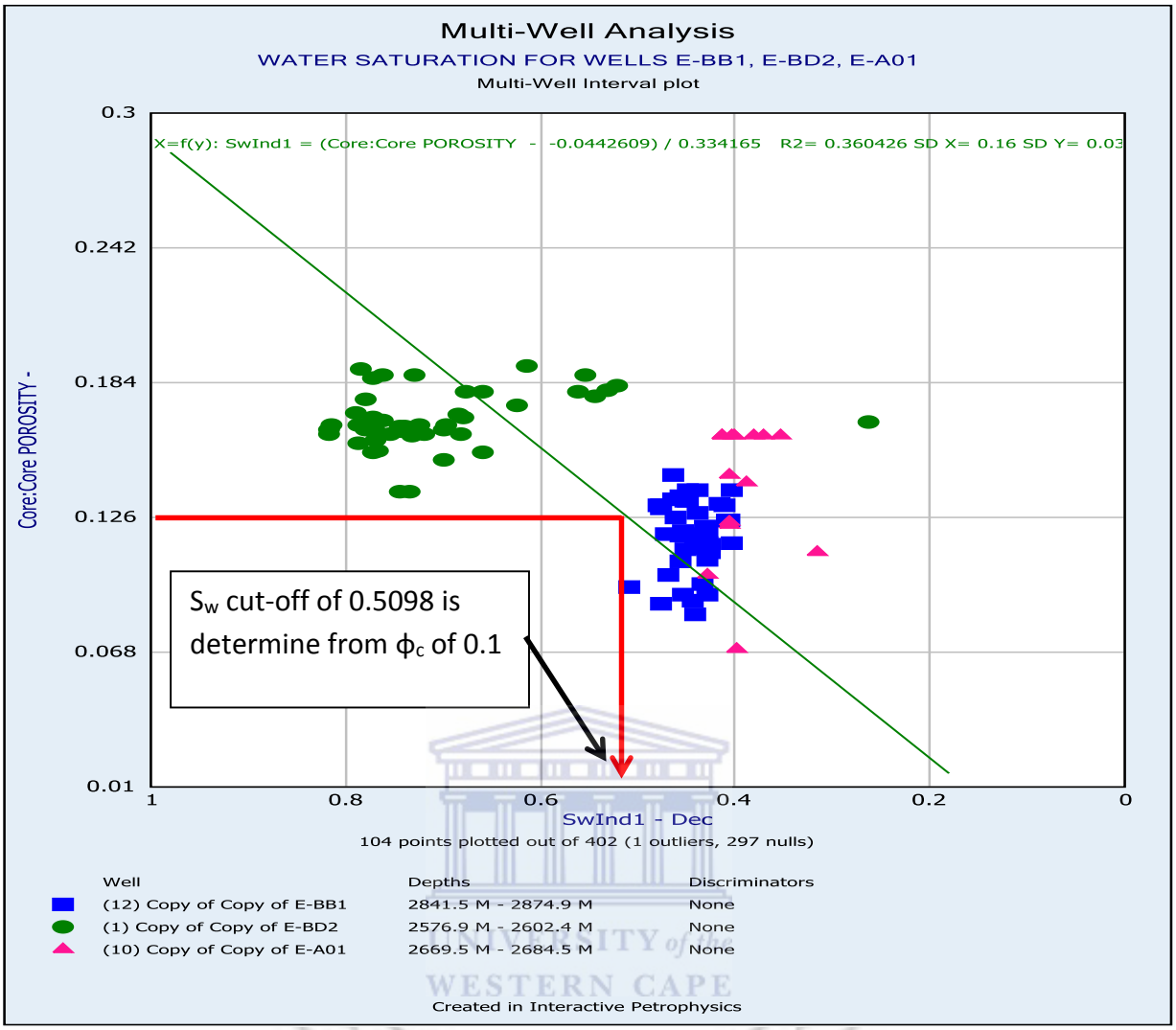

Figure 7.10 Sw determination of wells E-BB1, E-BD2 and E-A01 (courtesy of PASA).

The determination of Vcl is inconsistent since reservoir sandstone and clay are both porous hence porosity could not be used as a surrogate parameter to determine Vcl. A histogram chat (fig 7.11) was used to determine the cut-off value according to the discussion in the previous sub-chapter 7.2, the cut-off value can be picked to best suit the end result depending on what is set to be achieved based on hydrocarbon net pay and or NGR. The values ranges from the cut-off ≤ 0.38 are considered net pay and those values ranging from ≥ 0.38 are non-pay zone.

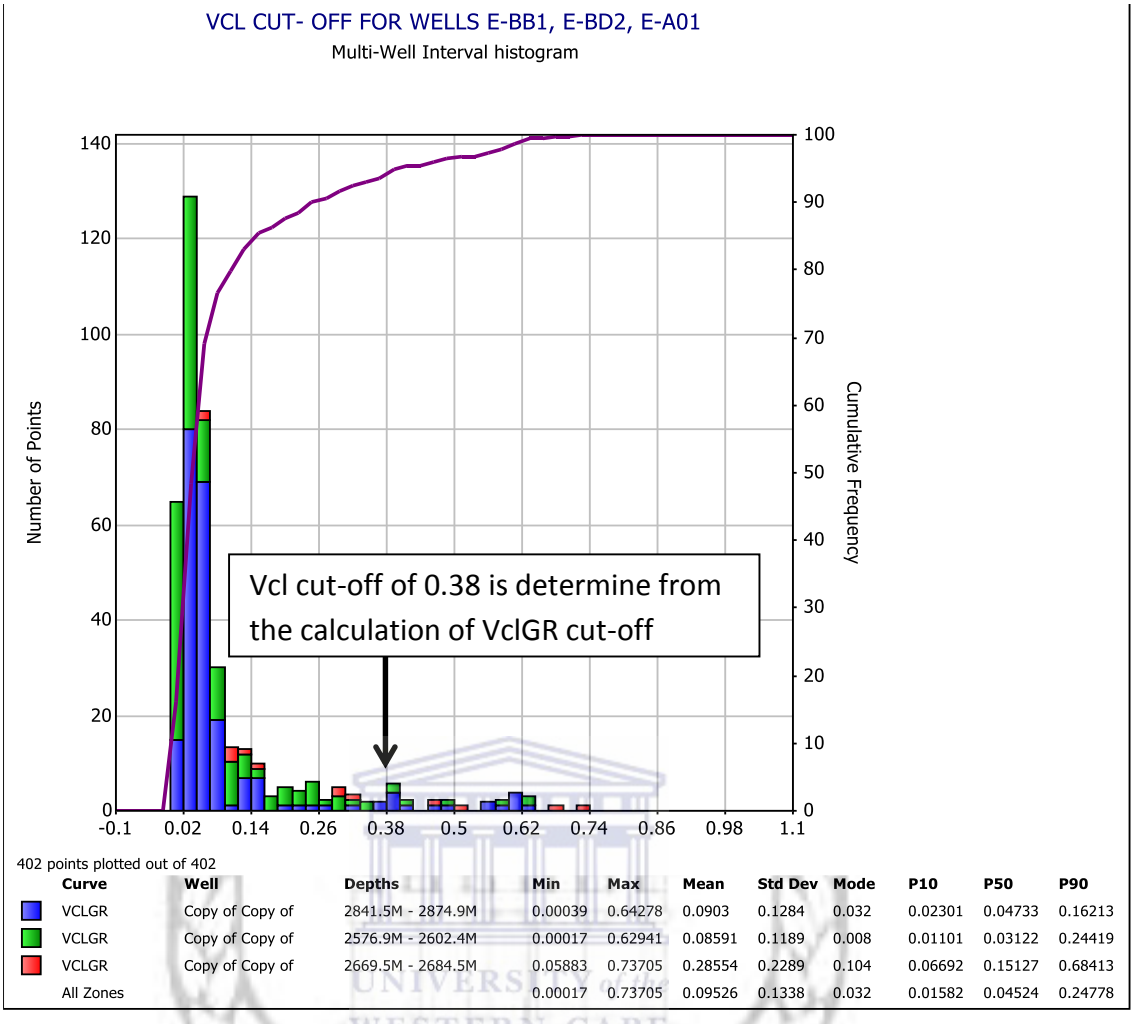

Figure 7.11 Vcl determination of wells E-BB1, E-BD2 and E-A01 (courtesy of PASA).

7.3 Determination of Net Pay

The gross is regarded as the thickness of the reservoir interval that contains zones of which hydrocarbon can be produced and zones which does not favour the production of hydrocarbon. Net pay is any interval within the reservoir that contains producible hydrocarbon at economic rate given a specific production method. It represents the portion of the reservoir that contains high storability and mobility and significant hydrocarbon saturation. Net pay is used to compute volumetric hydrocarbon in place and to determine the total energy of the reservoir which are both moveable and non-moveable hydrocarbons. Other use of net pay is to evaluate the potential amount of hydrocarbon available for secondary recovery (Cobb & Marek, 1998). The distinction between gross and net pay is made by applying cut-off values in the petrophysical analysis. In this research, cut-off values

of porosity (≥ 0.0663), volume of shale (≤ 0.38) and water saturation (≤ 0.5098) were used to identify pay intervals. The net to gross ratio is the thickness of net sand divided by the thickness of gross sand. This ratio is often used to represent the quality of a reservoir zone and for volumetric hydrocarbon calculations. Using the cut-off limits, flag curves were created in the database for net reservoir interval (red colour) and gross reservoir (green). The net to gross ratio determined could be used to calculate the volume of gas originally in place. However, the calculation of volume of hydrocarbon is not part of the scope of this study. Tables 7.3 to 7.5 below are the calculated net pay summary for wells with the corresponding graphics in Figure 7.12 to 7.14.

Two reservoirs encountered in well E-BB1 at depth 2841.5 -2874.9 and 2888.1-2910.5 respectively of which one proved to have net pay of (8.90m) having average porosity of 11.6%, average water saturation of 42.9% and 38% volume of clay as presented in table 7.3 and Figure 7.12 below.

RESERVOIR SUMMARY								**CUT-OFFS USED**		
	TOP DEPTH (m)	**BOTTOM DEPTH (m)**	**GROSS THICK (m)**	**NET PAY (m)**	**NET/ GROSS**	**AV. PHI (v/v)**	**AV. Sw (v/v)**	**PHI (v/v)**	**Sw (v/v)**	**Vcl (v/v)**
RES. #1	2841.5	2874.9	33.40	29.72	0.890	0.116	0.429	>=0.066		<=0.38
RES. #2	2888.1	2910.5	22.40	19.92	0.889	0.110	0.083	>=0.066		<=0.38
PAY SUMMARY										
RES. #1	2841.5	2874.9	33.40	29.57	0.885	0.116	0.429	>=0.066	<=0.5	<=0.38
RES. #2	2888.1	2910.5	22.40	1.48	0.066	0.120	0.083	>=0.066	<=0.5	<=0.38

Table 7.3 Showing summary of calculated net pay for well E-BB1 (courtesy of PASA).

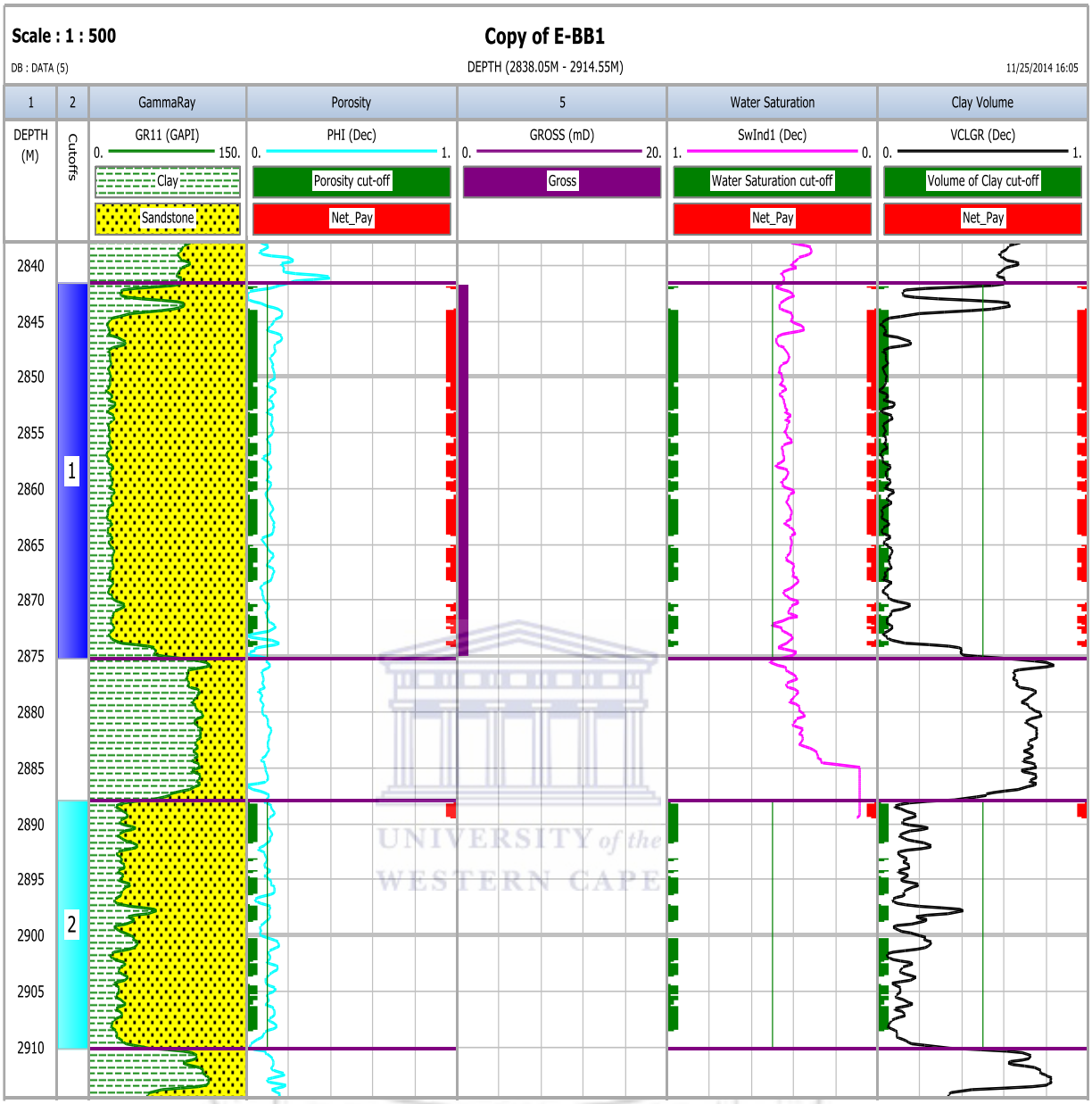

Figure 7.12 Showing ϕ, Sw, Vcl CUT-OFFS AND NET_PAY FOR WELL E-BB1 (courtesy of PASA).

In well E-A01, One reservoir was evaluated and it showed net pay potential as presented in Table 7.4 below. The net thickness range from 1.05m to 15.00m and average porosity is 0.066%, average water saturation is 38.8% and volume of clay is 38%.

RESERVOIR SUMMARY								CUT-OFFS USED		
	TOP DEPTH (m)	BOTTOM DEPTH (m)	GROSS THICK (m)	NET PAY (m)	NET/ GROSS	AV. PHI (v/v	AV. Sw (v/v)	PHI (v/v)	Sw (v/v)	Vcl (v/v)
	2669.5	2684.5	15.00	10.37	0.691	0.115	0.388	>=0.066		<=0.38
PAY SUMMARY										
	2669.5	2684.5	15.00	10.37	0.691	0.115	0.388	>=0.066	<=0.5	<=0.38

Table 7.4 Showing summary of calculate net pay for well E-A01 (courtesy of PASA).

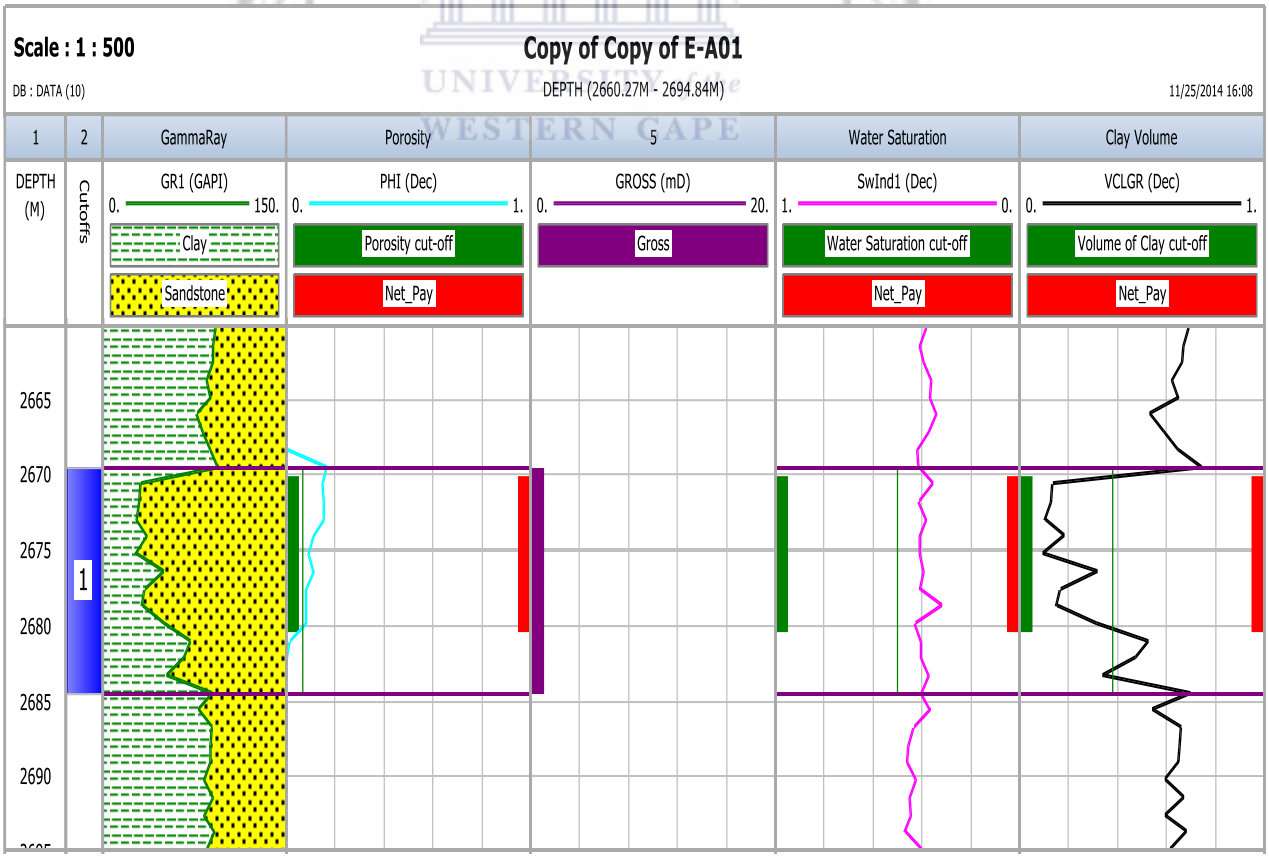

Figure 7.13 Showing ϕ, Sw, Vcl cut-offs and Net_Pay for well E-A01 (courtesy of PASA).

In well E-BD2, the gross thickness range 350m and net thickness is 28.96m. An average porosity of 14.6%, average water saturation of 69.9% and volume of clay is 38% were calculated as presented in Table 7.5 and Figure 7.14 below.

RESERVOIR SUMMARY								CUT-OFFS USED		
	TOP DEPTH (m)	BOTTOM DEPTH (m)	GROSS THICK (m)	NET PAY (m)	NET/ GROSS (m)	Av. PHI (v/v)	Av. Sw (v/v)	PHI (v/v)	Sw (v/v)	Vcl (v/v)
	2576.2	2602.5	350.00	28.96	0.083	0.146	0.659	>=0.066		<=0.38
PAY SUMMARY										
	2576.2	2602.5	350.00	4.57	0.013	0.128	0.358	>=0.066	<=0.5	<=0.38

Table 7.5 Showing summary of calculate net pay for well E-BD2 (courtesy of PASA).

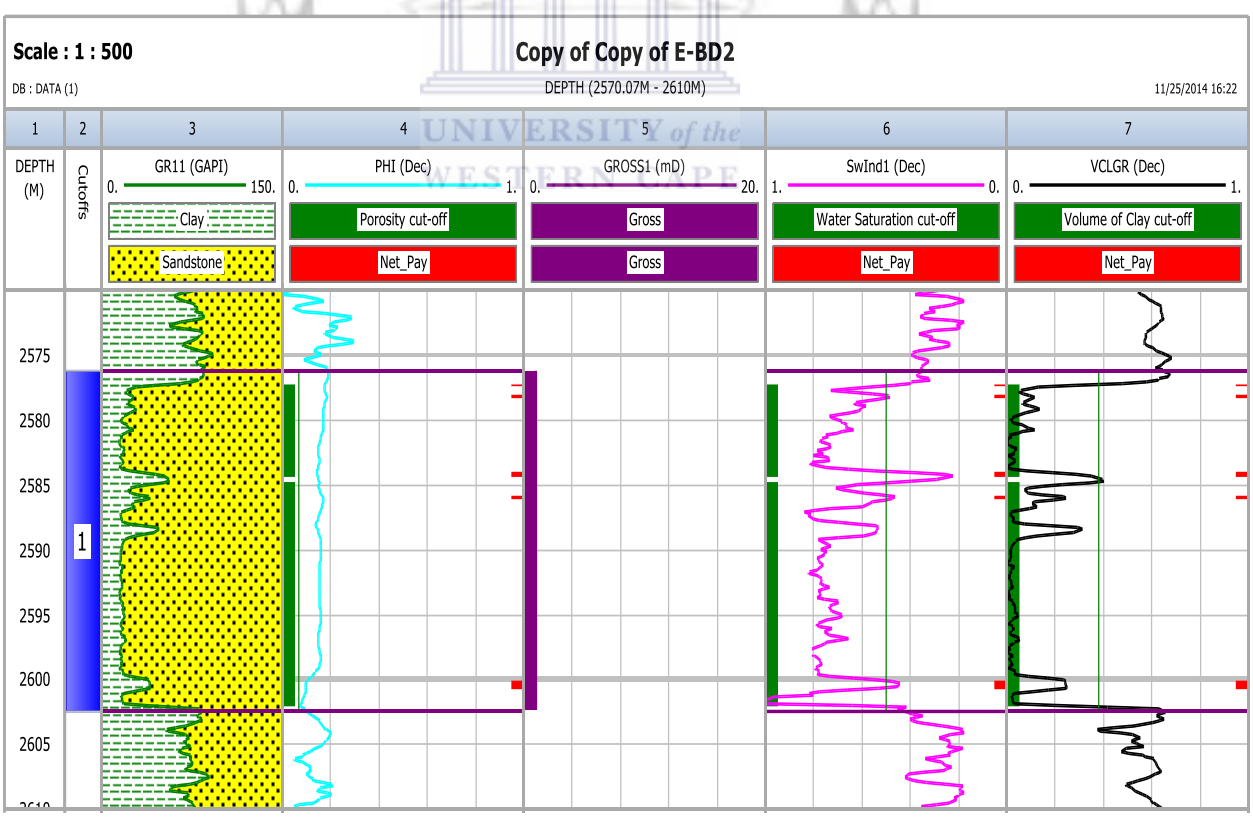

Figure 7.14 Showing ϕ, Sw, Vcl CUT-OFFS AND NET_PAY FOR WELL E-BD2 (courtesy of PASA).

8 CHAPTER

8.1 Conclusion and Recommendation

8.1.1 Conclusion

Petroleum systems are likely to account for all the discoveries made to date in the Bredasdorp Basin. The principal source rock is the deep water mudstone of the 13A seismic unit, and the reservoir unites responsible for the largest volume of reservoirs are the deep water sandstones of the 14A units and shallow marine sandstones of the upper part of the syn-rift sequence. It should be noted that a second unidentified post-rift source rock was invoked to explain geochemically distinct gas and condensate in the 14A play fairway Burden and Davies (1997). The source rock in the deep water organic-rich mudstones of the 13A seismic sequence immediately overlying the 13At1 unconformity. The research findings suggest that well E-BB1 and E-AO1 are stratigraphically located in the rich organic mudstone source rocks hence there was the formation and accumulation of hydrocarbons whereas well E-BD2 is stratigraphically located further away from E-BB1 and E-AO1 which shows very low hydrocarbons potentials. Successive basin wide unconformities (1At1, 5/6At1, 13At1, 15At1, etc) were overlain by deep water mudstones representing a relatively rapid deepening of the basin and development of anoxia due to poor circulation in a restricted basin with limited or non-existent access to the open ocean. More than one of these mudstones may have contributed hydrocarbons to the system but the 13A shales are particularly important as they presently lie in the oil window over significant areas and they are stratigraphically close to the 14A reservoir sands. Reservoirs are of two distinct groups. At the top of the syn-rift succession, Valanginian shallow marine glauconitic sandstones in tilted fault-block structures are hosts to the gas fields of the northern Bredasdorp sub-basin along the southern flanks of the Infanta Arch. Post-rift reservoirs are more intimately associated with the source rock being deep water fan/channel sandstones enclosed in the deep water mudstones that include the source of the hydrocarbons; traps are essentially stratigraphic. Post-rift reservoirs occur at several horizons above and below the 13A source rock but the 14A sandstones are the most important of these. The main play fairway lies along the northern flank of the Agulhas Arch. The stratigraphic extent of the petroleum system is from the deposition of the oldest reservoir rocks in the Valanginian (if the minor

basement reservoir is excluded), to the present. Its active duration is from the start of generation in the deeper parts of the basin in the Lower Cretaceous until the present although the oil and gas that are presently found probably date from generation not longer than than 60 Ma (Paleocene). The following factors are those most critical to effective trapping of hydrocarbons in the basin:

- Generation of hydrocarbons took place due to the depth of burial that had been reached by the Early Tertiary (60 Ma) with a second phase of generation in the Late Tertiary (5 Ma). As it is likely that other source rocks were mature for oil generation before the end of the Early Cretaceous, it seems probably that the volumes of oil and gas that have been generated in the basin are much larger than those that remain at the present-day. Evidence from the 14A play fairway indicates that earlier generated oils have been displaced from known reservoirs by more recently generated gas and gas liquids. The geothermal gradient in the western sub-basins is relatively high resulting in most of the Lower Cretaceous source rocks being in the gas window. Upper Cretaceous source rocks may however be mature and in the oil window in the deeper parts of the basin.

- Trap Formation: The structural component of the syn-rift traps was formed during the second phase of rifting in the Early Cretaceous (Valanginian). The stratigraphic traps of the post-rift succession were formed at the time of deposition possibly with some enhancement due to later compaction under burial.

- Early Sealing: Syn-rift traps were sealed at the earliest in latest Valanginian time with deposition of the oldest mudstones overlying the 1At1 unconformity. Post-rift stratigraphic traps were sealed syn-depositionally.

- Retention: It is very noticeable that the major economic discoveries are restricted to the western part of the Bredasdorp sub-basin. There have been only minor discoveries and shows in the eastern part of the basin. This trend is likely to relate to the increased influence of tectonics from west to east with greater proximity of the Agulhas-Falkland Fracture Zone. Fault-control of sedimentation persisted much later

in the basin history in the east and this is likely to have affected the capacity of the eastern sub-basins to retain any generated hydrocarbons. In addition, there area of deep water deposition in which the main source rocks formed is much less in the eastern sub-basins than the west.

8.1.2 Recommendation

8.1.2.1 Skin effect

Skin is the indication of altered permeability in the wellbore and near wellbore zones (Chen and Chang, 2006). The permeability in this zone is less than that of the formation. It is formed when mud (from drilling or acidization) penetrates or invades the formation near the wellbore (Chen and Chang, 2006). In boreholes E-BB1, E-BD2 and E-A01 in the Bredasdorp Basine, the calculated average Clay volume is 38%, attributed to "blockage" (Steyn, 1990) of the pore throats. These blockages were caused by various Clay minerals present in the formation and drop-out due to flow below dew points as well as mud which was dropped in perforations (PetroSA unpublished data).

8.1.2.2 Proposed Solutions for Enhanced Recovery.

Well testing techniques are essential in determining the lifespan of a well (Penuela and Civan, 2000). Gas-condensate reservoirs fall risk of diminishing at a rapid rate as a result of the drop of flowing bottom-hole pressure below saturation pressure of fluid at reservoir conditions (Penuela and Civan, 2000). Wells should be routinely stimulated for enhanced recovery and productivity. Many treatments conducted in the Ghawar field (Rahim and Al-Qhatani, 2003) have reveal that for high skin factors (38%), a matrix treatment would be more sufficient than fracturing. Most matrix acidization treatments can be performed in two phases, firstly a pre-flush phase of hydrochloric acid followed by a main flush of mud-based acid (Lievaart and Davies, 1987). The sandstones from boreholes E-BB1, E-BD2 and E-A01 display influential amounts of clays and cements which affect the porosity and permeability. These factors play a key role in selecting a suitable enhanced recovery method, along with

the heterogeneous nature of the reservoir zones in relation to porosity and permeability. Thus a secondary method can be applied, for instance matrix acidization injection coupled with hydraulic/acid fracturing. Fracturing is performed first by high pressure viscous injection (Mumallah, 1996) followed by an acid injection into the formed fracture. Heterogeneity within the reservoir zone could cause a problem where by acid will be more prone to enter higher permeability zones. A solution for this problem is the introduction of foam (Siddiqui et al., 2002) which would divert the acid towards lower permeability zones. This is favorable as the foam is clean, which minimizes damage to the formation and can be removed after the acidizing treatment. The redirected acid treatment moves along the fracture towards the lower permeable zones and the walls, dissolving and breaking up the clays and cements (Mumallah, 1996). The pressure is released and the fracture closed yet a pathway, formed by the etched surfaces, remains and acts as a conductive network from the formation into the wellbore. The aspect of Fines migration (Lievaart and Davies, 1987) poses a risk of clogging pore throats with dislodged clay particles. To alleviate this problem a suitable acid should be selected which would dissolve most of the clay particles. The low permeability barriers can be alleviated by fracturing to enhance connectivity for improved gas and gas-condensate flow hence the above methods of treatment can thus be considered to improve the flow rate of hydrocarbons in the wells and wells that will be drilled in future.

8.1.3 Problems encountered during research work;

- The data obtained from Petroleum Agency of South Africa (PASA), there was a massive problems with missing data from the conventional core report on borehole such Sg, Sw and So for well E-BD2 hence it was tough calculating the average water saturation and average temperatures of the cored reservoir zones.
- After loading data into Interactive Petrophysics (IP), there were incomplete or no logs (NHPI) that run through along the target zone of the borehole which makes it difficult to confirm the reading in terms of comparing the reading and interpretation of logs (LLD and LLS) as presented in (fig 7.02) above. Hence calculation of log using parameters in well E-BB1 which is this case is used as a key well that has complete data and the result was exported as LAS file in to wells E-BD2 and E-A01 that missing

data considering condition during basin formation was more or less the same cut across the area the wells are drilled in Bredasdorp Basin.

- The data was mixed up such that corrections was done so that i can be able to work with what I had e.g. top depth value was inverted with bottom depth value in wells E-BB1, E-BD2 and E-A01 hence that correction had to be made.
- It took too long to acquire the available data from PASA to ease research work carried out on time and smoothly.
- IP's licence expiration date is frequent and had to wait for activation since it not controlled by the department or university but by the licence operator and a general set back in network functionality as IP function with internet functionality of the university.
- Students have limited time to carry out research in the department, much and effective work is done late in to the day towards the pm since the department is very busy with undergraduate lectures, contractor of the newly build chemical science building that harbours the earth science department carry out construction works that create lot of interference in terms of noise level (banging and drilling noise). To add to the noise, at 16:00pm students are kicked out of the department for the day. These cause difficulties in caring out this research.

References:

Alvarez, L.W., Alvarez, W. Asaro, F and Michel, H.V. (1980). Extraterrestrial cause for the Cretaceous-Tertiary extension. Science, 208, 1095-1108.

Antonellini and Aydin (1995). Effect of faulting on fluid flow in porous sandstones: Geometry and spatial relations, Bull. Am. Ass. Petrol. Geol. 79, pages 642-671.

Amy, L.A., Talling, P.J., Peakall, J., Wyn, R.B. and Arzola Thynne, R.G. (2005). Bed Geometry used to test recognition criteria of turbidites and (sandy) debrites. Sedimentary Geology, vol. 179: 163-174.

Arthur, M.A., Schlanger, S.O. and Jenkyns, H.C. (1987). The Cenomanian-Turonian oceanic event, 11. Palaeoceanographic controls on organic matter production and preservation. In "Marine Petroleum Source Rocks". (eds) Brooks, J. and Fleet, A.J., Geo., Soc. Spec. publ. No. 26, Blackwell, London, 401-420.

Bailey, N.J.L, Burwood, R. and Harriman, G.E. (1990). Application of pyrolysate carbon isotope and biomarker technology to organofacies definition and oil correlation problems in the North Sea basins. Org. Geochem., 16/4-6, 1157-1172.

Balbinsky and Masters (AEA Technology). A New Flow Based Cut off Criterion for Permeability in Dry Gas Reservoirs.

Banks, N.L., Light, M.P.R. and Miles, J.A. (1992). Technical audit of the petroleum potential of offshore south Africa and its exploration to date. Unpublished report to SOEKOR, 110p.

Barker, C.E. (1990). Calculated volume and pressure changes during the thermal cracking of oil to gas in reservoirs. Am. Assoc. Pet. Geo. Bull., 74/8 1254-1261.

Barron, E.J. and Moore, G.T. (1993). Late Jurassic to mid-Cretaceous source rocks, reservoir and evaporitic seal distribution derived from general circulation model simulation, Ann. AAPG-SEPM-EMO-OPA-DEG Conv. Pap. Abstr., 72.

Barton, K.A. (1996). Participation opportunity in Block 9, offshore Republic of South Africa: borehole E-DE1 rcommendation. SOEKOR unpublished. Ript, SOE-EXP-RPT-370,17pp.

Barton, R.H., Tomlinson, W.D. and Bartington, G.W. (1988). Use of seabotton magnetic susceptibility measurements in hydrocarbon exploration. In "Remote sensing for geologist proceedings1". (eds.) 6th Environ. Res. Inst. Mich. et al., Thematic conference, 137-145.

Barton, K.A. and Grobbler, N.G. (1997). Re-appraisal of the E-CE/E-BD oil and gas field based on the 1996 reprocessing of the 3-D seismic data. SOE-EXPT-RPT-430,36pp.

Beamish, G.W.J. (1990). The seismic expression of depositional systerms tracts and its application to hydrocarbon exploration in the Bredasdorp Basin, offshore Southern Africa. In "Abstracts Geocongress 91", Geol. Soc. S. Afri., Cape Town, 638-641.

Ben-Avraham, Z., Hartnady, C.J.H. and Malan, J.A. (1993). Early tectonic extention between the Agulhas Bank and the Falklands Plateau due to the ration of the Lafonia microplate. Earth Planet. Sci. Lett., 117, 43-58.

Ben-Avraham, Z., Hartnady, C.J.H. and Kitchin, K.A. (1997 in press). Tectonics of the Agulhas-Falklands transform. Tectonophysics, 282, pp. unknown.

Benson, J.M. (1990). Palynofacies characteristics and palynological source rock assessment of the Cretaceous sediments of the northern Orange Basin (Kudu 9A-2 and 9A-3 wells). Communs. Geol. Surv. Namibia, 6, 31-39.

Benson, J.M., Van der Spuy, D. and Davies, C.P.N. (1990). Correlation between optical and chemical maturation indices and their application to the offshore petroleum geology of southern Africa. "Abstracts Geocongress 90". Geol. Soc. South Africa., Cape Town, 643-645.

Benson, J.M., Davies, C.P.N., Elliott, S., Hill, S.J., McMillan, I.K., Marot, J.E.B., Petrie, h., Pringle, A., Valicenti, V.H., Van der Spuy, D. and Wickens, H. deV. (1993). The correlation of sandstone within the 14A turbidite system, central Bredasdorp Basin. SOEKOR unpublished report., SOE-RPT-GEO-002,46pp.

Biddle, K.T., Uliana, M.A., Mitchum, R.M., Fitzgerald, M.G. and Wright, R.C. (1986). The stratigraphic and structural evolution of the central and eastern Magellanes Basin, Southern Africa. In "foreland Basin", (eds.) Allen, P.A. and Homewood, P., Int. Association. Sediment. Spec. Published. No. 8, 41-61.

Birch, G.F., Rogers, K. and Bremner, J.M. (1986). Texture and composition of surface sediments of the continental margin of the Republic of South Africa, Transkei and Ciskei. Marine Geoscience Series 3, Geo. Surv. S. Afr., Pretoria, 4 sheets.

Bishop, A.N. and Philip, R.P. (1994). Potential for amorphous kerogen formation via adsorption of organic material at mineral surfaces. Energy and Fuels, 8, 1494-1497.

Bishop, A.N. and Abbott, G.D. (1995). The interrelationship of biological marker maturity parameters and molecular yields during contact metamorphism. Geochim. et Cosmochim. Acta, 57, 3661-3668.

Boggs, Jr., S. (2001). Principles of Sedimentology and Stratigraphy, Third Edition. Prentice-Hall, Inc., New Jersey, pp 162-168.

Brink, G.J. and Winters, S.J. (1989). Overpressure study of the Bredasdorp Basin. SOEKOR unpublished report 8pp.

Brink, G.J., Kuhlmann, S., Winters, S.J., Fraser, N., Basson, W. and Blagg, J. (1991). Sequence 13A, Bredasdorp Basin: A case study of seismic/sequence stratigraphy integrated with seismic anomaly reservoir and source rock distribution trends. SOEKOR unpolished report. SOE-EXP-RPT-004, 33pp.

Broad, D.S. and Mills, S.R. (1993). South Africa offshore exploratory potential in variety of basins. Oil Gas Jour., 91/49, 38-44.

Broad, D.S. and Turner, J.R. (1982). Stratigraphy, facies and environments of deposition of the C-to-D sequence in the Bredasdorp Basin and Infanta Embayment. SOEKOR unpublished report., 58pp.

Brooks, J., Cornford, C. and Archer, R. (1987). The role of hydrocarbon source rocks in petroleum exploration. In “Marine Petroleum Source Rocks”. (eds.) Brooks, J. and Fleet, A.K., Geol. Soc. Spec. Published. No 26, 17-46.

Brown, D.M. and Ranoszek, M.A. (1990). E-BD1: geological well completion report. SOEKOE unpolished report., SOE-DRG-WCR-309, 18pp.

Brown, D.M. (1991). E-AQ1 post-mortem study and implications for overpressure compartments in the Bredasdorp Basin. SOEKOR unpolished report., 15pp.

Brown, L.F. and Dhorty, S. (1992). Drilling success for sequence stratigraphic targets by Soekor (Pty) Ltd., offshore South Africa, 1987-1992. (abs.). rocky Mountain Association. Geol. Appl. Sequ. Strat. Symp.

Brown, L.F., Benson, J.M., Brink, G.J., Doherty, S., Jollands, A., Jungslager, E.H.A., Keenan, J.H.G., Muntingh, A. and Van Wyk, N.J.S. (1995). "Sequence stratigraphy in offshore South Africa divergent basins". American Association of Petroleum Geology. No. 41,184pp.

Brown, R.W., Rust, D.J., Summerfield, M.A., Gleadow, A,J. and De Wit, M.J. (1990). An early Cretaceous phase of accelerated erosion on the south-western margin of Africa: evidence from apatite fission track analysis and the offshore sedimentary record. Nucl. Tracks Radiat. Meas., 17/3, 339-350.

Burden, P.L.A. (1992). Re-evaluation of the F-F structure south-eastern Bredasdorp basin. SOEKOR unpublished report., SOE-EXP-RPT-001, 28pp.

Burden, P.L.A (1992). Soekor, partners explore possibilities in Bredasdorp Basin off South Africa. Oil and Gas Jour., 90/51, 109-112.

Burden, P.L.A. (1993). Geology and prospectivity of the syn-rift succession in the Bredasdorp Basin. SOEKOR umpublished report., SOE-EXP-RPT-048, 53pp.

Burden, P.L.A. (1997). The geological evolution of the F-S structure in the eastern part of block 9. SOEKOR unpublished. Tech. Note No. 83,9pp.

Burden, P.L.A. and Gasson, M. (1992). Project: The geology of prospectivity of sequence 1A-to-8A in the Bredasdorp Basin. SOEKOR unpublished report., 34pp.

Burden , P.L.A. and Davies, C.P.N. (1997a). exploration to first production on Block 9 offshore South Africa. Oil Gas Journal., 95/36,92-65.

Burden, P.L.A. Davies, C.P.N. (1997b). Oribi field is South Africa's first offshore crude oil production. Oil Gas Jour., 95/37, 63-65.

Burnham, A.K. and Braun, R.L. (1985). General kinetic model of oil shale pyrolysis. In-situ, 9,1-23.

Burnham, A.K. Braun, R.L., Gregg, H.R. and Samoun, A.L. (1987). Comparison of methods of measuring kerogen pyrolysis rates and fitting kinetic parameters. Jour. Energy Fuels, 1/6, 452-458.

Burst, J.F. (1969). Diagenesis of Gulf Coast clays sediments and its possible relation to petroleum migration. Am. Assoc. pet. Geo. Bull., 53, 73-93.

Burwood, R., Cornet, P.J., Jacobes, L. and Paulet, J. (1990). Organofacies variation control on hydrocarbon generation: a Lower Cong coastal basin (Angola) case history. Org. Geochem., 16/1-3, 325-338.

Burwood, R., Leplat, P., Mycke, B. and Paulet, J. (1992). Rifted margin source rock deposition: a carbon isotope and biomarker study of a West African Lower Cretaceous "lacustrine section. Org. Geochem., 19/1-3, 41-52.

Bustin, R.M., Barnes, M.A. and Barnes, W.C. (1990). Determining levels of organic diagenesis in sediments and fossil fuels. In "Diagenesis" (eds.) Mcllreath, I.A. and Morrow, D.W., Geoscience Can. Repr. Ser., 4, 205-226.

Butler, R.W.H., Lickorish, W.H., Grasso, M., Pedley, H.M. and Ramberti, L. (1995). Tectonics and sequence stratigraphy in Messinian basins, Sicily: constraints on the initiation and termination of the Mediterranean salinity crisis. Geol. Soc. Am. Bull., 107/4, 425-439.

Butzer, K.W., Fock, G.J. Suckenrath, R. and Zilch, A. (1973). Palaeohydrology of late Pleistocene lake, Alexanderstontein, Kimberley, South Africa. Nature, 243, 328-330.

Cartwright, J.A. (1989). The structural and stratigraphic development of the Gamtoos and Algoa Basin. SOEKOR unpublished. Report., 26pp.

Cannan, J. and Dessort, D. (1987). Novel family of hexacyclic hopanoid alkanes (C32-C35) occurring in sediments and oils from anoxic palaeoenvironments. Org. Geochem., 11, 103-113.

Chen, C. and Chang, C. (2006). Theoretical evaluation of non-uniform skin effect on aquifer response under constant rate pumping, Journal of Hydrology 317: 190-201.

Chosson, P., Connan, K., Dessort, D. and Lanau, C. (1992). In vitro Biodegradation of steranes and terpanes: a clue to understanding geological situations. In "Biological Markers in sediments and Petoleum". (eds.) Moldowan, J.M., Albrecht, P. and Philp, R.P., Prentice Hall, New Jersey, 320-349.

Christie, A.D.M. (1990). Origin, classification and utilization of oil shales in South Africa. Suid-Afrikaanse Tydskrif vir Weterskap, 86, 9-15.

Clark, J.P. and Philp, R.P. (1989). Geochemical characteristics of evaporate and carbonate depositional environments and correlation of associated crude oils in the Black Creek Basin, Alberta. Bull. Can. Pet. Geol., 37, 401-416.

Clementz, D.M., Demaison, G.J. and Daly, A.R. (1979). Well site geochemistry by programmed pyrolysis. Offshore Tech. Conf. OTC 3410, 465-470.

Cole, D.I. (1992). Evolution and development of the Karoo Basin. In "Inversion tectonics of the Cape Fold Belt, Karoo and Cretaceous basins of Southern Africa." (eds.) De Wit, M.J. and Ransome, I.G.D., A.A. Balkema, Rotterdam, 87-99.

Cole, D.L. and McLachlan, I.R. (1990). Oil potential of the Permian Whitehill Formation in the main Karoo Basin, South Africa. In "Abstracts Geocongress'90". Geol. Soc. S. Afr., Cape Town, 103-105.

Comet, P.A., Rafalska, J.K. and Brooks, J.M. (1993). Sterane and triterpane patterns as diagnostic tools in the mapping of oils, condensates and source rocks of the Gulf of Mexico region. Org. Geochem., 20/8, 1265-1296.

Condie, K.C. (1989). "Plate Tectonics and Crustal Evolution". Pergamom Press, Oxford, 476pp.

Connan, J. (1984). Biodegradation of crude oils in reservoirs. In "Advances in " Petroleum Geochemistry Vol 1". (eds.) Brooks, J. and Welte, D.H., Academic, London, 299-335.

Cooles, G.P., Mackenzie, A.S. and Quigley, T.M. (1986). Calculation of petroleum masses generated and expelled from source rocks. Org. Geochem., 10, 235-245.

Cobb M.W., Marek F.J., (1998): Net pay determination and waterflood depletion mechanisms,SPE 48952,in the Annual Technical Conference and Exhibition;14.

Cornelius, C.D (1975). Geothermal aspects of hydrocarbon exploration in the North Sea area. Norsk. Geol. Ondersoek, 316, 26-67.

Cornford, C. (1986). Source rocks and hydrocarbons of the North Sea. In "introduction to the petroleum geology of the North Sea". (ed.) Glennie, K.W., Oxford Press, London, 197-236.

Conrford, C., Morrow, J.A., Turrington, A., Miles, J.A. and Brooks, J. (1983). Some geological controls on the oil composition in the UK North Sea. In " Petroleum Geochemistry and Exploration of Europe". (ed.) Brooks. J., Geol. Soc. Spec. Publ. No. 12, Blackwell, London, 175-194.

Coster, P.W., Lawrence, S.R. and Foster, G. (1989). Mozambique: a new geological framework for hydrocarbon exploration. Jour. Pet. Geol., 12/2, 205-230.

Creaney, S. and Passey, Q.R. (1993). Recurring patterns of total organic carbon and source rock quality within a sequence stratigraphic framework. Am. Assoc. Pet. Geol. Bull., 77/3, 386-401.

Dalziel, I.W.D. Garrett, S.W., Grunow, A.M., Pankhurst, R.J., Story, B.C.S. and Vennum, W.R. (1987). The Ellsworth-Whitmore Mountains crustal block: its role in the tectonic evolution of West Antarctica. In"Gondwana Six: structure, tectonics and geophysics". (eds.) McKenzie, G.D., Geophysics. Monograph No. 40, Am. Geophys. Union, Washington, 173-182.

Davies, C.P.N (1978). Geochemical report: borehole Gb-C1. SOEKOR unpubl. Rept., 13pp.

Davies, C.P.N (1979). Geochemical report for the Ga-D1 borehole. SOEKOR unpubl. Rept.10pp.

Davies, C.P.N (1988a). offshore hydrocarbon profiling (Sniffer) survey. SEOKOR unpul. Rept., 27pp.

Davies, C.P.N (1988b). Bredasdorp Basin- south flank hydrocarbon expulsion. SOEKOR unpubl. Rept., 17pp.

Davies, C.P.N (1990). Quantification of oil generation and expulsion from source rocks in the offshore Bredasdorp Basin. Abstracts Geocongress 90, Geol. Soc. S. Afr., Cape Town, 119-122.

Davies, C.P.N (1991). Geochemistry section: calcimetry analyses – accuracy and repeatability testing. SOEKOR unpubl. Rept., 17pp.

Davies, C.P.N (1992). Gamtoos Basin: geochemical correlation of oils and shale. SOEKOR unpubl. Rept.,17pp.

Davies, C.P.N (1993a). 14 megasequence project: the chemical contribution. SOEKOR unpubl. Rept., 37pp.

Davies, C.P.N (1993b). E-CB1: Modelling of expected hydrocarbon. SOEKOR sunpubl. rept., 34pp.

Davies, C.P.N (1993c). |Geochemistry report on features of borehole F-BB1. SOEKOR unpubl. Rept.,18pp.

Davies, C.P.N (1994a). Geochemical correlation of oils in 14A reservoirs in wells E-BT1, E-BTO1P, E-AR1, E-AA1 and E-AD1. SOEKOR unpubl. Rept., SOE-GCH-RPT-131, 41pp.

Davies, C.P.N (1994b). Kinetic, burial history and biomarker studies of the Neptuno XE-1, and Calafate PK-1 wells in the Magallanes Basin, Chile. SOEKOR unpubl. Rept., 27pp.

Davies, C.P.N (1995a). Log-derived salinity data: an investigation of sands in the Bredasdorp Basin. SOEKOR unpubl. Rept., SOE-GCH-RPT-249, 14pp.

Davies, C.P.N (1995c). Gas: Oil ratios. SOEKOR unpubl. Tech. Note No. 23, 7pp.

Demainson, G.J., Holck, A.J.J., Jones, R.W. and Moore, G.T. (1990). Anoxic environments and oil source bed genesis. Am. Assoc. Pet. Geol. Bull., 64/8, 1179-1209.

Demainson, G.J., Holck, A.J.J., Jones, R.W. and Moore, G.T. (1988). Predictive source bed stratigraphy; A guide to regional petroleum occurrence. In "Geochemistry". (comps.) Beaumont, E.A. and Foster, N.H., AAPG Treatise Pet. Geol. Rept. Ser. No. 8, 323-333.

Deming, D. (1994). Factors necessary to define a pressure seal. Am. Assoc. Pet. Geol. Bull., 78/6, 1005-1009.

De Paolo, D., Stolper, E. and Thomas, D. (1996). Hawaii scientific drilling project: summary of preliminary results. GSA Today, 6/8 1-8.

Derbyshire, J. (1964). A hydrological investigation of the Agulhas Current areas. Deep-sea Res., 11, 781-815.

De Swardt, A.M.J. and McLachlan, I.R. (1982). Petroleum in the South African offshore: the geological framework and hydrocarbon potential. Proc. 12th CMMI Congress. (eds.) Glen, H.W., S. Afr. Inst. Min. Metall., Johannesburg, 147-161.

Dingle, R.V. (1977). The anatomy of a large submarine slump on a sheared continental margin (SE Africa). Jour. Geol. Soc. Lond., 293-310.

Dingle. R.V. and Gentle, R.I. (1972). Early Tertiary volcanic rocks on the Agulhas bank, South African continental shelf. Goel. Mag., 109, 127-136.

Dingle. R.V., Siesser, W.G. and Newton, A.R. (1983). "Mesozoic and Tertiary Geology of Southern Africa". A.A. Balkema, Rotterdam,375pp.

Dow, W.G. (1974). Application of oil-correlation and source-rock data to exploration in Williston Basin. Am. Assoc. Pet. Geol. Bull., 58/7, 1253-1262.

Dow, W.G. (1977). Kerogen studies and geological interpretation. Jour. Geoch. Expl., 7, 79-99.

Duane, M.J. and Brown, R.W. (1991). Tectonic brines in sedimentary basins: further applications of fission track analysis in understanding Karoo Basin evolution (South Africa). Basin Res., 3, 187-195.

Duncan, R.A. (1981). Hotspots in the Southern Ocean, an absolute frame of reference for motion of the Gondwana continent. Tectonophys., 74, 29-42.

Duncan, R.A., Hargraves, R.B. and Brey, G.P. (1978). Age, palaeomagnetism and chemistry of melilite basalts in the Southern Cape, South Africa. Geol. Mag., 115/5, 317-327.

Du Toit, A.L. (1954). "Geology of South Africa". Oliver and Boyd, Edinburgh, 611pp.

Eglington, B.M., Auret, J.M. and Retief, E.A. (1990). Results of a Rb-Sr isotopic study of biotites from boreholes F-F2 and F-O1. EMATEK (CSIR) unpubl. Rept. to SOEKOR, EMA-C 90119, 4pp.

Eglinton, G. and Calvin, M. (1967). Chemical fossils. Sci. Amer., 219, 32-43.

Ekweozor, C.M. and Telnaes, N. (1990). Oleanane parameter: verification by quantitative study of the biomarker occurince in sediments of the Niger delta. Org. Geochem., 16/1-3, 401-413.

Ellis DV, Singer JM (1987): Well logging for Earth Scientist.

Erlank, A.J., Le Roex, A.P., Harris, C., Miller, R.McG. and McLachlan, I.R. (1990). Preliminary note on the geochemistry of basalt samples from the Kudu boreholes. Communs. Geol. Surv. Namibia, 6, 59-61.

Espitalié, J., Laporte, J.L., Madec, M., Marquis, F., Leplat, P., Paulet, J. and Boutefou, A. (1977). Méthod rapide de caratérisation des roches mères, de leur potential pétolier et de leur degré d'évolution. Rev. inst. Fr., 32, 23-42.

Espitalié, J., Deroo, G. and Marquis, F. (1985). La pyrolyse Rock-Eval et ses applications, Deuxiéme partie Rev. Inst. Fr. Du Petrole, 40/6, 755-784.

Eurotrack (1996). Fission track analyses of apatite from two samples. Unpubl. Rept. to SOEKOR, Eurotrack, London, 17pp.

Fleet, A.J. and Scott, A.C. (1994). Coal and coal-bearing strata as oil-prone source rocks: an overview. In "Coal and coal-bearing strata as oil-prone source rocks?". (eds.) Scott, A.J. and Fleet, A.C., Geol Soc. Lond. Spec. Publ. No 77, Geol. Soc., London, 1-8.

Fouche, J., Beate, K.J. and Van der Merwe. R. (1992). Pate tectonic setting of the Mesozoic basins, southern offshore, South Africa: a review. In "inversion tectonics of the Cape Fold

Belt, Karoo and Cretaceou Bains of Southern Africa". (eds.) De Wit, M.J. and Ransome, I.G.D., A.A. Balkema, Rottwerdam, 33-59.

Frakes, L.A. and Kemp, E.M. (1972). Incluence of continental positions on early Tertiary climates. Nature, 240, 97-100.

Friedinger, P.J.J. (1988). The hydrocarbon potential of the F-F structure (South eastern Bredasdorp Basin). SOEKOR unpubl. Rept., 11pp.

Funnel, R.H. and Allis, R.G. (1996). Hydrocarbon maturation potential of offshore Canterbury and Great south Basins. In "1996 New Zealand Pet. Conf. Proc. Vol. 1st, New Zealand Crown Minerals, Wellington, 22-30.

Gay, S.P.C. (1992). Epigenetic versus syngenetic magnetite as a cause of magnetic anomalies. Geopys. 57/1, 60-68.

George CJ, Stile LH (1978): Improve techniques for evaluating carbonate waterfloods in West Texas, Journal of Petroleum Technology, vol 30, no 6; 1547 -1554.

Gerrard, I. and Smith, G.C. (1983). Post-Palaeozoic succession and structure of the south-western African continental margin. In "studies in Continental Margin Geology" (eds.) Watkins, J.S. and Drake, C.L., Am. Assoc. Pet. Geol. Mem. No. 34, 49-74.

GETECH (1992). African magnetic mapping project-total magnetic field anomaly map. ULIS Ltd., England.

Gier, S. and Johns, W.D. (2005). Clay mineral diagenesis in interbedded sandstones and shales (Aderklaa-78, Vienna Basin): Comparisons and correlations, Geophysical Research Abstracts, vol. 7, European Geosciences Union 2005.

Gilbert, D. (1977). Organic facies variation in the Mesozoic south Atlantic. in "Initial Reports Deep Sea Drilling Project Leg 75". (eds.) Hay, W.W., Sibuet, J-C. et al., Washington (US Govt. Printers Office), 1035-1049.

Gilbert, C.E. and Roux, J. (1992). Evaluation of the 13A reservoirs at E-AR. SOEKOR unpubl. rept., SOE- PEN-ART-051, 29pp.

Gilbert, CE (1990). Sandstone distribution in the 14At1 level in the E-G area, south-central Bredasdorp Basin: implication for a predictive depositional model. In "Abstracts Geocongress 90",. Geol. Soc. S. Afr., Cape Town, 177-180.

Grobbleer, N. (1995). Formation water salinities in the Bredasdorp Basin. SOEKOR unpubl. rept. SOE-GEO-RPT-313, 14pp.

Gründlingh, M. (1984). Environmental observations: Sedco K- ocean current and temperature observations. CSIR-NRIO unpubl. rept. to SOEKOR No. C/SEA 7913 (rev.), 4pp.

Hälbich, I.W. (1983). The Cape Fold Belt-Agulhas transect across the Gondwana suture, Southern Africa. Global Geosci. Trans., 9, Geophys. Union, Washington, 18pp.

Hälbich, I.W., Fitch, F.J. and Miller, J.A. (1983). Dating the Cape orogeny. Spec. Publ. Geol. Soc. South Africa., 12, 149-164.

Hamel, C. and Thom, R. (2001). A petrographic comparison of Sandstones from the Hibernia Formation, Mississauga Sands and the Avalon Formation. In: Rock the Foundation Convention, Canadian Society of Petroleum Geologists, pp18-22.

Haszeldine, R.S., Cavanagh, A.J. and England, G.L. (2003). Effects of oil charge on illite dates and stopping quartz cement: calibration of basin models. Journal of Geochemical Exploration Abstracts 78-79: 373-376.

Haq, B.U. and Van Eysinga, F.W.B. (1987). "Geological Time Table", 4th ed., Elsevier, Amsterdam.

Haq, B.U., Hardenbohl, J. and Vail, P.R. (1987). The new chronostratigraphic basis of Cenozoic and Mesozoic sea level cycles. Cushman Foundation Foram. Res. Spec. Publ. No 24.

Hartnady, C.J.H. and Le Roex, A.P. (1985). Southern Ocean hotspot tracks and the Cenozoic absolute motion of the African, Antarctic and South American plates. Earth Planet. Sci. Let., 75, 245-257.

Hartnady, C.J.H. and Partridge, T.C. (1995). Neotectonic uplift in Southern Africa: a brief review and geodynamic conjecture. in "Centernnial Geocongress (1995): extended abstracts vol 11"., Geol. Soc. S. Afri., 456-459.

Hatch, F.H., Wells, A.K. and Wells, M.K. (1963). "Petrology of the Igneous Rocks". Thomas Murby, London, 515pp.

Hays, J.D., Imbrie, J. and Shackleton, N.J. (1976). Variations in the earth's orbit: pacemaker of the ages. Science, 194, 1121-1132.

Harbin, J.P., (1986). Sea-level curve for Pennsylvanian eustatic marine transgressive-regressive cycles along mid-continental outcrop belt, North America Geology, 14, 330-334.

Herbin, J.P., Magniez-Jannin, F. and Muller, C. (1986). Mesozoic organic rich sediments in the South Atlantic: distribution in time and space. SCOPE/UNEP Sonderbund, 60, 71-97.

Hildebrand, A.R., Renfield, G.T., Kring, D.A., Pilkington, M. Camargo, A., Jacoben, S.B. and Boynton, W.V. (1991). Chicxulub crater: a possible Cretaceous-Tertiary boundary impact crater on the Yucatán Peninsula, Mexico. Geology, 19, 867-871.

Hill, S.J. (1991). Petrographic subdivision and correlation of the 14A sandstones in the central Bredasdorp Basin. SOEKOR unpubl. rept., 10pp.

Hill, S.J. (1991). SOEKOR petrographic analysis- Borehole E-BB1.

Hill, S.J. (1995a). F-A gas field: petrographic appraisal. Halliburton unpubl. rept. to SOEKOR, HALPET R007/95, 22pp.

Hill, S.J. (1995b). Petrographic appraisal of pre1At1 sandstones from the northern flank of the Bredasdorp Basin. Halliburton unpubl. rept. to SOEKOR, HALPET R0194/95, 21pp.

Hill, S.J. (1996). Cabornate cementation of 14A sandstones in the southern part of the central Bredasdorp Basin. Halliburton unpubl. rept. to SOEKOR, HALPET R 004/96, 11pp.

Hodges, K. (1996). The geology of the deep marine sandstones of the 9At1-to-13At1 interval in the central Bredasdorp Basin. SOEKOR unpubl. rept., SOE-EXP-RPT-342, 16pp.

Holmes, A. (1994). "Principles of physical geology". Nelson, London 482-489.

Honiball, A. (1995). Palaeogeographyic maps of offshore South Africa. SOEKOR unpubl. rept., Tech, Note No. 56, 11pp.

Hovland, M., Croker, P.F. and Martin, m. (1994). Fault-associated seabed mounds (carbonate knolls?) off western Ireland and north-west Australia. Mar. Pet. Geol., 11/2, 232-246.

Howell, D.G. and Normark, W.R. (1982). Sedimentology of submarine fans. In: Scholle, P.A. and Spearing, D. (eds.), 1982. Sandstone Depositional Environments, The American Association of Petrtoleum Geology, 410pp.

Huber, B.T. and Watkins, D.K. (1992). Biogeography of Campanian-Maastrichtian calcareous plankton in the region of the Southern Ocean. In "The Antarctic palaeoenvironment: a perspective on global change-1".(ed.) Kennet, J.P. and Warnke, D.A., Antarctic research series No. 56, Am. Geophys. Union, 31, 60.

Johnson, M.R. (1990). Provenance and tectonic stting of the Cape-Karoo basin in the eastern Cape Province in "Abstracts Geocengress 90". Geol. Soc. S. Afr., Cape Town, 690-547.

Jungslager, E.H.A. (1996). The syn-rift of the Bredasdorp Basin. SOEKOR unpubl. rept., SOE-GEO-RPT-380, 61pp.

Karmakar, R., Manna, S.S. and Dutta, T. (2003). A geometrical model of diagenesis using percolation theory. Physica A 318: 113-120.

Kearey, P. (1996). Dictionary of Geology, Penguin Books Ltd., England, pp 366.

Kuntcheva, B., Kruhl, J.H. and Kunze, K. (2006). Crystallographic orientations of high-angle grain boundaries in dynamically recrystallized quartz: First results. Tectonophysics 421: 331-346.

Larsen, M. (1995). Overpressure study. SOEKOR unpubl. Tech. Note No. 29, 12pp.

Larsen, R.L. (1991). Geological consequences of superplumes. Geology, 19/10, 693-966.

Lawrence, S.R. and Johnson, M, (1995). Shelf north of Falklands may be new South Atalntic petroleum province. Oil Gas Jour., 93/9, 52-55.

Lawver, L.A., Gahagan, L.M. and Coffin, M.F. (1992). The development of palaeoseaways around Antarctica. In "The Antarctic palaeoenvionment: a perspective on global change". (eds.) Kennett, J.P. and Warnke, D.D., Antarctic Res. Ser. 56,c7-36.

Lee, Y.I., Sur, K.H. and Hisada, K. (2005). Assymmetric diagenetic changes in a half-graben basin: the Kanmon Group (Lower Cretaceous), SW Japan. Cretaceous Research 26: 73-84.

Le Roux, D.M., (1983). Geological structure in the little Karoo about 21°E longitude. Spec. Publ. Geol. Soc. South Africa., 12, 65-74.

Lievaart, L. and Davies, D.R. (1987). The role of fines during acidizing treatments, Marine and Petroleum Geology, Vol. 4: 127-131.

Loring, D.H, and Rantala, R.T.T. (1992). Manual for the geochemical analysis of marine sediments and suspended particulate matter. Earth Sci. Rev., 32, 235-283.

Loutit, T.S., Hardenbol, J., Vail, P.R. and Baum, G.R. (1989). Condensed sections: The key to age dating and correlation of continental margin sequences. In "Sea-level changes: an intergrated approach". (eds.) Wilgus, C.K., Hastings, B.S. Kendall, C.G.St.C., Posamentier, H.W., Ross, C.A. and Van Wagoner, J.C., Soc. Pal. Mineral. Spec. Publ. No. 42, 1-40.

Luca, C., (2001): Integrated reservoir studies Editions Technip Paris, p., 139-143.

Lutjeharms, J.R.E., Bang, N.D. and Valentine, H.R. (1981). Die fisiese oseanologie van die Agulhas Bank. WNNR Navorsingsverslag 386, Stellenbosch. 38pp.

Malan, J.A., Martin, A.K. and Cartwright, J.A. (1990). The structural and stratigaphic development of the Gamtoos and Algoa Basin, offshore South Africa. In "Abstracts Geocongress90". Geol. Soc. South Africa., Cape Town, 328-331.

Malan, J.A., (1993). Geology potential of Algoa, Gamtoos basins of South Africa. Oil and Gas Journal, 91 (46), 74-77. Pennwell, Tulsa, OK, United States.

Maslanyi, M., Light, M., Horn, I., Greenwood, J. and Davidson, K. (1992). How similar geology of West Africa and eastern South America evolved. Offshore, 52/2, 25-27.

Malcolm, H. Rider. (2002). The Geological interpretation of well logs 2nd Ed.

McAloon, W., Webster, M. and Elliott, S. (1990). The occurrence of overpressure in the South African continental shelf. Abstracts Geocongress 90, Geol. Soc. South Africa., 349-352.

McAloon, W., Barton, K., Egan, J., & Frewin, J. (2000): Pre-development characterisation of a marginal deep-marine channel/lobe-system reservoir: block 9, the Bredasdorp Basin, offshore South Africa. Journal of African Sciences, 31(1), 47.

Matthews, G.P. and Ridgway, C.J. (1996). Modelling of simulated clay precipitation within reservoir sandstones. Marine and Petroleum Geology, vol. 13, no. 5: 581-589.

McCarthy, T.S. (1978). Report on analytical services. Unpubl. rept. to SOEKOR, Wits. Univeristy., 2pp.

McIver, J.R. and Ferguson, J. (1978). Kimberlitic, melilitic, trachytic and carbonatitic eruptives at Saltpetre Kop, Sutherland, South Africa. In "Extended Abstracts to Second International Kimberlite Conference", October 3-7, 1977, Santa Fe, New Mexico, 3pp.

McLachlan, I.R. and McMillan, I.K. (1979). Microfaunal biostatigraphy, chronostratigraphy and history of Mesozoic and Cenozoic deposits on the coastal margin of South Africa. Geol. Soc. South Africa. Pub. No 6, 1614-181.

McLachlan, I.R. Du Toit, J.J.L., Davies, C.P.N., Wood, E.M. and Marot, J.E.B. (1979). Intial report on alteration and fushing of petroleum reseroirs in the distal Bredasdorp Basin. SOEKOR unpubl. rept., 21pp.

McLachlan, I.R., & Broad, D.S. (2000): Petroleum exploration offshore South Africa: Journal of African Sciences, 31(1), 50-51.

McMillan, I.K. (1986). Cenozoic planktonic and larger foraminifera distribution around Southern Africa and their implication for past changes of oceanic water temperature. South Africa. Jour. Sci., 82, 66-69.

McMillan, I.K. (1989). Victoriella conoidea (Rutten, 1914): A guide foraminifera for the Late Aquitanian (Early Miocene) marine rocks of Southern Africa. South Africa. Jour. Geol., 92/2, 95-101

McMillan, I.K. (1990). Foraminiferal definition and possible implications of the major Mid-Cretaceous (Albian to Conicacian) hiatuses of Southern-most Africa. In "Abstracts Geocongress 90". Geol. Soc. South Africa., Cape Town, 363-366.

McMillan, I.K. and Valicenti, V.H. (1986). Palaeontology summery borehole F-R1. SOEKOR unpubl. rept. 1pp.

McMillan, I.K., Broad, D.S. and Brink, G.J. (1992). Late Mesozoic basins off the South coast of South Africa. SOEKOR unpubl. rept., SOE-EXP-RPT-034-, 35pp.

McMillan, I.K., Brink, G.J., Broad, D.S. and Maier, J.J. (1997 in press). Late Mesozoic sedimentary basins of the South coast of South Africa. In "Sedimentary Basins of the World: The African Basins", (ed.) Selley, R.C., Elsevier, Amsterdam.

McHardy, W.J., Wilson, M.J. and Tait, J.M. (1982). Electron microscope and X-ray diffraction studies of filamentous illitic clay from sandstones of the Magnus Field. Clay Minerals, vol. 17: 23-39.

Miles, J.A. (1989). "Llustrated Glossary of Petroleum Geochemistry". Oxford, 137pp.

Miles, J.A. (1990). Secondary migration routes in the Brent sandstones of the Viking Graben and East Shetland Basin: evidence from oil residues and subsurface pressures. Am. Assoc. Pet. Geol. Bull., 74/11, 1718-1735.

Milner, S.C. (1992). The age and emplacement of the Etendeka Formation volcanic rocks and the Damaraland igneous complexes relative to the operating of the South Atlantic: a review. "Abstracts South Western African continental margin conference: evolution and physical characteristics". Geol. Soc. Namibia, April 1992, 44-47.

Mlaba, B.M. (1996). Evaluation of magnetic and seismic anomalies surrounding the F-F high. SOEKOR unpubl. rept., Tech. Note No. 76, 5pp.

Morgan, W.J. (1983). Hotspot tracks and the early rifting of the Atlantic. tectonophysics, 94, 123-139.

Mumallah, N.A. (1996). Hydrochloric acid diffusion coefficients at acidfracturing conditions, Journal of Petroleum Science and Engineering 15: 361-374.

Muntingh, A. (1993). Geology, prospects in Orange Basin offshore western south Africa. Oil Gas Jour., 91/4, 106-109.

NASOU, (1973). ” Standard encyclopaedia of Southern Africa”, 8 p284.

Nico G (2005). The Barremian to Aptian gas fairway, Bredasdorp Basin, South Africa. World Petroleum Congress, September 25 - 29, 2005 , Document ID 18-1001 Johannesburg, South Africa

North, F.K. (1985). “Petroleum Geology”. Allen and Unwin, Winchester, 607pp.

O’Brien, G. and Woods, P. (1995). Hydrocarbon-related diagenetic zones (HRDZs) in the Vulcan sub- basin, Timor Sea: recognition implications. APEA Jou., 35/1, 220-252.

Ocean Allen (1984). Sedimentary structures: their character and physical basis: Developments in Sedimentology, v. 30.

O’Connell, S.A., Chandler, M.A. and Ruedy, R. (1996). Implications for the creation of warm saline deep water: Late Palaeocene reconstructions and global climate model simulations. Geol. Soc. Am. Bull., 108/3, 270-284.

Opuwari Mimonitu, (2010). Petrophysical Evaluations of the Albian age gas bearing sandstone reservoirs of the O-M field, Orange Basin, South Africa

Partridge, T.C. and Maud, R.R. (1987). Geomorphic evolution of Southern Africa since the Mesozoic. South African. Jour. Geol., 90/2, 179-208.

Pasquini, C., Lualdi, A. and Vercesi, P. (2004). Depositional dynamics of glaucony-rich deposits in the Lower Cretaceous of the Nice arc, southeast France. Cretaceous Research 25: 179-189.

Paull, C.K., Buelow, W.J., Ussler III, W. and Borowski, W.S. (1996). Increased continental-margin slumping frequency during sea level lowstands above gas hydrate-bearing sediments. Geology, 24/2, 143-146.

Pederson, T.F. and Calvert, S.E. (1990). Anoxia vs productivity: what controls the formation of organic carbon-rich sediments and source rocks. Am. Assoc. Pet. Geol. Bull., 74/4, 454-466.

Penuela, G. and Civan, F. (2000). Prediction of the gas-condensate well productivity, Journal of Petroleum Science and Engineering 28: 95-110.

Peters, K.E. (1986). Guidelines for evaluating petroleum source rocks using programmed pyrolysis. Am. Assoc. Pet. Geol. Bull., 70/3, 318-329.

Petrie, H.S. (1996). F-F2, F-BC1, and F-S1 Tertiary biostratigraphic report. Unpubl. rept. to SOEKOR, Halliburton Services, HALL BIO R05/96, 7pp.

Petroleum Agency SA (2002-2005). South African Exploration Opportunities, South African Agency for Promotion of Petroleum Exploration and Exploitation, Cape Town, pp 27. **Press, F., Siever, R., Grotzinger, J. and Jordan, T.H. (2004)**. Understanding Earth, Fourth Edition, W.H. Freeman and Company, England, pp165-169.

Pferdekamper, H. and Winters, S.J. (1997). Evaluation of the 9At1-13At1 interval in boreholes E-BB/E-AA/E-AD/E-BB/E-CA. SOEKOR unpubl. Tech. Note. No. 61,10pp.

Philippi, G.T. (1956). Identification of oil source beds by chemical means. In Proc. 20th Int. Geol. Cong. (Mexico City) Sect. III Petr. Geol., 25-38.

Pirson, S. J., (1958): Oil reservoir engineering, McGraw-Hill, New York City, 735p.

Piper, D.J.W., Shor, A.N., Farre, J.A., O'Connell, S. and Jacobi, R. (1985). Sediment slides and turbidity currents on the Laurentian Fan: sidescan sonar investigations near the epicentre of the 1929 Grand Bank earthquake. Geology, 13, 538-541.

Platte River Associates (1995). "Basinmod 1-D-version 5.00". Platte River Associates, Denver, Colorado, pp. var.

Potter, P.E., Maynard, J.B. and Pryor, W.A. (1980). "Sedimentology of shale". Springer-Verlag, New York, 306pp.

Rafdal, J., (1991). Core analysis to calibrate well log interpretationhttp://scaweb.org/assets/papers/1991_papers/1-SCA1991-03EURO.pdf

Rahim, Z. and Al-Qahtani, M.Y. (2003). Selecting perforation intervals and stimulation technique in the Khuff reservoir for improved and economic gas recovery, Journal of Petroleum Science and Engineering 37: 113-122.

Rasmussen, B. (2005). Radiometric dating of sedimentary rocks: the application of diagenetic xenotime geochronology. Earth Science Reviews 68: 197-243.

Retallack, G.J. (1996). Acid trauma at the Cretaceous-Tertiary boundary in eastern Montana. GSA Today, 6/5, 1-7.

Rigassi, D.A. and Dixon, G.E. (1970). Cretaceous of the Cape Province, Republic of South Africa. Ibadan Uni. Conf. on African Geol., Dec. 1970, 513-527.

Reifenstuhl (2002). Reservoir Characterization Studies in Alaska, vol. 6,no 3, by, Alaska Division of Geological and Geophysical Surveys.

Renard, F., Ortoleva, P. and Gratier, J.P. (1997). Pressure solution in Sandstones: Influence of clays and dependence on temperature and stress. Tectonophysics 280: 257-266.

Rider M.H., (1996). The Geological Interpretation of Well Logs: Caithness.

Rider, M.H., (2000): The geological interpretation of well logs (2nd Edition). Whittle publishing,

Scotland. Printed by interprint Ltd., Malta

Rider MH (2002): The geological Interpretation of well logs; John Wiley and sons, New York. (2nd Edt).

Rogers, M.A., McAlary, J.D. and Bailey, N.J.L. (1974). Singnificance of reservoir bitumens to thermal maturation studies, Western Canada Basin. Am. Assoc. Pet. Geol. Bull., 58/9, 1806-1824.

Ronov, A.B. (1958). Organic carbon in sedimentary rocks (in relation to presence of petroleum). Translations in Geochemistry No. 5, 510-536.

Roux, J. (1995). Strutural evolution and prospectivity of the F-F/F-P prospect areas. SOEKOR unpubl. Tech. Note No. 34, 5pp.

Roux, J. (1996). Oil finds within the pre 1At1 succession of the4 Bredasdorp Basin (Block 9). SOEKOR unpubl. Tech. Note No. 45, 4pp.

Roux, J. (2005). Gas Exploration and Potential in South Africa. South Africa: Spintelligent. [Online]. Available http://www.esiafrica. com/archive/esi_1_2005/18_1.php

Rowsell, D.M. and De Swardt, A.M.J. (1976). Diagenesis in Cape and Karoo Basin, South Africa, and its bearing on their hydrocarbon potential. Trans. Geol. Soc. South Africa., 79/1, 81-145.

Rowsell, D.M., Winter, H. de la R. and Davies, C.P.N. (1979). Geochemical report borehole F-F2. SOEKOR. Unpubl. rept., 8pp.

SABS (1983). Analysis of E-G1 oil. Unpubl. rept. to SOEKOR. No 321/1264/W22, 4pp.

SADCC (1992). "Oil and Gas Exploration in the SADCC Region". SADCC Energy Sector Seminar, 26-29, Nov. 1986, Arusha, Tanzania, PUBL?, PP??

Schlanger, S.O., Arthur, M.A., Jenkyns, H.C. and Scholle, P,A. (1987). The Cenomanian-Turonian oceanic anoxic Event, 1. Stratigrapy and distribution of organic carbon-rich beds and the marine δC^{13} excursion, in "Marine Petroleum Source Rocks" (eds.) Brooks, J. and Fleet, A.J., Geol. Soc. Spec. publ. No 26, Blackwell, London, 371-399.

Schlumberger (1991a). Petroleum Geology. In "Well evaluation conference-Angola", (eds.) Stark, D.M., Editions Galilée, Paris, 1-11-95.

Schlumberger (1991b). Log interpretation charts. Schlumberger educ. services, Houston, Texas, 171pp.

Schalkwyk, H. J. M., (2005). Assessment controls on reservoir performance and the addects of granulation seam mechanics in the Bredasdorp Basin, South Africa thesis.

Shanmugam, G. and Moiola, R.J. (1985). Submarine Fan Models: Problems and Solutions. In: A.H. Bouma, W.R. Normark and N.E. Barnes (eds.). Submarine Fans and Related turbidite Systems. Springer-Verlag New York, Inc., pp29-33.

Siddiqui, S.; Talabani, S.; Saleh, S.T. and Islam, M.R. (2002). Foam flow in low permeability Berea Sandstone cores: a laboratory investigation, Journal of Petroleum Science and Engineering 36: 133-148.

Smith, G.J. (1992). Geology and prospectivity of the 9A-to-12A sequence, Bredasdorp Basin. SOEKOR unpubl. rept., SOE-EXP-RPT-046, 33pp.

Smith, G.J. (1990). Milankovitch cyclicity and the stratigraphic record, a review Terra Nova, 1, 402-404.

Snyder, R. H., (1971): A review of the concepts and methodology of determining "net pay", SPE 3609, in the Annual Technical Conference and Exhibition, 12p.

Steyn, C. (1990). E-BA1 DST#1 & 1A : Test Analysis Report, Soekor Library, PetroSA unpublished data.

Storvoll, V., Bjørlykke, K., Karlsen, D. and Saigal, G. (2002). Porosity preservation in reservoir sandstones due to grain-coating illite: a study of the Jurassic Garn Formation from the Kristin and Lavrans fields, offshore Mid- Norway. Marine and Petroleum Geology 19: 767-781.

Stow, D.A.V. (1985). Brae Oilfield Turbidite System, North Sea. In: A.H. Bouma, W.R. Normark and N.E. Barnes (eds.). Submarine Fans and Related turbidite Systems. Springer-Verlag New York, Inc., pp231-236.

Stow, D.A.V., Howell, D.G. and Nelson, C.H. (1985). Sedimentary, tectonic, and Sea-Level Controls. In: A.H. Bouma, W.R. Normark and N.E. Barnes (eds.). Submarine Fans and Related turbidite Systems. Springer-Verlag New York, Inc., pp15-22.

Strauss, P., Noble, R.D.P. and Davies, C.P.N. (1996). Reconmmendation to drill borehole E-DC1. SOEKOR unpubl. rept., SOE-EXP-RPT-0360, 19pp.

Talwani, M. and Eldholm, O. (1973). Boundary between continental and oceanic crust at the margin of rifted continents. Nature, 241, 325-330.

Tarling, D.H. (1973). Metallic deposits and continental drift. Nature, 243, 193-196.

Taylor, K.G., Gawthorpe, R.L. and Fannon-Howell, S. (2004). Basin-scale diagenetic alteration of shoreface sandstones in the Upper Cretaceous Spring Canyon and Aberdeen Members, Blackhawk Formation, Book Cliffs, Utah. Sedimentary Geology 172: 99-115.

Theron, J.A. (1970). A stratigraphical study of the Bokkerveld Group (series). In "Second Gondwana symposium- proceedings and papers". Int. Union. Geol. Sci. Comm. Strat., CSIR, Pretoria, 197-204.

Thomas, B.M. Moller-Pedersen, P., Whitaker, M.F. and Shaw, N.D. (1985). Organic facies and hydrocarbon distribution in the Norwegian North Sea. In (eds.) Thomas, B.M. et al. "Petroleum Geochemistry in Exploration of the Norwegian Shelf". Graham and Trotman, London, 3-26.

Tissot, B.P. and Welte, D.H. (1984). "Petroleum Formation and Occurrrence". Springer-Verlag, Berlin, 699pp.

Underhill, J.R. and Partington, M.A. (1993). Jurassic thermal dorming and deflation in the North Sea: implications of the sequence stratigraphic evidence. In "Petroleum Geology of Northwest Europe" (eds.) Parker, J.R., Geol. Soc. Lond., 337-345.

Vail, P.R., Bubb, J.N., Hatelid, W.G., Mitchum, R.M., Sangree, J.B., Thomson, J.B. 111., Todd, R.G. and Widmier, J.M. (1977). Seismic stratigraphy and global changes of sea level, Parts I to II. In " Seismic Stratigraphy, application to hydrocarbon exploration". AAPG Mem. No. 26, 49-212.

Vail, P.R. (1987). Seismic stratigraphy interpretation procedure. In "Atlas of Seismic Stratigraphy". (eds.) Bally, A.W., Am. Assoc. Pet. Geol. Studies Geol. No. 27, AAPG, Tulsa, 1-10.

Valincenti, V.H. (1995). Biostatigraphy, sequence stratigraphy and a depositional model for the Bredasdorp Basin synrift sediments. SOEKOR unpubl. Tech. Note No. 19, 9pp.

Valicenti, V.H. and Broad, D.S. (1994). Dating of the drift onset unconformity in South Africa. SOEKOR unpubl. rept., SOE-PAL-RPT-015, 6pp.

Valicenti, V.H. and Stephens, J.M. (1984). Ostracods from the Upper Valanginian and Upper Hauterivian of the Sundays River Formation, Algoa Basin, South Africa. Revista Española de Micropal., 16, 171-239.

Van der Merwe, R. and Fouché, J. (1992). Inversion tectonics in the Bredasdorp Basin, offshore South Africa. In "Inversion Tectonics of the Cape Fold Belt, Karoo and Cretaceous Basins of Southern Africa". (eds.) De Wit, M.J. and Ransome, I.G.D., A.A. Balkema, Rotterdam, 49-59.

Van der Spuy, D. (1991). Application of the delta logR method of source rock indentification. SOEKOR unpubl. rept., SOE-GCH-RPT-003, 12pp.

Van Heerden, I.Li. (1984). Report on Agulhas Current measurements –FQ1 site. Specialist offshore Surveys unpubl. rept. to SOEKOR, 25pp.

Van Wyk, A. and Guest, M. (1992). Depth conversion: Southern Outeniqua Basin. SOEKOR unpubl. rept. SOE-EXP-RPT-004, 23pp.

Van Wyk, N.J.S. (1990). Applacation of sequence stratigraphy to oil and gas exploration in the Bredasdorp Basin, offshore South Africa. Abstracts Geocongress 90, Geol. Soc. South Africa., 566-569.

Veevers, J.J. (1990). Tectonic-climate supercycle in the billion-years plate-tectonic eon: Permian Pangean icehouse alternates with Cretaceous dispersed-continents greenhouse. Sed. Geol., 68, 1-16.

Vertaille, E.J.J. (1993). A synopsis of RFT data acquired in wells in the Bredasdorp Basin, including regional plots. SOEKOR unpubl. rept., SOE-PET-RPT-107, 6pp.

Weaver, C. E. and Pollard, L. D., (1975): The chemistry of clay minerals. Development insedimentology -15. Elsevier Scientific publishing company. P.213

Wenham, M.A., Van Wyk A. and Guest, M. (1991). Re-evaluation of the Souther Outeniqua Basin. SOEKOR unpubl. Rept., SOE-EXP-RPT-001-25pp.

White, R. and McKenzie, D. (1989). Magmatism at rift zones: the generation of volcanic continental margins and flood basalts. Jou. Geophys. Res., 94/B6, 7685/7729.

Wickens, H. de V. (1993). Sedimentology of the 14A reservoir sandstones, central Bredasdorp Basin, Southern offshore South Africa. SOEKOR unpubl. rept., SOE-ED-RPT-001, 80pp.

Wickens, H. de V. and McLachlan, I.R. (1990). The stratigraphy and sedimentology of the reservoir interval of the Kudu 9A-2 and 9A-3 boreholes. Communs. Geol. Surv. Namibia, 6, 9-22.

Williams, J.A. (1974). Characterization of oil types in Williston Basin. Am. Assoc. Pet. Geol. Bull., 58/7, 1243-1252.

Wilde, P., Normark, W.R., Chase, T.E. and Gutmacher, C.E. (1985). Potential petroleum reservoirs on Deep-Sea Fans off Central California. In: A.H. Bouma, 145 W.R. Normark and N.E. Barnes (eds.). Submarine Fans and Related turbidite Systems. Springer-Verlag New York, Inc., pp35-41.

Wilkinson, M., Milliken, K.L. and Haszeldine, R.S. (2001). Systematic Destruction of K-feldspar in deeply buried rift and passive margin sandstones, Journal of the Geological Society, London, Vol. 158: 675-683.

Winter, A. and Martin, A.K. (1990). Late Quatenary history of the Agulhas Current. Palaeoceanography, 5/4, 479-486.

Winter, H. de la R. (1981). Progress report on geopressure interpretation: volumes 1 and 2. SOEKOR. Unpubl. rept. 57pp.

Wood,E.M. (1995). Development potential seen in Bredasdorp Basin off South Africa. Oil and Gas Jour., 93/22,54-58.

Worthington PF, Cosentino (2005): The role of Cut-Offs in Integrated Reservoir Studies. SPE Reservoir Evaluation and Engineering (4). SPE 84387.

Wright, J.B. (1973). Continental drift, magmatic provinces and mantle plumes. Nature, 244, 565-567.

Zimmerman, H.B., Boersma, A. and McCoy, F.W. (1987). Carbonaceous sediments and palaeoenvironment of the Cretaceous South Atlantic. In “Marine petroleum source rocks” (eds.) Brooks, J. and Fleet, A.J., Geol. Sec. Spec. Publ. No 26, London, 271-286.

Related sites

www.corelab.com/petroleum services/geological/thin.asp

www.panterra.nl/geoscienc/geology/reservoir quality.php

http://pubs.usgs.gov/of/2003/ofr-03-420/ofr-03-420.html

http://www.petroleumagencysa.com/index.php/contact?view=contact

http://blogs.denison.edu/geosciences/2012/04/27/the-erosive-and-depositional-poperties-of-turbidty-currents/

http://www.studyblue.com/notes/note/n/planet-earth-16-deep-ocean/deck/4681998

(http://www.petroleum-engineering.net/basic-logging-formation-evaluation-component/).

Appendix

Result obtained from the conventional core measurements of well E-BB1(Hill 1991), PASA.

Depth (m)	Porosity (%)	K (mD)	Kair (mD)	Sg (%)	So (%)	Sw (%)	Calcite (%)	Dolomite (%)	Grain Density (g/cc)
2846.05	13.8	26.29	29.05	70	5	25	0.0	1.0	2.67
2846.25	11.7	12.95	14.56						2.66
2846.54	13.1	27.66	30.06						2.65
2846.79	13.1	29.29	32.17						2.65
2847.05	13.0	23.56	25.94	66	4	30	0.0	1.0	2.66
2847.25	10.1	4.82	5.67						2.65
2847.50	11.2	12.41	13.88						2.65
2847.75	11.5	10.65	12.11						2.65
2848.03	11.2	9.04	10.34	67	5	28	0.5	1.0	2.65
2848.25	13.1	24.83	27.47						2.64
2848.50	13.2	24.87	27.25						2.65
2848.75	13.8	25.79	28.40						2.67
2849.05	12.6	28.11	30.47	67	0	33	0.5	1.0	2.65
2849.27	14.4	39.29	42.73						2.65
2849.53	8.9	1.01	1.40						2.66
2849.78	9.3	1.30	1.74						2.66
2850.05	12.0	14.44	16.10	67	4	29	0.5	1.0	2.65
2850.25	13.3	27.49	29.95						2.65
2850.47	13.3	20.03	22.31						2.65
2850.72	10.7	4.27	5.12						2.65
2851.05	11.9	7.78	9.04	66	5	29	1.0	1.0	2.66
2851.22	11.3	6.50	7.70						2.65
2851.46	13.5	18.19	20.22						2.66
2851.72	13.4	15.81	17.83						2.65
2852.03	8.4	0.10	0.21	47	19	34	0.0	2.0	2.67
2852.29	9.0	0.61	0.89						2.65
2852.79	12.8	12.56	14.33						2.65
2853.11	13.8	16.70	18.48	73	0	27	1.0	3.0	2.68
2853.33	12.2	10.62	12.12						2.65
2853.58	11.5	7.04	8.19						2.66
2853.83	11.8	9.00	10.33						2.65
2854.05	12.5	9.91	11.36	65	4	31	0.0	1.0	2.67
2854.22	12.0	10.49	12.01						2.65
2854.51	9.3	1.12	1.72						2.65
2854.76	9.7	1.97	2.56						2.64
2855.05	11.3	4.68	5.64	66	5	29	0.0	1.5	2.66

2855.22	11.4	6.15	7.31						2.65
2855.47	10.8	5.87	6.97						2.64
2855.72	12.5	9.70	11.28						2.68
2856.05	11.1	2.65	3.38	62	8	30	1.0	0.5	2.67

Result obtained from the conventional core measurements of well E-BD2 (Hill 1991), PASA.

DEPTH (m)	POROSITY (%)	Kair (mD)	K (mD)	GRAIN DENSITY
2579.30	19.8	935.94	929.28	2.64
2580.35	18.6	502.55	496.59	2.67
2580.60	18.6	282.96	275.57	2.66
2580.85	17.5	235.05	227.52	2.65
2581.60	19.2	672.96	670.18	2.65
2581.85	16.9	121.36	116.44	2.64
2582.35	19.7	645.21	645.10	2.64
2582.64	19.4	489.34	485.87	2.64
2583.80	16.0	165.59	159.19	2.64
2584.30	17.3	156.57	150.40	2.64
2585.80	19.0	422.15	421.45	2.64
2586.32	19.4	755.32	747.28	2.64
2586.82	19.7	204.11	197.60	2.67
2587.35	17.4	68.05	63.97	2.64
2587.85	15.6	177.83	173.97	2.64
2588.10	18.0	299.54	295.98	2.64
2588.35	18.7	392.54	329.52	2.64
2588.60	18.5	448.35	445.58	2.64
2588.85	18.9	531.57	529.74	2.66
2589.10	17.1	147.35	141.91	2.64
2589.35	17.0	200.50	197.79	2.64

2589.60	17.0	211.49	206.98	2.64
2589.85	16.9	242.98	239.65	2.64
2590.10	17.3	253.21	248.39	2.64
2590.35	17.5	244.77	239.01	2.65
2590.60	17.2	221.71	215.48	2.64
2590.98	17.6	237.96	229.99	2.65
2591.17	16.8	189.51	183.87	2.64
2591.42	17.5	262.06	258.82	2.64
2591.69	17.1	158.28	151.44	2.65
2591.94	16.8	192.63	189.02	2.64
2592.19	17.3	205.04	201.48	2.64
2592.44	16.1	107.96	103.43	2.64
2592.69	16.0	159.57	154.51	2.64
2592.94	14.4	107.15	103.09	2.64
2593.19	18.6	199.70	196.71	2.72
2593.50	16.6	148.80	144.94	2.65
2583.75	17.9	149.68	145.31	2.65
2594.00	17.0	97.09	90.84	2.65
2594.28	16.7	179.49	174.86	2.64
2594.53	16.7	120.87	117.09	2.64
2594.78	17.3	120.12	115.01	2.65
2595.03	16.8	112.02	107.51	2.64
2595.28	17.6	215.58	211.62	2.65
2595.53	14.3	79.67	76.10	2.65
2595.78	16.3	151.83	145.54	2.64
2596.05	17.0	160.11	153.82	2.65
2596.30	17.3	159.00	155.19	2.66

Result obtained from the conventional core measurements of well E-A01 (Hill 1991), PASA.

Depth (m)	Gas Exp.	Sum of fluids	Air Perm (mD)	Liq Perm (Md)	Sw	So	Sg	Cal.	Dol.	Grain density
2674.05	16.1	17.3	111.57	106.44	84	00	16	1	05	2.73
2674.05	15.7	17.3	104.80	99.75	84	00	16	1	05	2.73
2674.30	15.5		109.31	105.18						2.68
2674.30	14.9		103.48	99.47						2.68
2674.55	15.9		77.11	73.33						2.67
2674.55	14.4		72.75	69.16						2.67
2674.80	15.3		96.83	92.44						2.68
2674.80	14.8		91.54	87.15						2.68
2675.05	14.6	15.0	88.00	83.34	89	00	11	1	09	2.68
2675.05	14.2	15.0	82.99	78.43	89	00	11	1	09	2.68
2675.25	13.8		55.89	52.74						2.69
2675.25	13.3		52.74	49.62						2.69
2675.50	14.0		37.13	34.27						2.69
2675.50	13.5		35.15	32.43						2.69
2675.75	12.7		10.22	8.88						2.70
2675.75	12.3		9.60	8.34						2.70
2675.90	14.8	15.5	5.19	4.09	63	00	37	1	08	2.70
2675.90	14.3	15.5	4.81	3.79	63	00	37	1	08	2.70
2676.20	14.2		1.56	1.10						2.68
2676.20	13.5		1.29	.92						2.68
2676.45	11.9		1.61	1.18						2.67
2676.45	11.3		1.38	1.02						2.67
2676.70	12.9		2.15	1.61						2.67
2676.70	12.3		1.80	1.36						2.67
2676.96	14.7	14.4	1.62	1.10	67	00	33	1	02	2.68
2676.96	14.1	14.4	1.25	.85	67	00	33	1	02	2.68
2677.30	10.4		.16	.07						2.66
2677.30	9.8		.09	.04						2.66
2677.55	12.4		.69	.44						2.68
2677.55	11.8		.57	.37						2.68
2677.80	12.0		1.63	1.16						2.68
2677.80	11.5		1.32	.96						2.68
2677.97	12.9	13.6	1.64	1.14	59	0	41	3	05	2.69
2677.97	12.4	13.6	1.25	.87	59	00	41	3	05	2.69
2678.25	11.8		.33	.18						2.68
2678.25	10.9		.18	.10						2.68
2678.50	12.0		1.36	.94						2.68
2678.50	11.3		1.00	.70						2.68
2678.75	5.5		.04	.02						2.72
2678.75	5.0		.01	.00						2.73
2678.93	11.1	11.2	1.18	.80	56	00	44	3	04	2.70
2678.93	10.6	11.2	.90	.62	56	00	44	3	04	2.70
2679.15	11.7		1.32	.92						2.68

2679.15	11.1		1.08	.77						2.68
2679.40	11.7		1.21	.83						2.67
2679.40	11.2		.97	.68						2.67
2679.65	11.9		1.35	.94						2.67
2679.65	11.3		1.10	.78						2.67
2679.89	11.5	11.1	1.36	.95	49	00	51	2	02	2.67
2679.89	11.1	11.1	1.16	.82	49	00	51	2	02	2.67
2680.20	10.6		.28	.15						2.67
2680.20	10.1		.19	.10						2.67
2680.45	10.7		.36	.21						2.68
2680.45	9.4		.26	.15						2.68
2680.70	9.4		.19	.09						2.69
2680.70	9.7		.12	.06						2.69
2680.89	7.3	7.3	.12	.05	48	00	52	6.5	04	2.68
2680.89	6.8	7.3	.07	.03	48	00	52	6.5	04	2.68
2680.15	7.5		.08	.03						2.68
2680.15	6.9		.04	.01						2.68

STANDALONE PICKETT CROSSPLOTS FOR WELLS E-BB1, E-BD2 AND E-A01 (courtesy of PASA).